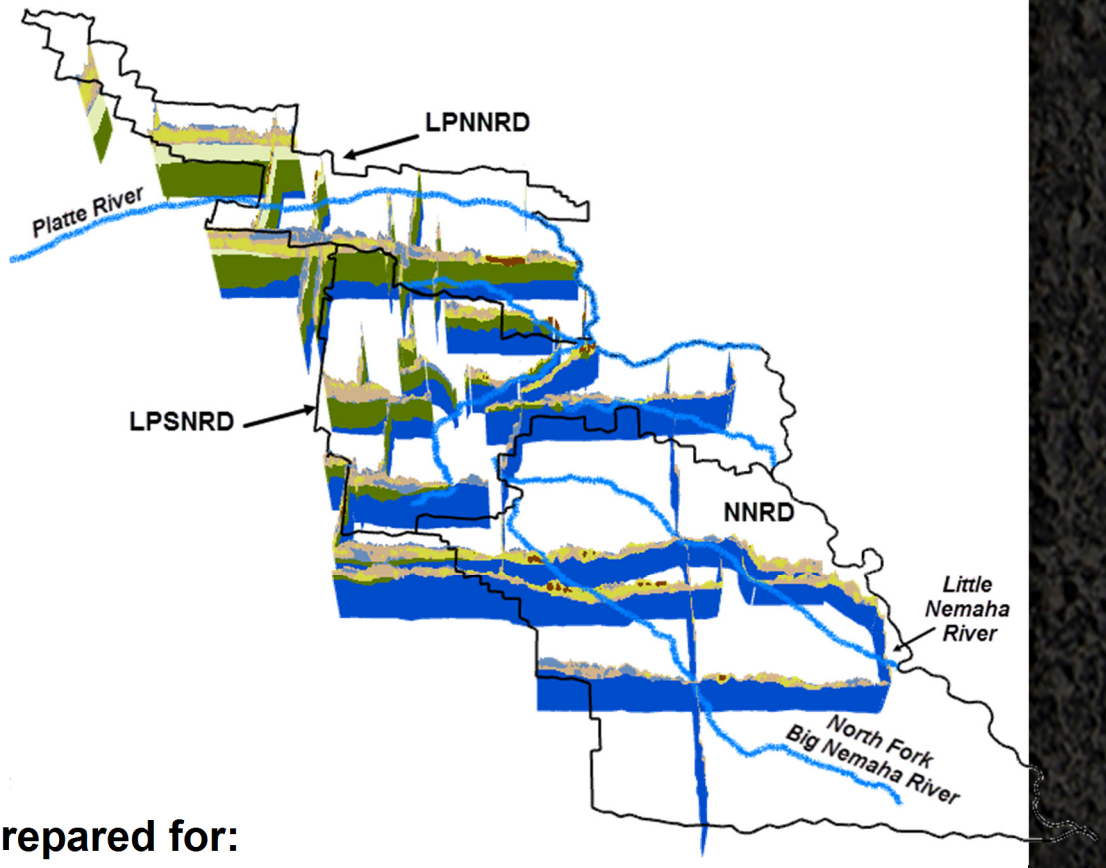
# Final Report on Airborne Electromagnetic Geophysical Surveys and Hydrogeologic Framework Development for the Eastern Nebraska Water Resources Assessment

Volume II – Including the Lower Platte North, Lower Platte South, and Nemaha Natural Resources Districts




**Prepared for:**

**Eastern Nebraska Water Resources Assessment**
**3125 Portia Street**
**Lincoln, NE 68521**

**July 20, 2015**

EXPLORATION RESOURCES INTERNATIONAL

EXPLORATION RESOURCES INTERNATIONAL

July 20, 2015

# Final Report on Airborne Electromagnetic Geophysical Surveys and Hydrogeologic Framework Development for the Eastern Nebraska Water Resources Assessment – Volume II, including the Lower Platte North, Lower Platte South, and Nemaha Natural Resources Districts

Prepared for:
Eastern Nebraska Water Resources Assessment

Submitted by:
Exploration Resources International Geophysics, LLC
6207 Hwy 80 East
Vicksburg, MS 39180
Phone: (866) 974-6867

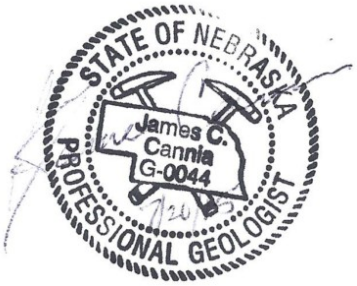
Clint P. Carney, P.G.
Clint.Carney@xrigeo.com

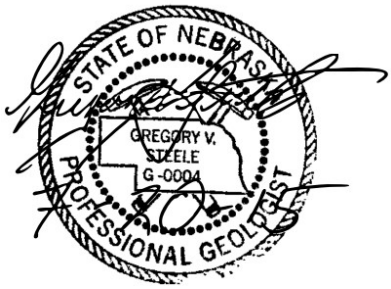
Jared D. Abraham
Jared.Abraham@xrigeo.com

James C. Cannia, P.G.
Jim.Cannia@xrigeo.com

Gregory V. Steele, P.G.
Greg.Steele@xrigeo.com



## Executive Summary

Exploration Resources International (XRI) is pleased to submit our report to the Eastern Nebraska Water Resources Assessment titled "*Final Report on Airborne Electromagnetic Geophysical Surveys and Hydrogeologic Framework Development for the Eastern Nebraska Water Resources Assessment- Volume II, including the Lower Platte North, Lower Platte South, and Nemaha Natural Resources Districts*." The ENWRA AEM survey investigation discussed here was separated into two operational phases and, thus, two reports. Volume I describes the methods, background information, and findings of Phase 1, the airborne survey conducted in the Fall of 2014, that covered approximately the northern half of the ENWRA area, which included the Lewis and Clark, Lower Elkhorn, and Papio-Missouri River Natural Resources Districts. Volume II describes the methods, background information, and findings from Phase 2, the Spring 2015 airborne survey, that covered, approximately, the southern half of the project area, including the Lower Platte North, Lower Platte South, and Nemaha Natural Resource Districts. This project was conducted to address ENWRA's water resource concerns by completing reconnaissance flight lines in the glacial terrain of eastern Nebraska. This hydrogeologically complex area has undergone increased groundwater development in recent years, which prompted ENWRA to seek additional information on the aquifers underlying the region. XRI entered into an agreement with ENWRA to undertake this study on September 15, 2014. The scope of work for this project is as follows:

**1. SCOPE OF WORK**

1.1 An Airborne Electromagnetic (AEM) survey was flown in two phases over a specified area in eastern, NE within the ENWRA area to support creation of a regional hydrogeological framework of this area. XRI subcontracted with a qualified aircraft company to complete the flights of the area in order to acquire the data necessary to complete the Survey. This framework will be provided both as preliminary AEM data and as a final product in an Interpretative Report. Approximately 1,298 line miles of AEM and magnetic data were collected in the two phases.

1.2 Phase 1 commenced on Oct. 11, 2014. The Contractor entered into a contract with a subcontractor to fly 750 line miles over the specified area of the ENWRA to obtain the data for Phase 1 of the Survey, which was then used by XRI to provide the hydrogeological framework contained in the interim report presented on April 9, 2015. XRI provided status reports to the ENWRA group, concerning the progress of the flights on a daily basis including the areas flown, production rates, and flight plan for the following day. The ENWRA group was updated on a regular basis on progress of the interim report. After completion of the framework for Phase 1, an interim Interpretative Report was produced and delivered to the ENWRA on April 9, 2015 (Completion of Phase 1).

1.3 XRI contracted to fly approximately 550 flight miles over the specified area of the ENWRA to obtain the data for Phase 2 of the Survey, which was then used by XRI to develop the hydrogeological framework discussed in this volume. XRI provided status reports to the ENWRA concerning the progress of the flights on a daily basis which included the areas flown, production rates, and flight plan for the following day. The ENWRA group was updated on a regular basis on progress of the interim report.

1.4 XRI processed and performed quality assurance and quality control protocols on all of the data collected from the Surveys.

1.5 Upon completion of data acquisition of each phase of the Survey, XRI began the geophysical processing, including numerical inversions to create a preliminary and final datasets to be shared with the ENWRA.

1.6 XRI inverted the AEM data and derived a 3D electrical model of the surveyed area. These inverted georeferenced data will be delivered to the ENWRA and incorporated into the two volume Interpretative Report.

1.7 XRI's Interpretative Report includes locations of aquifer(s), a hydrogeologic framework that presents the AEM relationship to geologic test holes, as well as delineation of potential recharge areas along two-dimensional profiles. The Interpretative Report will also include all data and metadata files and will be delivered to the ENWRA in PDF digital format.

1.8 The final Interpretative Report for both phases will be delivered no later than July 30, 2015 (Completion of Phase 2).

**2. SCHEDULE**

2.1 Upon completion of data acquisition of each phase of the Survey, XRI began the geophysical processing, including numerical inversions to create a preliminary and final datasets to be shared with the ENWRA.

2.2 Post geophysical processing, XRI began development of the hydrogeologic framework. At times during its development, XRI interacted with ENWRA staff to keep the ENWRA group apprised of progress. After completion of the framework for Phase 1, an interim Interpretative Report was produced and delivered to the ENWRA on April 9, 2015 (Completion of Phase 1). The final Interpretative Report for both phases will be delivered no later than July 30, 2015 (Completion of Phase 2).

For organizational purposes, as discussed above, this report (Volume II) formally discusses the findings of the AEM survey for the LPNNRD, LPSNRD, and the NNRD. A small portion of the flight lines in the PMRNRD were collected in the Spring 2015 survey and are included in Volume I. Volume I of this report includes the assessments of the LCNRD, LENRD, and the PMRNRD.

The AEM data for Phase 2 of the project was successfully collected on April 16-21, 2015, including all quality control, quality assurance, and initial inversions of the data. In total, 685 line-miles of data were collected during this phase of the survey. Data interpretation and report writing started in April 2015 and will be completed with delivery of this final report to ENWRA. All contracted activities within the scope and schedule of work were met or exceeded.

Interpretation of the AEM data collected in 2015 provides a subsurface characterization of the principal aquifer beneath the southern ENWRA project area that correlated with pre-existing geologic information. The AEM provides detailed verification and quantification of the geology that underlies the flight lines within the project area. The interpretation also provided an improved understanding of the glacial, bedrock, water quality, and structural features present in the subsurface. Lithologic descriptions from test holes (University of Nebraska-Conservation and Survey Division) and oil and gas records (Nebraska Oil and Gas Conservation Commission) provided the most useful historical information in the development of the new hydrogeologic framework. Additional supporting data included historic cross sections and a limited number of geophysical logs from the Conservation and Survey Division.

The nature of the AEM reconnaissance line flight pattern (i.e. the large distance between the flight lines) limits the display of the subsurface to two-dimensional (2D) sections along the flight lines, which resulted in insufficient information for accurate estimation of aquifer volumes or the amount of groundwater in storage. However, the 2D sections do provide the location, orientation, groundwater levels (1995 CSD regional water table surface map), and connectivity between the deposits comprising the principal aquifer and the local streams that were crossed by flight lines in the project area. The hydrogeologic framework also provides locations at the land surface where the potential for recharge to the principal aquifer along the flight lines is likely the greatest. The 2D sections of the glacial till and loess areas provide limited insight into the confined and unconfined nature of the groundwater system and where water quality management could be impacted by the presence or absence of these materials.

Within the southern ENWRA project area, the principal aquifer primarily consists of unconsolidated Quaternary sediments found mainly in paleovalleys (buried and surficial) as well as alluvial valley deposits. In some locations, these aquifer materials are in hydrogeologic connection with each other. Within the Quaternary system, the materials detected by the AEM survey, were divided into non-aquifer (aquitard), marginal, principal, and coarse, sand-rich principal materials. Principal aquifer material, including sand-rich zones, is found primarily within paleovalleys and beneath the valleys of the major surface water drainages covering the area. Marginal aquifer deposits are found throughout much of the area and comprise most of the aquifer resources in the western LPSNRD, in the LPNNRD between the Platte River valley and the major paleovalley mapped along the southern district border, and through most of the southern and eastern NNRD. Aquitard materials are generally less thick than in the northern ENWRA project and are most prevalent in the north central area of the LPNNRD, the eastern LPSNRD, and the western and southern NNRD. Potential Cretaceous Dakota Formation bedrock aquifers are likely present where areas of high electrical resistivity were detected. These are considered “potential,” as limited information on the aquifer is available in the area. Paleozoic strata are detected in the AEM survey but minimal information on water quality as well as a lack of deep test hole logs limit conclusive hydrogeologic interpretation on these units. Structure in the Paleozoic sequence, is clearly evident across several profiles, including faults, dipping strata, and the Nemaha Uplift. Brackish and saline groundwater were detected and mapped across parts of the southern ENWRA project area, particularly in the Lower Platte South and Nemaha Natural Resources Districts. Although these saline groundwater types can be mapped by AEM methods (they represent as highly conductive, low resistivity features), there is, however, limited historical data or new supporting data on water quality in the project area to

fully characterize the brackish/saline conditions detected in the survey. The body and appendices of this Volume II report contain the information used in the AEM interpretation and development of the hydrogeologic framework.

Key findings include:

1.) Aquifer resources beneath the southern ENWRA project area vary considerably within the Quaternary system, and with the exception of the Platte River valley, aquifer materials, whether principal or marginal, are considerably more limited in areal extent as compared to the northern half of the ENWRA project area (Volume I).

2.) LPNNRD - The AEM survey revealed that in the LPNNRD the subsurface beneath the Platte River valley is composed of widespread deposits of principal aquifer material, and in many locations, sand-rich principal aquifer materials. In the uplands south of the Platte River valley across the southern LPNNRD and northern LPSNRD, the Quaternary system primarily consists of marginal and aquitard materials, and in some areas, nearly the entire Quaternary sequence consists of aquitard materials. In the south central area of the southeastern half of the LPNNRD, a paleovalley is present that consists of upwards of 200 ft of principal aquifer deposits underlain by 100-200 ft of marginal and aquitard deposits. In the far western area of the northwestern half of the LPNNRD, the principal aquifer consists of Quaternary deposits and Tertiary Ogallala Group (*To*) materials. On the eastern side of the district, the Todd Valley hosts sand-rich principal aquifer material through nearly the entire thickness of the valley. In the far southeast corner of the district, the Quaternary system is relatively thin compared to other sections of the LPNNRD and consists of interlayered marginal and principal aquifer material with variable degrees of saturation.

3.) LPSNRD - The Quaternary system beneath the LPSNRD is variable in material thickness and texture, with a majority of the materials west of Lincoln consisting of marginal and aquitard deposits with isolated intervals of principal aquifer. The most extensive bodies of principal aquifer deposits are found in the northwest corner of the district where paleovalleys are underlain by aquitard and marginal aquifer deposits, and to the south of Lincoln where a paleovalley crosses beneath the district with variable width, depth, and thickness. Immediately north of Lincoln, the Quaternary system is relatively thin, typically not exceeding 200 ft in thickness, and in many locations, less than 100 ft thick with variable electrical resistivity. This trend continues along the Salt Creek valley northeast of Lincoln, where less than 100 ft of interlayered marginal and principal aquifer materials comprise the local groundwater source. On the northern outskirts of Lincoln, low resistivity (conductive) intervals were detected in the shallow subsurface. These intervals correspond to high-TDS conditions in the shallow aquifer and surface water features. East of Lincoln, the Quaternary system consists primarily of marginal aquifer and aquitard material ranging from 100 ft to 200 ft in thickness, with only isolated principal aquifer features, mostly overlying the underlying Cretaceous Dakota Formation (*Kd*) and Paleozoic bedrock. The Quaternary system generally thins eastward, and is mostly marginal aquifer material ranging from 100 to 150 ft in thickness.

4.) NNRD - The Quaternary system beneath the NNRD ranges from areas of thick paleovalleys in the northwest and north-central areas of the district to areas of only thin, unsaturated marginal aquifer and aquitard materials overlying Paleozoic bedrock. The AEM survey revealed insight into the structure of known palevalleys that exist beneath parts of the district. In some areas of Johnson County, principal aquifer materials are present near the land surface and extend to near the base of the Quaternary system, a condition that provides greater potential for aquifer recharge. In the east-central area of the NNRD, the AEM survey revealed a thin distribution of marginal aquifer material with isolated areas of principal aquifer materials. Overall, the Quaternary system is less than 100 ft thick with variable saturated thickness.

5.) Dakota Formation - The full extent and thickness of the Dakota Formation, a secondary aquifer resource in eastern Nebraska (Divine et al., 2009), is revealed in the AEM survey of the southern ENWRA area. The southeastern terminus of this regionally extensive formation is evident in the AEM data, which also includes isolated remnants of the formation beyond the primary eastern Dakota Formation margin in the LPSNRD. The Dakota Formation ranges in thickness from nearly 600 ft beneath parts of the western LPNNRD to less than 40 ft along the margin of the formation. A very slight apparent westward dip in the Dakota Formation is indicated along west-east flight lines in the LPNNRD, and the topographic expression of the Dakota Formation is generally flat beneath much of the western half of the Dakota Formation's extent, with more local relief beneath some areas in the eastern LPNNRD and LPSNRD. The depth to the top of the Dakota Formation ranged from over 900 ft to less than 50 ft.

The AEM data captured the variability in resistivity of the Dakota Formation providing an inventory of potential drill targets in this formation for bedrock aquifer development. Intervals of 20-40 ohm-m ranging from less than 100 ft thick to nearly 400 ft thick are present throughout much of the LPNNRD and the eastern half of the LPSNRD, some containing thinner intervals of 40 ohm-m or greater material. An area of expected high TDS water within the Dakota Formation is evident in the central LPSNRD (immediately north of Lincoln) where the Dakota Formation is relatively shallow and where high TDS surface water is detected in numerous wetlands and surface drainages. This area of the Dakota Formation extends westward along flight line 300701, but does not appear to extend north or south, as resistive intervals are found in the Dakota Formation within flight lines in both directions from this conductive area.

6.) Paleozoic Strata - The AEM survey of the southern portion of the ENWRA project area revealed over 1,000 ft of Paleozoic strata beneath much of the surveyed locations, particularly in the eastern LPSNRD and most of the NNRD. Although undifferentiated in the interpretation in this report, the AEM data revealed considerable variability in the resistive nature of the Paleozoic deposits, from bodies with resistivities exceeding 30 ohm-m, to other strata with resistivity less than 10 ohm-m. Resistivities greater than 60 ohm-m are encountered along flight lines 401101 and 301501 in the southern NNRD that are associated with granite of the Nemaha Uplift. The depths to the Paleozoic sequence ranges from over 1,500 ft bgl beneath the northwestern half of the LPNNRD to only a few feet beneath overburden along gullies and valleys of the southern NNRD. Numerous Paleozoic outcrops are present across the NNRD and the parts of the LPSNRD.

The AEM survey revealed several structural features in the Paleozoic system beneath the southern ENWRA survey area, including faults and dipping strata associated with the TRSZ and resistive zones of the Nemaha Uplift and Elk Creek Carbonatite complex. These features are identified in the AEM profiles by offsets in the strata as indicated by changes in resistivities within the Paleozoic strata. The Union and Humboldt Faults are evident on several AEM profiles, and tilted strata are clearly evident along flight line 401101. The basement rock of the Nemaha Uplift, consisting of Precambrian granite, is also evident along flight line 401101 and 301501. This uplift, which also hosts the Elk Creek Carbonatite, is indicated as a large resistor immediately west of the Humboldt Fault. Although interpretation of Paleozoic features was beyond the purview of this project, the depth and detail revealed by the AEM within the Paleozoic sequence can allow for refined interpretation of regional structure, as well as identifying possible sources for groundwater exploration in southeast Nebraska, particularly along faults.

7.) Survey Line Spacing - The variable grid spacing across the southern ENWRA project area provided insight and information on a regional scale, allowing for greater understanding of where future investigations could potentially provide more detailed characterization of the subsurface. Due to the larger population centers and infrastructure, along with areas of particular interest from ENWRA, the design of the survey lines was more variable as compared to the more gridded design of the northern ENWRA survey area conducted in the Fall of 2014.

The hydrostratigraphic framework resulting from the AEM reconnaissance survey provides a database of information on the structure of the groundwater resources available beneath the southern half the ENWRA area. The body and appendices of the report contain the information used in the AEM interpretation and in the development of the hydrogeologic framework. Recommendations for future work include:

1.) Additional AEM surveys in areas where the reconnaissance survey located potentially extensive zones of sand-rich, principal aquifer materials.

2.) The connectivity between groundwater and surface water features along the streams and rivers within the project area is not well understood at all locations, particularly in areas where high densities of irrigation wells exist. The addition of a near-surface, high resolution AEM streambed mapping program of the riparian area is recommended. This data would provide finer detail of the lithology of these critical areas, and, more precisely, characterize the extent and shape of the aquifers and aquitards that affect hydrologic connection to streams. This is of particular importance in the narrow stream valleys in the NNRD where the alluvial volume is limited.

3.) A tightly-spaced AEM survey grid in the area northeast of Lincoln to target the shallow subsurface, a complement to the present investigation of the Dakota Formation beneath this area, could further characterize the extent of the areas affected by the high-TDS waters in the shallow subsurface. This will assist in development of new groundwater resources in the area.

4.) For locations where the target of the investigation involves localized aquifer features, a tighter grid spacing on the order of 600 to 1,500 ft separation is recommended. Surveys of this scale will allow for creation of 3D voxel models of aquifer materials, from which estimations of aquifer volume and

groundwater in storage can be made. This will provide NRD managers greater insight into the quantity of groundwater available in their areas of interest.

5.) A CSD test hole program that includes penetration through the Dakota Formation, ideally in the areas where the most extensive Dakota Formation resistors were detected in the AEM survey.

6.) The AEM survey identified areas along the flight lines where a greater probability of groundwater recharge is likely to occur. A high resolution AEM survey of these areas would serve to quantify the geographic extent of these areas and the hydrologic connection to the subsurface.

7.) Utilize aquifer characterization techniques in conjunction with the AEM survey flight lines to improve the understanding of important changes in hydraulic conductivity, storage, and yield.

## Table of Contents

1 Introduction ..... 1
1.1 Purpose of Project ..... 1
1.2 Previous Work ..... 2
1.3 Description of Project Area ..... 3
2 Project Area Hydrogeology ..... 5
2.1 Geologic Setting ..... 5
2.1.1 Surficial Geology ..... 8
2.1.2 Tertiary Geology ..... 9
2.1.3 Cretaceous Geology ..... 9
2.1.4 Jurassic and Triassic Geology ..... 10
2.1.5 Paleozoic System ..... 10
2.1.6 Structural Geology ..... 12
2.2 Hydrogeologic Characteristics of the Quaternary System ..... 17
2.2.1 Surface Hydrology ..... 17
2.2.2 Groundwater Flow System ..... 20
2.2.3 Aquifer Characteristics ..... 22
2.2.4 Aquifer-Surface Water Connection ..... 23
2.2.5 Connectivity to other Aquifers ..... 24
2.3 Bedrock Aquifer Conditions ..... 24
2.3.1 Extent and Structure of Kd Aquifer ..... 24
2.3.2 Aquifer Characteristics ..... 25
2.3.3 Connectivity to Surface Water ..... 26
2.3.4 Connectivity to other Aquifers ..... 26
2.4 Water Quality ..... 26
2.4.1 Quaternary Aquifer Water Quality ..... 29
2.4.2 Bedrock Aquifer Water Quality ..... 30
2.5 Water Use ..... 31
3 Additional Background Information ..... 35
3.1 Borehole Data ..... 35
3.2 Historic Geologic Cross Sections ..... 38

4 Geophysical Methodology, Acquisition and Processing ..... 42
4.1 Geophysical Methodology ..... 42
4.2 Utility Mapping ..... 43
4.3 AEM Survey Instrumentation ..... 44
4.4 Data Acquisition ..... 47
4.5 Data Processing ..... 48
4.5.1 Primary Field Compensation ..... 48
4.5.2 Automatic Processing ..... 49
4.5.3 Manual Processing and Laterally-Constrained Inversions ..... 49
4.5.4 Power Line Noise Intensity (PLNI) ..... 51
4.5.5 Magnetic Field Data ..... 53
4.6 Spatially-Constrained Inversion ..... 55
4.6.1 Determination of the DOI ..... 60
5 Results and Interpretation ..... 62
5.1 AEM Results and Interpretation ..... 63
5.1.1 Interpretive Process ..... 63
5.1.2 Resistivity-Lithology Relationship ..... 66
5.2 Hydrogeologic Framework Interpretation ..... 78
5.2.1 Quaternary Geologic and Depositional Features Revealed in the AEM Survey ..... 79
5.2.2 Brackish/Saline Conditions in the Subsurface ..... 86
5.2.3 Structural Features ..... 91
5.2.4 Comparison with CSD Geologic Cross Sections and Test Holes ..... 94
5.3 Hydrogeologic Interpretation for the Individual NRDs ..... 102
5.3.1 Lower Platte North NRD ..... 102
5.3.2 Lower Platte South NRD ..... 111
5.3.3 Nemaha NRD ..... 117
5.3.4 Flight Lines beyond the ENWRA Area ..... 123
5.3.5 Comparison of AEM Results with Previous Studies ..... 126
5.4 Summary and Recommendations ..... 135
5.4.1 Key AEM Survey Findings ..... 135
5.4.2 Applicability and Recommendations Regarding Future Groundwater Investigations ..... 139
6 Description of Data Delivered ..... 143

7 References ..... 149
Appendix 1: AEM Profiles and Interpretation ..... A1-1
Appendix 2: Comparison of CSD Holes with AEM Profiles ..... A2-1
Appendix 3: Depth of Investigation ..... A3-1
Appendix 4: Data Delivery ..... A4-1
Appendix 5: Water Quality Diagrams ..... A5-1

## List of Figures

Figure 1-1: Map of ENWRA project area, with the southern extent of the survey area (Phase II) and flight lines highlighted in bolded orange and blue, respectively. The northern half of the project area (Phase I) is outlined in green. NRD boundaries are shown in red with individual NRD initials shown in white. ..... 2

Figure 1-2: Map of the southern ENWRA project area, including the largest cities and major roads within the study area. NRD boundaries are displayed in the insert map. ..... 4

Figure 1-3: Land surface elevation and topographic expression of the southern ENWRA project area. ..... 5

Figure 2-1: Bedrock geology of the southern ENWRA project area (Burchett, 1986). ..... 6

Figure 2-2: Geologic time scale with lithostratigraphic sequence underlying Nebraska as defined by UNL-CSD (modified from Korus and Joeckel, 2011; Burchett, 1986; Condra and Reed, 1959). ..... 7

Figure 2-3: Generalized till thickness map of Quaternary deposits in the southern ENWRA project area (CSD, 2014). ..... 8

Figure 2-4: Geographic extent of the Midcontinent Rift in the central United States (Ojakangas, 2001; obtained from www.interstatefalls.org). ..... 14

Figure 2-5: Generalized map of structural features present beneath southeastern Nebraska (Burchett et al., 1985). The numbered features are: 1) Richfield Arch; 2) Denton Arch; 3) Union Fault, and 4) Burchard Fault. Note the Humboldt Fault Zone and the Forest City Basin are identified individually, and the outline of the extent of the Midcontinent Rift is identified by the area within the dashed line labeled "Midcontinent Geophysical Anomaly." ..... 14

Figure 2-6: Cross section modified from Korus et al. (2012) indicating locations of the Northern Bounding Fault and the Union Fault (red) in the Douglas-Saunders-Cass-Otoe County portion of the transect. The location of the cross section is identified in Figure 3-5 and the full transect is provided in Appendix 2. .. 15

Figure 2-7: Cross section across northern Kansas and southeastern Nebraska showing the Nemaha Uplift and the folded Paleozoic and Permian strata draped over the uplifted granite block (Carlson, 1971). .... 15

Figure 2-8: Depth to the Precambrian basement rock (in feet) in the southeast corner of Nebraska. ..... 16

Figure 2-9: Locations of known, mapped faults in the project area. The Thurman-Redfield Structural Zone (TRSZ) and the Nemaha Uplift Area are displayed in transparent orange shading. ..... 16

Figure 2-10: Map displaying the major streams and rivers within the southern ENWRA project area. .... 18

Figure 2-11: Mapped alluvial valley areas hosting alluvial aquifers in the southern ENWRA project area, modified from the Nebraska Groundwater Atlas (Korus et al., 2013b). ..... 19

Figure 2-12: Major paleovalleys in the southern ENWRA project area, modified from the Nebraska Groundwater Atlas (Korus et al., 2013b). ..... 20

Figure 2-13: Elevation of the groundwater surface in the southern ENWRA project area. Regional groundwater movement is from areas of higher groundwater elevations to lower elevations as displayed by the contours. ..... 21

Figure 2-14: Thickness contours of the *Kd* /Maha aquifer in eastern Nebraska (Ellis, 1984). The green area indicates where the *Kd* is the uppermost bedrock subcrop in eastern Nebraska (Burchett, 1986). Note that the contours and the extent of the *Kd* subcrop are from different map sources. Thus, there are mapped *Kd* intervals from the Nebraska bedrock geology map (Burchett, 1986) that exist east of the 0 ft thickness contour from Ellis (1984). ..... 25

Figure 2-15: Concentrations of calcium, chloride, sodium, and TDS (x-axis) in groundwater samples verses depth (y-axis). Data are from the USGS NWIS. ..... 28

Figure 2-16: Box and whiskers plots of major ions and nutrients concentrations of in groundwater samples by aquifer type across the southern ENWRA project area. Data are from the USGS NWIS. ..... 29

Figure 2-17: Public supply wells within the southern ENWRA project area. ..... 32

Figure 2-18: Registered wells in the southern ENWRA project area with depth to static water level indicated by color ..... 33

Figure 2-19: Progression of irrigation well development from the pre-1960s (upper left) to 2015 (lower right). Blue dots indicate existing wells, yellow dots indicate new wells constructed during the indicated decade (NDNR). ..... 34

Figure 3-1: Locations of CSD tests holes examined in the southern ENWRA project area. ..... 36

Figure 3-2: Locations of boreholes used containing lithologic information in the southern ENWRA project area. ..... 36

Figure 3-3: Locations of boreholes used containing stratigraphic information in the southern ENWRA project area. ..... 37

Figure 3-4: Locations of boreholes containing geophysical logs in the southern ENWRA project area. .... 37

Figure 3-5: Locations of geologic cross sections examined within the southern ENWRA project area. .... 39

Figure 3-6: Original cross section from CSD OFR 109 (left) and the digitized cross section (right). CSD test hole locations were used to orient images in 3D space. (Divine et al., 2010; Korus et al., 2012). Note that blank areas in the digitized cross section indicate where no lithologic information was available on the original cross section..... 40

Figure 3-7: Example 3D view of geo-referenced geologic cross sections used to supplement the AEM interpretation of the southern ENWRA project area..... 41

Figure 4-1: Schematic of an AEM survey. ..... 42

Figure 4-2: A) Example of a dB/dt sounding curve. B) Corresponding inverted model values. C) Corresponding resistivity earth model. ..... 43

Figure 4-3: Map of the expected utilities in the southern ENWRA project area. ..... 44

Figure 4-4: SkyTEM 508 frame including instrumentation locations and X and Y axes. ..... 45

Figure 4-5: Photos of the SkyTEM508 system on the ground (above) and in suspension beneath the helicopter (below). ..... 46

Figure 4-6: Flights lines as collected by date for the southern ENWRA project area. ..... 48

Figure 4-7: Example locations of EM coupling with pipelines or power lines. ..... 50

Figure 4-8: A) AEM data affected by coupling, shown in Figure 4-7, in Aarhus Workbench editor. The top group of lines is the Low Moment and the bottom is the High Moment. B) AEM data with area affected by coupling removed. ..... 50

Figure 4-9: A) Inversion results where AEM data affected by coupling with pipelines and power lines were not removed. B) Inversion results where AEM data affected by coupling were removed prior to inversion..... 51

Figure 4-10: Power Line Noise Intensity (PLNI) map of the southern ENWRA project area. ..... 52

Figure 4-11: Locations of inverted data along the AEM flight lines in the southern ENWRA project area. Red lines indicate where data was used in the inversion and black line segments indicate where data removed due to em coupling. ..... 52

Figure 4-12: Magnetic Total Field data corrected for diurnal drift, with IGRF removed. ..... 53

Figure 4-13: Regional magnetic Total Field data within the southern ENWRA project area boundary. Derived from Bankey et al. (2002). ..... 54

Figure 4-14: 3D magnetic field analytical signal calculated from the diurnal and IGRF corrected magnetic Total Field data. ..... 54

Figure 4-15: An example of an AEM profile illustrating the increase in model layer thickness with depth. ..... 56

Figure 4-16: Borehole resistivity logs compared with inverted AEM models. A: Well 1-A-68, 1,606 ft from the AEM line. B: Well 1-A-76, 1,478 ft from AEM line. C: Well 1-B-65, 1,867 ft from AEM line. D: Well 2-A-65, 1,699 ft from AEM line. ..... 58

Figure 4-17: Cross-plot of inverted resistivities compared with the resampled borehole resistivities for the 13 boreholes located within close proximity to the flight lines. ..... 58

Figure 4-18: Difference between data point residuals produced by SCIs with and without using the borehole conductivity data as a-priori information. Red indicates an improvement in the residuals by greater than 0.1. ..... 59

Figure 4-19: Data residuals distribution produced by the SCIs in the 10-mile recon lines both using the resistivity logs as a-priori and without them. ..... 59

Figure 4-20: Sample of AEM resistivity inversion model with the 0.1 DOI marked as grey dots at the bottom of the image. ..... 61

Figure 5-1: AEM flight lines with line numbers in the southern ENWRA project area. ..... 62

Figure 5-2: Color codes for aquifer materials, stratigraphy, and lithology used the interpretive profiles and 3D figures in this section and in the report appendices. ..... 63

Figure 5-3: Box and whisker plots for the resistivity ranges for the nine most common unconsolidated materials encountered in the Quaternary system. ..... 67

Figure 5-4: Histogram plot displaying the distribution of resistivities by major aquifer material color categories (blue- non-aquifer material, tan- marginal aquifer, yellow- principal aquifer, brown- sand-rich, coarse intervals of the principal aquifer). ..... 68

Figure 5-5: Pie charts of the distribution of material within each resistivity range for the 4 aquifer materials used in the interpretation of the AEM data- 0-12 ohm-m (left) and 12-20 ohm-m (right). ..... 69

Figure 5-6: Pie charts of the distribution of material within each resistivity range for the 4 aquifer materials used in the interpretation of the AEM data- 20-50 ohm-m (left), and 50 ohm-m (right) and above ..... 69

Figure 5-7: Pie chart of the overall lithology indicated in the 58 e-logs used to characterize the relationship of lithology and resistivity in the project area. ..... 70

Figure 5-8: Pie charts showing overall percentage of lithologies in selected CSD test holes in the southern ENWRA project area. ..... 71

Figure 5-9: Histogram of the distribution of the fractional difference in the thickness of the principal aquifer materials using 20 and 21 ohm-m resistivity thresholds. ..... 72

Figure 5-10: Example cross section illustrating the small difference between selecting a 20 ohm-m threshold or a 21 ohm-m threshold to define the principal aquifer. The solid black line enclosing the yellow (principal aquifer material) represents the 20 ohm-m threshold and the dotted black line enclosing the principal aquifer material represents the 21 ohm-m threshold. ..... 73

Figure 5-11: Box and whiskers plot of the resistivity distribution of the Tertiary, Cretaceous and Paleozoic bedrock units discussed in the interpretation of the AEM data..... 74

Figure 5-12: Deep oil and gas borehole resistivity logs compared with inverted AEM models. A: Well 2616719000, 5,186 ft from the AEM line, B: Well 2616721003, 12,838ft from AEM line. ..... 75

Figure 5-13: Box and whisker plot for the major lithologic texture categories within the *Kd* from CSD e-logs located across the entire ENWRA project area. ..... 76

Figure 5-14: Resistivity count distribution by major grain size category for CSD test holes screened in the *Kd*. Plot A (top) represents all coarse unconsolidated and consolidated deposits; plot B (middle) represents all unconsolidated and consolidated fines, and plot C (bottom) represents a composite of both coarse and fine materials, color coded by the ranges of 0-20, 20-40, and 40 ohm-m and above used in the interpretive figures of the *Kd* beneath the ENWRA project area. ..... 77

Figure 5-15: A northward view of the 3D hydrostratigraphic framework of the southern ENWRA project area, including geologic materials ranging from Quaternary deposits to Paleozoic bedrock. See Figure 5-2 for the color codes of the materials and geologic strata displayed. ..... 80

Figure 5-16: An eastward view of the 3D hydrostratigraphic framework of the southern ENWRA project area. See Figure 5-2 for the color codes of the materials and geologic strata displayed..... 81

Figure 5-17: A westward view of the 3D hydrostratigraphic framework of the southern ENWRA project area. See Figure 5-2 for the color codes of the materials and geologic strata displayed..... 81

Figure 5-18: 3D representation of shallow subsurface resistivity intervals of 8 ohm-m or less and at the land surface near the north side of the city of Lincoln in the LPSNRD. ..... 88

Figure 5-19: Profile of conductivity (in Siemens/m) within the *Kd* along flight line 300302. The conductivity profile is from a depth at the top of the low resistivity interval within the *Kd*. ..... 89

Figure 5-20: Profile of conductivity (in Siemens/m) at the land surface along the Little Salt Creek drainage in the LPSNRD exhibiting areas of high TDS water in areas underlain by low-resistivity *Kd*. ..... 89

Figure 5-21: 3D and 2D representations of regionally extensive, low-resistivity zones revealed in the southern ENWRA AEM survey. The gray surface demarcates the top of the Paleozoic system. ..... 90

Figure 5-22: AEM profile 401101 displaying the Nemaha Uplift area on the left and Union Fault within the Paleozoic system. Note the resistivity color scale ranges from 10 to 70 ohm-m. ..... 92

Figure 5-23: AEM profile 301501 displaying the Nemaha Uplift/Elk Creek Carbonatite and the Humboldt Fault within the Paleozoic system. Note the resistivity color scale ranges from 3 to 60 ohm-m. ..... 92

Figure 5-24: AEM profile 301101 displaying the presence of the Humboldt Fault within the Paleozoic system. Note the resistivity color scale ranges from 7 to 70 ohm-m. ..... 93

Figure 5-25: AEM profile 400901 and CSD cross section on the LPNNRD-PMRNRD boundary displaying the Northern Bounding Fault beneath the Platte River valley. Note the resistivity color scale ranges from 10 to 70 ohm-m. ..... 93

Figure 5-26: AEM profile 400803 in the western NNRD showing the western extent of the Union Fault in the Paleozoic system. Note the resistivity color scale ranges from 4 to 50 ohm-m. ..... 94

Figure 5-27: Northwestward view of the southern ENWRA project area displaying the locations of historic and contemporary CSD geologic cross sections. The color scale is shown in Figure 5-2. ..... 96

Figure 5-28: Northeastward view of the southern ENWRA project area displaying the locations of historic and contemporary CSD geologic cross sections. The color scale is shown in Figure 5-2. ..... 97

Figure 5-29: Combined display of AEM data (top panel), hydrostratigraphic interpretation (middle panel), and CSD cross section (bottom panel) for a section of flight line 201001 in the southeastern half of the LPNNRD. The location of the AEM flight line and CSD cross section is displayed on the top pane to the right. ..... 98

Figure 5-30: Close-in view of CSD test hole 8-A-54 along a segment of the southern extent of AEM flight line 201001 in the LPNNRD, demonstrating the thin intervals of material indicated in the test hole logs that correspond to only the averaged resistivity data across intervals of greater thickness. ..... 99

Figure 5-31: Combined display of AEM data (top panel), hydrostratigraphic interpretation (middle panel), and CSD cross section (bottom panel) for flight line 400901 near Ashland, NE. The location of the AEM flight line and CSD cross section is displayed on the panel to the right. ..... 100

Figure 5-32: Combined display of AEM data (second panel), hydrostratigraphic interpretation (third panel), and CSD cross section (bottom panel) for flight lines 300701 and 300702 which cross the LPSNRD from west to east. The location of the AEM flight line and CSD cross section is displayed in the top panel. ..... 101

Figure 5-33: Flight lines within the LPNNRD acquired in the both phases of the ENWRA AEM survey. .. 103

Figure 5-34: 3D hydrogeologic framework from the reconnaissance AEM survey within the LPNNRD using flight lines from both the Fall 2014 and Spring 2015 AEM surveys. Vertical exaggeration is 60x. . 103

Figure 5-35: A northwestward view of the 3D hydrostratigraphic framework interpretation in the LPNNRD displaying the hydrogeologic character of the Platte River valley. Terrace features are marked with a white “T”, and the incised valley in flight line 201301 is marked with a white “V.” Vertical exaggeration is 60x. ..... 105

Figure 5-36: AEM flight line 300101 across the center of the southeastern half of the LPNNRD. West is on the left, east to the right. The 1995 water level surface is displayed as a blue dashed line. The blue fill indicates undifferentiated Paleozoic strata. ..... 107

Figure 5-37: AEM flight line 400501 across the south central section of the southeastern half of the LPNNRD. South is on the left, north to the right. The 1995 water level surface is displayed as a blue dashed line. The blue fill indicates undifferentiated Paleozoic strata. ..... 108

Figure 5-38: Flight lines within the LPSNRD acquired in the second phase of the ENWRA AEM survey. 111

Figure 5-39: 3D hydrogeologic framework from the reconnaissance AEM survey only within the LPSNRD. Vertical exaggeration is 30x. ..... 112

Figure 5-40: Hydrogeologic interpretation of AEM profile 300701 west of Lincoln in the LPSNRD. ..... 113

Figure 5-41: Hydrogeologic interpretation of AEM profile 400801 northeast of Lincoln in the LPSNRD. The blue dashed line is the 1995 CSD regional water table surface and the solid blue color is undifferentiated Paleozoic strata. ..... 114

Figure 5-42: Hydrogeologic interpretation of AEM profile 300702 east of Lincoln in the LPSNRD. The blue dashed line is the 1995 CSD regional water table surface and the solid blue color is undifferentiated Paleozoic strata. ..... 114

Figure 5-43: Eastward view of the3D hydrogeologic framework of the southern LPSNRD showing principal aquifer materials of the Dorchester-Sterling paleovalley aquifer. Vertical exaggeration is 30x. ..... 116

Figure 5-44: Flight lines within the NNRD acquired in the ENWRA AEM survey. ..... 118

Figure 5-45: 3D hydrogeologic framework from the reconnaissance AEM survey only within the NNRD. ..... 118

Figure 5-46: Close-in view of the paleovalley system in the northwest NNRD. Vertical exaggeration is 50x. ..... 120

Figure 5-47: View of flight line 400803 displaying the Dorchester-Sterling paleovalley on the south side (left) of the profile. ..... 121

Figure 5-48: AEM profile of flight line 301301 displaying the confluence of two paleovalleys in northeastern Johnson County. ..... 121

Figure 5-49: Flight line from AEM profile 401401 in the eastern NNRD. ..... 122

Figure 5-50: Flight lines within the UBBNRD acquired in the second phase of the ENWRA AEM survey. 124

Figure 5-51: Flight lines within the LBBNRD acquired in Phase 2 of the ENWRA AEM survey. ..... 124

Figure 5-52: AEM profile of flight line 400101 in the northeastern corner of the UBBNRD. ..... 125

Figure 5-53: AEM profile of flight line 400303 in the northern LBBNRD. See Figure 5-2 for the strata color coding. ..... 125

Figure 5-54: Locations of prior study airborne geophysical survey studies in the southern ENWRA project area. ..... 127

Figure 5-55: Locations where inversion results between surveys were compared. ENWRA Fall 2014 and Spring 2015 were compared at points A and B. The compared models at point A were 252 ft apart and 601 ft at point B. ENWRA Spring 2015 were compared with the Dwight-Valparaiso-Brainard 2014 flights at points C, D, and E. The compared models were 77 ft, 48 ft, and 110 ft apart, respectively. ..... 127

Figure 5-56: Comparison of inverted model results between ENWRA 2015 and ENRWA 2014 at two locations. Depths of investigations for each survey are shown. ..... 128

Figure 5-57: Comparison of inverted models between the ENWRA 2015 survey and the Dwight-Valparaiso-Brainard surveys. ..... 130

## List of Tables

Table 2-1: Aquifers in Quaternary to Cretaceous stratigraphic units beneath eastern Nebraska. ..... 22

Table 2-2: Statistical results of water-quality analyses from groundwater samples collected in or near the project area, from all aquifer sources. Units in milligrams per liter unless stated otherwise. Data are from the USGS NWIS, Lower Platte North NRD, and Nemaha NRD (NA- not analyzed; N- number of samples). ..... 28

Table 2-3: Statistical results of water quality analyses from groundwater samples collected in or near the project area, from Quaternary surficial aquifer wells. Units are in milligrams per liter unless stated otherwise. Data are from the USGS NWIS, Lower Platte North NRD, and Nemaha NRD (NA- not analyzed; N- number of samples). ..... 30

Table 2-4: Statistical results of water quality analyses from groundwater samples collected in or near the project area from bedrock aquifer wells. Units are in milligrams per liter unless stated otherwise. Data are from the USGS NWIS, Lower Platte North NRD, and Nemaha NRD (NA- not analyzed; N- number of samples). ..... 31

Table 3-1: Geologic cross sections from OFR-109 that were digitized and geo-referenced (Divine et al., 2010; Korus et al., 2012). ..... 38

Table 4-1: Positions of instruments on the SkyTEM508 frame, using the center of the frame as the origin in feet. ..... 46

Table 4-2: Positions of the SkyTEM508 transmitter coil corners, using the center of the frame as the origin in feet. ..... 46

Table 4-3: Locations of magnetic field base station instruments. ..... 46

Table 4-4: Airports and state parks used for landing and refueling by date of acquisition. ..... 47

Table 4-5: Production log displaying the number of production flights conducted each day and total line miles and kilometers surveyed. A limited number of flight lines did overlap. ..... 48

Table 4-6: Thickness and depth to bottom for each layer in the SCI inverted AEM models. The thickness of the model layers increase with depth as the resolution of the AEM technique decreases. ..... 55

Table 4-7: List of wells with borehole resistivity logs used as a-priori information for the SCI. ..... 57

Table 6-1: Channel name, description, and units for EM_20150428_Nebraska_Final01.xyz with EM, mag, DGPS, Inclinometer, altitude, and associated data. ..... 144

Table 6-2: Channel name, description, and units for ENWRA2015_SCI_Results.xyz with EM inversion results. ..... 145

Table 6-3: Files containing borehole information. ..... 146

Table 6-4: Channel name, description, and units for collar files. ..... 146

Table 6-5: Channel name description and units for borehole data. ..... 147

Table 6-6: Channel name description and units for the interpretation results file. ..... 148

## List of Abbreviations

| | |
|---|---|
| 1D | One-dimensional |
| 2D | Two-dimensional |
| 3D | Three-dimensional |
| A* $m^2$ | Ampere meter squared |
| AEM | Airborne Electromagnetic |
| Bgl | Below Ground Level |
| dB/dt | Change in amplitude of magnetic field with time |
| CSD | Conservation and Survey Division, Nebraska Geological Survey |
| DOI | Depth of Investigation |
| DGPS | Differential global positioning system |
| em, EM | Electromagnetic |
| ENWRA | Eastern Nebraska Water Resources Assessment |
| FDHEM | Frequency-Domain Helicopter Electromagnetic |
| Ft | Feet |
| Ft/d | Feet per day |
| $Ft^2/d$ | Feet squared per day |
| $Ft^3/s$ | Cubic feet per second |

| | |
|---|---|
| GIS | Geographic Information System |
| gpd/ft | Gallons per day per foot |
| GX | Geosoft executable |
| HEM | Helicopter Electromagnetic |
| IGRF | International Geomagnetic Reference Field |
| in/yr | Inches per year |
| *Kc* | Carlile Formation |
| *KcKgg* | Carlile & Greenhorn-Graneros Formations |
| *Kd* | Dakota Formation |
| km | Kilometers |
| LCI | Laterally-Constrained Inversion |
| LBBNRD | Lower Big Blue Natural Resources Dsitrict |
| LPNNRD | Lower Platte North Natural Resources District |
| LPSRD | Lower Platte South Natural Resources District |
| MAG | Magnetic (data); Magnetometer (instrument) |
| MCG | Minimum curvature gridding |
| mg/L | Milligrams per liter |
| mi | Miles |
| $mi^2$ | Square miles |
| Ma | Megaannus (Million years) |
| µS/cm | Microsiemens per centimeter |
| NAD83 | North American Datum of 1983 |
| NDNR | Nebraska Department of Natural Resources |
| NNRD | Nemaha Natural Resources District |
| NRD | Natural Resources District |
| NOGCC | Nebraska Oil and Gas Conservation Commission |
| NWIS | National Water Information System |
| OM | Oasis montaj |
| PFC | Primary Field Compensation |
| PLNI | Power Line Noise Intensity |
| PMRNRD | Papio-Missouri River Natural Resources District |
| Rx | Receiver |
| SCI | Spatially-Constrained Inversion |
| STD | Standard Deviation |
| TDS | Total Dissolved Solids |
| TEM | Transient Electromagnetic |
| TDEM | Time-Domain Electromagnetic |
| TRSZ | Thurman-Redfield Structural Zone |
| Tx | Transmitter |
| UBBNRD | Upper Big Blue Natural Resources District |
| USGS | United States Geological Survey |
| UTM | Universal Transverse Mercator |
| $V/m^2$ | Volts per meter squared |
| XRI | Exploration Resources International |

# 1 Introduction

## 1.1 Purpose of Project

Sound management of groundwater and surface water in eastern Nebraska has become increasingly important in recent years. There are expanding pressures placed on the resource by the ever growing demands for agricultural production, population growth and urbanization, potential contamination from natural and anthropogenic sources, industrial needs, and the persistent threat of drought. The combination of these stresses on water resources has increased the need for detailed hydrogeologic frameworks of the subsurface.

This report describes the findings of the second phase of an airborne electromagnetic (AEM) investigation conducted across several natural resource districts (NRDs) that are part of the Eastern Nebraska Water Resources Assessment (ENWRA) in eastern Nebraska. This phase, with data acquisition conducted in April 2015, covered the southern half of the ENWRA area (Figure 1-1), and hereafter will be referred in this report as the "southern ENWRA project area." The AEM survey data were collected along reconnaissance (recon) lines with various spacing and orientations from the northernmost extent of the Platte River valley to the Nebraska-Kansas border and from the Polk-Butler County line eastward to the Missouri River valley. The AEM survey in the second phase of flights included parts of four NRDs participating in ENWRA- the Papio-Missouri River (PMRNRD), the Lower Platte North (LPNRD), the Lower Platte South (LPSNRD), and Nemaha (NNRD). Additionally, AEM data were acquired in limited sections of the Upper Big Blue and Lower Big Blue NRDs. For organizational purposes, this report (Volume II) formally discusses the findings of the AEM survey for the LPNNRD, LPSNRD, and the NNRD, although some inclusion of the PMRNRD occurs due to the northern extent of the phase II flight lines (see Volume I of this report for a full discussion of the AEM survey findings in the PMRNRD).

In addition to the AEM data acquired during this investigation, data and findings from previous studies, along with geologic descriptions and geophysical logs from University of Nebraska-Lincoln Conservation and Survey Division (CSD) and Nebraska Oil and Gas Conservation Commission test holes (NOGCC) were utilized to develop the hydrogeologic framework of the region.

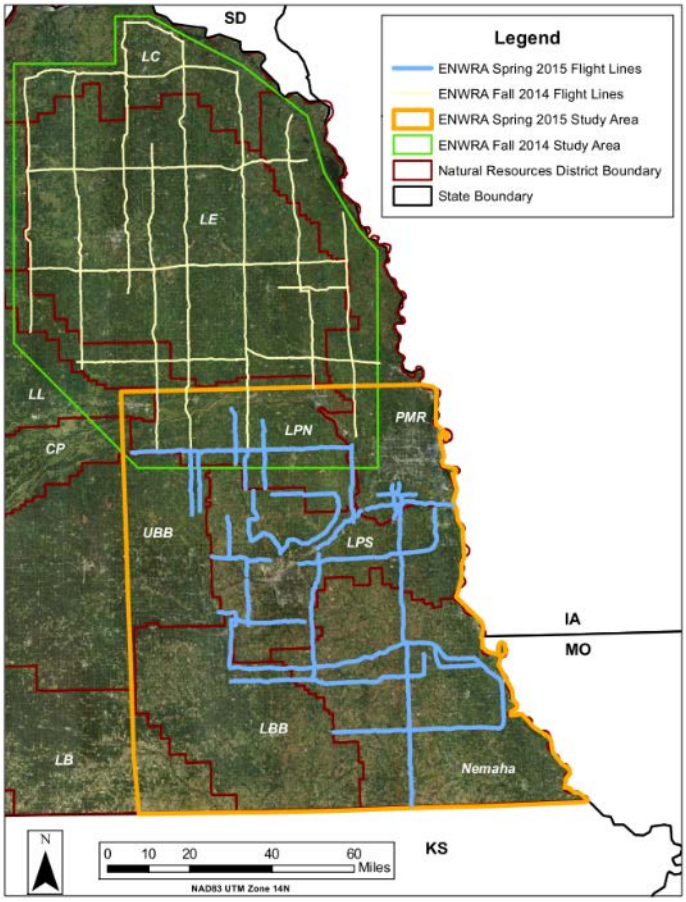



**Figure 1-1: Map of ENWRA project area, with the southern extent of the survey area (Phase II) and flight lines highlighted in bolded orange and blue, respectively. The northern half of the project area (Phase I) is outlined in green. NRD boundaries are shown in red with individual NRD initials shown in white.**

## 1.2 Previous Work

The use of AEM technology to map and evaluate groundwater resources has gained momentum over the last 20 years in the United States and abroad. The state of Nebraska has been on the forefront of implementing AEM for water resources management over the last decade with projects across the state in a variety of geologic settings. In recent years, ENWRA has coordinated efforts between area Natural Resources Districts (NRDs), CSD, the U.S. Geological Survey (USGS), the Nebraska Department of Natural Resources (NDNR), and Exploration Resources International Geophysics, LLC (XRI) in support of several projects designed to characterize glacial outwash and buried paleovalley aquifers across the eastern part of the state.

In March 2007, AEM methods were implemented to characterize the hydrogeologic conditions in the Platte River valley near Ashland, NE, as well as in areas underlain by glacial till near Firth and Oakland, NE (Abraham et al., 2011; Korus et al., 2013a). In the following years, individual reports utilizing the AEM data collected in 2007 were released by the USGS and CSD. In 2009, a multi-faceted investigation incorporating the 2007 AEM data and 2009 ground-based geophysical techniques was conducted by the

USGS to characterize the hydrogeologic setting near Oakland, NE. In 2009, the Lower Platte South NRD funded development of a three-dimensional (3D) hydrostratigraphic framework of the subsurface near Swedeburg, NE based on an AEM survey. Also in 2009, the Lower Platte South NRD (LPSNRD) funded a similar investigation of the hydrostratigraphy near Sprague, NE (Smith et al., 2009; Divine and Korus, 2012).

In 2013, the LENRD funded XRI to conduct an AEM survey near the towns of Clarkson and Howells, NE to characterize the extent of the Quaternary aquifer beneath the area following the 2012 drought (Abraham et al., 2013). Also in 2013, XRI completed an AEM survey covering over 800 line-miles in Butler and Saunders counties northwest of the city of Lincoln, NE (Carney et al., 2014). This survey revealed extensive, buried paleovalley aquifers beneath thick sequences of till. Additionally, intervals of Cretaceous bedrock units were revealed in the survey. In the fall of 2014, XRI conducted an AEM survey of nearly 1,500 line-miles across a subsection of the LENRD at a three mile flight line spacing to assess the general hydrogeologic character of the subsurface and upper bedrock in the northwest portion of the district and to investigate the appropriate length of flight line spacing for conducting airborne investigations in the glaciated terrain of eastern Nebraska. The survey revealed the subsurface character to depths beyond 1,200 ft in this investigation (Exploration Resources International, 2015). Also, a survey was conducted in conjunction with the LENRD survey of the northern half the ENWRA project area at a grid spacing ranging from 10-20 miles. Findings of this survey are described in Volume I of this report. This body of work exemplifies how AEM surveys of the glacial terrain of eastern Nebraska have followed a progressive, long-term plan spanning nearly eight years, and each project shows continuing advancements in the science and application of AEM to support groundwater management.

## 1.3 Description of Project Area

The approximately 8,894 square-miles ($mi^2$) of the southern ENWRA project area (Figure 1-2) lie within southeast Nebraska and overlies five of Nebraska's eight topographic regions—Plains, Rolling Hills, Bluffs and Escarpments, Valley-Side Slopes, and Valleys (Conservation and Survey Division, 1951). The elevation of the area, presented in Figure 1-3, ranges from 835 ft to over 2,200 ft above sea level**.** The surface topography of the area is generally rolling hills dissected by south and southeastward oriented drainages, with broad floodplains associated with the Platte River on the north and the Missouri River on the east.

Omaha and Lincoln are the two largest cities within or near the project area (Omaha is adjacent to the northeastern extent of the flight lines). The estimated 2010 population of Nebraska (1.8 million) shows that collectively Omaha (population 408,958) and Lincoln (population 258,379), the two largest cities in the state, comprise 36% of Nebraska's total 2010 population (Nebraska Department of Economic Development, 2014). First Class cities (populations of 5,000 to 100,000) within the project area are Bellevue (50,137) and Papillion (18,894), Nebraska City (7,289) and Plattsmouth (6,502) (U.S. Census Bureau, 2015). Bellevue and Papillion, like Omaha, lie outside the AEM flight areas. Second Class cities (populations 800 to 5,000) with 2010 population estimates of at least 1,500 inhabitants include Wahoo (4,508), Gretna (4,441), Auburn (3,460), Ashland (2,453), and Tecumseh (1,677). The total population of these first and second class cities totals nearly 100,000 inhabitants (Nebraska Department of Economic Development, 2015; U.S. Census Bureau, 2015).

Beyond the developed urban areas, land use/land cover within the project area is primarily agricultural, including irrigated and non-irrigated corn, soybeans, and alfalfa. Secondary land use is mostly rangeland, pastureland, and grasslands, urban areas, riparian forest, and woodlands (CALMIT, 2007). Center-pivot irrigation is the primary groundwater irrigation method within the project area, using approximately 11,900 registered irrigation wells (NDNR). Section 2.5 of this report includes further discussion on groundwater use and the history of irrigation well development in the southern ENWRA project area.

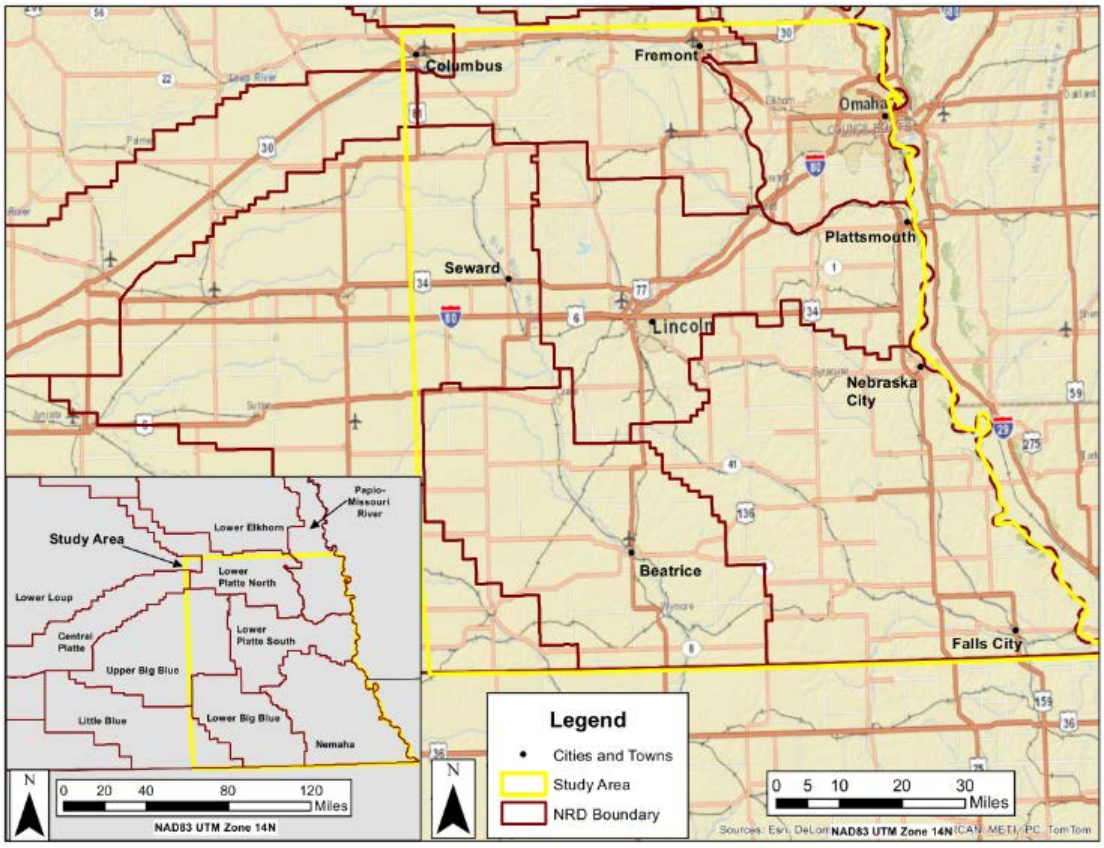



**Figure 1-2: Map of the southern ENWRA project area, including the largest cities and major roads within the study area. NRD boundaries are displayed in the insert map.**

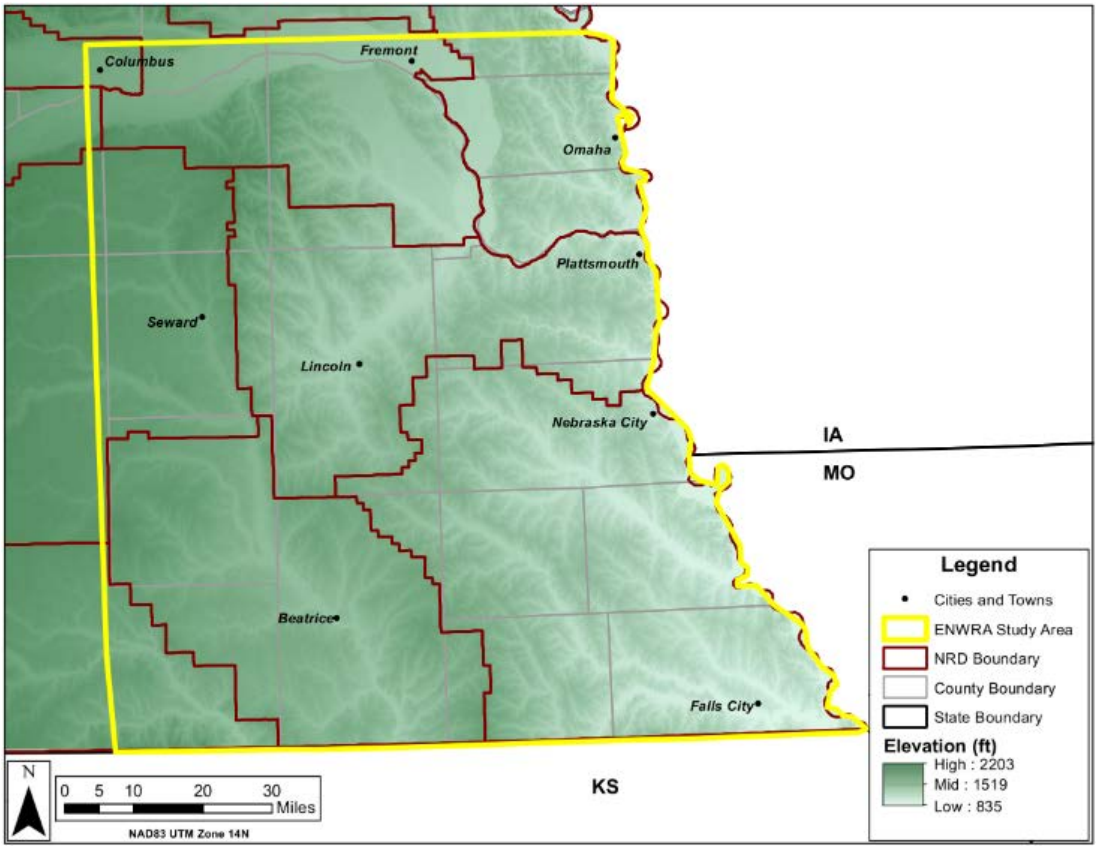



**Figure 1-3: Land surface elevation and topographic expression of the southern ENWRA project area.**

# 2 Project Area Hydrogeology

## 2.1 Geologic Setting

Bedrock geology in the project area is comprised of late Paleozoic and Cretaceous deposits (Figure 2-1). Cretaceous deposits underlie the northwestern half of the southern ENWRA project area, and Paleozoic deposits underlie the entire area. Within the Paleozoic sequence, Pennsylvanian deposits include the Marmaton, Pleasanton, Kansas City, Lansing, Douglas, Shawnee, and Wabaunsee Groups. Overlying these units are the Permian Admire, Council Grove, and Chase Groups. For purposes of this report, only undifferentiated Paleozoic strata are identified in the AEM interpretations. Collectively, these Paleozoic deposits subcrop in most of the eastern part of the project area and unconformably lie below the Cretaceous units in the northwestern part of the project area. Some outcrops of Paleozoic units occur in the LPSNRD and NNRD, mostly along surface drainages. Deeper units from the Mississippian through Cambrian periods are present, but are not discussed in detail as they are typically beyond the depth of investigation of the AEM system.

Cretaceous bedrock units in the project area include the Niobrara Formation, the Carlile Shale, the Greenhorn-Graneros Formations, which underlie only a small section of the northwestern corner of the southern ENWRA project area, and the Dakota Formation, which is present beneath the LPNNRD and most of the LPSNRD. Some intervals of the Dakota Formation can locally yield potable water and are

considered a secondary aquifers in Nebraska (Divine et al., 2009). This unit will be discussed in greater detail in following sections of this report.

Figure 2-2 displays the geologic time scale with CSD's lithostratigraphic sequence that underlies the state modified from Korus and Joeckel (2011).

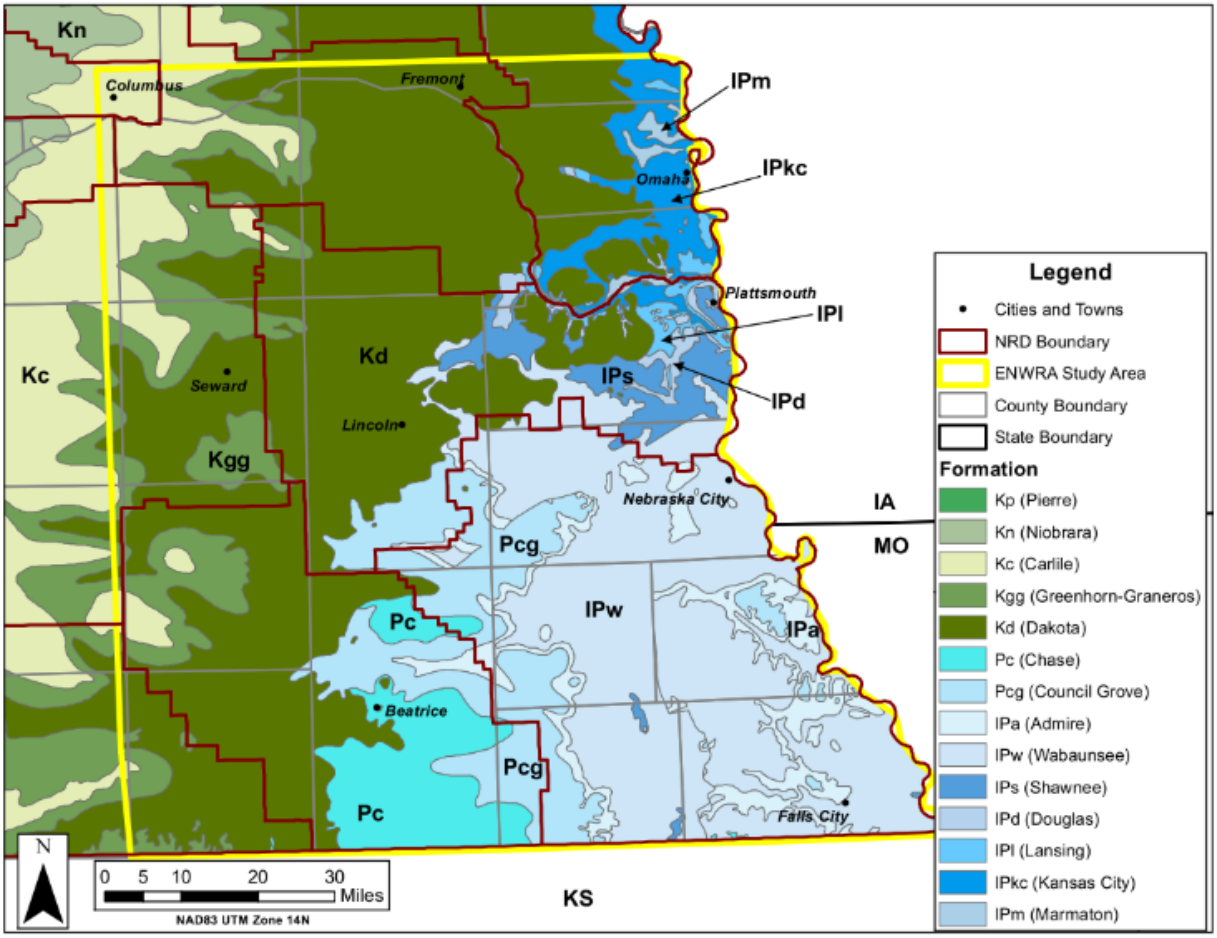



**Figure 2-1: Bedrock geology of the southern ENWRA project area (Burchett, 1986).**

| Age (Ma) | Era | Period | | Epoch | Lithostratigraphy | Lithology | Max Thickness (ft) | Lith/ Strat Color Code |
|---|---|---|---|---|---|---|---|---|
| 0.01 | Cenozoic | Quaternary | | Holocene | DeForest Fm, other units | dune sand, alluvium | NA | |
| | | | | Pleistocene | Peoria Loess | loess (silt) | 35 | |
| | | | | | Gilman Canyon Fm. | loess (silt) | 5 | |
| | | | | | Loveland Loess | loess (silt) | 25 | |
| | | | | | Kennard Fm. | loess (silt) | 25 | |
| | | | | | Pre-Illinoian glacial deposits | till, outwash, fines | >400 | |
| 2.6 | | Tertiary (*T*) | Neogene | Pliocene | Broadwater Fm, corr. units | sand and gravel | 70 | |
| 5.3 | | | | Miocene | Ogallala Group (*To*) | sand, sandstone, silt, siltstone, gravel, caliche | 650 | |
| 23 | | | Paleogene | Oligocene | *Only unnamed units in NE Nebraska identified in early Eocene* | sandstone & conglomerate | NA | |
| 33.9 | | | | Eocene | | | | |
| 55.8 | | | | Paleocene | | | | |
| 65.5 | Mesozoic | Cretaceous (*K*) | | Late Cretaceous | *Upper Late Cretaceous units absent* | | | |
| | | | | | Pierre Shale (*Kp*) | shale, shaly chalk, siltstone, sandstone | 1,970 | |
| | | | | | Niobrara Fm (*Kn*) | shaly chalk, limestone | 570 | |
| | | | | | Carlile Shale (*Kc*) | shale, minor sandstone | 300 | |
| | | | | | Greenhorn Limestone & Graneros Shale (*Kgg*) | limestone, shale | 60 | |
| 99.6 | | | | Early Cretaceous | Dakota Group (*Kd*) | sandstone, conglomerate, siltstone, mudstone, shale | 600 | |
| | | | | | *Lower Early Cretaceous units absent* | | | |
| 251 | Paleozoic | Permian (*P*) | | | Chase Group | limestone, evaporites, shale | 300 | |
| 299 | | | | | Council Grove Group | | 300 | |
| | | Carboniferous | Pennsylvanian (*IP*) | | Admire Group | limestone, shale, mudstone, sandstone | 150 | |
| | | | | | Wabaunsee Group | | 300 | |
| | | | | | Shawnee Group | | 200 | |
| | | | | | Douglas Group | | 100 | |
| | | | | | Lansing Group | | 75 | |
| | | | | | Kansas City Group | | 200 | |
| | | | | | Pleasanton Group | | 40 | |
| | | | | | Marmaton Group | | 125 | |
| | | | | | Cherokee Group | | 300 | |
| 318 | | | Mississippian (*M*) | | Osage-Meramec, Kinderhook Groups | limestone, shale, dolomite, siltstone, chert | 500 | |
| 359 | | Devonian | | | *Strata only subcrops in Nebraska, generally below investigative depth of AEM system* | | 560 | |
| 416 | | Silurian | | | | | 450 | |
| 444 | | Ordovician | | | | | >600 | |
| 488 | | Cambrian | | | Elk Creek Carbonatite | intrusion complex | NA | |
| 542 | Precambrian | | | | | | | |

**Figure 2-2: Geologic time scale with lithostratigraphic sequence underlying Nebraska as defined by UNL-CSD (modified from Korus and Joeckel, 2011; Burchett, 1986; Condra and Reed, 1959).**

### *2.1.1 Surficial Geology*

The complex Pleistocene and Holocene (Quaternary) geology in southeast Nebraska consists of myriad sequences of clay, silt, till, sand, and gravel overlying bedrock units. These deposits are capped by loess at many locations across the region. The surficial geology of the project area is typical of western mid-continental glaciated areas of North America where buried Quaternary sand and gravel glacial outwash deposits or paleovalleys comprised of unconsolidated Plio-Pleistocene sand and gravel units underlie vast areas of glacial till. In most areas of southeast Nebraska, including the project area, glacial till often underlies loess units (e.g., Peoria, Gillman Canyon Formation, and Loveland Loess). Present day surface water systems have incised the loess and till units such that in some locations wide stream valleys exist (e.g., Platte River valley).

CSD test hole records and drillers logs obtained from NDNR indicate glacial till and loess deposits are prevalent across the project area and make up the majority of the surficial geology (Figure 2-3). These units, which can exceed 200 ft in thickness, serve as the upper confining units to hydrogeologically confined units such as buried paleovalley aquifers. These till deposits vary and thin southward typically, to thicknesses of less than or near 100 ft at many locations. These deposits also inhibit or dampen recharge to groundwater systems because of low permeability of the clay within the till.

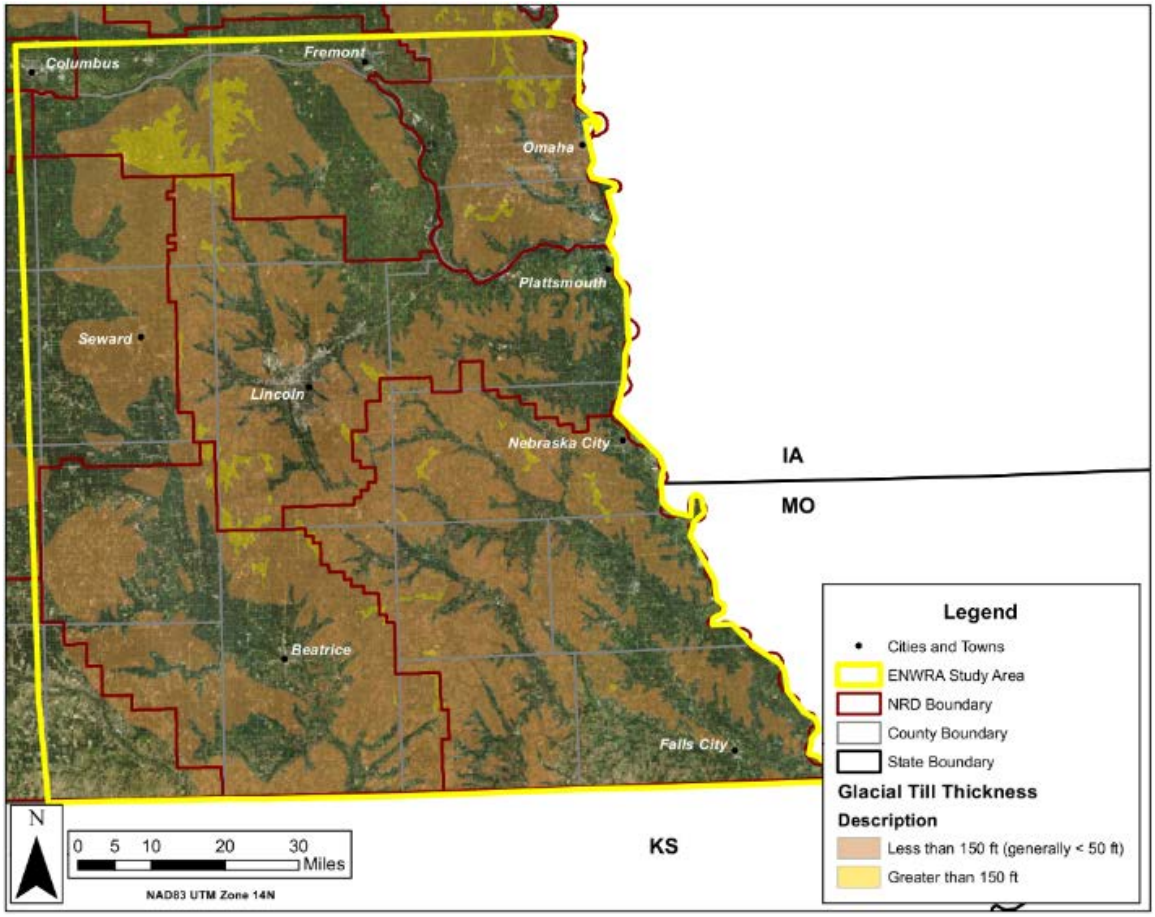



**Figure 2-3: Generalized till thickness map of Quaternary deposits in the southern ENWRA project area (CSD, 2014).**

Unconsolidated sand and gravel (glacial outwash) of Plio-Pleistocene age occupy paleovalleys that sit unconformably on the erosional surface of Cretaceous or Paleozoic bedrock. It should be noted that the topography of the bedrock surface undulates across the project area and shows appreciable relief in some locations, particularly areas where paleovalleys are carved into the consolidated sedimentary strata. Thicknesses of the sand and gravel deposits vary by location but can be over 5 miles wide and 200 ft thick (Tanner and Steele, 1991). The paleovalley units "are not well constrained and may be preglacial, synglacial, or inter-glacial in origin" (Gates et al., 2014). Moreover, the paleovalley units underlying thick till sequences in eastern Nebraska in some cases can be greater than 6 mi wide, 62 mi long, (Gates et al., 2014) and up to 200 ft thick (Fredrick et al., 2006). Locally, CSD test holes indicate that the sand and gravel units are typically not clean but interlayered with silts and clays. The paleovalleys are overlain by fine-grained glacial deposits intermixed with local sand and gravel lenses. Most glacial deposits are overlain by loess deposits that are 30-40 ft thick and thin to the west (Tanner and Steele, 1991). Certain paleovalleys in eastern Nebraska extend eastward (Divine et al., 2009) and some paleovalleys trend southeastward (Condra and Reed, 1959, pg. 9). Hence, easterly to southeasterly trends for paleovalley aquifers in eastern Nebraska appear to be the most common orientation of these features.

### *2.1.2 Tertiary Geology*

The Ogallala Group (*To*) is present only in the northern half of the ENWRA project area and does not extend into the southern area discussed in this report. However, *To* is present beneath the far northwestern section of the LPNNRD, which is included in the interpretive analysis of this report. For further description of the *To*, see section 2.1.2 in Volume I of this report. No other Tertiary deposits are noted to be present within the southern ENWRA project area flight coverage.

### *2.1.3 Cretaceous Geology*

Cretaceous deposits within the project area include the Carlile Shale (*Kc*), the Greenhorn-Graneros Formations (*Kgg*) and the regionally extensive Lower Cretaceous Dakota Formation (*Kd*) (also commonly referred to as the "Dakota Sandstone"). The *Kd* underlies approximately the northwestern half of the southern ENWRA area, and in the extreme western sections of the project area, the formation lies unconformably beneath Upper Cretaceous deposits. Across the rest of the *Kd*'s extent in eastern Nebraska, the unit lies unconformably beneath unconsolidated Quaternary deposits. The *Kd* is comprised primarily of massive to interbedded sandstone with ironstone and shale, and some argillaceous to slightly sandy beds (Condra and Reed, 1959). Sandstone in the *Kd* typically has low permeability and storage compared to unconsolidated units overlying it. However, a hydraulic connection can exist in locations where the *Kd* is in contact with overlying saturated Quaternary deposits, allowing for a secondary source of groundwater storage (Gutentag et al., 1984). Locally the *Kd* can serve as the primary groundwater source to irrigation, municipal, or domestic wells. In some areas, the Quaternary system and the *Kd* are included within the same well and are screened across both intervals for water supply production. In some locations along the Platte River valley and other associated tributary surface drainages within the southern ENWRA project area, the *Kd* outcrops along hillsides (Burchett et al., 1972; Burchett et al., 1975; Joeckel and Dillon 2005; Mason and Joeckel, (2002);

Hanson et al., 2012; Korus et al., 2014). These areas are revealed in some of the AEM profiles displayed in the interpretive sections of this report.

### *2.1.4 Jurassic and Triassic Geology*

Strata considered correlating with Jurassic and Triassic deposits have been identified in cuttings in western Nebraska. However, these units are not known to exist in eastern Nebraska (Condra and Reed, 1959).

### *2.1.5 Paleozoic System*

Paleozoic strata forms the uppermost bedrock beneath the southeastern half of the project area and lie unconformably beneath Quaternary deposits. In the northwestern half of the southern ENWRA survey area, these units are situated unconformably beneath the *Kd*. The Paleozoic system is primarily composed of alternating carbonates and clastic materials. At numerous locations in the southern ENWRA project area, particularly within the NNRD, outcrops of Paleozoic strata exist along hillsides and drainages (Burchett et al., 1972; Burchett et al., 1975; Joeckel and Dillon (2000); Korus et al., 2014). Although historic cross sections and lithologic logs from deep oil and gas wells could allow for the identification of Paleozoic units in limited locations of the southern ENWRA project area, it was determined by XRI that insufficient information was available to characterize the individual formations as revealed by the AEM. Thus, strata are identified in the following subsections by geologic period, but all Paleozoic units are undifferentiated in the interpretive analysis for this report.

#### *2.1.5.1 Permian Geology*

Permian deposits in Nebraska are extensive in the southern and western parts of the state (Burchett, 1982). Some Permian formation outcrops are present in southeast Nebraska, but all are mostly absent in the northern parts of the project area (Burchett, 1982, 1983; Korus, 2012). Predominant Permian deposits present in southeast Nebraska that subcrop beneath the project area include the Chase and Council Grove Groups. These units are comprised primarily of massive to bedded limestone with fossiliferous intervals. Some of the Permian strata can be dolomitic with interbedded shale, evaporites, sandstone, and siltstone. Shale deposits can be substantial sequences that are a mixture including argillaceous, arenaceous, fissile, and/or limy type shales (Condra and Reed, 1959; Burchett, 1983). These units are not distinguished by formation names for purposes of this study.

#### *2.1.5.2 Carboniferous Geology*

Carboniferous deposits composed of Pennsylvanian and Mississippian subsystems underlie all of Nebraska except for a few square miles in the northeast part of the state (Condra and Reed, 1959). Undifferentiated deposits of the Carboniferous System include the Admire, Wabaunsee, Shawnee, Douglas, Pedee, Lansing, Kansas City, Bronson, Marmaton, Cherokee, Osage-Meramec, and Kinderhook Groups. Korus (2012) reports Pennsylvanian deposits that extend beneath parts of the project area are the undifferentiated Kansas City and Lansing Groups, and the undifferentiated Marmaton and Pleasanton Groups. Similar to the Permian deposits, these Carboniferous groups are comprised of massive to bedded and fossiliferous limestone that can be dolomitic with interbedded shale, evaporites, sandstone, and siltstone. Shale deposits can be substantial sequences that are a mixture including

argillaceous, arenaceous, fissile, and/or limy type shale (Condra and Reed, 1959). The Kansas City and Lansing Groups are primarily inter-bedded limestone and shale (Hanson et al., 2012). In addition, the Kansas City, Lansing, Marmaton, and Pleasanton Groups are part of the Western Interior Plains confining system overlying the upper aquifer unit of the Western Interior Plains aquifer system—part of which a member is the Kinderhook Group (Jorgensen et al., 1993; Signor et al., 1996). These units are not distinguished by individual formation names for purposes of this study.

#### *2.1.5.3 Devonian Geology*

Devonian deposits underlie most of the southeastern one-third of Nebraska and unconformably underlie Carboniferous units. The Devonian deposits are largely a sequence of limestones, dolomites, and shales that thin westward and northwestward, and are absent over the Cambridge Arch (Condra and Reed, 1959). It is unknown to what extent Devonian rocks underlie the project area.

#### *2.1.5.4 Silurian Geology*

Silurian deposits underlie the east to southeast one-fourth of Nebraska and are thickest in the extreme southeast part of the state and thin northward. Condra and Reed (1959) report most Silurian rocks in Nebraska have been dolomitized, but play an important groundwater reservoir in the Omaha area.

#### *2.1.5.5 Ordovician Geology*

Ordovician deposits underlie parts of eastern Nebraska. Principal units in eastern Nebraska are the Richmond and Trenton Groups of which "the Trenton Group is well represented in the subsurface of eastern Nebraska" (Condra and Reed, 1959). Ordovician deposits in eastern Nebraska generally are oolitic and hematitic shales overlying dolomites. Similar to Silurian deposits, Ordovician deposits produce some groundwater to deep wells in the Omaha area. Condra and Reed (1959) report that yields of groundwater from Ordovician deposits increases to the west, however, these water resources are highly mineralized and thus are not suitable for extensive use in the region.

#### *2.1.5.6 Cambrian Geology*

Cambrian deposits are present at considerable depth in eastern Nebraska and include sandstones (Jordan Sandstone, Dresbach Sandstone) and carbonates of the Trempealeau-Franconia Formation (Condra and Reed, 1959). The Jordan Sandstone is utilized as a regional bedrock aquifer source east of Nebraska (Young, 1992), but the formation's potential for production is unknown within the state's borders. Another Cambrian aged deposit is present in the project area, the Elk Creek Carbonatite, and is discussed in the following subsection.

#### *2.1.5.7 Precambrian Geology*

A section of the project area is underlain by relatively shallow Precambrian granite in eastern Johnson and Pawnee Counties, within 1,000 ft bgl across much of this area, and less than 500 ft bgl in the southeastern corner of Pawnee County. The depth to Precambrian granite approaches 2,000 ft near Omaha and ranges from 1,800 to 2,100 ft bgl in the Lincoln area (Condra and Reed, 1959). The composition of the Precambrian base in the project area is poorly constrained, but Condra and Reed (1959) note that the Precambrian is comprised of quartzite beneath the Lincoln area. In other areas, the Precambrian sequence, igneous and metamorphic rocks can be prevalent, particularly in structurally-low areas (Condra and Reed, 1959; Carlson and Treves, 2005). One area where the Precambrian composition

is well understood is in southeastern Johnson County near the town of Elk Creek, where the Precambrian granite serves as a host rock for a Cambrian igneous intrusion defined as the Elk Creek Carbonatite. The feature hosts the largest known niobium deposit in the United States and contains a variety of other rare earth elements of high economic value (Drenth, 2014). The intrusion ranges from 3 to 5 miles in width beneath a 500 to 600 ft thick sequence of Quaternary deposits and Paleozoic strata. The dolomitic-carbonatite intrusion consists of numerous mineralogy, including apatite beforsite, syenite, undifferentiated mafic rocks, beforsite breccia, and barite and magnetite beforsite. An airborne aeromagnetic survey was conducted in 2012 (Blessington, 2014; Drenth, 2014) and revealed the 3D distribution and depth of the intrusion. At its upper surface, the intrusion has a general concentric shape, but with depth, the intrusion narrows in a conical shape to give the feature and apparent narrowing, funnel-like shape with depth (Drenth, 2014). The feature is apparent in the AEM survey profiles and will be discussed in following sections of this report.

### *2.1.6 Structural Geology*

Southeast Nebraska is underlain by numerous structural features, including faults, arches, basins, anticlines, and synclines. The features are a result of tectonic activity related to the Midcontinent Rift System (MRS) as well as from the Nemaha Uplift that extends southward from southeast Nebraska to central Oklahoma (Dolton and Finn, 1989). Little is understood regarding the influence of the related fault systems on the regional hydrogeology. However, these features warrant a brief discussion, as structural features are evident in the subsurface profiles from the AEM survey. Additionally, understanding the regional structural geology could point to future areas of potential groundwater exploration and development.

Detailed explanation of the complex processes leading to origin of these features is beyond the scope of this report. However, the following description summarizes briefly the tectonic history that led to the structural features beneath present-day southeastern Nebraska. The MRS, which extends from the Great Lakes region southwestward to central Kansas, is a failed rift (splitting) of the continental crust that occurred during Precambrian time (approximately 1,100 Ma). Through the remainder of Precambrian time, the rifted zone filled with allocthonous sediments as well as igneous rock from basalt flows and other intrusive and extrusive igneous features. The rift extends into Nebraska from the east beneath an area from Douglas County to Otoe County and extends as far west as Saline County before curving southward into Kansas (Figure 2-4 and Figure 2-5). The structural features resulting from the MRS are part of the Thurman-Redfield Structural Zone (TRSZ), a system of faults, basins, arches and horsts present across Iowa and eastern Nebraska (Anderson, 1988; Witzke el al., 2003). During the middle to late Paleozoic Era, compressional forces from continental collision activated on multiple occasions deeper Proterozoic faults, which resulted in folding and faulting of the sequence of strata deposited during the Cambrian through the early Pennsylvanian Periods. Subsequent compressional activity is believed to have extended into Permian time as folds in these strata and late Pennsylvanian units are apparent across the region. This structural activity resulted in the Union Fault and the Northern Bounding Fault, which form the margins of the TRSZ on the south and north, respectively. The resulting displacements in the strata are evident along the CSD cross section from Thurston to Pawnee Counties, Nebraska (Korus et al., 2012) as displayed in Figure 2-6 (the full cross section is available in Appendix 2). *Pennsylvanian* strata within the TRSZ dips southward considerably, whereas *Permian* strata is absent.

South of the Union Fault, the bedrock units have a more subtle north/northwestward dip with the Permian/Pennsylvanian Council Grove Group being the uppermost bedrock unit beneath Nemaha and Richardson Counties. Faulting is not believed to extend into Mesozoic time, as structural displacement of the *Kd* has not been observed in eastern Nebraska or western Iowa. However, deformation of these units is believed to have occurred due to tectonic movement associated with the uplift of the modern-day Rocky Mountains to the west (Laramide Orogeny) (Tikoff and Maxson, 2001; Maher, 2014).

The compressional forces resulting from continental collision during the Paleozoic Era also resulted a second major group of structural features in southeast Nebraska, the Nemaha Uplift and associated folding and faulting. Burberry and others (2014, in review) suggest that the compressional forces creating the Nemaha Uplift also activated faulting associated with the Midcontinent Rift/TRSZ in the northern extent of the project area. The Nemaha Uplift is an upward thrust of pre-Cambrian basement rock in Johnson, Pawnee, and Gage Counties that resulted in folding of the overlying Paleozoic and Permian strata (Figure 2-7). At its shallowest depth, the pre-Cambrian igneous and metamorphic rocks are less than 500 ft bgl (Figure 2-8). Bounding the uplifted area on the east is the Humboldt Fault System (HFS), which consists of high-angle reverse faults with downthrown eastern blocks. The HFS extends from beneath the city of Omaha in southern Douglas County southward into Kansas near the Pawnee-Richardson County line. The HFS intersects with the Union Fault approximately 8 miles northwest of Nebraska City near the Otoe-Cass County line. Geologic maps (Burchett and Carlson, 1966) display the fault as a single feature that splits into two traces in southwest Nemaha County. The fault system, however, is believed to consist of multiple smaller faults along the eastern edge of the Nemaha Uplift. Displacement is around 1,000 ft in southeastern Nebraska (Condra and Reed, 1959) and exceeds 4,000 ft in northern Kansas (Stander, 1989). The Nemaha Uplift is bounded by the Burchard Fault on the west, with a western downthrown block that offsets Paleozoic strata that dips westward towards the Central Nebraska/Salina Basin. East of the Nemaha Uplift and the HFS is the Forest City Basin, a structural depression consisting of upwards of 4,000 ft of Paleozoic carbonates and clastics (Carlson, 2011). Figure 2-9 displays the major faults and structurally altered areas presented in this discussion beneath the southern ENWRA project area.

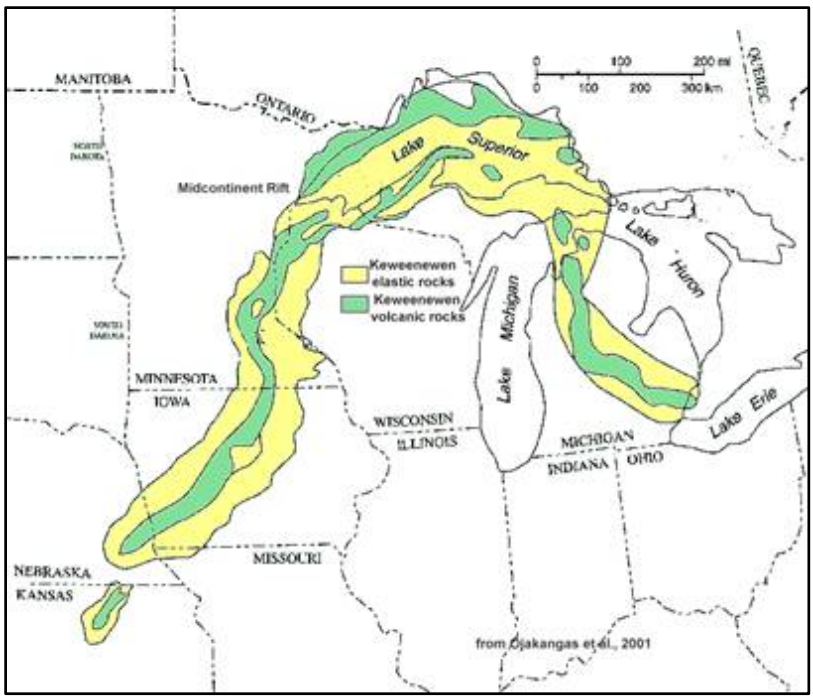



**Figure 2-4: Geographic extent of the Midcontinent Rift in the central United States (Ojakangas, 2001; obtained from www.interstatefalls.org).**

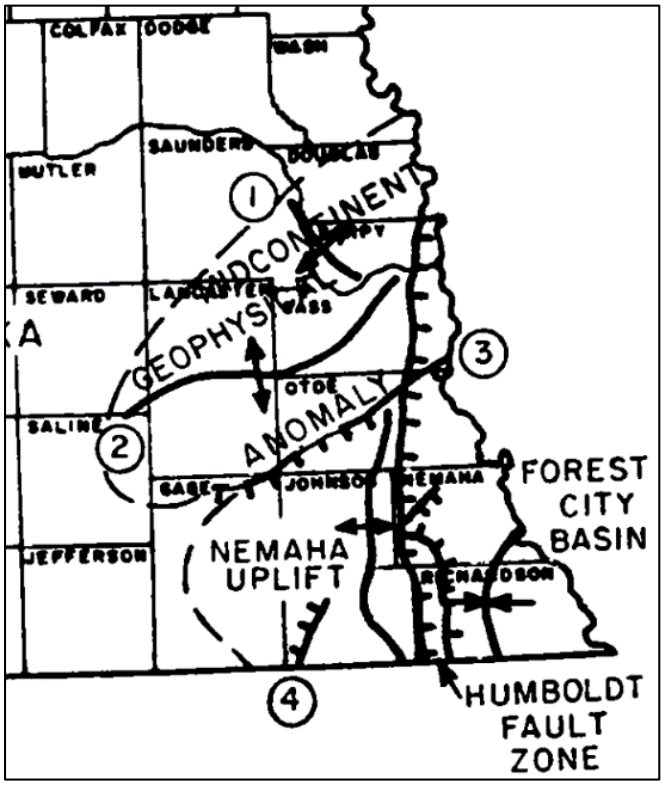



**Figure 2-5: Generalized map of structural features present beneath southeastern Nebraska (Burchett et al., 1985). The numbered features are: 1) Richfield Arch; 2) Denton Arch; 3) Union Fault, and 4) Burchard Fault. Note the Humboldt Fault Zone and the Forest City Basin are identified individually, and the outline of the extent of the Midcontinent Rift is identified by the area within the dashed line labeled "Midcontinent Geophysical Anomaly."**

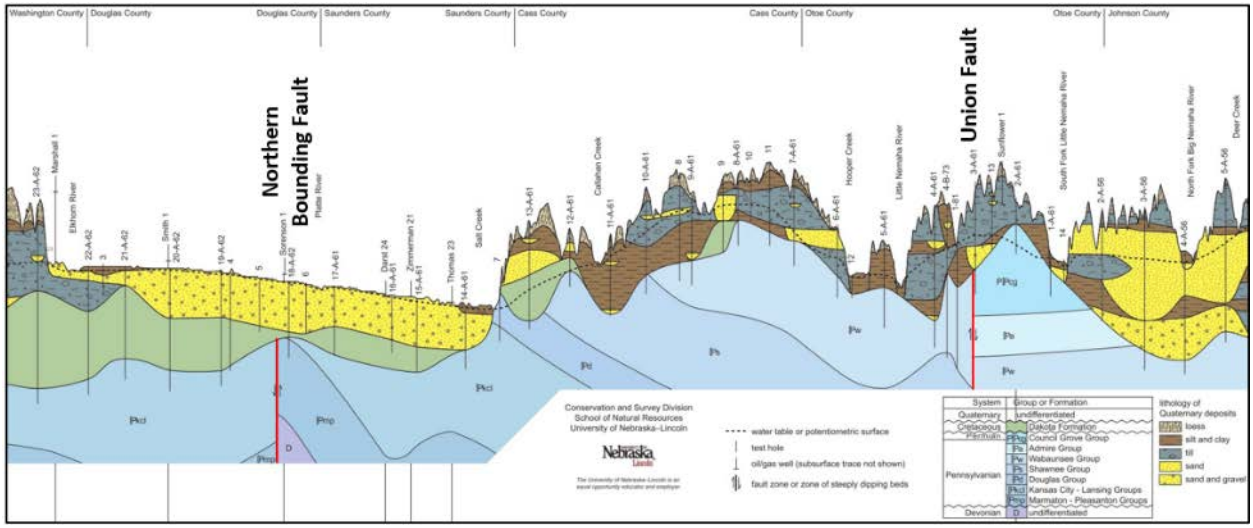



**Figure 2-6: Cross section modified from Korus et al. (2012) indicating locations of the Northern Bounding Fault and the Union Fault (red) in the Douglas-Saunders-Cass-Otoe County portion of the transect. The location of the cross section is identified in Figure 3-5 and the full transect is provided in Appendix 2.**

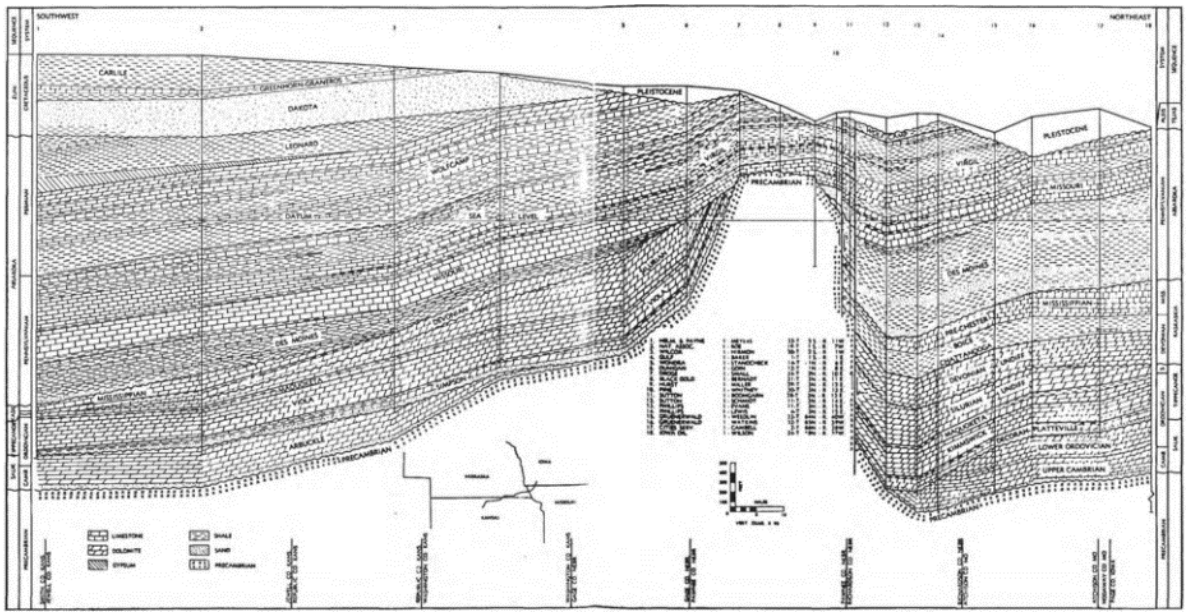



**Figure 2-7: Cross section across northern Kansas and southeastern Nebraska showing the Nemaha Uplift and the folded Paleozoic and Permian strata draped over the uplifted granite block (Carlson, 1971).**

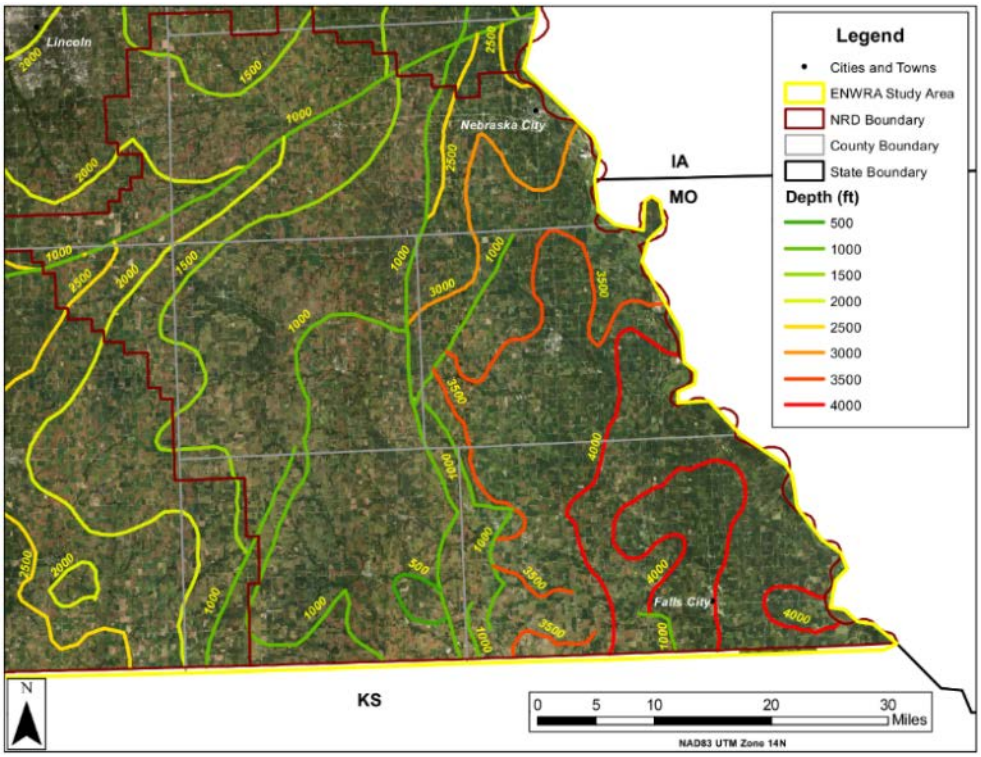



**Figure 2-8: Depth to the Precambrian basement rock (in feet) in the southeast corner of Nebraska.**

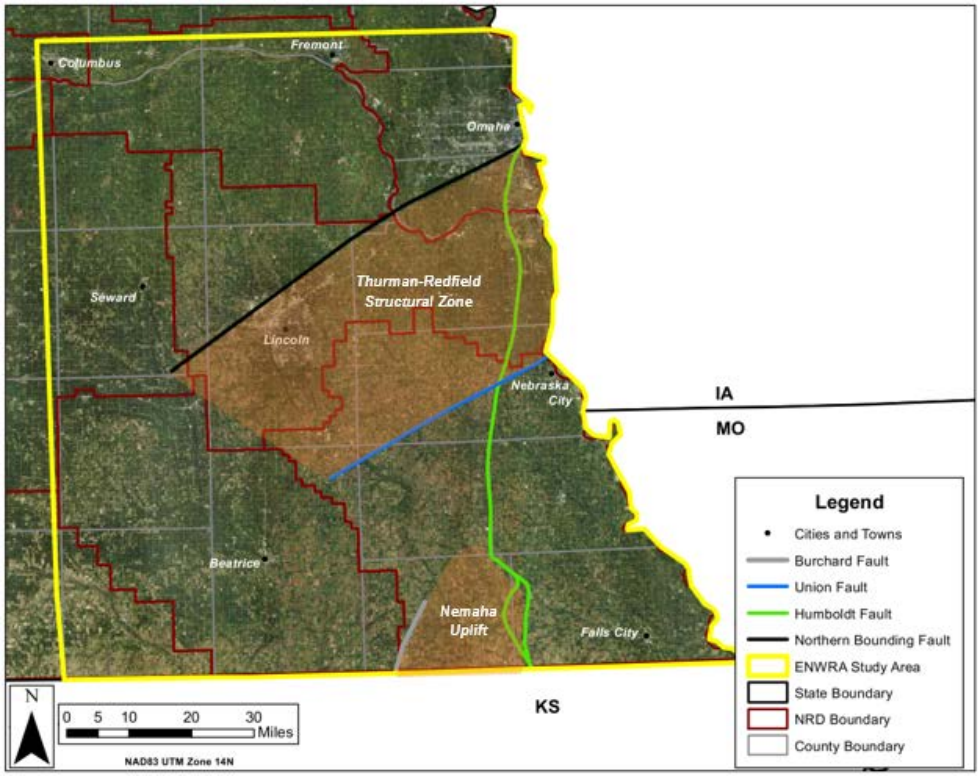



**Figure 2-9: Locations of known, mapped faults in the project area. The Thurman-Redfield Structural Zone (TRSZ) and the Nemaha Uplift Area are displayed in transparent orange shading.**

## 2.2 Hydrogeologic Characteristics of the Quaternary System

The principal Quaternary hydrogeologic units or surficial aquifers in the project area include (1) saturated alluvial deposits that make up the stream-valley (valley fill) aquifers, and (2) glacial-drift aquifers- alluvial and paleo-alluvial or paleo-glacial deposits of Plio-Pleistocene age that underlie till and loess deposits in the uplands and/or that make up the paleovalley deposits. Saturated Quaternary deposits in northeast Nebraska are a complex mixture of saturated sand and gravel deposits. These saturated deposits can be confined, unconfined, deep, shallow, and/or regional and local intermixed with glacial till (Miller and Appel, 1997; Flowerday et al., 1998; Gates et al., 2014). Stream-valley and glacial-drift systems both occur within the project area and locally can be hydraulically connected with each other, similar systems, and/or bedrock aquifers. In addition, aquifers in the project area typically are associated with modern or abandoned stream valleys or within elongated paleovalleys (Gates et al., 2014).

### *2.2.1 Surface Hydrology*

The surficial hydrologic system of the project area is comprised of numerous dendritically-patterned, perennial and seasonal streams that developed through drainage-dissection of glacial till and loess deposits. Figure 2-10 displays the project area's major surface drainages. The largest surface-water system in the project area is the Platte River, which flows easterly from western Nebraska to its confluence with the Missouri River south of Omaha. USGS surface water station number 06805500 at Louisville, NE reported a 2013 annual mean discharge for the Platte River of 5,421 cubic feet per second ($ft^3/s$)) (USGS, 2015). Tributaries in the project area include larger systems with respect to mean-annual discharges such as Salt Creek near Greenwood, NE (USGS station number 06803555; 2014 annual mean discharge of 369.9 $ft^3/s$), the Little Nemaha River at Auburn, NE (USGS station number 06811500; 2014 annual mean discharge of 164.9 $ft^3/s$), the North Fork Big Nemaha River at Humboldt, NE (USGS station number 06814500; 1997 through 2013 stage and annual maximum discharge computation only; 2014 annual mean discharge of 127.5 $ft^3/s$), and Wahoo Creek as Ashland, NE (USGS station number 06804700; 2014 annual mean discharge of 160.7 $ft^3/s$) (USGS, 2015). Many other tributaries to these smaller systems are present in the project area but are not listed or discussed.

Wetlands exist in Lancaster and southern Saunders Counties. Harvey et al. (2007) report many saline wetlands exist in discharge areas of the Cretaceous Dakota aquifer system and are located within the flood plains of Rock, Salt, and Little Salt Creeks. Discussion on the presence of salinity in these areas is discussed in following sections of this report.

Recharge contribution from surface water features to the groundwater system largely is unknown. The larger lakes in the project area are generally located in or directly adjacent to Lancaster County within the Salt Creek or Big Nemaha River basins, and were built by the U.S. Army Corps of Engineers for flood control/recreational use. The largest surface feature is Branched Oak Lake northwest of Lincoln that covers approximately 1,800 acres. Many smaller water bodies, such as Czechland Lake (85 acres) and Two River State Recreation Area (4 acres) are scattered throughout the project area, and most flood control/recreation lakes are in the 200 to 600 acre size (Nebraska Game and Parks Commission, 2015). In addition, many smaller lakes built and maintained by the NRDs also exist within the project area.

However, because the large and small lakes lie in glaciated areas of eastern Nebraska, recharge to or interaction with the groundwater system is unknown.

Besides wetland systems, larger lakes within the project area are present; however, their recharge
Extent of Aquifers

As mentioned in the beginning of this section, two primary surficial aquifer types exist in the project area—stream-valley and glacial-drift systems. Outside the major surface water drainage valleys (Figure 2-11), the primary aquifers in the project area lie in paleovalleys. Many paleovalleys have easterly trends and lie beneath thick assemblages to thin veneers of glacial-drift deposits. Todd Valley, a paleo-stream-drift valley located in Saunders County in the LPNNRD, deviates from this trend with a northwest to southeast orientation. Todd Valley (Figure 2-12) is a remnant of the ancestral Platte River valley and, unlike the paleovalleys, is not overlain by glacial-drift deposits.

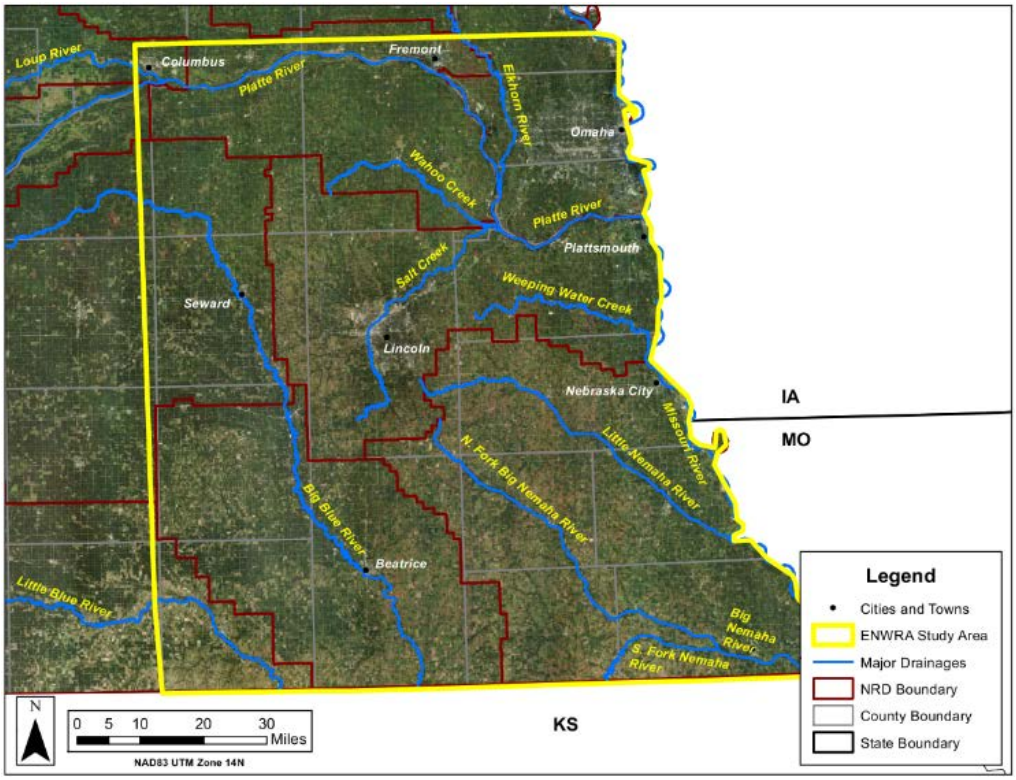



**Figure 2-10: Map displaying the major streams and rivers within the southern ENWRA project area.**

Larger paleovalleys in the project area lie in two general regions. The first region is in the northern extent of the project area, primarily in Butler and Saunders Counties. The second region lies in southern Lancaster and Otoe Counties, and northern Johnson County. Smaller paleovalleys include one that is located mostly in northern Richardson to extreme northeast Pawnee and southern Nemaha Counties, and another that extends into the western edge of Pawnee County (Figure 2-12). Consequently, mapped paleovalleys of substantial size are absent in much of the central part of the project area.

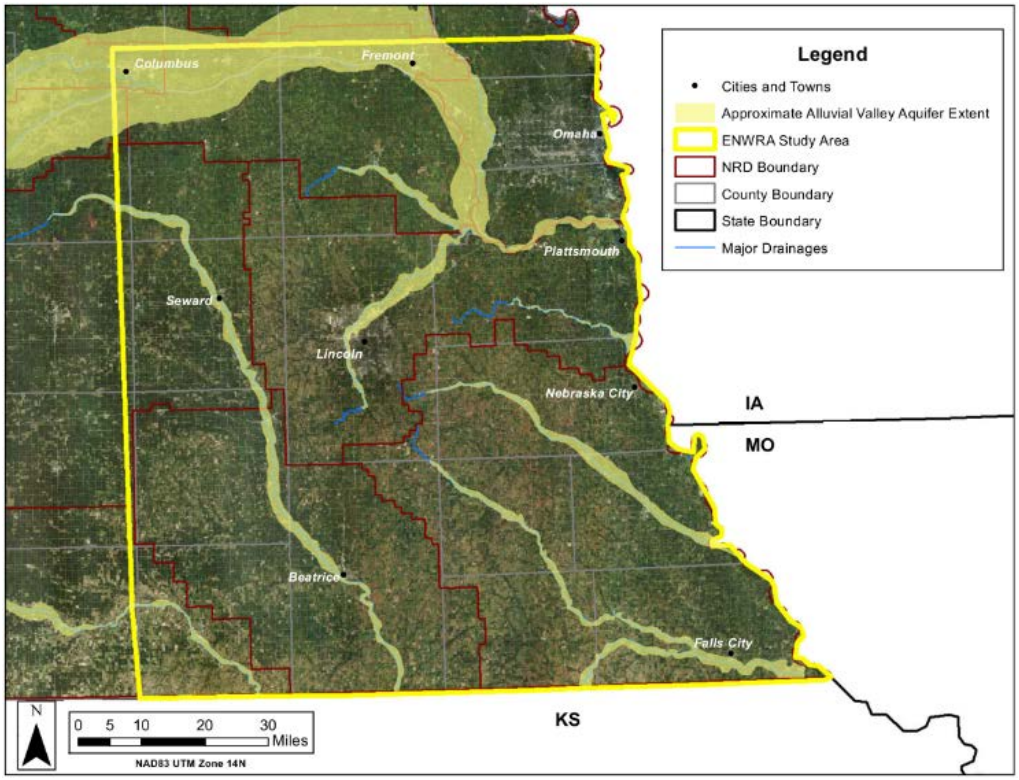



**Figure 2-11: Mapped alluvial valley areas hosting alluvial aquifers in the southern ENWRA project area, modified from the Nebraska Groundwater Atlas (Korus et al., 2013b).**

Availability of groundwater in stream-valley aquifers is adequate for most purposes, specifically within the larger streams such as the Platte River, Big and Little Nemaha Rivers, and Salt Creek. Most of the water in stream-valley or alluvial aquifers is under unconfined or water-table conditions with local confined conditions where overlying fine sediments cap the aquifers. Stream-valley aquifers consist mostly of Holocene sand and gravel with local deposits of Pleistocene age. The stream-valley sand and gravel deposits in many locations have been reworked from older glacial-drift deposits, thus these materials are difficult to distinguish from glacial outwash (Miller and Appel, 1997). Locally, stream-valley aquifers can be hydraulically connected to underlying semi-consolidated or bedrock aquifers, such as the *Kd*.

Availability of groundwater in glacial-drift aquifers is highly variable. The potentiometric head in glacial-drift aquifers is a composite surface and comprised of unconfined and confined systems due to the complex interbedding of deposits with varying permeability and large numbers of local confining units (Miller and Appel, 1997). Consequently, groundwater in glacial-drift aquifers could be under confined conditions in one area and unconfined conditions in other areas.

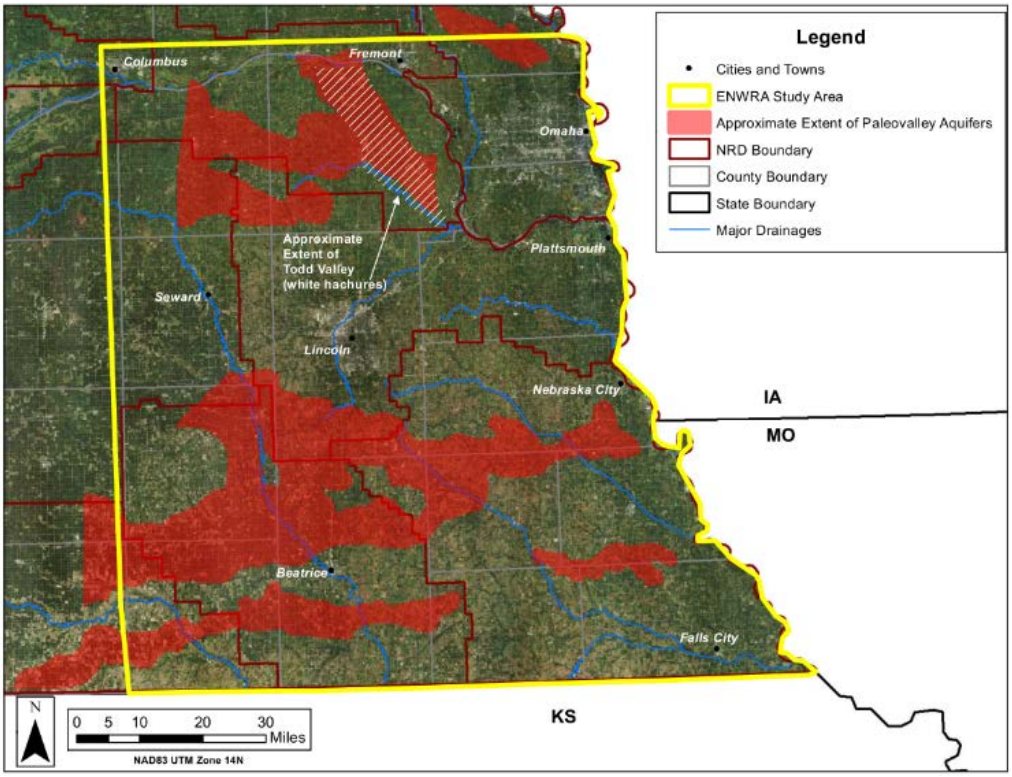



**Figure 2-12: Major paleovalleys in the southern ENWRA project area, modified from the Nebraska Groundwater Atlas (Korus et al., 2013b).**

### *2.2.2 Groundwater Flow System*

Much of the hydrologic information used in the preparation of this report was gathered from studies with a regional scope. These reports include hydrogeologic maps, geologic cross sections, and water-quality analyses in but are not limited to Burchett et al. (1972, 1975), Ellis (1984), Tanner and Steele (1991), Gosselin et al. (1996, 2001), Flowerday et al. (1998), Summerside et al. (2001), Divine et al. (2009), and Gates et al. (2014).

Regional groundwater-flow direction for the project area largely is northeast to southwest (Tanner and Steele, 1991; Flowerday et al., 1998; Gates et al., 2014) (Figure 2-13). Regional groundwater flow can be hydraulically connected to shallower aquifers or surface water systems, although their interconnection is not fully understood.

Groundwater levels in the project area vary spatially and temporally. Spatially, groundwater levels are located at shallower depths in the alluvial valleys and at deeper depths under the glaciated terrain. Temporally, groundwater levels typically reach maximum depths from extensive groundwater pumpage during the pumping season (typically June through September) then return to pre-stress levels or their shallowest depths the following spring (e.g. March to June). Annual depths of drawdown and recharge of aquifers highly depend on the type of aquifer (e.g., confined or unconfined), proximity of the aquifer to the land surface, and the amount of stress and number of stress points exhibited during the pumping season, combined with the amount of recharge available to the aquifer. Groundwater under confined systems, such as in aquifers beneath glacial till, typically exhibit more drawdown than groundwater in unconfined systems that are present in alluvial settings.

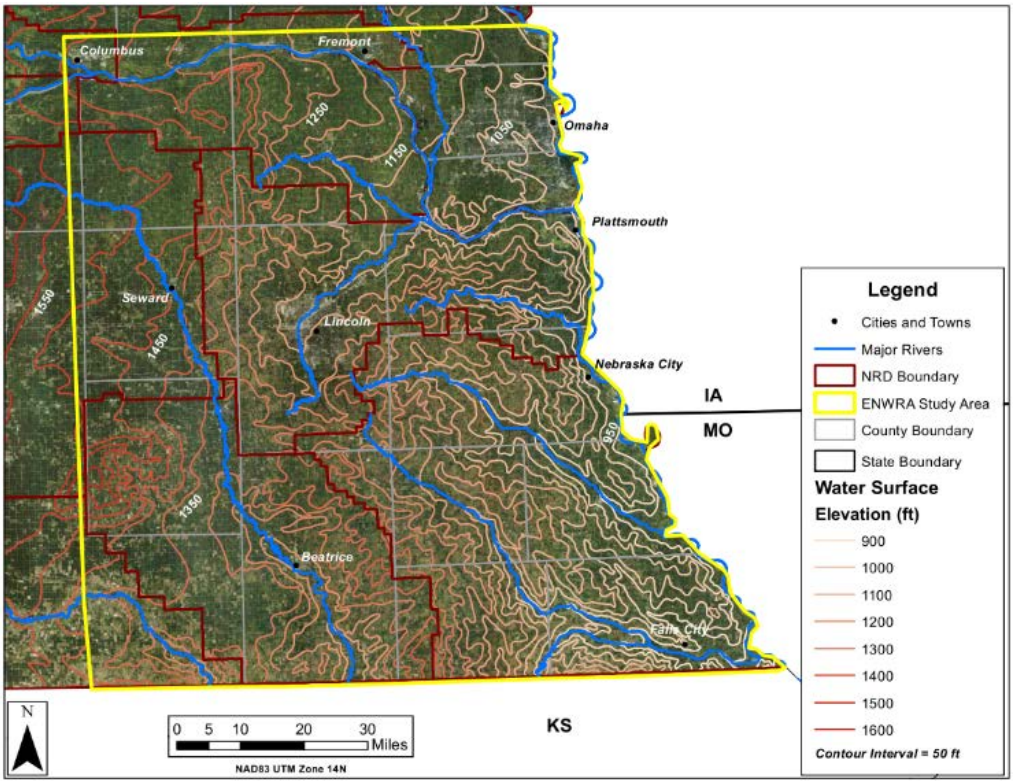



**Figure 2-13: Elevation of the groundwater surface in the southern ENWRA project area. Regional groundwater movement is from areas of higher groundwater elevations to lower elevations as displayed by the contours.**

Contrasts of hydraulic conductivity within the principal aquifers of eastern Nebraska, including the *Kd*, cause common significant vertical groundwater-flow gradients (Summerside et al., 2001). Potentiometric gradients show groundwater movement from upland areas toward stream valleys. Hilly topography and complex heterogeneity within the glacial-drift terrain can create local flow systems (Gates et al., 2014). In wetland areas, Harvey et al. (2007) report groundwater flows mostly toward the surface but local downward gradients can be present. Also, within the wetlands or near streams adjacent to wetlands, potentiometric surfaces can lie above land surface. Carbon-14 dating of the deeper groundwater in the wetland systems showed recharge dates ranging from about 16,000 to 36,000 years before present (Harvey et al., 2007).

Confined and unconfined conditions as well as the general makeup of the aquifer create differences in well yields from the surficial Quaternary systems. In these systems well yields range from 50 to 1,000 gallons per minute (gpm) with local yields up to 1,500 gpm (Tanner and Steele, 1991).

Recharge to stream-valley aquifers largely is from local precipitation, although additional sources of recharge can occur from downward percolation of irrigation waters or inflow from underlying permeable aquifers. Szilagyi et al. (2005) estimated regional mean annual recharge rates for stream valleys within the project area ranging from about 3.7 to 5.5 in/yr, with local annual recharge rates up to 6.4 in/yr. In the uplands beyond the stream valleys, regional estimated annual recharge rates generally ranged from 2.4 to 5.5 in/yr. Gates et al. (2014) used extracted data from Szilagyi and Jozsa's (2013) statewide data to determine regional-scale mean annual recharge in the glaciated area of eastern Nebraska. This analysis determined that the total recharge for the Nebraska glaciated region averaged

about 2.2 in/yr (converted from a reported as 56 mm/yr) and was similar to rates determined using other methods (Gates et al., 2014).

**Table 2-1: Aquifers in Quaternary to Cretaceous stratigraphic units beneath eastern Nebraska.**

| System | Series | Hydrologic unit | Maximum thickness (ft) |
|---|---|---|---|
| **Quaternary** | Holocene, Pleistocene | Aquifer in undifferentiated alluvial deposits | Generally less than 100 ft |
| Undifferentiated sand and gravel units in stream-valley systems. Stream-aquifer systems can be intermixed with older glacial sand and gravel making the deposits difficult to distinguish from older glacial outwash. Hydraulic head is typically unconfined. Recharge is principally from local precipitation and is rapid if the source area is primarily sand and gravel. Wells are capable of yielding up to several thousand gpm. | | | |
| **Quaternary** | Holocene, Pleistocene | Aquifer in undifferentiated glacial-drift deposits | Up to 300 ft |
| Undifferentiated sand and gravel units in glacial-drift aquifers. Hydraulic head generally under confined conditions, but can be under unconfined conditions elsewhere. Thickness of glacial-drift aquifers vary greatly. Comprised largely of sand and gravel from ancestral river channels or glacial outwash that became capped by till or loess. Some paleovalleys are several miles wide and tens of miles long. Recharge mostly from precipitation infiltration or inflow from adjacent hydraulically connected aquifers. Well yields are highly variable; some capable of up to several thousand gallons per minute but vary by location. Isolated aquifers are capable of sustaining potable quality water for domestic or stock purposes only. | | | |
| **Cretaceous** | Upper | Confining units of the Pierre, Niobrara, Carlile, or Greenhorn–Graneros Formations | Variable |
| Where present, largely serve as regional confining units. Niobrara Formation may produce water where secondary fracturing occurs. | | | |
| **Cretaceous** | Lower | Aquifer in sandstone of the *Kd* | Total thickness variable. Up to 600 ft in the project area |
| Locally, the *Kd* serves as an aquifer or as a confining unit. The aquifer is generally located in loosely-cemented, medium- to fine-grained sandstone. Hydraulic head is typically confined with local unconfined conditions encountered. Groundwater is more potable in eastern part of the state, where the *Kd* underlies saturated Quaternary deposits, hydrologic connection can occur. Westerly, the *Kd* becomes more mineralized and is found deeper beneath the surface. Where *Kd* units lie in close proximity to the land surface, recharge is primarily from local precipitation, otherwise largely from inflow from adjacent hydrologically-connected aquifers. Sandstones are capable of producing potable water to irrigation and municipal wells with yields can be as much as 1,000 gallons per minutes locally. | | | |

### *2.2.3 Aquifer Characteristics*

Transmissivity values in the project area's unconsolidated aquifers range from less than 20,000 gpd/ft (2,700 $ft^2$/d) to highs of greater than 150,000 gpd/ft (20,000 $ft^2$/d) with localized areas of 200,000 gpd/ft (27,000 $ft^2$/d) (Summerside and Myers, 2005b; Olafsen-Lackey and Summerside, 2005b). Transmissivity values are predominantly 50,000 to 150,000 gpd/ft or greater in alluvium and unconfined systems with local areas of 20,000 gpd/ft. Results of a composite aquifer test conducted in a paleovalley aquifer south of Lincoln, NE (U.S. Geological Survey, written comm., 2009) indicated a transmissivity for a paleovalley aquifer of approximately 28,000 gpd/ft (3,700 $ft^2$/d) and a hydraulic conductivity of about 56 ft/d. This aquifer test was performed in the lateral parts of a much larger paleovalley. Consequently, higher transmissivity and likely larger hydraulic conductivity values would be expected in the larger and deeper parts of the aquifer. As shown by Summerside and Myer (2005b) and Olafsen-Lackey and Summerside (2005b), larger transmissivity values would represent aquifers where coarser sand and gravel deposits or thicker deposits are encountered.

Specific yield in the project area generally ranges from 0.05 to 0.15 with localized areas of 0.20 (Summerside and Myer, 2005a, Olafsen-Lackey and Summerside, 2005a). Specific yield in alluvium and unconfined systems generally ranged from 0.10 to 0.15. Specific yield in confined areas generally were slightly smaller than the alluvial and unconfined areas—ranging from 0.05 to 0.10 in the areas underlying the loess and till (Summerside and Myer, 2005a; Olafsen-Lackey and Summerside, 2005a).

Very little information is available for storativity values in the project area. However, in 2009 ENWRA and the USGS conducted a 94-hour constant-discharge aquifer test to determine the general hydraulic characteristics of a glacial aquifer south of Hickman, Lancaster County, Nebraska. The aquifer test was conducted in the northern edge of a large paleovalley aquifer. The paleovalley aquifer is characterized by regional glacial deposits overlying permeable sand and gravel units that primarily trends northwest to the southeast. The northern edge of the paleovalley aquifer is hydraulically-connected to an overlying separate aquifer from which the test was conducted. These two aquifers connect into a larger distinct single aquifer south of the aquifer-test site. Calculated storativity values from the constant-discharge aquifer test were computed to be around $5x10^{-4}$ for most individual wells and $6x10^{-4}$ for the composite analysis. Although this aquifer test behaved like an unconfined system, the calculated storativity values were consistent with those described by Lohman (1972) for most confined systems ($10^{-3}$ to $10^{-5}$). Similarly, storativity values for most of the confined paleovalley aquifers within the project area are likely within a magnitude of the range calculated from the aquifer test (e.g. $10^{-3}$ to $10^{-5}$).

### *2.2.4 Aquifer-Surface Water Connection*

Groundwater flow connectivity to surface water is largely undocumented in the glaciated areas of eastern Nebraska. Review of USGS 7.5-minute topographic maps show some springs exist or existed along the South Fork Little Nemaha River Basin (USGS, 1966a). Several flowing artesian wells in the South Fork Little Nemaha River valley near Cook, NE are shown by the USGS (1966b). The former USGS groundwater-recorder well 403032096104801 was located about 0.3 mi north and 20 ft higher in elevation than one of these flowing artesian wells (USGS, 1966b). From 1977 through 2001, the median water level for the Cook recorder well was about 15.5 ft below land surface or about 4 ft higher than the land surface elevation of flowing artesian well located in section 9.

Gosselin et al. (2001) report a 2,463 ft exploratory well drilled in 1887 had artesian conditions that allowed groundwater to flow to the land surface. Three saline zones were identified in this well; lower part of the *Kd*, and the Pennsylvanian Shawnee and Kansas City Groups. Moreover, they reported the presence of the Denton Arch (Burchett, 1982) creating feasible pathways for deep groundwater to migrate to the land surface. This well is another example of how deep groundwater flow can reach the land surface along preferential pathways. For example, in northern Lancaster County, Harvey et al. (2007) report saline wetland areas in Salt Creek Basin that result from upward movement of groundwater to the land surface. These wetland areas serve as groundwater sinks—e.g. discharge points into a surface-water system. As a result, the saline groundwater from deeper bedrock aquifers provides a saline influx to Salt, Little Salt, and Rock Creeks.

### *2.2.5 Connectivity to other Aquifers*

Gosselin et al. (1996) report Plio-Pleistocene deposits in some locations are in hydrologic connection to shallow aquifers and streams. Where connected, the deeper aquifers can discharge into the shallow aquifers or streams. For example, Harvey et al. (2007) reported where connected deeper aquifers play an important role in the water chemistry of the shallow deposits with the creation of saline wetlands through upward groundwater flow from deep bedrock aquifers. The rate of communication between aquifers is unknown, however. In southeast Nebraska, some paleovalley aquifers are inadequately delineated, therefore, hydrologic connection between aquifers cannot be fully understood. Although connection, either horizontally or vertically, is not well understood, some communication between stream-valley, glacial-drift (e.g., paleovalley), and bedrock aquifers does occur temporally and/or aerially. Changes in the flux across the temporal hydrologic connection likely occur with increased pumping during irrigation season (June to September). Pumpage of high capacity wells during this time can cause magnitude changes in groundwater gradients.

## 2.3 Bedrock Aquifer Conditions

The primary bedrock aquifer in the project area is hosted by the *Kd,* which locally can serve as a secondary aquifer in eastern Nebraska (Divine et al., 2009) with regional confining units to unconsolidated Quaternary deposits overlying the *Kd*. Well yields from the *Kd* generally are about 10 to 750 gpm (Tanner and Steele, 1991). The *Kd* can yield some freshwater locally and serve as a source of groundwater to irrigation or domestic wells, but it can also serve as a confining unit to the overlying unconsolidated deposits. Well yields from aquifers in the Paleozoic bedrock generally are about 20 to 50 gpm in areas where secondary porosity has developed fractured zones in the limestone sequences (Tanner and Steele, 1991).

Some bedrock aquifers are found in Paleozoic strata, but these aquifers are limited in extent and production. The Western Interior Plains aquifer system, comprise of Ordovician and Cambrian strata are present in parts of eastern Nebraska, particularly within the Forest City Basin. These units are absent near Nemaha Uplift in Johnson and Pawnee Counties. Due to the depth and high mineralization of the water, including total dissolved solids (TDS), the aquifer is not highly utilized across the project area (Miller and Appel, 1997).

### *2.3.1 Extent and Structure of Kd Aquifer*

The bedrock aquifer system within the permeable sandstone of the *Kd* is defined as the Maha aquifer in Nebraska (Miller and Appel, 1997; Gosselin et al., 2001). Ellis (1984) presented a structural map of the "Dakota aquifer system" (Maha) in eastern Nebraska indicating the unit thinning eastward with a relatively steep gradient immediately beneath the project area (Figure 2-14). From west to east the unit thins from approximately 600 ft to about 100 ft. Regionally, the system thickens northwestward to over 900 ft in north-central Nebraska.

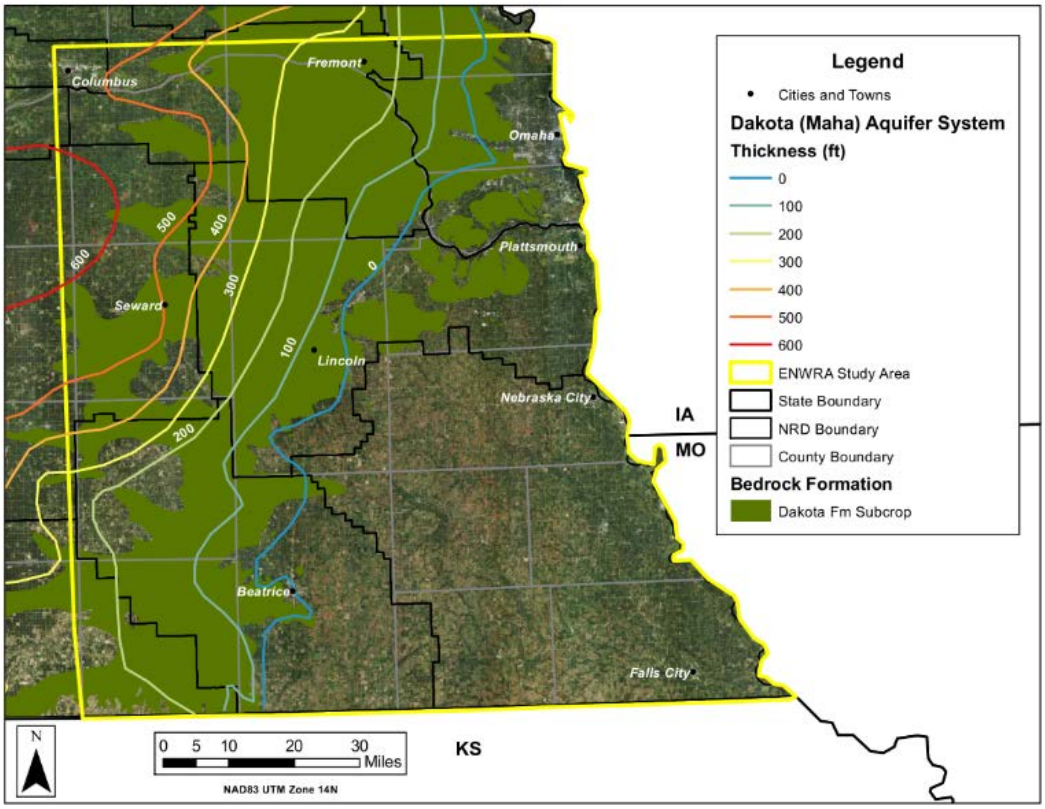



**Figure 2-14: Thickness contours of the *Kd* /Maha aquifer in eastern Nebraska (Ellis, 1984). The green area indicates where the *Kd* is the uppermost bedrock subcrop in eastern Nebraska (Burchett, 1986). Note that the contours and the extent of the *Kd* subcrop are from different map sources. Thus, there are mapped *Kd* intervals from the Nebraska bedrock geology map (Burchett, 1986) that exist east of the 0 ft thickness contour from Ellis (1984).**

### *2.3.2 Aquifer Characteristics*

Available aquifer data are based primarily on regional aquifer evaluations. Transmissivity within the Maha aquifer beneath the project area ranges from around 7,500 to 75,000 gpd/ft (1,000 to 10,000 $ft^2/d$). In the northern portion of the project area, transmissivities exceed 75,000 gpd/ft (10,000 $ft^2/d$) beneath Colfax and northern Butler Counties (Helgesen et al., 1993).

Limited information exists on the porosity of the Maha aquifer. Helgesen et al. (1993) present a regional porosity map within this aquifer based on borehole geophysical logs and laboratory-derived values (core tests) from literature originating in the oil and gas industry. The nearest contour to the project area, which sits north-south across central Nebraska, indicates a porosity value of 0.3. Specific yield estimates for sandstones in the Dakota aquifer in Kansas and Colorado range from 0.1 to 0.2. No storage coefficient values for the confined portion of the system have been identified. However, a specific storage value of $9.5 \times 10^{-7}$ per ft of aquifer was reported (Helgesen et al., 1993). Multiplying this by 400 ft (the average thickness of the Maha aquifer beneath of the project area) results in a storage coefficient of $3.8 \times 10^{-4}$.

### *2.3.3 Connectivity to Surface Water*

Recharge to the Maha aquifer beneath the project area is limited to locations where the bedrock is close to the surface. This occurs most often along deeply-incised surface drainages. In other regions of the Maha aquifer, recharge occurs via infiltration of precipitation along exposed outcrops or shallow subcrops (Helgesen et al., 1993).

Connection to surface water features is limited to where outcrops of the *Kd* are in direct contact with streams at the surface or where permeable bedrock and or fractures are separated from the surface streams by highly permeable streambed sediments.

### *2.3.4 Connectivity to other Aquifers*

Communication with overlying buried glacial outwash aquifers likely occurs, but specific quantification of these fluxes is not known. Gosselin et. al (2001) identified geochemical groundwater signatures that indicated a source from overlying glacial outwash. The degree of communication between the Quaternary and Cretaceous groundwater flow systems is not well understood and likely varies considerably due to local, ambient vertical gradients or through influence of pumping that occurs from both aquifers. Upward vertical communication of groundwater from underlying bedrock units is also possible. The highly saline sources in the *Kd*/Maha aquifer southeast of the project area in Lancaster County have been attributed to sources from the underlying Paleozoic units (Helgesen et al., 1993).

## 2.4 Water Quality

Understanding water quality is a primary function of any AEM investigation, as the presence of electrically-conductive water at the land surface or within the subsurface can affect the AEM signal and thus the geologic interpretation. Understanding the water quality of a hydrogeologic framework also can aid in understanding flow system dynamics such as recharge and discharge areas, flow tubes, potential interaction between aquifers and streams or aquifers with other aquifers, and trends in water chemistry that can impact human health. This section briefly discusses the characterization of groundwater in and around the project area through a brief overview of historic water samples obtained from the USGS National Water Information System (NWIS) database. No assessment of the water quality within or adjacent to the project area was completed, as much of that data already was analyzed in previous studies (e.g., Tanner and Steele, 1991; Helgesen et al., 1993; Harvey et al., 2007; Arnold et al., 2008; Divine et al., 2009; and Gates et al., 2014). Moreover, all of the focus is on groundwater quality, as even several large tracts of land within the project area are classified as saline wetlands. Wetland areas were documented and described by Harvey et al. (2007).

A total of 778 historic groundwater-quality samples from 220 wells were analyzed to determine water chemistry characteristics of the project area—719 water samples from 167 Quaternary surficial wells, 44 water samples from 41 Cretaceous wells (most likely *Kd/*Maha aquifer) wells, 13 water samples from 11 wells completed in Paleozoic strata, and 2 water samples from one well that had no aquifer source classification. Some of the 43 wells that were part of a USGS PMRNRD study near Springfield, NE were not classified as to what aquifer type they were constructed in. Most, if not all, were shallow domestic wells located in alluvial or glacial-drift areas. Consequently, all of these wells were classified as

Quaternary for this this report. The specific conductance values in each of these wells were below 1,000 µS/cm. Therefore, a Quaternary aquifer designation was considered justified. The three wells where specific conductance values exceeded 1,000 µS/cm (1,090, 1,190, and 1,990 µS/cm) were likely in the Platte River alluvium or very shallow bedrock (i.e., 15 ft in depth).

Water samples from the Quaternary surficial deposits include all alluvial (stream-valley) and glacial-drift (paleovalley) aquifers. The chemical characteristics of the samples collected from the Quaternary surficial system show that most groundwater is a calcium-bicarbonate type; whereas most samples collected from the bedrock toward a sodium-sulfate type. The Quaternary and bedrock systems, however, had groundwater samples that were discordant from the majority of samples from their system. Groundwater samples collected from the *Kd* show a mixture of calcium-bicarbonate and sodium-sulfate type groundwater (Piper diagram for bedrock wells in Appendix 5). In addition to the 778 water samples collected for chemical analysis, 1,416 water samples from 359 wells were examined to evaluate the presence of nitrate as N in the project area. The results for nitrates are only presented in the overall statistical analysis (Table 2-2) and all water-quality data is available in the data deliverables.

Median specific conductance for all 778 groundwater samples was 615 µS/cm (Table 2-2). Median calcium, sodium, chloride, sulfate, and TDS from these samples were 72.6, 30.9, 13.6, 61.0, and 376 mg/L, respectively (Table 2-2). For all groundwater samples the maximum specific conductance value was 62,700 µS/cm and the maximum calcium, sodium, chloride, sulfate, and total dissolved solids concentrations were 610, 16,600, 24,400, 2,950, and 43,800 mg/L, respectively. The maximum value for specific conductance, sodium, chloride, and TDS was from a well screened in the *Kd*. Figure 2-15 displays an overall plot of concentrations for calcium, chloride, sodium and TDS for the entire suite of groundwater samples versus depth in the project area. Figure 2-16 shows in a series of box plots the concentration distributions for major ions and nutrients, categorized by aquifer source, across the project area (note that larger images of Figure 2-15 and Figure 2-16 are provided in Appendix 5).

In general, the groundwater of the project area appears mostly to be fresh but with localized areas of high concentrations of specific conductivity, sulfate, and TDS concentrations. The local areas of groundwater salinity may pose interpretation problems during analysis of the AEM data.

**Table 2-2: Statistical results of water-quality analyses from groundwater samples collected in or near the project area, from all aquifer sources. Units in milligrams per liter unless stated otherwise. Data are from the USGS NWIS, Lower Platte North NRD, and Nemaha NRD (NA- not analyzed; N- number of samples).**

| Composite of Groundwater Samples | Minimum | 1st Quartile | Median | Mean | 3rd Quartile | Maximum | NA's | N |
|---|---|---|---|---|---|---|---|---|
| Water temperature, in °C | 5.90 | 12.1 | 13.0 | 13.3 | 14.0 | 26.1 | 82 | 696 |
| Specific conductance, in µS/cm at 25°C | 243 | 525 | 615 | 1,354 | 808 | 62,700 | 16 | 762 |
| pH, in standard units | 5.90 | 7.00 | 7.20 | 7.28 | 7.50 | 8.60 | 270 | 508 |
| Dissolved oxygen | 0.10 | 0.30 | 0.95 | 2.34 | 4.00 | 11.1 | 214 | 564 |
| Bicarbonate | 110 | 287 | 365 | 398 | 429 | 1,280 | 715 | 63 |
| Calcium | 2.50 | 60.0 | 72.6 | 82.2 | 90.0 | 610 | 0 | 778 |
| Magnesium | 0.40 | 12.9 | 16.3 | 20.5 | 21.0 | 268 | 0 | 778 |
| Sodium | 6.90 | 24.6 | 30.9 | 126 | 46.0 | 16,600 | 33 | 745 |
| Sodium adsorption ratio | 0.16 | 0.65 | 0.89 | 5.53 | 1.25 | 1,300 | 35 | 743 |
| Potassium | 1.32 | 3.61 | 6.27 | 7.15 | 8.54 | 98.0 | 64 | 714 |
| Chloride | 0.00 | 6.56 | 13.6 | 223 | 25.0 | 24,400 | 0 | 778 |
| Sulfate | 1.00 | 27.9 | 61.0 | 107 | 93.0 | 2,950 | 1 | 777 |
| Fluoride | 0.10 | 0.30 | 0.37 | 0.48 | 0.41 | 8.40 | 406 | 372 |
| Silicate | 1.30 | 28.6 | 31.2 | 31.0 | 34.0 | 58.0 | 381 | 397 |
| TDS | 108 | 328 | 376 | 682 | 491 | 43,800 | 63 | 715 |
| Nitrate as N | <0.02 | 0.08 | 0.97 | 5.40 | 4.62 | 580 | 0 | 1,416 |

*computed with censored data equal to LRL

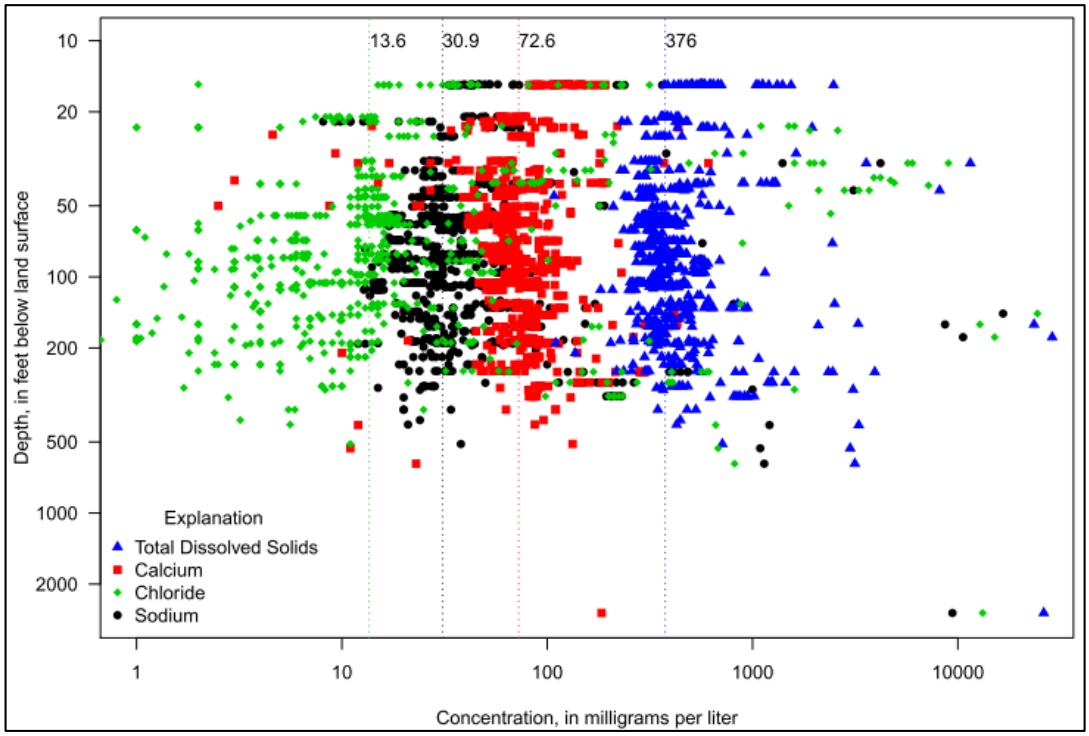



**Figure 2-15: Concentrations of calcium, chloride, sodium, and TDS (x-axis) in groundwater samples verses depth (y-axis). Data are from the USGS NWIS.**

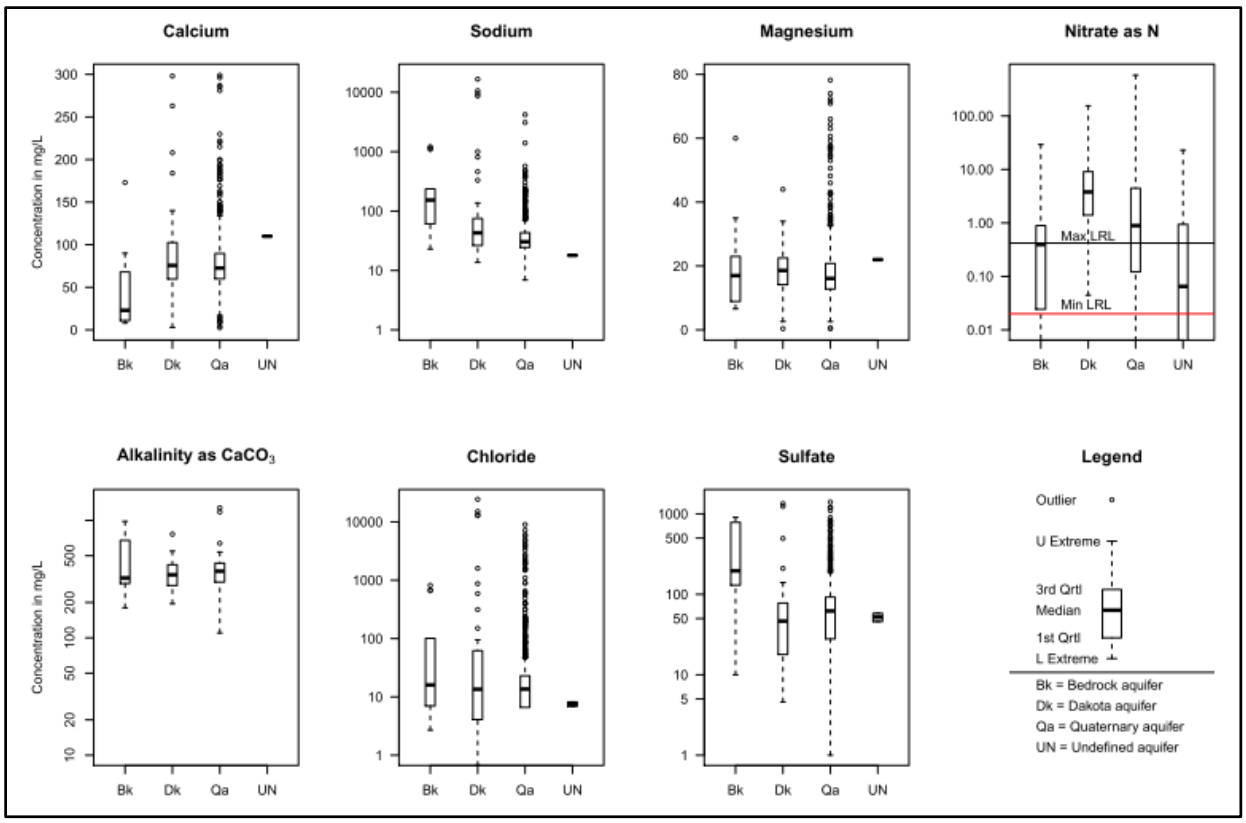



**Figure 2-16: Box and whiskers plots of major ions and nutrients concentrations of in groundwater samples by aquifer type across the southern ENWRA project area. Data are from the USGS NWIS.**

### *2.4.1 Quaternary Aquifer Water Quality*

Groundwater quality of the Quaternary aquifers depends largely on overlying deposits. In areas where low yield deposits (i.e., till and loess) overlie aquifers, groundwater quality is often less impacted than those where sand and gravel deposits are near land surface. In stream-valley systems, groundwater is in close proximity to the land surface and therefore subject to water-quality changes due to land use/land cover.

Median specific conductance values from 778 water-quality samples collected from alluvial, paleovalley and glacial-drift wells were around 610 µS/cm (Table 2-3). This value was slightly smaller than the median specific conductance value from water samples collected from bedrock wells, 802 µS/cm. Quaternary surficial wells contained median calcium, sodium, chloride, sulfate, and TDS concentrations of 72.6, 30.4, 13.6, 62.0, and 374 mg/L, respectively (Table 2-3). The maximum specific conductance value was 28,700 µS/cm and the maximum calcium, sodium, chloride, sulfate, and TDS concentrations were 610, 4,200, 9,000, 1,400, and 11,500 mg/L, respectively. These data show some influence of other groundwater systems (e.g., *Kd*/Maha aquifer) or the saline wetlands present in the project area.

**Table 2-3: Statistical results of water quality analyses from groundwater samples collected in or near the project area, from Quaternary surficial aquifer wells. Units are in milligrams per liter unless stated otherwise. Data are from the USGS NWIS, Lower Platte North NRD, and Nemaha NRD (NA- not analyzed; N- number of samples).**

| Quaternary Surficial Aquifers | Minimum | 1st Quartile | Median | Mean | 3rd Quartile | Maximum | NA's | N |
|---|---|---|---|---|---|---|---|---|
| **Well depth, in feet** | 15.3 | 42.9 | 70.4 | 95.2 | 118 | 422 | 27 | 751 |
| **Water temperature, in degrees C** | 5.90 | 12.0 | 13.0 | 13.2 | 14.0 | 26.1 | 72 | 706 |
| **Specific conductance, in µS/cm at 25°C** | 243 | 521 | 610 | 1,110 | 781 | 28,700 | 13 | 765 |
| **pH, in standard units** | 5.90 | 7.10 | 7.20 | 7.27 | 7.50 | 8.60 | 266 | 512 |
| **Dissolved oxygen** | 0.10 | 0.30 | 0.80 | 2.18 | 3.70 | 11.1 | 179 | 599 |
| **Bicarbonate** | 110 | 304 | 369 | 402 | 426 | 1,280 | 683 | 95 |
| **Calcium** | 2.50 | 60.0 | 72.6 | 81.3 | 89.7 | 610 | 0 | 778 |
| **Magnesium** | 0.40 | 12.8 | 16.1 | 19.5 | 20.8 | 189 | 0 | 778 |
| **Sodium** | 6.90 | 24.4 | 30.4 | 58.6 | 43.2 | 4,200 | 32 | 746 |
| **Sodium adsorption ratio** | 0.16 | 0.65 | 0.88 | 1.58 | 1.19 | 120 | 34 | 744 |
| **Potassium** | 1.32 | 3.60 | 6.40 | 6.95 | 8.47 | 69.4 | 61 | 717 |
| **Chloride** | 0.00 | 6.62 | 13.6 | 141 | 23.0 | 9,000 | 0 | 778 |
| **Sulfate** | 1.00 | 27.9 | 62.0 | 89.5 | 92.3 | 1,400 | 1 | 777 |
| **Fluoride** | 0.20 | 0.30 | 0.37 | 0.40 | 0.40 | 3.20 | 402 | 376 |
| **Silicate** | 1.30 | 29.0 | 31.3 | 31.3 | 34.0 | 53.0 | 376 | 402 |
| **TDS** | 108 | 326 | 374 | 491 | 480 | 11,500 | 61 | 717 |

### *2.4.2 Bedrock Aquifer Water Quality*

Water quality within the bedrock aquifers—inclusive of *Kd* and Paleozoic limestones and shales—varies considerably by location and depth. For example, groundwater quality in the *Kd* in eastern Nebraska varies from (1) a Ca(±Mg)$HCO_3$-type water associated with precipitation and where the *Kd*/Maha aquifer is unconfined, (2) a $CaSO_4$ and Ca-Na $SO_4$-type water associated with meltwater from Pleistocene glaciers and where the confining unit is thick, or (3) mixed waters of either $CaSO_4$ and Ca-Na $SO_4$-type water or NaCl-type water, which represent a possible interaction of the first two types of water or recharge waters have been displaced by NaCl at depth (Gosselin et al., 2001). In the project area, water quality in the *Kd* generally varies between a Ca(±Mg)$HCO_3$ and a Ca-Na $SO_4$-type water (Appendix 5).

In areas where the *Kd* is unconfined or subject to recharge from precipitation, water can be potable. Concentrations of TDS at these locations can be 500 mg/L or less (Ellis, 1984), whereas elsewhere groundwater in the *Kd* can be highly mineralized as shown with some TDS concentrations ranging from 29,000 to 44,000 mg/L. The previous range of TDS concentrations are an example of what can affect an AEM survey, which could potentially lead to an improper hydrogeologic interpretation.

Four times as many wells were sampled from the *Kd* as compared to Paleozoic sources. Consequently, most of the statistical analyses of the water-quality data are weighted on wells in the *Kd*. However, since median and maximum/minimum results are discussed, weighted means were not calculated. The

median specific conductance value from water-quality samples collected from bedrock wells was 802 µS/cm.

**Table 2-4: Statistical results of water quality analyses from groundwater samples collected in or near the project area from bedrock aquifer wells. Units are in milligrams per liter unless stated otherwise. Data are from the USGS NWIS, Lower Platte North NRD, and Nemaha NRD (NA- not analyzed; N- number of samples).**

| Bedrock Aquifers | Minimum | 1st Quartile | Median | Mean | 3rd Quartile | Maximum | NA's | N |
|---|---|---|---|---|---|---|---|---|
| **Well depth, in feet** | 39.0 | 129 | 170 | 228 | 192 | 2,650 | 6 | 53 |
| **Water temperature, in degrees C** | 11.0 | 12.5 | 13.5 | 13.8 | 14.4 | 18.0 | 10 | 49 |
| **Specific conductance, in µS/cm at 25°C** | 337 | 570 | 802 | 4,400 | 1,280 | 62,700 | 3 | 56 |
| **pH, in standard units** | 6.70 | 7.00 | 7.10 | 7.36 | 7.80 | 8.50 | 4 | 55 |
| **Dissolved oxygen** | 0.10 | 4.55 | 6.75 | 6.14 | 8.83 | 10.7 | 35 | 24 |
| **Bicarbonate** | 180 | 282 | 332 | 392 | 428 | 980 | 32 | 27 |
| **Calcium** | 3.00 | 55.1 | 71.1 | 93.4 | 102 | 430 | 0 | 59 |
| **Magnesium** | 0.40 | 14.0 | 18.5 | 32.7 | 22.5 | 268 | 0 | 59 |
| **Sodium** | 13.7 | 26.9 | 44.2 | 930 | 149 | 16,600 | 1 | 58 |
| **Sodium adsorption ratio** | 0.31 | 0.73 | 1.25 | 52.2 | 3.44 | 1,300 | 1 | 58 |
| **Potassium** | 2.12 | 3.73 | 4.80 | 9.48 | 9.20 | 98.0 | 3 | 56 |
| **Chloride** | 0.67 | 5.56 | 13.0 | 1,220 | 62.5 | 24,400 | 0 | 59 |
| **Sulfate** | 4.60 | 24.6 | 52.0 | 318 | 169 | 2,950 | 0 | 59 |
| **Fluoride** | 0.10 | 0.30 | 0.30 | 0.93 | 0.50 | 8.40 | 4 | 55 |
| **Silicate** | 6.90 | 24.2 | 29.6 | 29.3 | 35.7 | 58.0 | 5 | 54 |
| **TDS** | 227 | 359 | 487 | 2,890 | 772 | 43,800 | 2 | 57 |

The median calcium, sodium, chloride, sulfate, and TDS concentrations from water samples in bedrock wells were 71.1, 44.2, 13.0, 52.0, and 487 mg/L, respectively (Table 2-4). Median specific conductance values and median concentrations of sodium and TDS were higher in samples from the bedrock wells than the Quaternary wells, but median concentrations of calcium and sulfate were lower. The maximum specific conductance value and maximum concentrations of sodium, chloride, sulfate, and TDS from samples of bedrock wells all were higher than those from the Quaternary wells. Groundwater samples from Quaternary deposits had maximum concentrations of calcium and bicarbonate, likely indicating older groundwater within the bedrock deposits since the $Ca(\pm Mg)HCO_3$, changes to a Ca-Na $SO_4$ and finally to NaCl water.

## 2.5 Water Use

Public supply well locations within the southern ENWRA project area, provided by the NDNR, are displayed in Figure 2-17. The greatest concentrations of public wells are near the more populated areas of Saunders, Douglas, and Sarpy Counties. Registered wells other than public supply wells are found throughout the southern ENWRA area, with irrigation wells being the most numerous. The densest concentrations of irrigation wells are in the northwestern and eastern parts of the LPNNRD as well as in smaller, more scattered areas in the LPSNRD and the central NNRD. Domestic wells are found throughout the southern ENWRA area, with the greatest concentrations in the LPSNRD and the

northwestern extent of the NNRD. Commercial/industrial wells are located typically near population centers, and non-consumptive (geothermal) wells are found throughout the project area. Overall, the distribution of wells of any type (Figure 2-18) demonstrates where aquifer resources are generally lacking. In particular, there are numerous areas of several contiguous square miles where no registered wells of any type exist in the southeastern half of the NNRD.

Figure 2-18 displays the depth to groundwater in the registered wells across the southern ENWRA area. Relatively shallow groundwater (less than 50 ft below the subsurface) is present along the major surface water drainages, as well as beneath the Todd Valley in the LPNNRD. The static water level depth is more variable in the western half of the LPSNRD and the portions of the LPNNRD beyond the major drainages and Todd Valley, where depths can approach 200 ft bgl. Amongst the more scattered distribution of registered wells in the NNRD, static water levels are typically 0 to 50 ft bgl, with the exception of an area in northwest Johnson County that coincides with a paleovalley where depths typically range from 100-200 ft bgl. Immediately west of the survey area in the UBBNRD and LBBNRD, static water levels are typically 50-100 ft bgl.

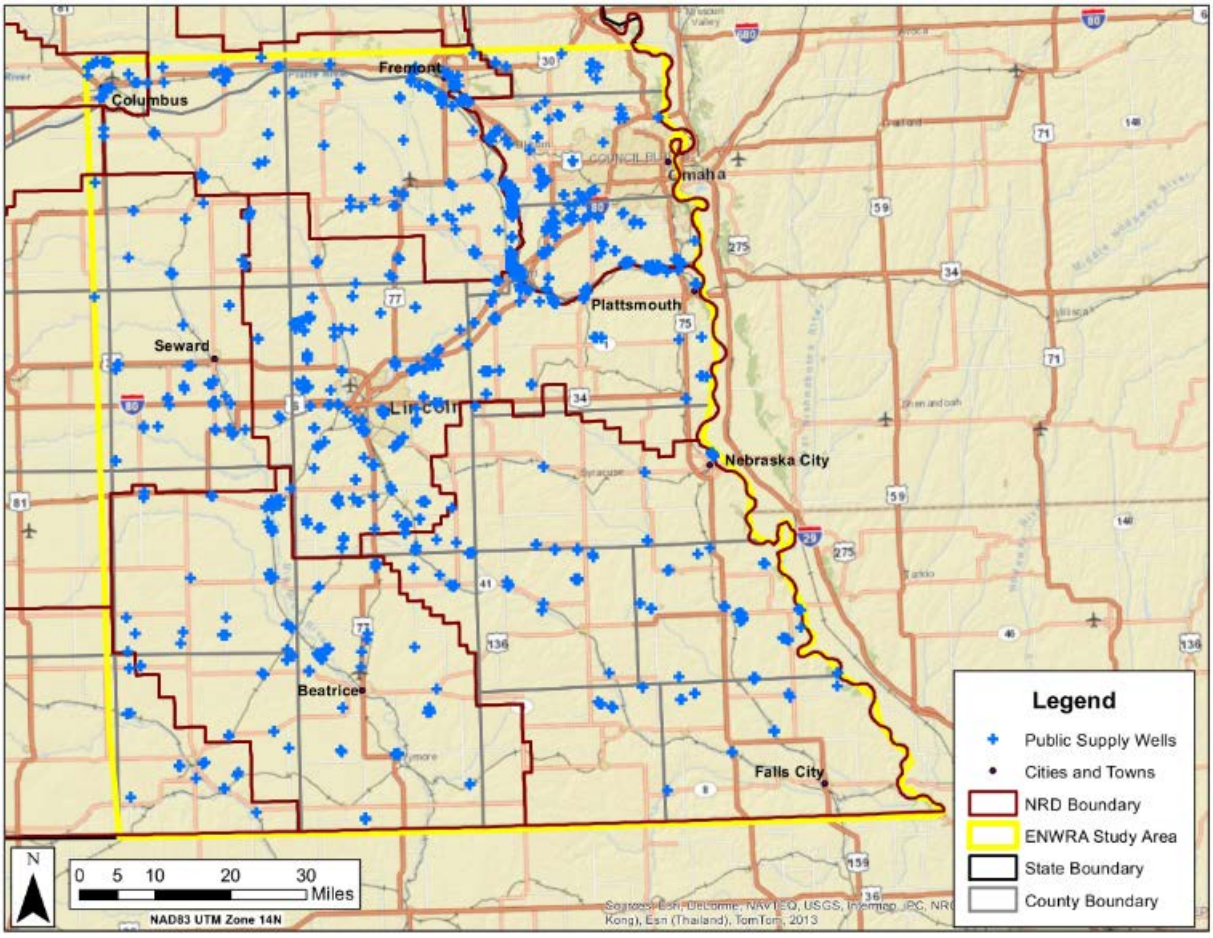



**Figure 2-17: Public supply wells within the southern ENWRA project area.**

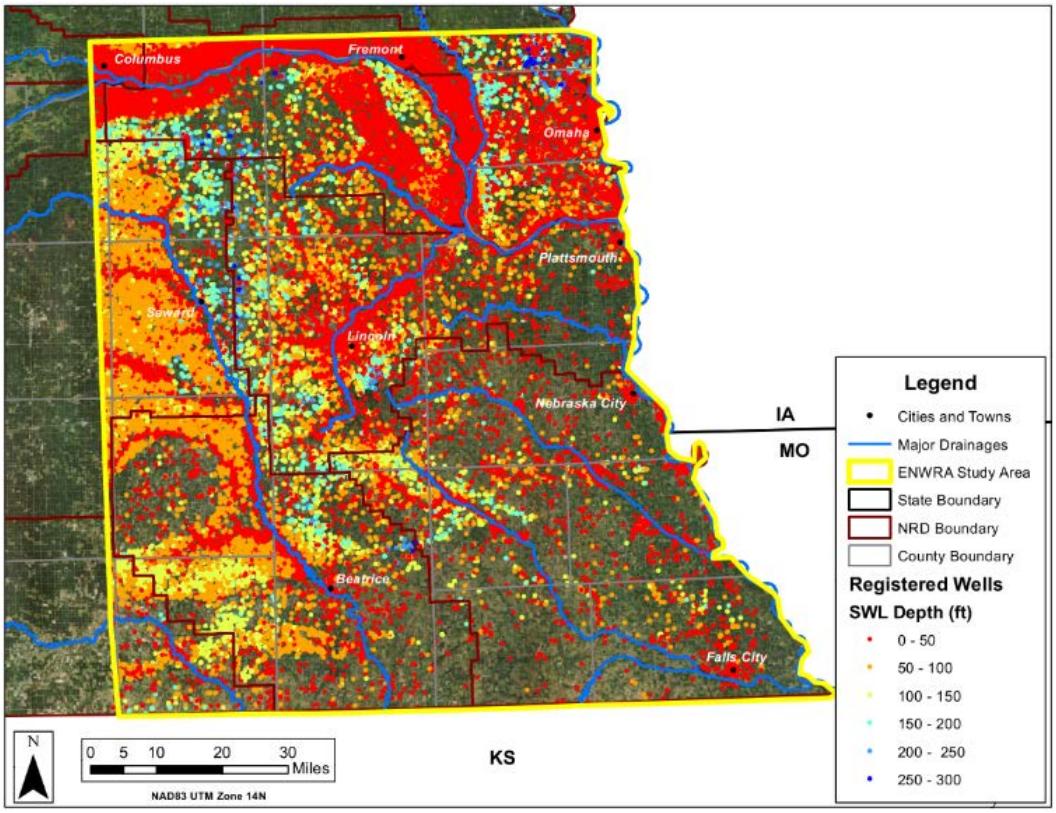



**Figure 2-18: Registered wells in the southern ENWRA project area with depth to static water level indicated by color.**

Figure 2-19 demonstrates the increase in the number of registered irrigation wells across the southern ENWRA area from the mid-20$^{th}$ century through the spring of 2015 (DNR registered well database, accessed May, 2015). Before the 1960s, irrigation wells were mainly prevalent along the Platte River valley in the LPNNRD and in the far western extent of the project area. Over time, technological advancements of pumps and center-pivot systems allowed for more widespread implementation of irrigation above deeper aquifers and more variable terrain across Nebraska. However, in southeastern Nebraska, the lack of productive aquifer materials limited irrigation well development, even with improvements in pump and distribution technology. Irrigation well density increased modestly in the LPSNRD and the NNRD by the 1970s, but overall the development of groundwater as an irrigation source was less robust than other regions of the state during this era. The largest gains in irrigation wells occurred along the Platte River valley and in the far western portion of the project area beneath the UBBNRD and LBBNRD. By the 2000s, another pulse of irrigation well development occurred in the NNRD in an area that corresponds with mapped paleovalleys displayed in Figure 2-12.

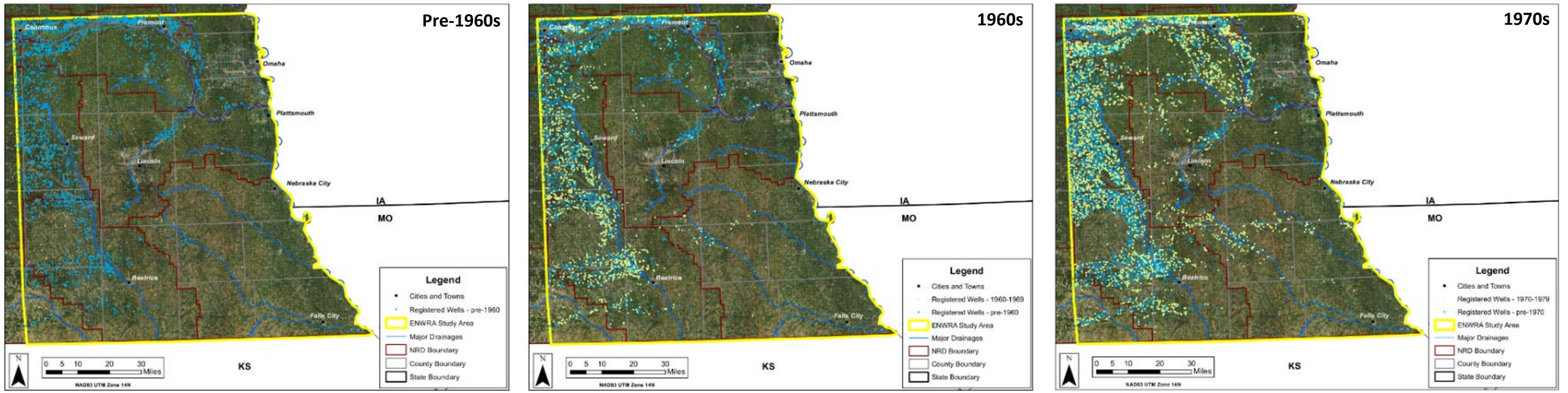



**Figure 2-19: Progression of irrigation well development from the pre-1960s (upper left) to 2015 (lower right). Blue dots indicate existing wells, yellow dots indicate new wells constructed during the indicated decade (NDNR).**

# 3 Additional Background Information

Various sources of background information were used to interpret the AEM data, which is discussed in Section 5. Section 3 discusses the background data sources and the methods used to prepare this data for use in the interpretation.

## 3.1 Borehole Data

Borehole data for this project consisted of a combination of lithologic, stratigraphic, and downhole geophysical logs. Appendix 4 contains all borehole data utilized. The majority of borehole data were acquired from the Nebraska Statewide Test Hole Database (Conservation and Survey Divsion, 2014), which contains information from boreholes drilled between 1930 and 2003 by the CSD and other cooperating agencies. CSD test holes drilled subsequent to 2003 were provided as a dataset directly from ENWRA and are shown in Figure 3-1. Additional borehole data were also acquired from the Nebraska Oil and Gas Conservation Commission (NOGCC) (Nebraska Oil and Gas Conservation Commision, 2008).

The CSD test holes are more numerous and generally much shallower than the oil and gas boreholes, typically less than 500 feet in depth and most do not extend far into bedrock material. Oil and gas boreholes can extend to depths greater than the AEM earth-resistivity models (discussed in Section 5). However, they typically lack the level of near-surface detail provided by the CSD boreholes.

The lithologic and stratigraphic borehole data from both the CSD and oil and gas boreholes were examined in detail. In some instances, specific interval descriptions were generalized to present both datasets with concise lithology and stratigraphy logs. A total of 953 lithology logs and 869 stratigraphy logs were obtained from CSD boreholes; 28 lithology logs and 29 stratigraphy logs were obtained from NOGCC oil and gas boreholes. The locations of the boreholes containing lithology and stratigraphy data used are depicted in Figure 3-2 and Figure 3-3.

Geophysical logs from both CSD boreholes and oil and gas boreholes contained resistivity logs collected from a variety of downhole resistivity and/or induction tools. A total of 60 resistivity logs were obtained from CSD boreholes, with all of these logs from boreholes drilled since 1998. The geophysical logs from boreholes drilled after 1998 contain a combination of natural gamma, self- potential, single-point resistivity, 16-inch normal resistivity, 64-inch normal resistivity, lateral resistivity, specific conductance of borehole fluid, and borehole fluid temperature data. One geophysical log was obtained from an oil and gas well. These data were acquired as an image of the original paper log which was then converted into digital format. Oil and gas borehole geophysical logs contain a combination of self-potential, short normal resistivity, lateral resistivity, spherically-focused resistivity and deep- and medium-induction log data. A variety of factors can lead to geophysical borehole data that does not accurately measure subsurface physical properties, such as drilling fluid infiltration and improper or infrequent borehole tool calibration.

Each resistivity log was compared to the initial AEM data for correlation, both in magnitude of the reported resistivity values and structural interval delineation. A total of 25 resistivity logs were

considered to be high quality data and located in close proximity to the AEM flight lines. These logs were used as constraints in the final AEM data inversion (Section 4.6). The locations of the boreholes containing geophysical logs used in this project are displayed in Figure 3-4.

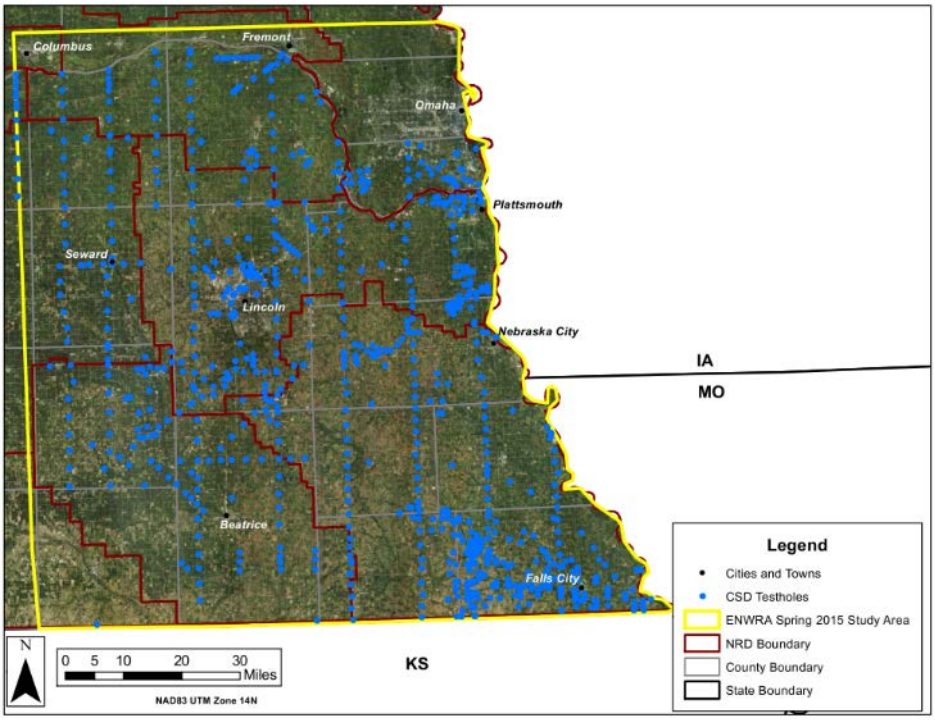



**Figure 3-1: Locations of CSD tests holes examined in the southern ENWRA project area.**

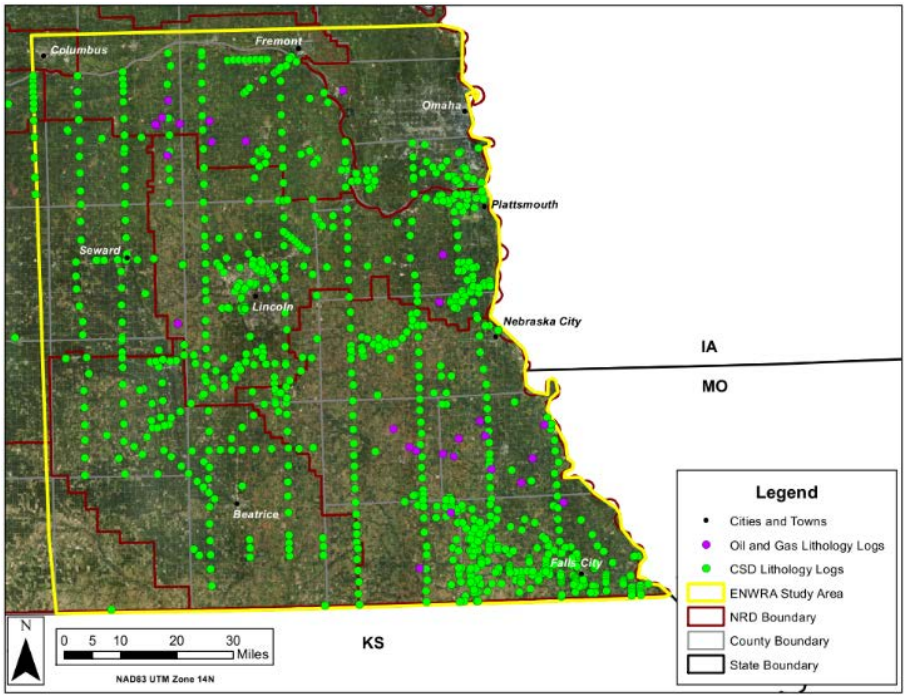



**Figure 3-2: Locations of boreholes used containing lithologic information in the southern ENWRA project area.**

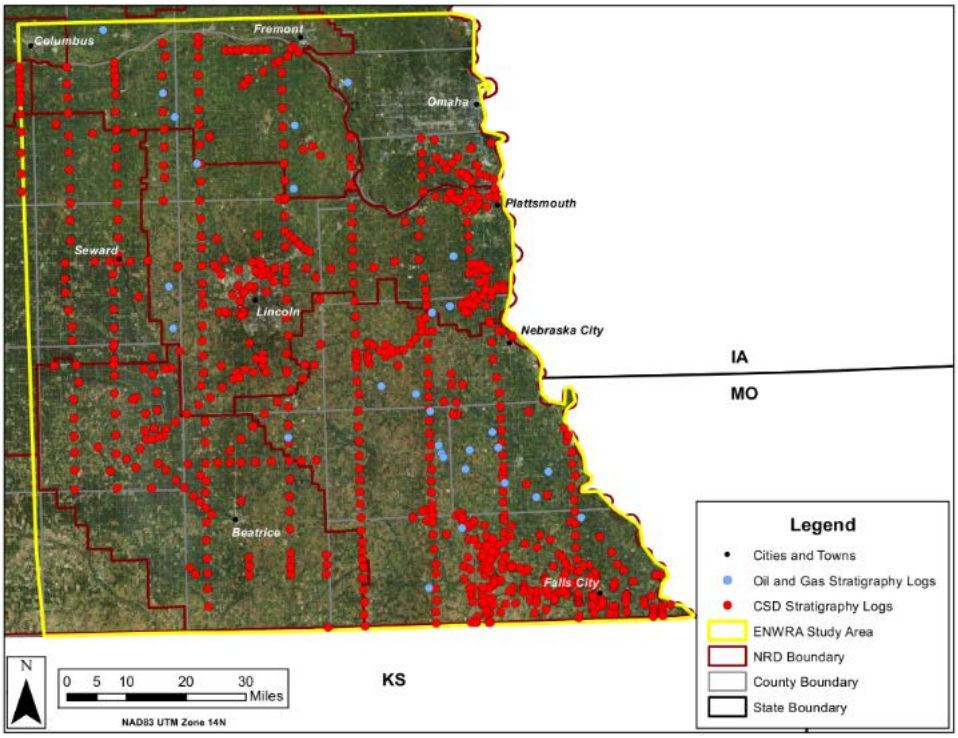



**Figure 3-3: Locations of boreholes used containing stratigraphic information in the southern ENWRA project area.**

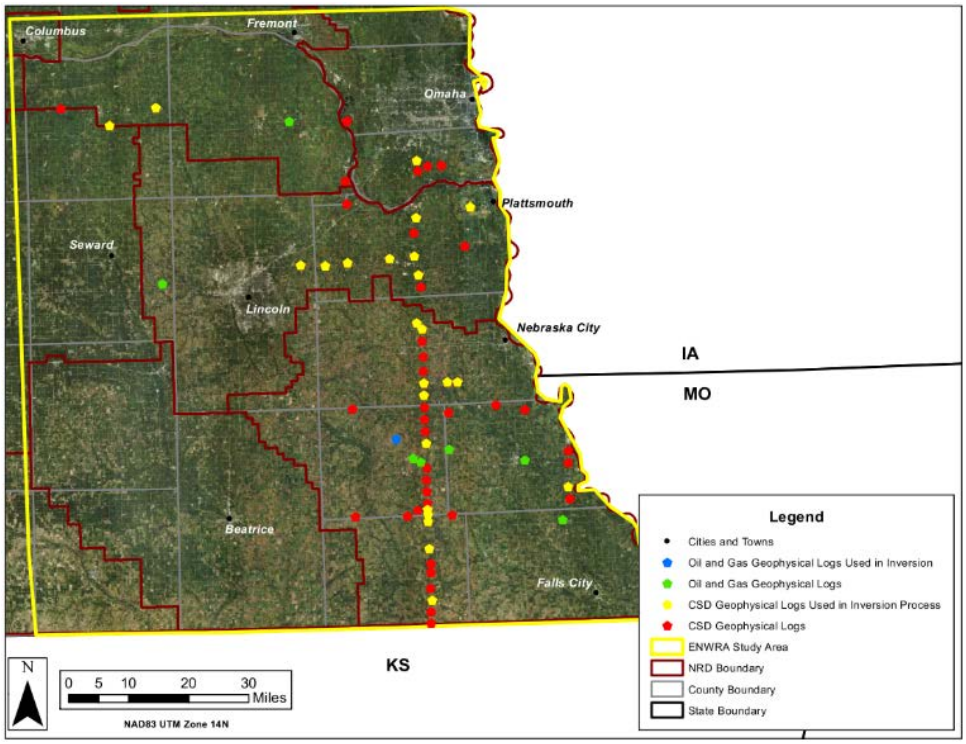



**Figure 3-4: Locations of boreholes containing geophysical logs in the southern ENWRA project area.**

## 3.2 Historic Geologic Cross Sections

Several published and previously unpublished geologic cross sections were digitized and geo-referenced (Divine et al., 2010; Korus et al., 2012). The quality of the sections ranged from rough pencil drafts to publishable quality cross sections. Table 3-1 lists the cross sections used and Figure 3-5 shows their locations.

**Table 3-1: Geologic cross sections from OFR-109 that were digitized and geo-referenced (Divine et al., 2010; Korus et al., 2012).**

| Image Name | Associated Line Name |
|---|---|
| Washington_Pawnee.jpg | 1811E0112E |
| Thurston_Pawnee.jpg | 2509E0110E |
| Douglas_Pawnee.jpg | 1610E0210E |
| Seward_Cass.jpg | 1103E1113E |
| SAU-205_Valparaiso.jpg | 1405E1205E |
| Saunders_Gage_1.jpg | 1607E0208E |
| Butler_secC.jpg | 1603E1203E |
| Saline_EW_north.jpg | 0801W0805E |
| Hamilton_Lancaster.jpg | 1105W1107E |
| SaltCreek.jpg | 1207E1108E |
| Butler_secA.jpg | 1601E1201E |
| Gage_NS_west.jpg | 0705E0105E |

Corel Draw was used to digitize each cross section and an example is shown in Figure 3-6. Care was taken to properly place identified CSD borings as these were used to geo-reference each image. Each digitized image was broken up into smaller panels, where each panel began and ended at a known borehole. Encom Profile Analyst (PA) (pbEncom, 2015) was used to apply positional data to each panel. Figure 3-7 shows the cross-sections in a 3D view in PA. These digitized profiles were used in the interpretation of the AEM results discussed in Section 5.

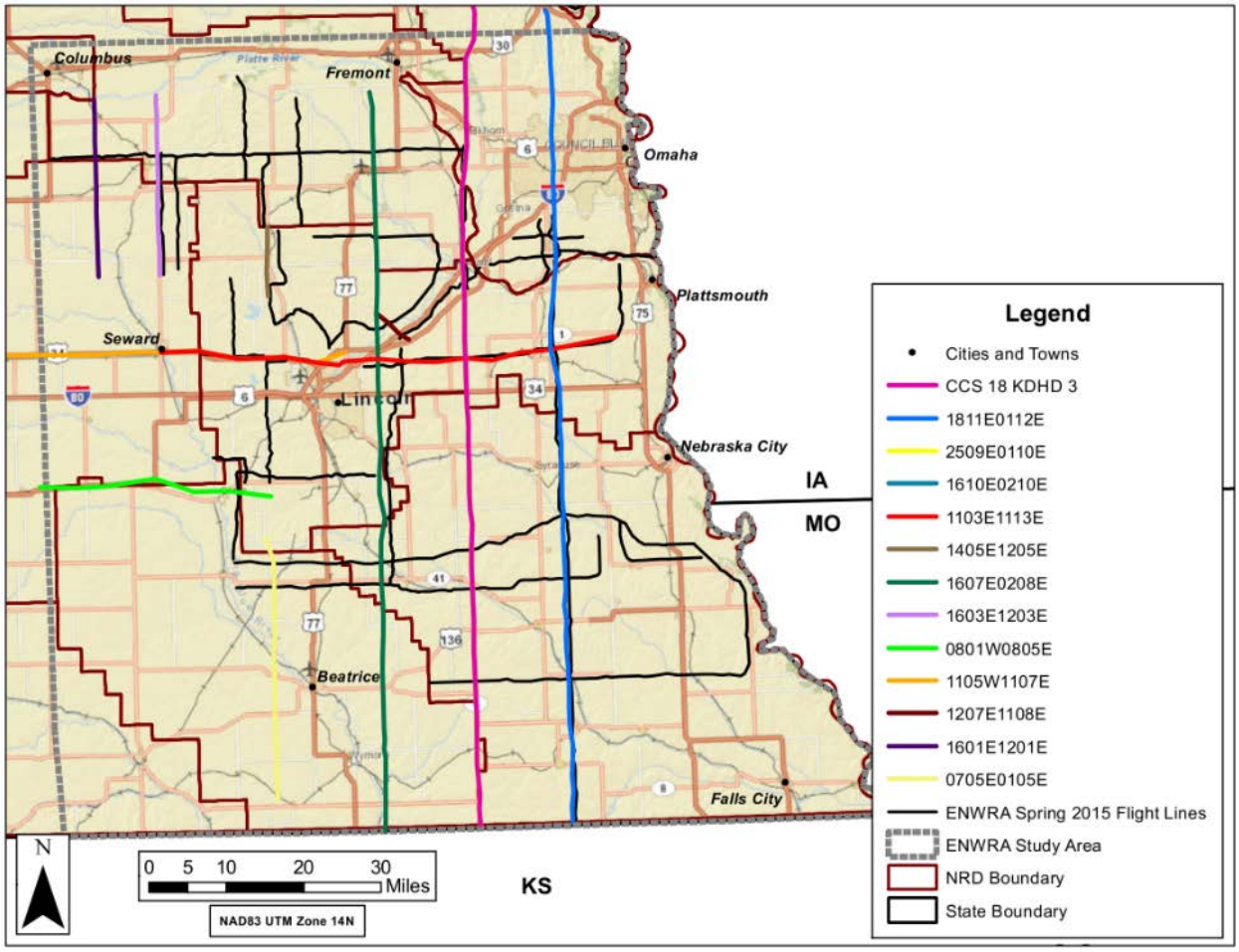



**Figure 3-5: Locations of geologic cross sections examined within the southern ENWRA project area.**

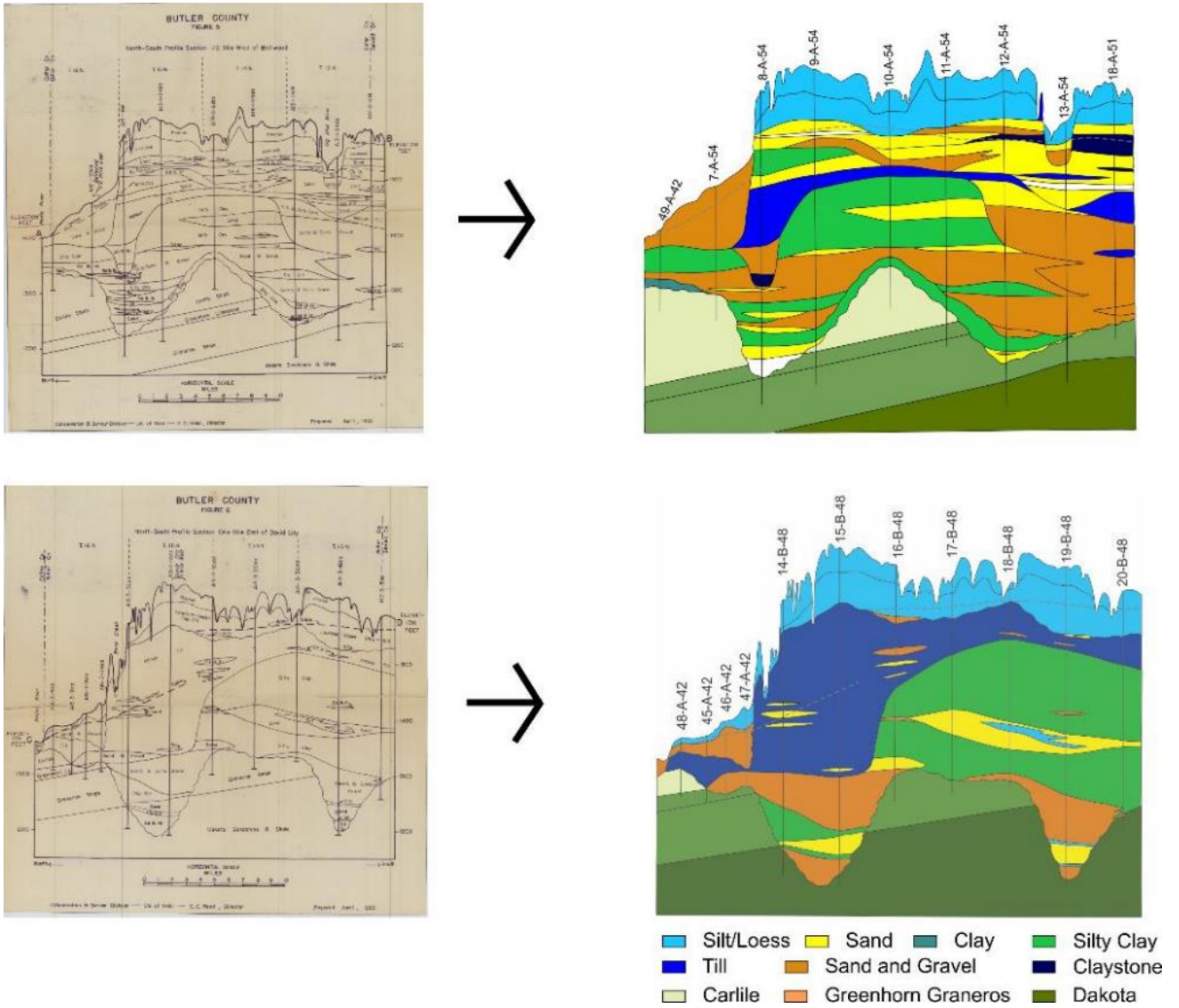



**Figure 3-6: Original cross section from CSD OFR 109 (left) and the digitized cross section (right). CSD test hole locations were used to orient images in 3D space. (Divine et al., 2010; Korus et al., 2012). Note that blank areas in the digitized cross section indicate where no lithologic information was available on the original cross section.**

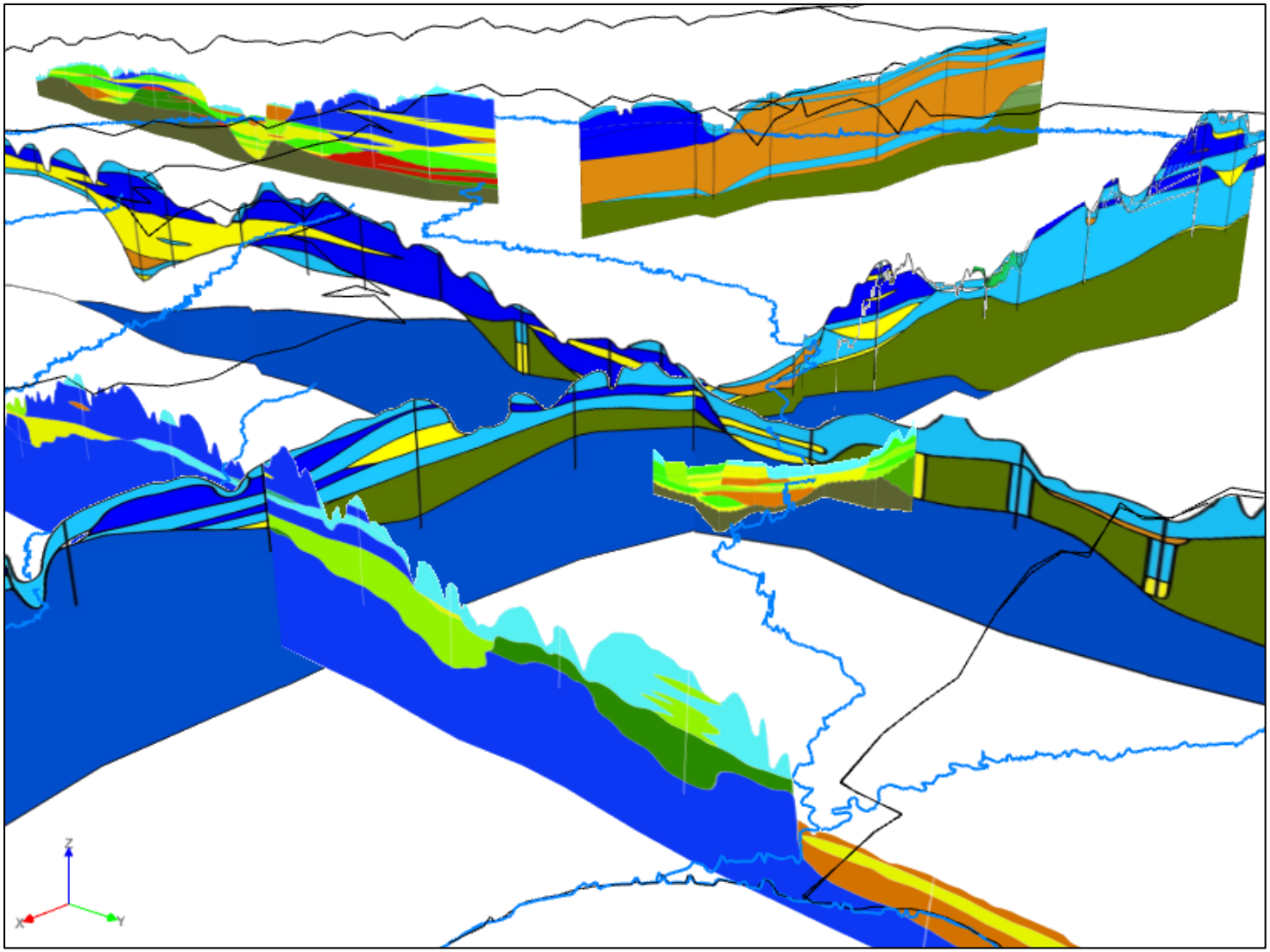



**Figure 3-7: Example 3D view of geo-referenced geologic cross sections used to supplement the AEM interpretation of the southern ENWRA project area.**

# 4 Geophysical Methodology, Acquisition and Processing

## 4.1 Geophysical Methodology

AEM (Airborne Transient Electromagnetic (TEM)) investigations provide characterization of electrical properties of earth materials from the land surface downward using electromagnetic induction. Figure 4-1 gives a conceptual illustration of the airborne TEM method.

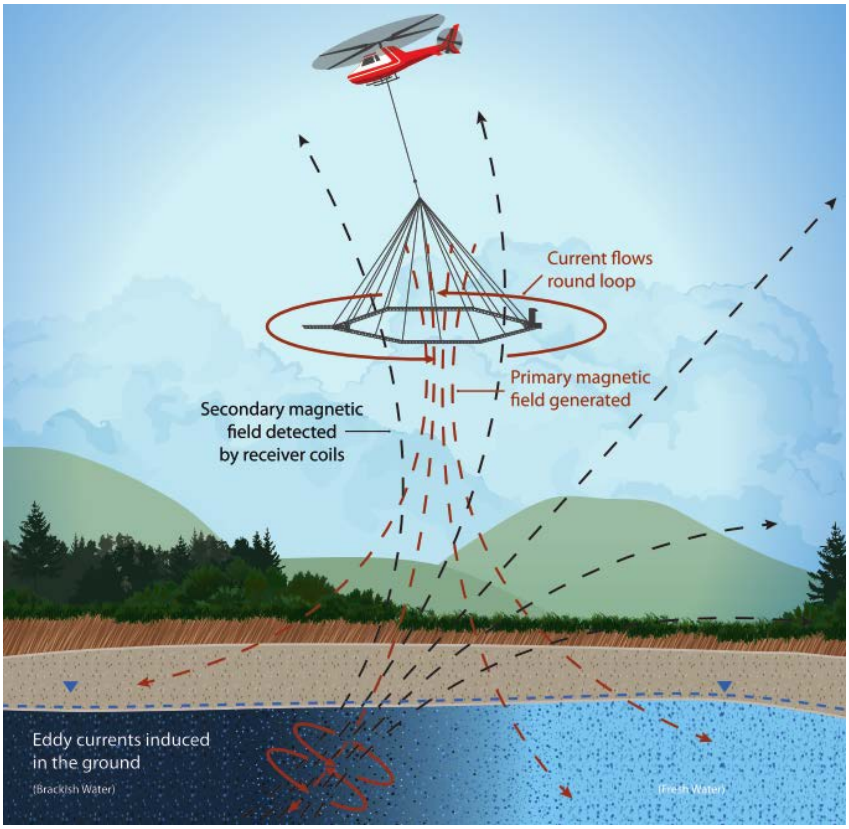



**Figure 4-1: Schematic of an AEM survey.**

To collect TEM data, an electrical current is sent through a large loop of wire consisting of multiple turns which generates an electromagnetic (em) field. This is called the transmitter (Tx) coil. After the em field produced by the Tx coil is stable, it is switched off as abruptly as possible. The em field dissipates and decays with time, traveling deeper and spreading wider into the subsurface. The rate of dissipation is dependent on the electrical properties of the subsurface (controlled by the material composition of the geology including the amount of mineralogical clay, the water content, the presence of dissolved solids, the metallic mineralization, and the percentage of void space). At the moment of turnoff, a secondary em field, which also begins to decay, is generated within the subsurface. The decaying secondary em field generates a current in a receiver (Rx) coil, per Amperes Law. This current is measured at several different moments in time (time gates). From this current, the time rate of decay of the magnetic field, B, is determined (dB/dt). When compiled in time, these measurements become a “sounding” at that location. Each AEM measurement produces an em sounding at one point on the surface.

The sounding curves are numerically inverted to produce a model of subsurface resistivity as a function of depth. Inversion relates the measured geophysical data to probable physical earth properties. Figure 4-2 shows an example of a dual-moment TEM dB/dt sounding curve and the corresponding inverted electrical resistivity model.

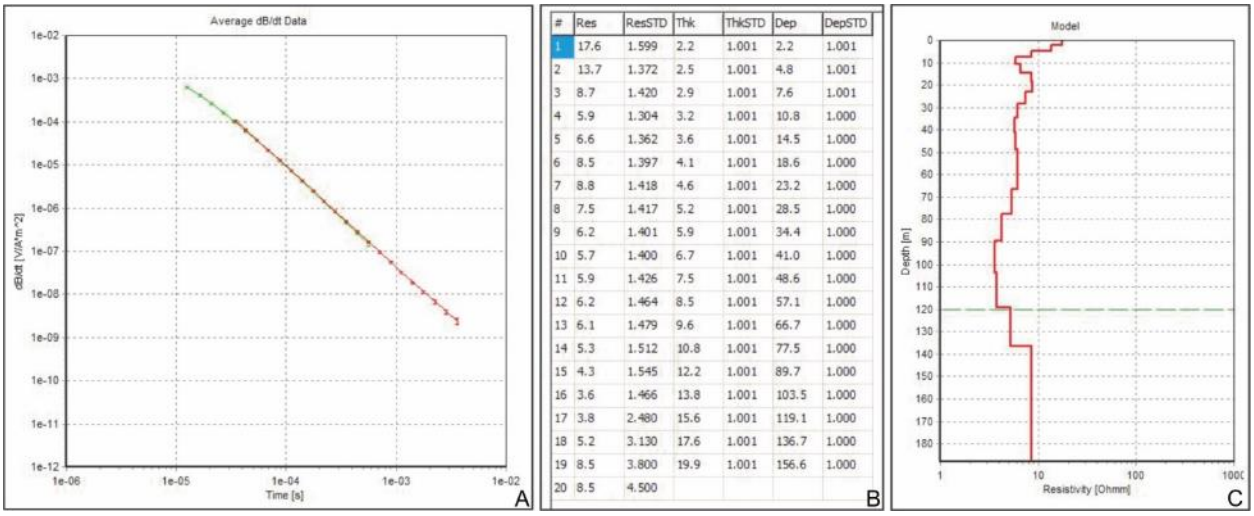



**Figure 4-2: A) Example of a dB/dt sounding curve. B) Corresponding inverted model values. C) Corresponding resistivity earth model.**

## 4.2 Utility Mapping

The primary source of noise in geophysical electromagnetic surveys are other electromagnetic devices that are part of typical municipal utility infrastructure. These include, for example, power lines, railroads, pipelines, and water pumps. Prior to AEM data acquisition, during the survey design of the ENWRA area, three types of utilities (pipelines, railroads, and power lines) were located. Various public power districts in eastern Nebraska provided power line locations, in either a Google Earth ".kmz" or ".cad" format that were then converted to a Geographic Information Systems (GIS) Arc shapefile format. Public power entities that provided power line location data included: Auburn Board of Public Works, Burt County Power District, Butler County Power District, Cedar-Knox Power District, City of Freemont, Cornhusker Public Power District, Cuming County Power District, Elkhorn Rural Public Power District, Lincoln Electric Systems, Loup Power District, Nebraska Public Power District, Nemaha-Marshall Electric Cooperative, Norris Public Power District, North Central Public Power District, Northeast Nebraska Public Power District, Omaha Public Power District, Polk County Rural Public Power District, Seward County Public Power District, and the Stanton County Public Power District.

A GIS Arc shapefile of railroads in Nebraska was downloaded from the United States Department of Agriculture's Natural Resource Conservation Service (United States Department of Agriculture, 2014) and a shapefile of the pipelines in Nebraska was purchased from Platts (Platts, 2014). Maps, shown in Figure 4-3, of the three utilities were exported in GeoTIFF and .kmz formats and were used during data processing and interpretation.

The locations of the flight lines were modified from a regularly spaced design grid to one with flight lines optimized in order to avoid electromagnetic coupling with the previously mentioned utilities.

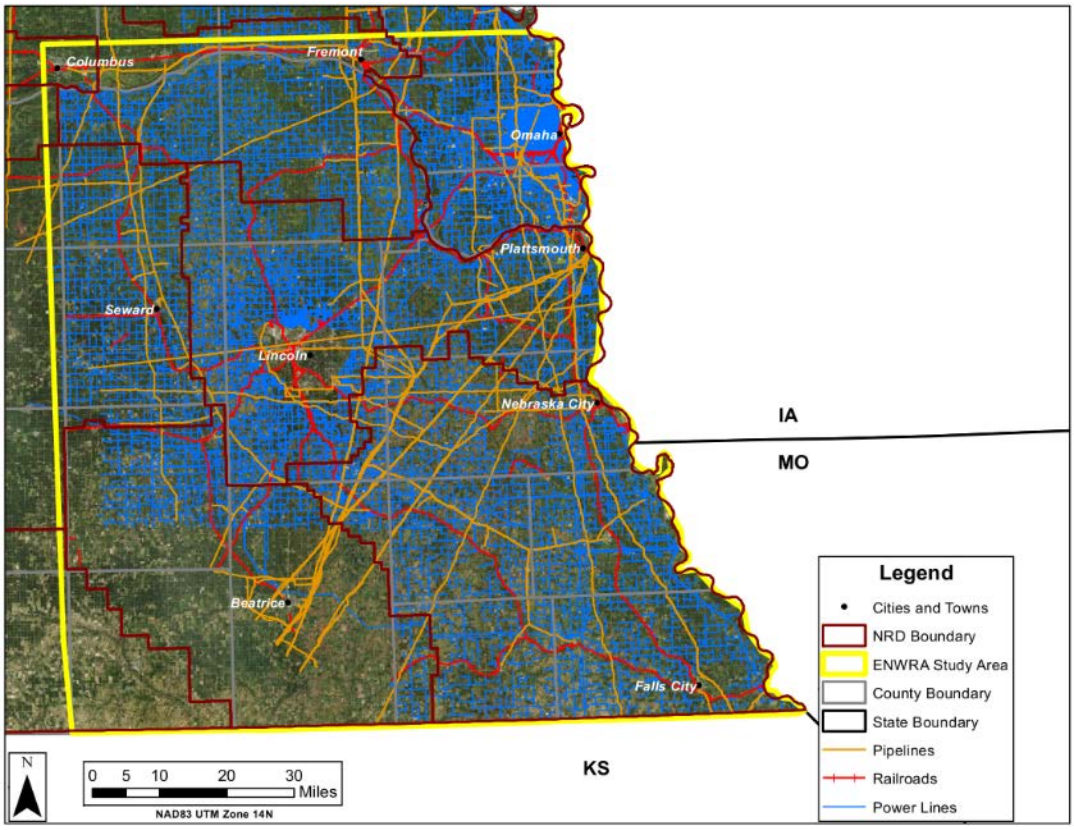



**Figure 4-3: Map of the expected utilities in the southern ENWRA project area.**

## 4.3 AEM Survey Instrumentation

AEM data were acquired using the SkyTEM 508 (508) airborne electromagnetic system (SkyTem Airborne Surveys Worldwide, 2015). The 508 is a rigid frame, dual-magnetic moment (Low and High) transient airborne electromagnetic (TEM) system. The area of the 508 Tx coil is 5,769.5 ft2 (536 m2) and the coil contains eight (8) turns of wire. A peak current of 8.6 amps is passed through one turn of wire in the Tx for Low Moment measurements and a peak current of 127 amps is passed through the eight turns of wire for High Moment measurements. This results in peak Tx Low and High magnetic moments of ~4,600 Ampere-meter-squared ($A*m^2$) and ~540,000 $A*m^2$, respectively.

The SkyTEM 508 system utilizes an offset Rx positioned slightly behind the Tx resulting in a 'null' position which is a location where the intensity of the primary field from the system transmitter is minimized. This is desirable because you want to minimize the amplitude of the primary field at the Rx to maximize the sensitivity of the Rx to the secondary fields. The SkyTEM 508 multi-turn Rx coil has an effective area of 1,130 $ft^2$ (105 $m^2$). In addition to the Tx and Rx that constitute the TEM instrument, the SkyTEM 508 is also equipped with a Total Field magnetometer and data acquisition systems for both of these instruments. The SkyTEM 508 also includes two each of laser altimeters, inclinometers/tilt meters, and differential global positioning system (DGPS) receivers. Positional data from the frame mounted DGPS receivers are recorded by the AEM data acquisition system. The magnetometer includes a third DGPS receiver whose positional data is recorded by the magnetometer data acquisition system. Figure 4-4 gives a simple illustration of the SkyTEM 508 frame and instrument locations. The image is viewed along

the +z axis looking at the horizontal x-y plane. The axes for the image are labeled with distance in meters. The magnetometer is located on a boom off the front of the frame (right side of image). The Tx coil is located around the octagonal frame and the Rx Coil is located at the back of the frame (left side of image).

The coordinate system used by the 508 defines the +x direction as the direction of flight, the +y direction is defined 90° to the right and the +z direction is downward. The center of the transmitter loop, mounted to the octagonal SkyTEM frame is used as the origin in reference to instrumentation positions. Table 4-1 lists the positions of the instruments (in feet) and Table 4-2 lists the corners of the transmitter loop (marked with red circles in Figure 4-4).

The DGPS and magnetometer mounted on the frame of the SkyTEM508 require the use of base stations, which are located on the ground and are positioned in an area with low cultural noise. Data from the magnetometer and DGPS base stations were downloaded each day following completion of the AEM flights. The DGPS and magnetometer base stations were placed at the Universal Transverse Mercator (UTM) coordinate system locations listed in Table 4-3.

The horizontal geodetic reference used is North American Datum of 1983 (NAD83 in feet). All elevations are from USGS's National Elevation Dataset, referenced to the North American Vertical Datum of 1988; with feet as the unit of measurement.

For this ENWRA survey, the 508 system was flown at an average speed of 50.0 mi/hr (80.5 km/hr) at an average flight height of 141.4 ft (43.1 m) above land surface, using the sling-load cargo system of an AS350 FX2 helicopter. Figure 4-5 displays pictures of the 508 system on the ground and in operation.

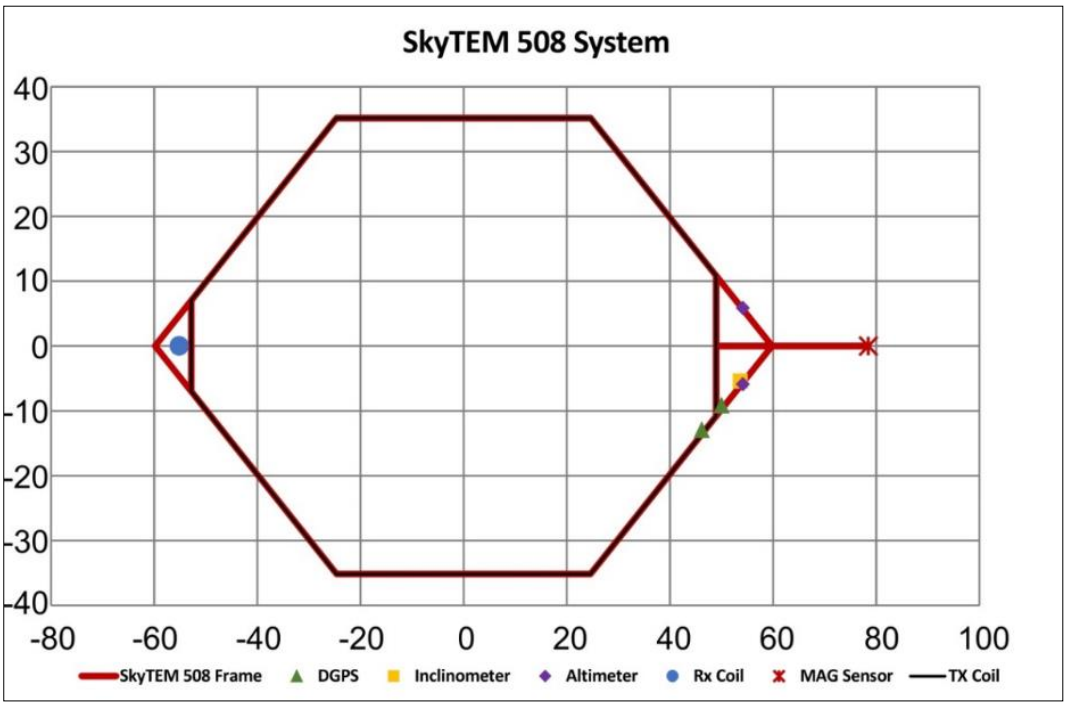



**Figure 4-4: SkyTEM 508 frame including instrumentation locations and X and Y axes.**

**Table 4-1: Positions of instruments on the SkyTEM508 frame, using the center of the frame as the origin in feet.**

| | DGPS 1 | DGPS 2 | Inclinometer 1 | Inclinometer 2 | Altimeter 1 | Altimeter 2 | MAG Sensor | Rx Coil |
|---|---|---|---|---|---|---|---|---|
| **X** | 50.00 | 46.16 | 53.64 | 53.64 | 54.13 | 54.13 | 79.79 | -55.12 |
| **Y** | 9.15 | 12.96 | 5.38 | 5.38 | 5.87 | -5.87 | 0.00 | 0.00 |
| **Z** | -0.52 | -0.52 | -0.39 | -0.39 | -0.39 | -0.39 | -1.51 | -6.56 |

**Table 4-2: Positions of the SkyTEM508 transmitter coil corners, using the center of the frame as the origin in feet.**

| Tx Corners | 1 | 2 | 3 | 4 | 5 | 6 | 7 | 8 |
|---|---|---|---|---|---|---|---|---|
| **X** | 24.64 | 48.95 | 48.95 | 24.64 | -24.64 | -52.82 | -52.82 | -24.64 |
| **Y** | 35.17 | 10.86 | -10.86 | -35.17 | -35.17 | -6.99 | 6.99 | 35.17 |

**Table 4-3: Locations of magnetic field base station instruments.**

| Instrument | Easting (ft) | Northing (ft) | UTM Zone |
|---|---|---|---|
| Magnetometer Base Station 1 | 2067151 | 15254064 | 14 N |
| Magnetometer Base Station 2 | 2065339 | 15255616 | 14 N |
| DGPS Base Station | 2065311 | 15255605 | 14 N |



**Figure 4-5: Photos of the SkyTEM508 system on the ground (above) and in suspension beneath the helicopter (below).**

## 4.4 Data Acquisition

All SkyTEM systems are calibrated to a ground test site in Lyngby, Denmark prior to being used for production work (HydroGeophysics Group Aarhus University, 2010; HydroGeophysics Group Aarhus University, 2011; Foged et al., 2013). The calibration process involves acquiring data with the system hovering at different altitudes from 16.4 to 164 ft (5 to 50 m) over the Lyngby site. Acquired data are processed and a scale factor (time and amplitude) is applied so that the inversion process produces the model that approximates the known geology at Lyngby.

For the ENWRA survey, upon installation of the navigational instruments in the helicopter and assembly of the SkyTEM508 system, several test flights were flown to ensure that the equipment was operating within technical specifications. Initial survey set-up procedures included measurement of the transmitter waveforms, verification that the receiver was properly located in a null position, and verification that all positioning instruments were functioning properly. High altitude tests, used to verify system performance, were flown once at the beginning of the survey and repeated throughout the survey. In the field, visual quality control of the operational parameters for the EM and magnetic field sensors including current levels, positioning sensor dropouts, acquisition speed, and system orientation were conducted with proprietary SkyTEM software following each flight.

Airborne data were collected over the survey grids across the project area from 16-21 April 2015 and approximately 685 line-miles (1,102 line-kilometers) were acquired. Various airports and state parks were used as landing and refueling locations. These locations are listed in Table 4-4 and the daily flights lines are shown in Figure 4-6.

**Table 4-4: Airports and state parks used for landing and refueling by date of acquisition.**

| Date | Flight Number | Area Working |
|---|---|---|
| **4/16/2015** | 1 | Crete and Tecumseh, NE |
| **4/16/2015** | 2 | Tecumseh and Pawnee City, NE |
| **4/16/2015** | 3 | Pawnee City and Tecumseh, NE |
| **4/17/2015** | 1 | Tecumseh and Plattsmouth, NE |
| **4/17/2015** | 2 | Plattsmouth and Tecumseh, NE |
| **4/17/2015** | 3 | Tecumseh and Crete, NE |
| **4/20/2015** | 1 | Crete and Wahoo, NE |
| **4/20/2015** | 2 | Wahoo and David City, NE |
| **4/20/2015** | 3 | David City and Wahoo, NE |
| **4/21/2015** | 1 | Wahoo, NE |
| **4/21/2015** | 2 | Wahoo and Plattsmouth, NE |

**Table 4-5: Production log displaying the number of production flights conducted each day and total line miles and kilometers surveyed. A limited number of flight lines did overlap.**

| Date | Production Flights | Line (mi) | Line (km) |
|---|---|---|---|
| **4/16/2015** | 3 | 181.9 | 292.7 |
| **4/17/2015** | 3 | 204.3 | 328.8 |
| **4/20/2015** | 3 | 143.2 | 230.4 |
| **4/21/2015** | 2 | 155.6 | 250.3 |
| | Total | 684.9 | 1102.3 |

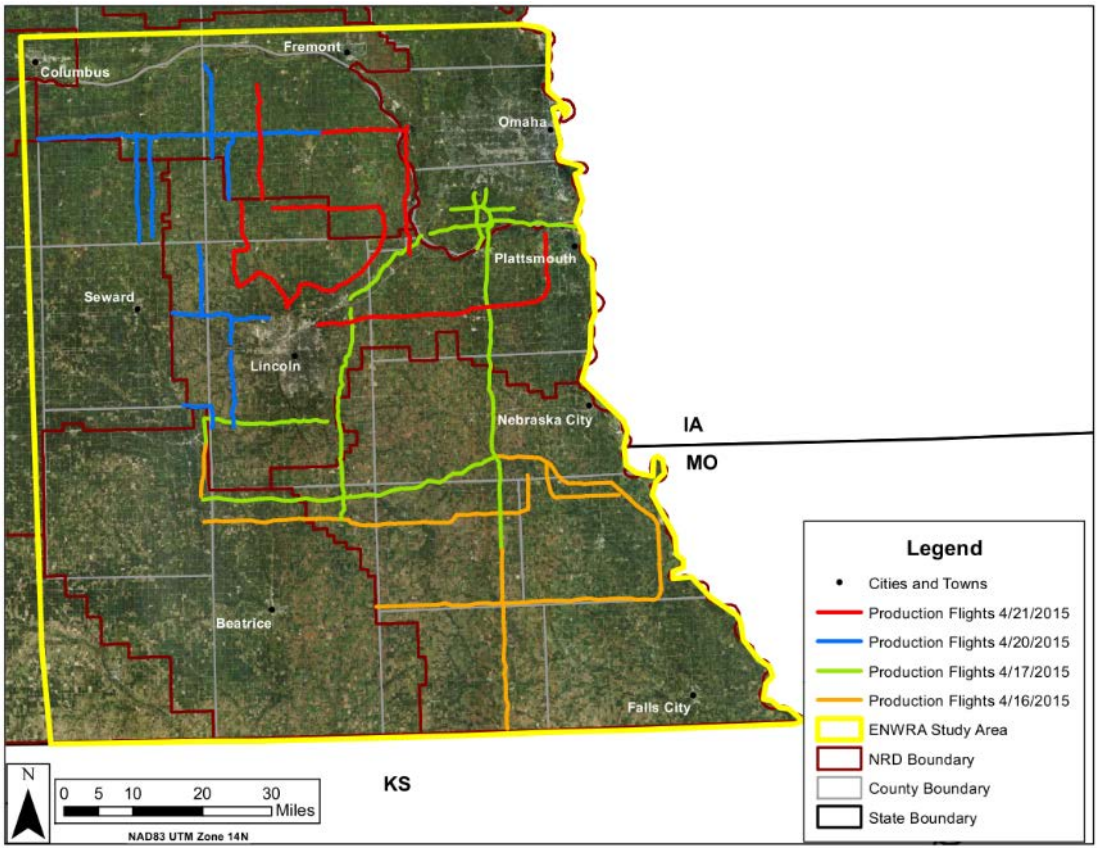



**Figure 4-6: Flights lines as collected by date for the southern ENWRA project area.**

## 4.5 Data Processing

### *4.5.1 Primary Field Compensation*

A standard SkyTEM data acquisition procedure involves testing the acquired raw data by SkyTEM in Denmark for Primary Field Compensation (PFC) prior to continued data processing by XRI (Schamper et al., 2014). The primary field of the transmitter affects the recorded early time gates, which in the case of the Low Moment, are helpful in resolving the near surface resistivity structure of the ground. The Low Moment uses a saw tooth waveform which is calculated and then used in the PFC correction to correct the early time gates.

### 4.5.2 Automatic Processing

The AEM data collected by the 508 were processed using Aarhus Workbench version 4.2.7.2 (HydroGeophysics Group Aarhus University, 2011). Automatic processing algorithms provided within the Workbench program are initially applied to the AEM data. GPS locations were filtered using a stepwise, second-order polynomial filter of 9 seconds with a beat time of 0.5 seconds, based on flight acquisition parameters. The AEM data are corrected for tilt deviations from level and so filters were also applied to both of the tilt meter readings with a median filter of 3 seconds and an average filter of 2 seconds. The altitude data were corrected using a series of two polynomial filters. The lengths of both eighth-order polynomial filters were set to 30 seconds with shift lengths of 6 seconds. The lower and upper thresholds were 1 and 100 meters, respectively.

Trapezoidal spatial averaging filters were next applied to the AEM data. The times used to define the trapezoidal filters for the Low Moment were $1.0x10^{-5}$ sec, $1.0x10^{-4}$ sec, and $1.0x10^{-3}$ sec with widths of 5, 8 and 10 seconds. The times used to define the trapezoid for the High Moment were $1.0x10^{-4}$ sec, $1.0x10^{-3}$ sec, and $1.0x10^{-2}$ sec with widths of 8, 10, and 20 seconds. The trapezoid sounding distance was set to 2.5 seconds and the left/right setting, which requires the trapezoid to be complete on both sides, was turned on. The spike factor and minimum number of gates were both set to 25 percent for both soundings. Lastly, the locations of the averaged soundings were synchronized between the two moments.

### 4.5.3 Manual Processing and Laterally-Constrained Inversions

Following implementation of the automatic filtering, the AEM data were manually examined using a sliding two minute time window. The data were examined for possible electromagnetic coupling with surface and buried utilities and metal, as well as for late time-gate noise. Data affected by these were removed. An example of locating areas of EM coupling with pipelines or power lines, and recognizing and removing coupled AEM data in Aarhus Workbench is shown in Figure 4-7 and Figure 4-8, respectively. Examples of two inversions, one without EM coupling and the other with EM coupling, are shown in Figure 4-9. The AEM data were then inverted using a Laterally-Constrained Inversion (LCI) algorithm (HydroGeophysics Group Aarhus University, 2011). The profile and depth slices were examined, and any remaining electromagnetic couplings were masked out of the data set.

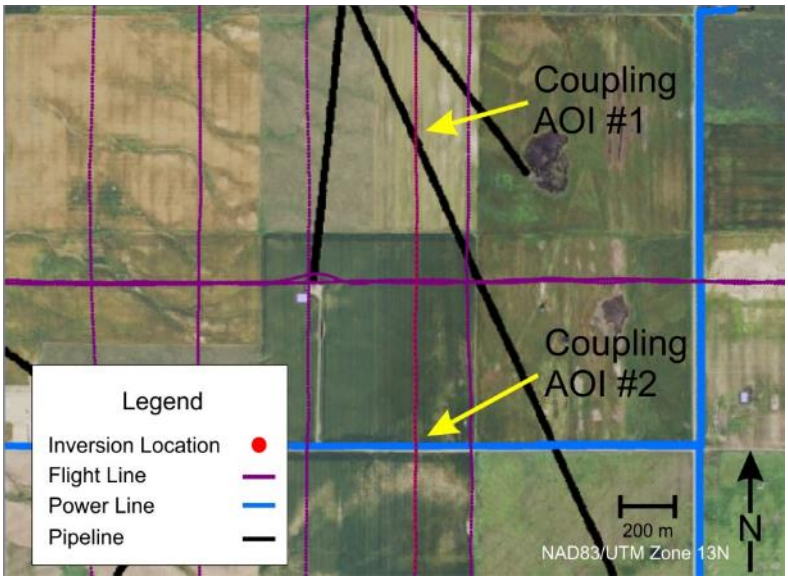



**Figure 4-7: Example locations of EM coupling with pipelines or power lines.**

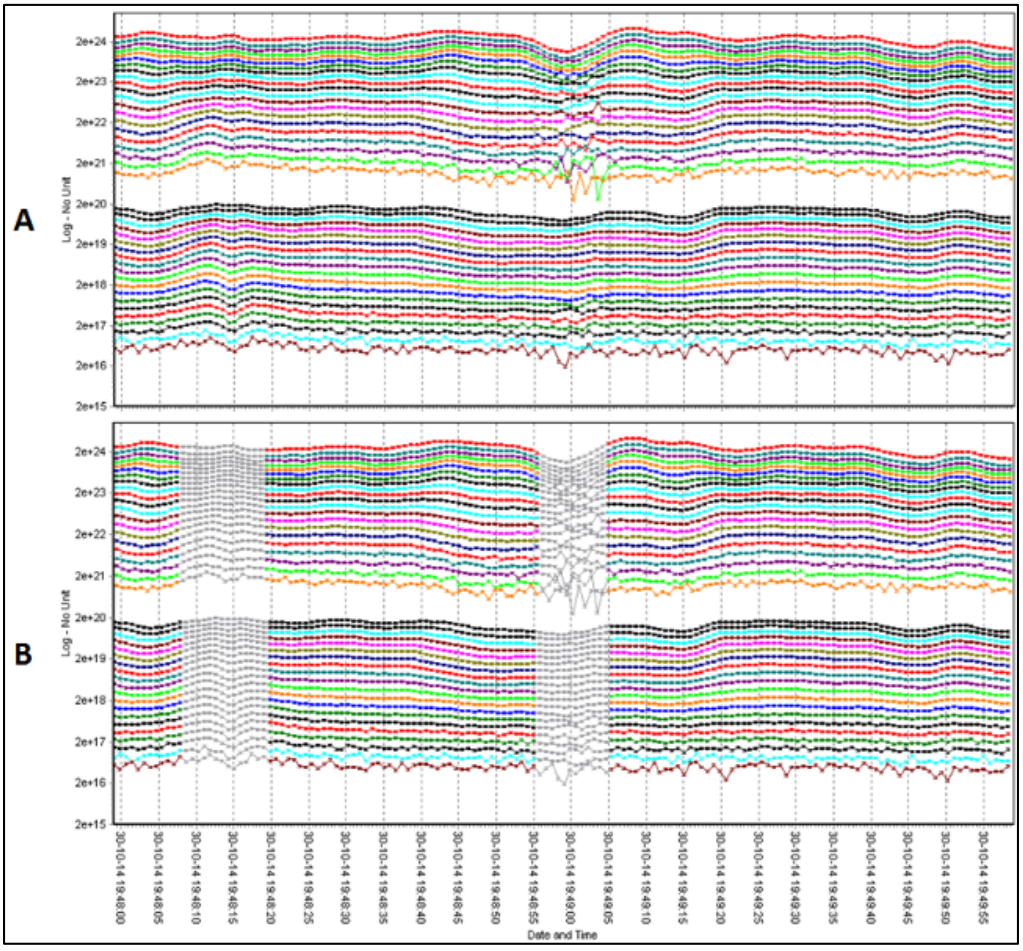



**Figure 4-8: A) AEM data affected by coupling, shown in Figure 4-7, in Aarhus Workbench editor. The top group of lines is the Low Moment and the bottom is the High Moment. B) AEM data with area affected by coupling removed.**

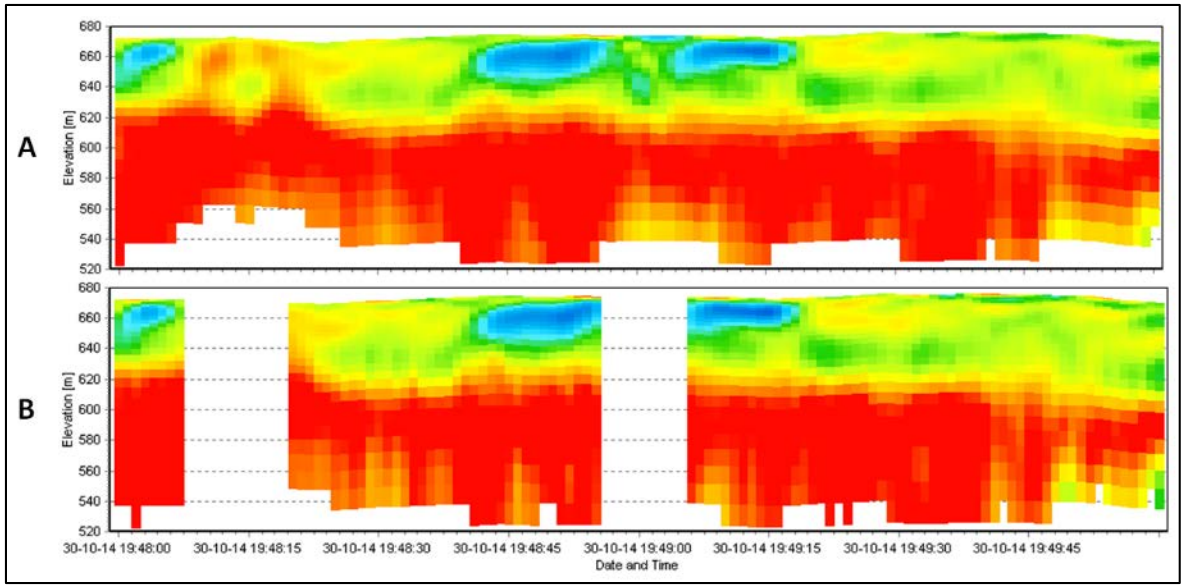



**Figure 4-9: A) Inversion results where AEM data affected by coupling with pipelines and power lines were not removed. B) Inversion results where AEM data affected by coupling were removed prior to inversion.**

### *4.5.4 Power Line Noise Intensity (PLNI)*

The PLNI channel assists in identifying possible sources of noise from power lines. The PLNI is produced by performing a spectral frequency content analysis on the raw received Z-component SkyTEM data. For every Low Moment data block, a Fourier Transform (FT) is performed on the latest usable time gate data. The FT is evaluated at the local power line transmission frequency (60 Hz) yielding the amplitude spectral density of the local power line noise. The PLNI data for the ENWRA survey area are presented in Figure 4-10. Pipelines, unless they are cathodically-protected, are not mapped by the PLNI. Figure 4-11 shows the flight lines where data was removed following decoupling of data due to infrastructure and late time-gate noise.

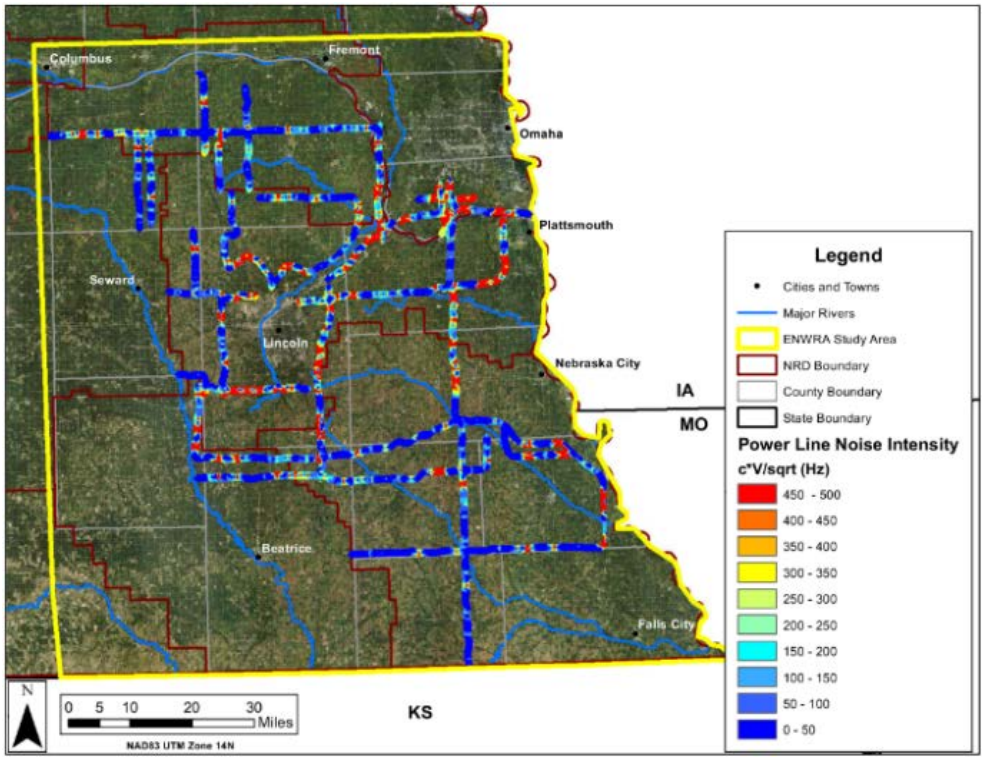



**Figure 4-10: Power Line Noise Intensity (PLNI) map of the southern ENWRA project area.**

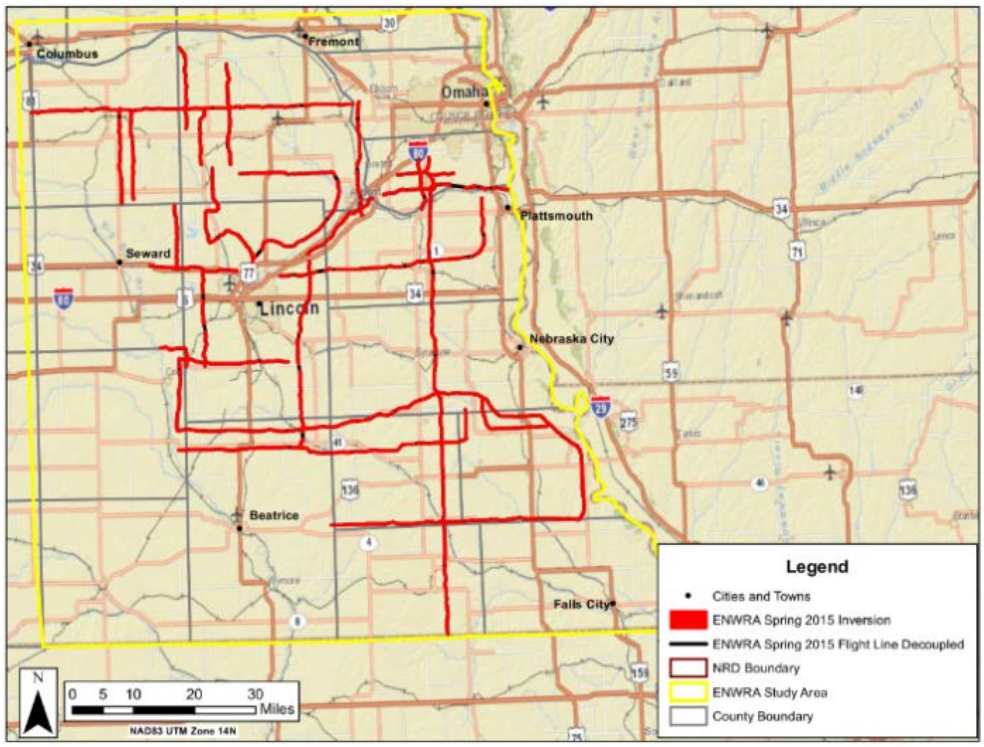



**Figure 4-11: Locations of inverted data along the AEM flight lines in the southern ENWRA project area. Red lines indicate where data was used in the inversion and black line segments indicate where data removed due to em coupling.**

### *4.5.5 Magnetic Field Data*

As discussed above, the SkyTEM 508 includes a Total Field magnetometer. The magnetic field data can yield information about infrastructure as well as geology. Figure 4-12 shows the magnetic Total Field data after correcting for diurnal drift and removing the International Geomagnetic Reference Field (IGRF). This data compares well with the regional magnetic data shown in Figure 4-13 (Bankey et al., 2002) with the exception of the high anomaly surrounding the city of Wayne, NE. The line spacing of the regional data is 5 miles which could explain the difference in amplitude magnitude in this area.

The 3D magnetic field analytic signal is presented in Figure 4-14. The analytic signal indicates areas of sharp changes in the magnetic field such as those caused by metallic infrastructure. This data is used in decoupling efforts.

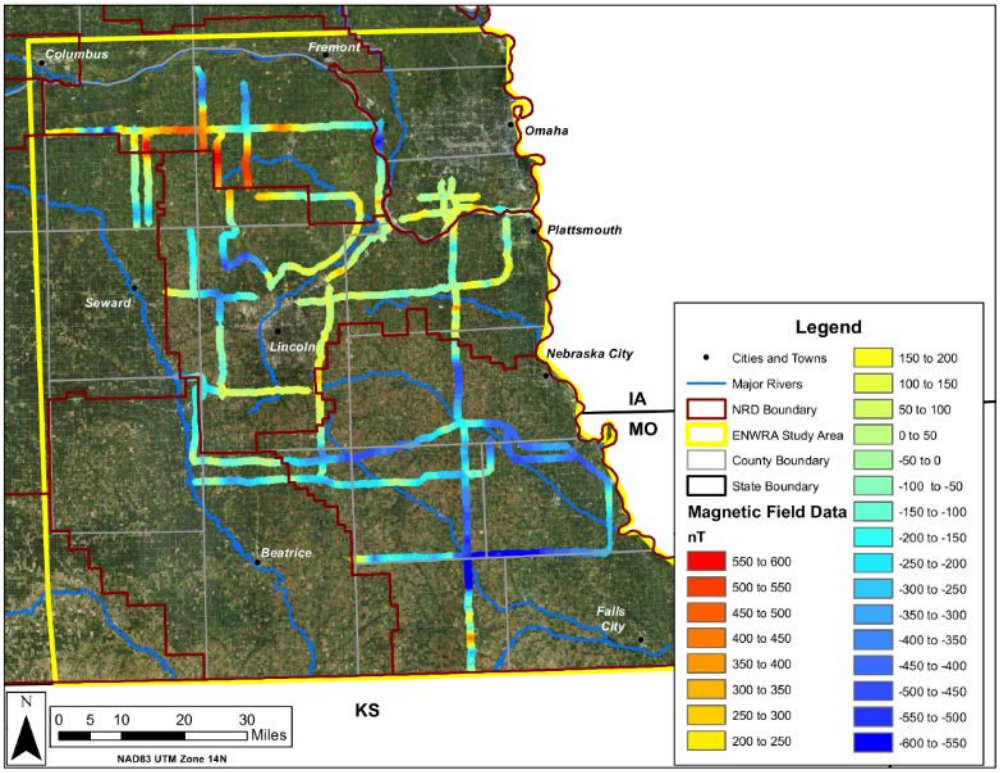



**Figure 4-12: Magnetic Total Field data corrected for diurnal drift, with IGRF removed.**

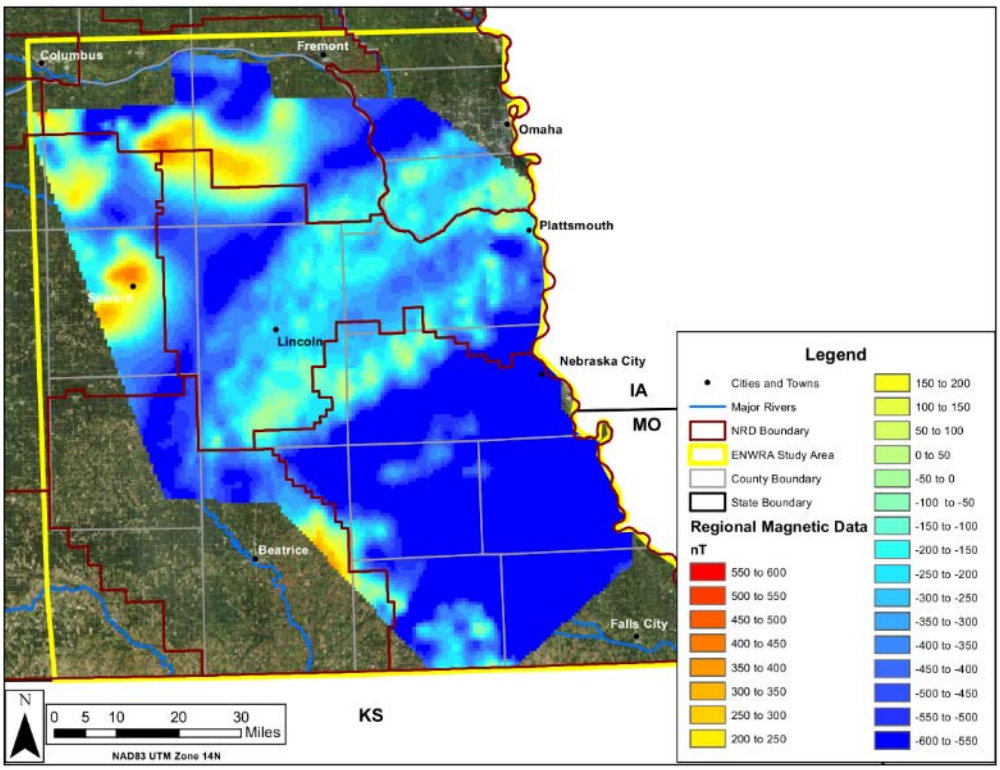



**Figure 4-13: Regional magnetic Total Field data within the southern ENWRA project area boundary. Derived from Bankey et al. (2002).**

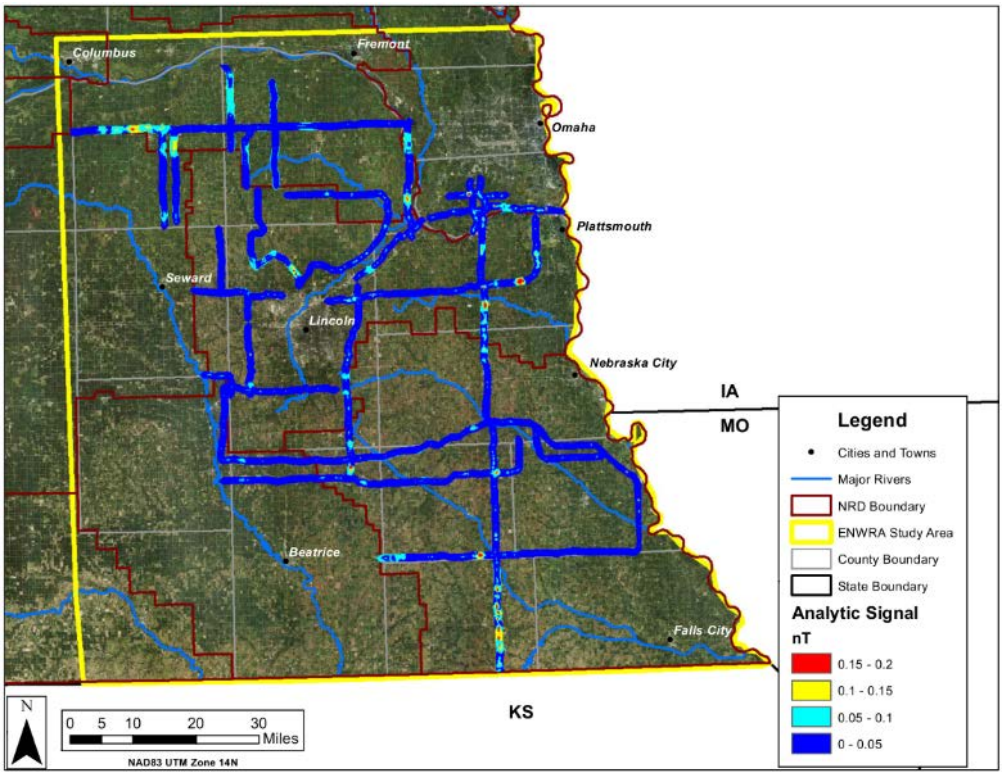



**Figure 4-14: 3D magnetic field analytical signal calculated from the diurnal and IGRF corrected magnetic Total Field data.**

## 4.6 Spatially-Constrained Inversion

Following the initial decoupling and LCI analysis, a Spatially-Constrained Inversions (SCI) was performed. SCI inversions use EM data along, and across flight lines within user-specified distance criteria (Viezzoli et al., 2008).

A smooth model inversion of 30 layers, each with a starting resistivity of 10 ohm-m, was used (equivalent to a 10 ohm-m half space). The thickness of the first layer of the model was 16.4 ft (5 m) with the thickness of each consecutive layer increasing by a factor of 1.1. The bottom of the 29$^{th}$ layer was set to 1,640.4 ft (500 m), and it had a thickness of 133.5 ft (40.7 m). The thickness of the layers increases with depth (Table 4-6 and Figure 4-15) as the resolution of the technique decreases. The reference distance was set to 328 ft (100 m) with a power law of 0.5. The constraint levels, ResVerSTD and ResLatStD, were set to 2 and 1.3, respectively, for all layers.

In addition to the recovered resistivity models, the SCI also produces data residual values (single sounding error residuals), total residual values (total model residual error values), and Depth of Investigation (DOI) estimates. The data residual compares the measured data with the response of the inverted model. The total residual is a weighted average of the data residual and the model residual (Christensen et al., 2009; SkyTEM Airborne Surveys Worldwide, 2012). The DOI estimates the depth to which the AEM data are sensitive to changes in the resistivity distribution (Christiansen and Auken, 2012).

**Table 4-6: Thickness and depth to bottom for each layer in the SCI inverted AEM models. The thickness of the model layers increase with depth as the resolution of the AEM technique decreases.**

| Layer | Depth to Bottom (ft) | Thickness (ft) | Layer | Depth to Bottom (ft) | Thickness (ft) |
|---|---|---|---|---|---|
| **1** | 16 | 16 | **16** | 488 | 51 |
| **2** | 34 | 18 | **17** | 543 | 54 |
| **3** | 53 | 19 | **18** | 601 | 59 |
| **4** | 74 | 21 | **19** | 665 | 63 |
| **5** | 96 | 22 | **20** | 733 | 68 |
| **6** | 120 | 24 | **21** | 806 | 73 |
| **7** | 145 | 26 | **22** | 885 | 79 |
| **8** | 173 | 28 | **23** | 971 | 85 |
| **9** | 203 | 30 | **24** | 1062 | 92 |
| **10** | 235 | 32 | **25** | 1161 | 99 |
| **11** | 270 | 35 | **26** | 1268 | 107 |
| **12** | 307 | 37 | **27** | 1383 | 115 |
| **13** | 347 | 40 | **28** | 1507 | 124 |
| **14** | 391 | 43 | **29** | 1641 | 133 |
| **15** | 438 | 47 | | | |

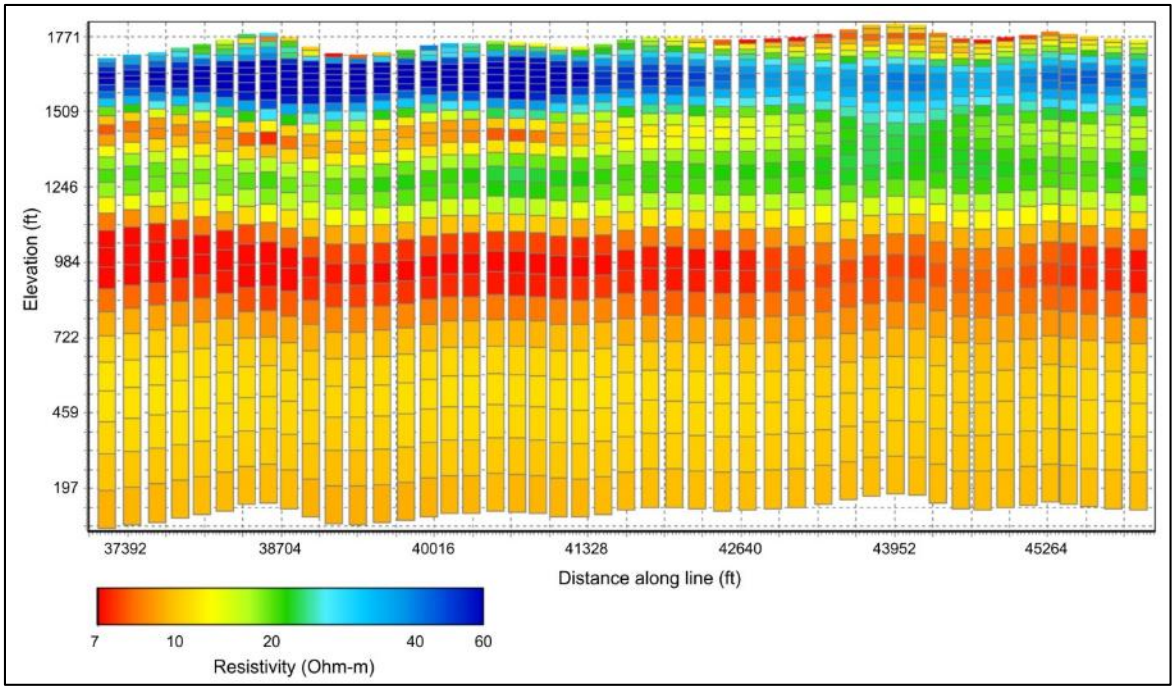



**Figure 4-15: An example of an AEM profile illustrating the increase in model layer thickness with depth.**

Lastly, 25 of the borehole conductivity logs, listed in Table 4-7, were used to constrain the inversion with a lateral standard deviation (STD) constraint of 2 and a reference distance of 3,280 ft (1,000 m) (HydroGeophysics Group Aarhus University, 2011). A variety of a-priori STD values and reference distances were tested including STDs of 1.5 and 2, and reference distances of 3,280 ft (1,000 m) and 9,840 ft (3,000 m). Workbench resamples the geophysical logs to match the layer widths and depths set for the SCI results Figure 4-16 compare the borehole logs with the starting model and the inverted model results for select boreholes. Figure 4-17 shows a cross plot of the inverted resistivities compared with the resampled borehole resistivity for the 13 boreholes that were located very close to the flight lines.

The data residuals for the inversion using the resistivity logs were compared to those that didn't include the borehole logs. A STD value of 2 with a reference distance of 3,280 ft (1,000 m) produced the best results with improved data residuals, shown in Figure 4-18. Their distribution is shown in Figure 4-19.

**Table 4-7: List of wells with borehole resistivity logs used as a-priori information for the SCI.**

| Well | Easting (ft) | Northing (ft) |
|---|---|---|
| **1-A-68** | 2331244.000 | 14855078.000 |
| **1-A-76** | 2163210.750 | 14977701.000 |
| **1-B-65** | 2409688.000 | 14860928.000 |
| **1-B-68** | 2352868.000 | 14854338.000 |
| **11-A-67** | 2441681.000 | 14698524.000 |
| **13-81** | 2432954.750 | 14804230.000 |
| **13-B-67** | 2442893.500 | 14640682.000 |
| **14-80** | 2480209.000 | 14906308.000 |
| **19-A-61** | 2439520.500 | 14740737.000 |
| **2-A-62** | 2433447.000 | 14946944.000 |
| **2-B-73** | 2460199.750 | 14752267.000 |
| **20-A-61** | 2439645.750 | 14751328.000 |
| **22-B-67** | 2566327.750 | 14660762.000 |
| **24-A-61** | 2438079.000 | 14799016.000 |
| **25-A-61** | 2435001.000 | 14846535.000 |
| **26-A-61** | 2430914.750 | 14862781.000 |
| **28-A-61** | 2432630.250 | 14896794.000 |
| **3-B-73** | 2469297.250 | 14752294.000 |
| **5-A-67** | 2446912.250 | 14561095.000 |
| **5-B-77** | 2204289.250 | 14993553.000 |
| **8-A-67** | 2443316.250 | 14636213.000 |
| **8-B-67** | 2444195.250 | 14606185.000 |
| **9-A-61** | 2372595.750 | 14857170.000 |
| **9-B-67** | 2442247.500 | 14656598.000 |
| **260972100** | 2415129.458 | 14702349.110 |

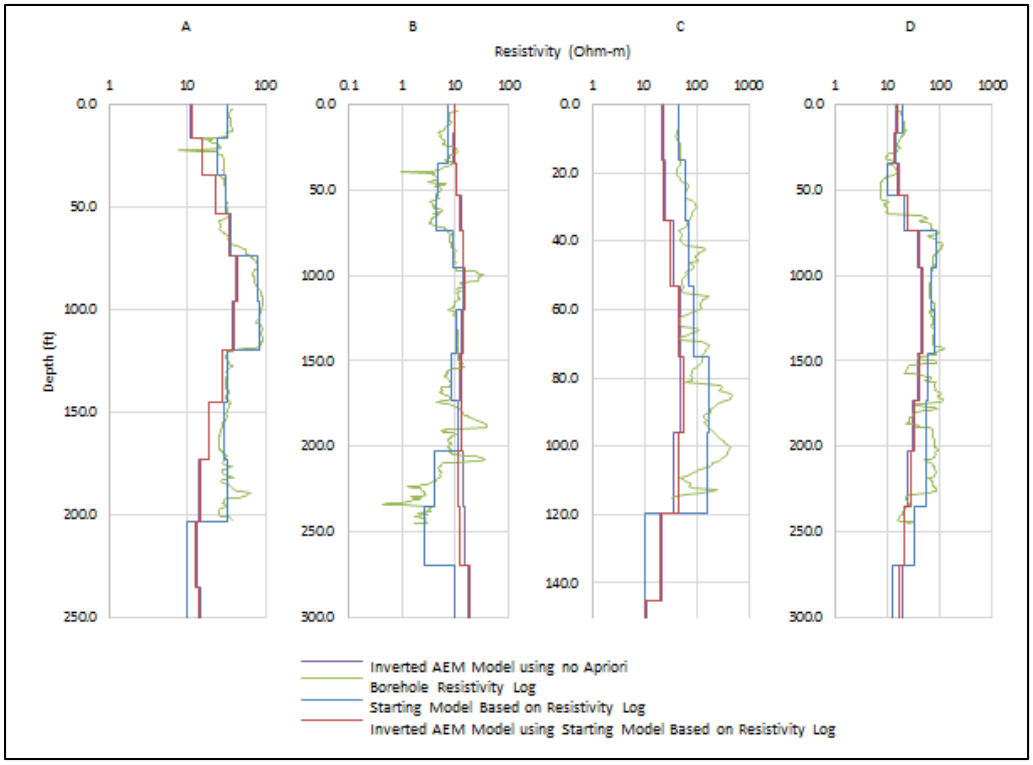



**Figure 4-16: Borehole resistivity logs compared with inverted AEM models. A: Well 1-A-68, 1,606 ft from the AEM line. B: Well 1-A-76, 1,478 ft from AEM line. C: Well 1-B-65, 1,867 ft from AEM line. D: Well 2-A-65, 1,699 ft from AEM line.**

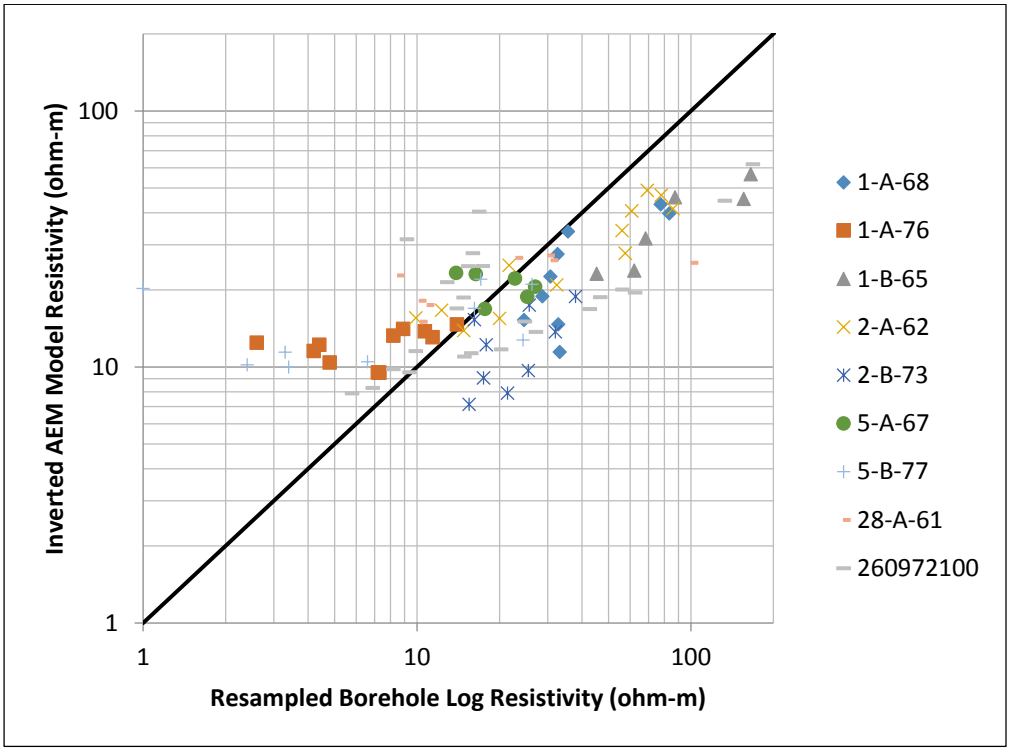



**Figure 4-17: Cross-plot of inverted resistivities compared with the resampled borehole resistivities for the 13 boreholes located within close proximity to the flight lines.**

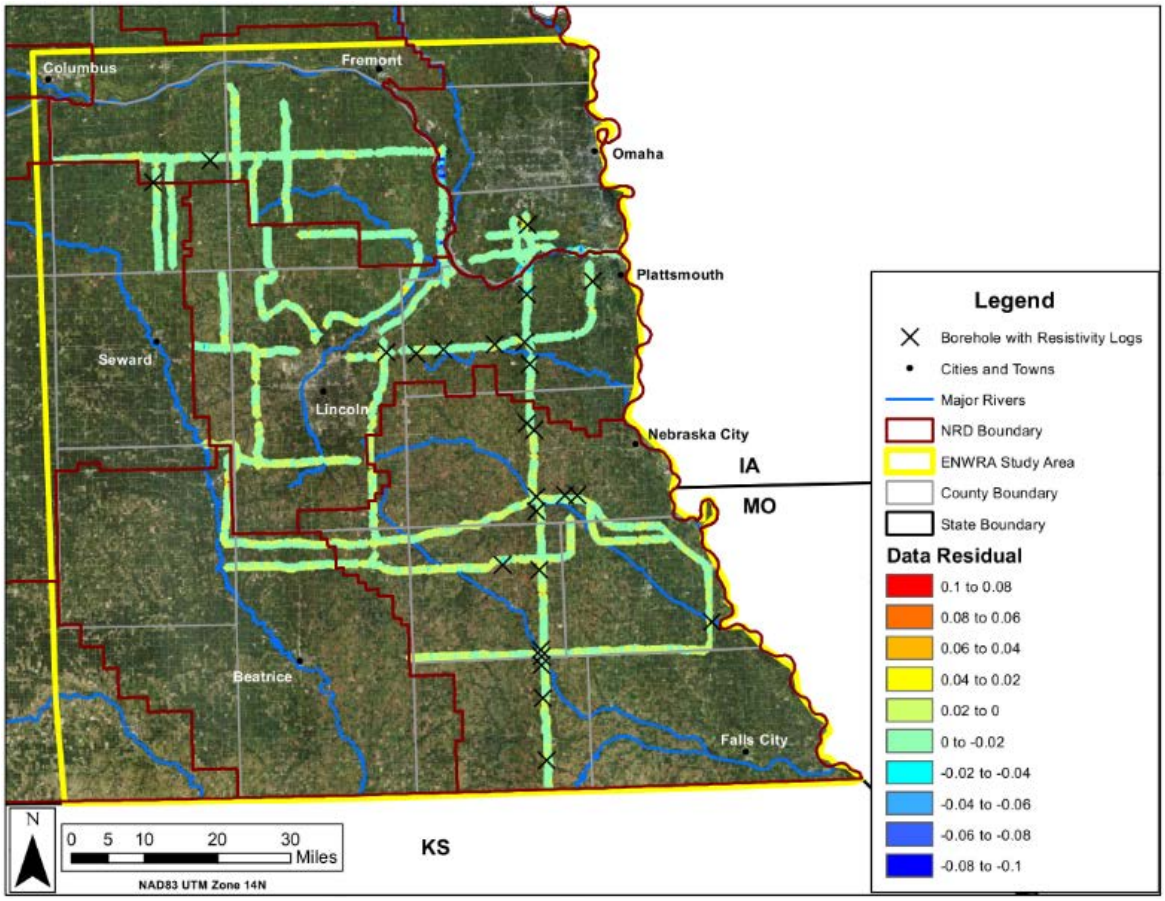



**Figure 4-18: Difference between data point residuals produced by SCIs with and without using the borehole conductivity data as a-priori information. Red indicates an improvement in the residuals by greater than 0.1.**

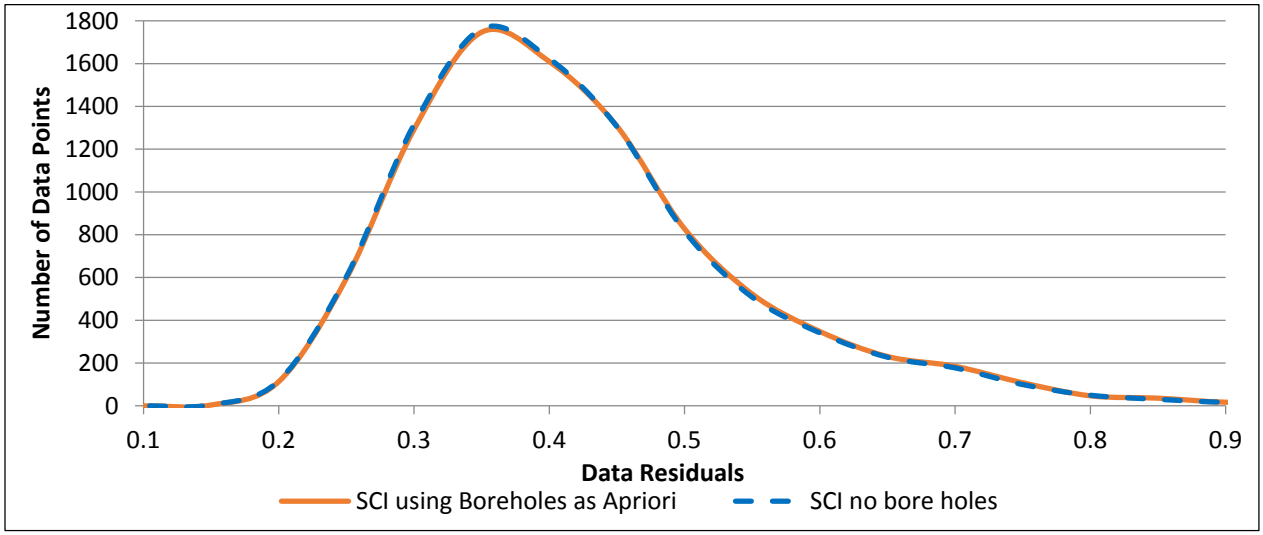



**Figure 4-19: Data residuals distribution produced by the SCIs in the 10-mile recon lines both using the resistivity logs as a-priori and without them.**

### *4.6.1 Determination of the DOI*

The Depth of Investigation (DOI) plays a critical role in data interpretation. The DOI is a numerical estimation of the depth below which the resolution of a model, resulting from a numerical inversion, diminishes. This depth develops primarily due to the limitations of the TDEM method including: the equipment and methodology used for data acquisition, the noise in the data, and the resistivity structure (the geology) being investigated (Christiansen and Auken, 2012).

In addition to inverting the AEM data, Aarhus Workbench also calculates depths of investigation (DOI) for each inverted sounding, both a DOI Upper and a DOI Lower. 'Upper' refers to a shallower DOI estimate while 'Lower' refers to a deeper one. The derivation of these depths is presented in Christiansen and Auken (2012) and discussed in more detail in Appendix 3.

The Aarhus Workbench uses inverted model sensitivities (the Jacobian) determined during the last inversion step, along with an estimate of data uncertainty to calculate the DOI's. The Jacobian matrix is the sensitivity of the data to perturbations at the current location in model-space. As such, the Jacobian is also a representation of the sensitivity of changes in the model to the observed data.

The last step in this process is calculation of the cumulative sensitivities, by summing up the individual thickness-normalized sensitivities, starting with the bottom layer. That is, for a 30-layer model (which is usually used in all the XRI Workbench inversions) the cumulative sensitivity for the 30$^{th}$ layer is the thickness-normalized sensitivity for the 30$^{th}$ layer. Then the cumulative sensitivity for the 29$^{th}$ layer is the sum of the cumulative sensitivity for the 30$^{th}$ and the thickness-normalized sensitivity for the 29$^{th}$ layer. The cumulative sensitivity for the 28$^{th}$ layer would be the sum of the cumulative sensitivity for the 29$^{th}$ layer and the thickness-normalized sensitivity for the 28$^{th}$ layer.

However, there is a difference between *resolution* of a property and *detection* of a property. Resolution means that the properties of interest are accurately recovered through inversion. Detection indicates that while the true value of a property may not be accurately resolved, there is still some sensitivity, in the data, to changes in that property. The DOI is generally the line of demarcation between resolution and detection.

Christiansen and Auken (2012) define the global threshold value as that cumulative sensitivity which indicates "*the miminum amount of sensitivity needed for indicative information.*" They further state that "*setting the threshold value is very much a question of fine-tuning based on experience, intuition, and comparing different models with different methods. The threshold value suggested here is purely empiric. Setting a higher threshold value will decrease the DOI, and a lower value will increase the DOI.*"

The upper and lower DOIs typically exported by the Aarhus Workbench are for cumulative sensitivities 1.2 (upper DOI) and 0.6 (lower DOI). However, additional cumulative sensitivity values can also be developed and exported including 0.4, 0.2, and 0.1. Variations in the character of the DOI's are functions of the resistivity of the sounding for which the DOI is calculated. The DOI contours for the cumulative sensitivity thresholds will be much deeper under resistive zones and shallower under conductive zones. An example of a DOI produced using a 0.1 cumulative sensitive is shown on the profiles in Figure 4-20 and in Appendix 3.

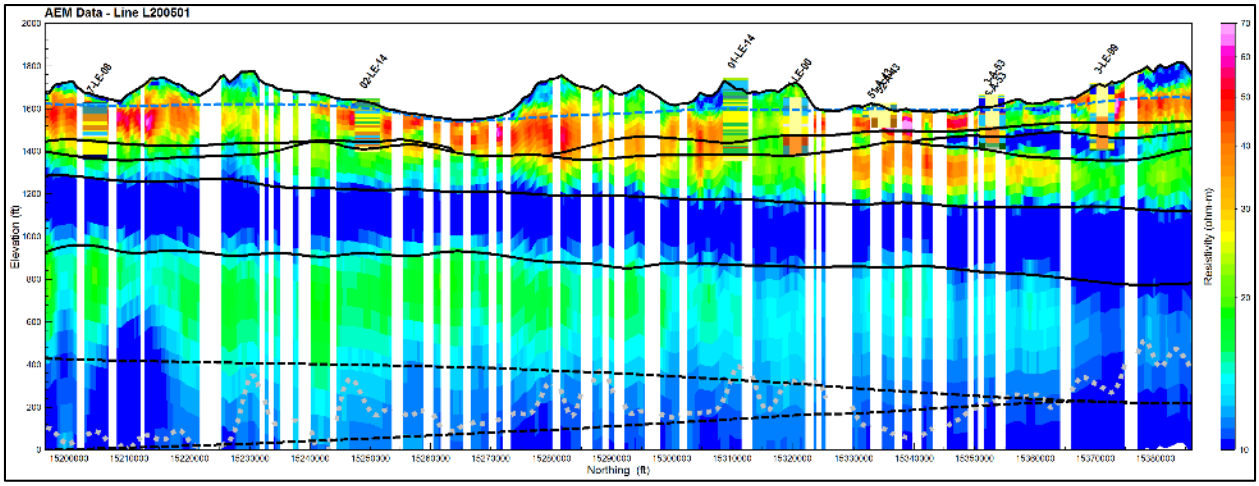



**Figure 4-20: Sample of AEM resistivity inversion model with the 0.1 DOI marked as grey dots at the bottom of the image.**

# 5 Results and Interpretation

A total of 684.9 line miles (1102.3 line km) of AEM data were collected in Phase 2. Of that total, 167.7 lines miles (269.8 line km), or 24.4%, were removed due to electromagnetic coupling with infrastructure, leaving a total of 517.3 line miles (832.5 line km) for inversion and interpretation. Had the flights line paths not been optimized prior to data collection, the expected data retention would have been 40.6% instead of 75.6% (using a radius of interference from the noise source of approximately 820.2 ft (250 m)). Locations of where data were removed are provided in the previous section in Figure 4-11. Figure 5-1 shows the locations of where data were collected along with the flight line numbers in the southern ENWRA project area.

Figure 5-2 includes the color codes for the aquifer materials as well as the stratigraphy and lithology labels used in figures in this section as well as in the appendices of this report.

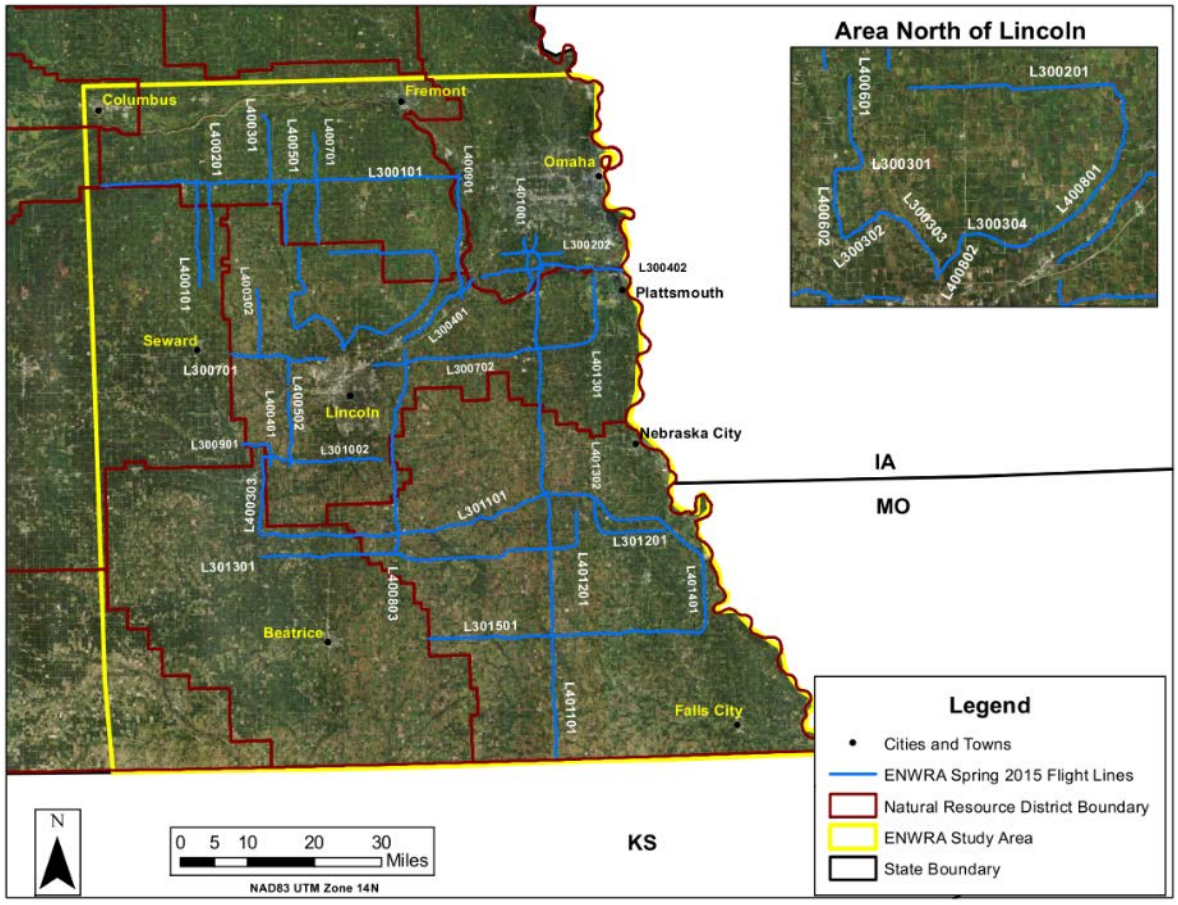



**Figure 5-1: AEM flight lines with line numbers in the southern ENWRA project area.**

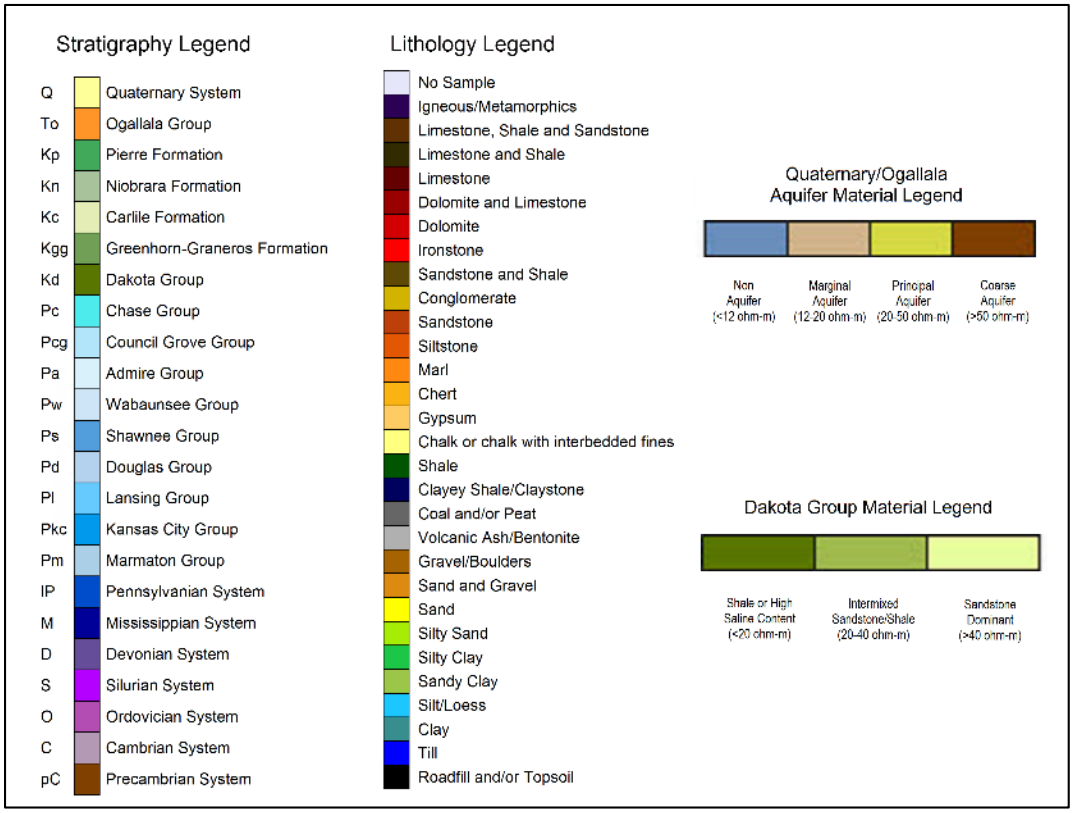



**Figure 5-2: Color codes for aquifer materials, stratigraphy, and lithology used the interpretive profiles and 3D figures in this section and in the report appendices.**

## 5.1 AEM Results and Interpretation

### *5.1.1 Interpretive Process*

After final processing of the AEM data, characterization of the subsurface was performed in cross-section format using Encom PA (pbEncom, 2015). In this step, contacts between the bedrock (Paleozoic and Cretaceous), and Quaternary deposits were delineated for every flight line in the project area. The interpreted geological units included the Quaternary system, *Kc, Kgg, Kd*, and undifferentiated Paleozoic units from the upper surface to the DOI. The Greenhorn Limestone and Graneros Shale (*Kgg*) were not geophysically distinct (poor resistivity contrast) from the *Kc* at all locations. Since these units generally function as aquicludes over the project area, they were grouped as one (*KcKgg*) in the representation of the AEM data and the hydrostratigraphic framework of the project area. The selection process benefited from the use of CSD and NOGCC borehole logs, which provided lithologic, stratigraphic, and geophysical information. The historical CSD cross-sections (Divine et al., 2010; Korus et al., 2012) were projected in Encom PA to aid in interpreting the AEM data. The interpretations were simultaneously checked against the CSD's Nebraska bedrock geology map (Burchett, 1986) and other geological maps in the southern portion of the project area (Burchett and Carson 1966a, b, c, d; Burchett et al., 1972; Burchett et al., 1975; Ellis, 1984). Historic bedrock geology maps were used to assist in the interpretation of the AEM inversion results (Divine et al., 2010; Korus et al., 2012). The contours from these data sources were georeferenced and digitized with GIS software. The resulting digitized contour lines were then gridded to create either surfaces of the bedrock unit tops and bases or thickness maps.

An additional geologic map of outcrops along the flight line 401101 in the Table Rock area of the NNRD (Korus et al., 2014) was georeferenced and digitized using GIS software. These maps were particularly useful in interpreting the contact between the Quaternary system and the Paleozoic along valley edges and upland areas. After the cross-section interpretations of the geological contacts were completed, the results were compared in 3D with the NOGCC boreholes, CSD boreholes, CSD historic bedrock surface, and CSD cross-sections (Divine et al., 2010; Korus et al., 2012).

Areas of offsets between intersecting AEM flight lines were minimized by reinterpreting the information based on visualization of the AEM data in a 3D display.

Regional surface grids of geologic formations were produced during this process. To create these grids, the elevations of the interpreted top of the formation as well as data from CSD and NOGCC holes were imported to a Geosoft Oasis montaj (OM) database. The interpreted elevation data were then gridded for each formation independently using the OM minimum curvature gridding (MCG) algorithm with a 1,500 ft cell size, a blanking distance of 50,000 ft, and the cells to extend beyond set to 50. All other parameters were either left as the default or blank. The large blanking distance was required to fill in between the broadly spaced reconnaissance lines, where 15 miles or more separated adjacent flight lines. CSD and NOGCC holes were used to provide additional formation elevation data throughout the project area. The 1,500 ft cell size preserved most of the spatial resolution obtained from the AEM data but minimized artifacts from the MCG routine. While the MCG routine performs reasonably well with honoring the data, in areas where the spatial density of data points is low, the MCG routine may trend towards an overall average data value. This may cause artifacts in the final grid in the form of grid values that are not supported by data in the general vicinity. A smaller cell size resulted in these gridding artifacts on the boundary of the project area and where only reconnaissance lines were available (i.e. no CSD or NOGCC holes available). A 9-point convolution filter was applied to each grid using a pre-defined Hanning filter under the GRIDFILT GX within OM. This type of filter is common in image processing and was used to reduce high-frequency noise in the grid.

The parameters utilized in this process resulted in grids that were continuous across the project area but also extended outside the project area or beyond the areal extent of the interpreted feature in the AEM data. Once generated, each individual grid was masked to remove gridded data that was either outside the project area or in areas where that geologic surface was not identified. The mask was generated from the AEM interpretation, CSD and NOGCC test holes, and the project area bedrock geology map. In areas where no AEM data or drill holes were available, the contours for each geologic unit were followed as depicted on the CSD bedrock geology map (Burchett, 1986). These masks were also set at the eastern edge of the continuous *Kd* contact as defined by Burchett (1986). The isolated areas of eroded *Kd* were excluded from the surface due to the limited control from the reconnaissance lines and the limited drilling data. As the edges of the *Kd* are encountered, the irregular erosional surface of the *Kd* is variable and requires greater detail in both drilling and AEM data coverage.

Once masked, the grids were then sampled to the location of the AEM data within OM and visually inspected for consistency. In areas of sparse data, grid surfaces did not meet or overlap (e.g. the gridded bedrock surface exceeded the DEM elevation by a small interval (< 5 ft) in a minor number of instances). In areas of incongruity, data were manually adjusted to ensure geologic surfaces met

appropriately or did not overlap. This manual editing was conducted only on the geologic surface data that coincided with the location of the AEM data and used to generate the cross section plots presented in this report. The digital regional grids provided with this report will show discontinuities throughout the project area where different geologic surfaces meet or pinch out. In most cases, this is typically less than 30 feet, but some areas exist where the elevation offset of successive geologic units is 75 ft or more where no drilling or AEM control exists. Some of the bedrock surfaces that are exposed near the geological formation surfaces also required manual editing due to elevation tares where the geological unit was above the DEM sampled at 1,500 ft. In those instances, the top of the geological unit was set to the DEM elevation minus 15 ft. These only occurred in areas where there was no drilling or AEM control. To improve theses surfaces without additional data would require an interpreted, hand-drawn surface to assist in filling in the areas without drilling and AEM control and was beyond the scope of this report.

Following construction of the bedrock surface, the consolidated and unconsolidated deposits were isolated within the AEM data. A voxel resistivity grid was made of the AEM data using a 1,000 $ft^2$ horizontal cell with the thickness related to the model cell thickness (Section 4.6). The voxel was then sliced at the bedrock surface. This surface was the top of the *KcKgg*, *Kd,* or top of the Paleozoic system depending on location in the project area. Note that the *Kc* and *Kgg* are combined as one hydrostratigraphic unit (further discussion on this merging of units is provided later in this section). The voxel values were then sampled on the AEM flight path cross-sections to indicate the location of the resistive intervals that are interpreted as unconsolidated Quaternary aquifer materials. The aquifer and non-aquifer materials in the Quaternary system were separated by four major resistivity thresholds selected in Encom PA. These ranges include 1-12 ohm-m, representing non-aquifer materials ("aquitard"- primarily glacial till, loess), 12-20 ohm-m, representing marginal aquifer deposits with potential for interlayered silt and clay, 20-50 ohm-m, indicating the Quaternary system's principal aquifer, and an interval of 50 ohm-m or greater, indicating the coarsest, sand-rich intervals within the principal aquifer (further discussion regarding the selection of these threshold ranges is provided in the following section regarding the selection of these threshold ranges). These surfaces were then gridded to provide formation or geologic material top and bottom along the flight line. *T*he *Kd* resistors were also sampled from a sliced voxel model at a resistivity range of 20 ohm-m or greater.

To assist in the approximation of the saturated materials along the surveyed AEM flight lines, the 1995 CSD statewide water table was mapped into the cross-sections. It should be noted that this inclusion provides only a generalized characterization of saturated thickness of the aquifer, as the CSD's dataset is two decades old at the time of the Spring 2015 AEM survey, and local conditions likely deviate in areas with variable topography.

It should be noted that care must be exerted not to use the voxel information beyond the flight lines, as the voxels are not constrained and thus will not provide information due to the large interpolation distances between flight lines. In some areas on the interpretation profiles, there are slight differences at the land surface and the underlying geologic interpretation. This is an artifact of displaying a 3D model along a line profile feature.

### 5.1.2 Resistivity-Lithology Relationship

#### 5.1.2.1 Quaternary System

A critical aspect of a geophysical survey, for whatever purpose, is assessing the nature of the material detected by the geophysical method applied in the investigation. In regards to the ENWRA reconnaissance survey, assessment of the sediment character in both the Quaternary system and the consolidated bedrock strata was conducted to determine the overall composition of the major categories used to define the aquifer and aquitards in eastern Nebraska. A numerically robust assessment of the resistivity thresholds used to characterize non-aquifer, marginal and principal aquifer, including sand-rich intervals in the principal aquifer was calculated. This allows for the characterization of the ranges of resistivities present in the major geologic units described in this report. It should be noted that this analysis encompasses all Quaternary and bedrock data from both subregions of the ENWRA project area as defined in this report. Separate analyses were conducted for both areas, and results confirmed that virtually no differences were evident between the two areas, thus justifying the application of the resistivity thresholds described in this section for the entire ENWRA area.

Data for this analysis was utilized from locations across the ENWRA reconnaissance line area. The relationship between resistivity and lithology type was assessed by performing an association function that linked nine lithologic descriptor codes for Quaternary sediments used in the CSD test hole lithologic characterization with the resistivity values across that particular depth interval as indicated in the 58 high-graded resistivity logs applied in the AEM data inversion (25 from the southern area, 33 from the northern area). With this approach, several thousand points became available for each lithologic description in the test holes used in this analysis. From this list of associated resistivity levels and pre-categorized lithologies, statistical analyses were performed to aide in defining the various thresholds used to determine the aquifer material type in the project area subsurface. The following paragraphs contain descriptions of each analysis performed.

Figure 5-3 displays a box and whiskers plot of the resistivity range for each of the nine unconsolidated materials in the Quaternary system. These plots indicate the spread of the range of resistivities for each of the materials, including the $75^{th}$ and $25^{th}$ quartiles, median values, and the IRQ*1.5 (whiskers) (Tukey, 1977). Included in the background of the plot are the divisions in resistivity between the aquitard and the three aquifer designations in the AEM interpretations. Glacial till (blue) has an interquartile range of resistivities from approximately 17 to 45 ohm-m, with a median value of 25 ohm-m and maximum and minimum values of around 90 and 11 ohm-m, respectively. This plot indicates that for glacial till, there is a wide spread of resistivity. This should not be unexpected, as glacial till can be composed of a wide variety of unsorted sediment sizes, including gravel and sand intermixed with fines.

Silt/loess has a similar resistivity distribution as glacial till, but with a higher median near 29 ohm-m, and a lower minimum value near 2 ohm-m. This wide range could be a result of silt and loess being combined in one category, where silt from different horizons that are intermixed with other fines such as fine sand or clay could create the wide range in values for this material.

For the lithologic category clay, the median value is close to glacial till, but with a lower maximum value (approximately 40 ohm-m) and lower minimum value (3 ohm-m). These differences should be expected, as glacial till is typically composed of more resistive materials in comparison to clay materials alone.

Silty clay has the lowest median value of the 9 categories displayed in Figure 5-3 (approximately 14 ohm-m). Silty sand and sandy clay each have very similar characteristics in this plot, which should be expected as these lithologic categories are similar.

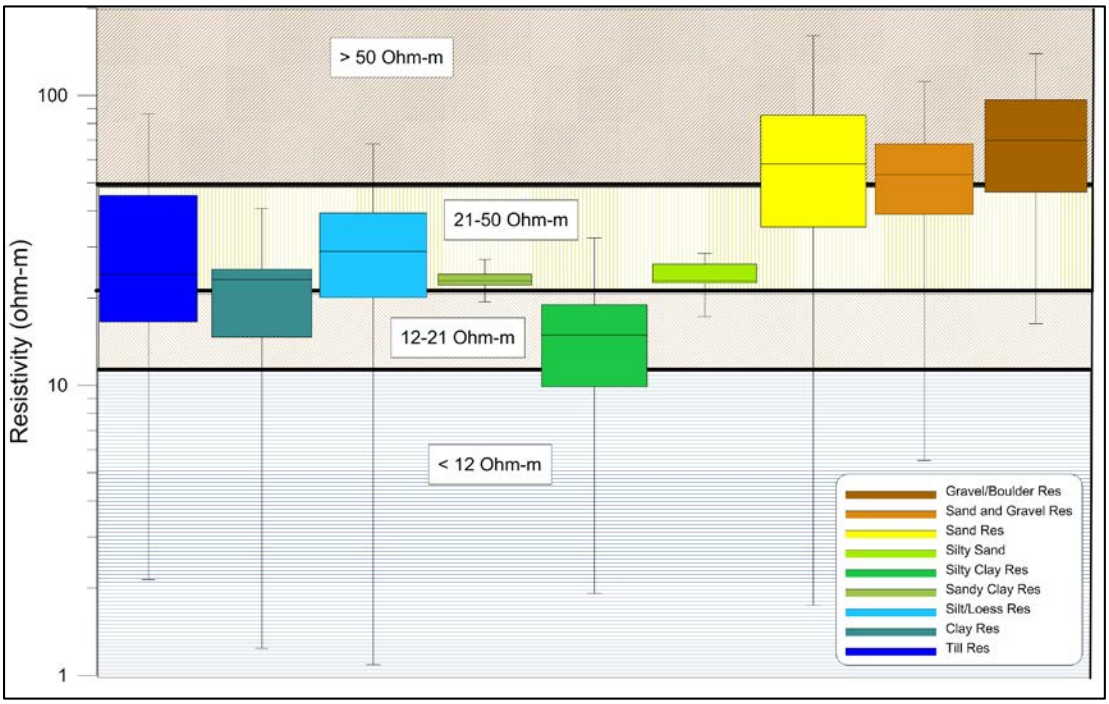



**Figure 5-3: Box and whisker plots for the resistivity ranges for the nine most common unconsolidated materials encountered in the Quaternary system.**

The distribution of sand, sand and gravel, and gravel and boulder categories are considerably higher than the median and interquartile ranges of the fine materials displayed in Figure 5-3. The median resistivity of the three coarse sediment ranges is 55 ohm-m or higher, and the lowest 25$^{th}$ quartile (sand) is 35 ohm-m, indicating that 75 percent of the resistivity values for each of these three coarse categories is 35 ohm-m or higher. Sand also has the maximum (117 ohm-m) and the minimum (7 ohm-m) values of the three coarse sediment categories.

Figure 5-4 displays a histogram of the unconsolidated material distribution by frequency count of materials associated with resistivities from the 58 borehole geophysical logs assessed from across the project area. The color-defined bins of the histogram show the thresholds for resistivity used to define the major aquifer material type in the interpretation of the AEM data. Non-aquifer material (blue), shows a distribution on the log-scale x-axis from 1 to 12 ohm-m. This material range corresponds primarily to intervals of resistivity associated with silty clay, clay, silt/loess, and till. The tan area, between 12 and 20 ohm-m, is defined by a mix of fine to coarse sediments, with abundant silty clay still present. The principal aquifer (yellow), is defined by materials ranging from 20 to 50 ohm-m. This interval has a considerable peak of material with a resistivity approximately in the 22-27 ohm-m range

and a secondary peak in the 45 to 50 ohm-m range. The fourth category on the histogram (brown area) represents materials 50 ohm-m and greater, which corresponds to the coarse, sand-rich intervals of the principal aquifer. This interval is considerably lower in the frequency count than the primary aquifer, but by highlighting this interval, discreet sections of the aquifer are revealed showing possible depositional trends in the Quaternary deposits as well as identifying areas where the potential for high-yield wells is the greatest.

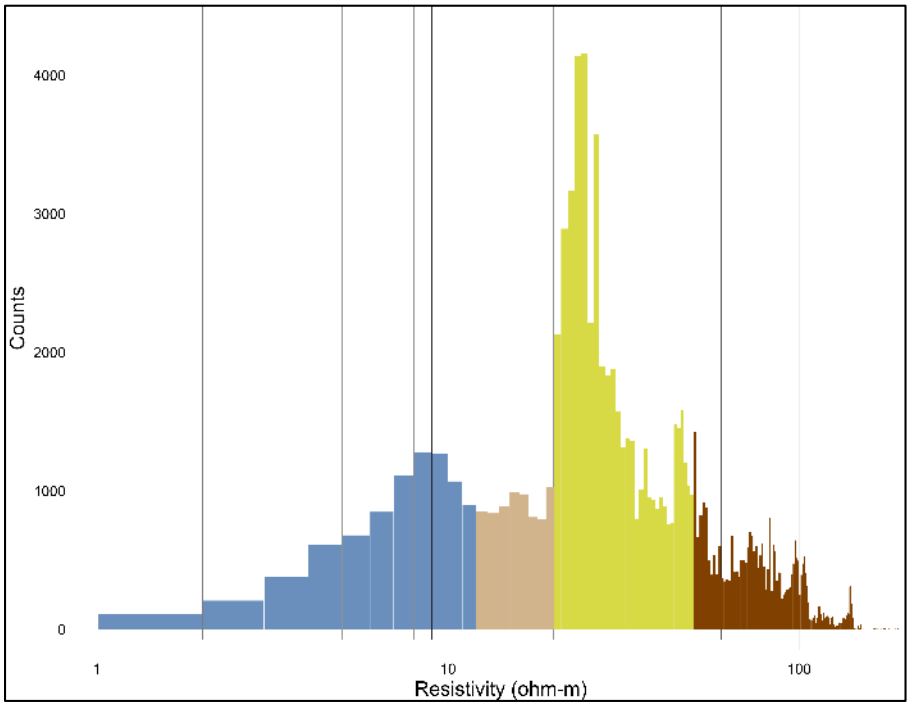



**Figure 5-4: Histogram plot displaying the distribution of resistivities by major aquifer material color categories (blue- non-aquifer material, tan- marginal aquifer, yellow- principal aquifer, brown- sand-rich, coarse intervals of the principal aquifer).**

Figure 5-5 and Figure 5-6 display pie charts that indicate the distribution of sediment type within each aquifer material range (0-12, 12-20, 20-50, >50 ohm-m). Fine materials (silt/loess, clay, till) are the predominant material types for the non-aquifer material (0-12 ohm-m). For marginal aquifer material (12-20 ohm-m), slightly over 14% of the material in this range has a component of sand, with silt/loess, till, and clay comprising over 75% of this range. For principal aquifer material, over 37% of the material consists of coarse materials, and for the coarse portion of the principal aquifer at 50 ohm-m or greater, over 85% of the lithology consists of coarse material.

Figure 5-7 contains the overall distribution of sediment type as indicated in the 58 e-logs used to assess the lithology-resistivity relationship across in the project area. Over 48 percent of the lithologies indicated by the e-logs were categorized as sand, sand and gravel, or gravel and boulders. Silt/loess was the second highest category at 27.2 percent. This should be expected, considering the presence of silt within the many of the major depositional features in the project area (loess, till, outwash, alluvium). Glacial till is the second most abundant non-coarse material at over 13 percent. The remaining categories containing some component of clay is just over 10 percent of the overall distribution.

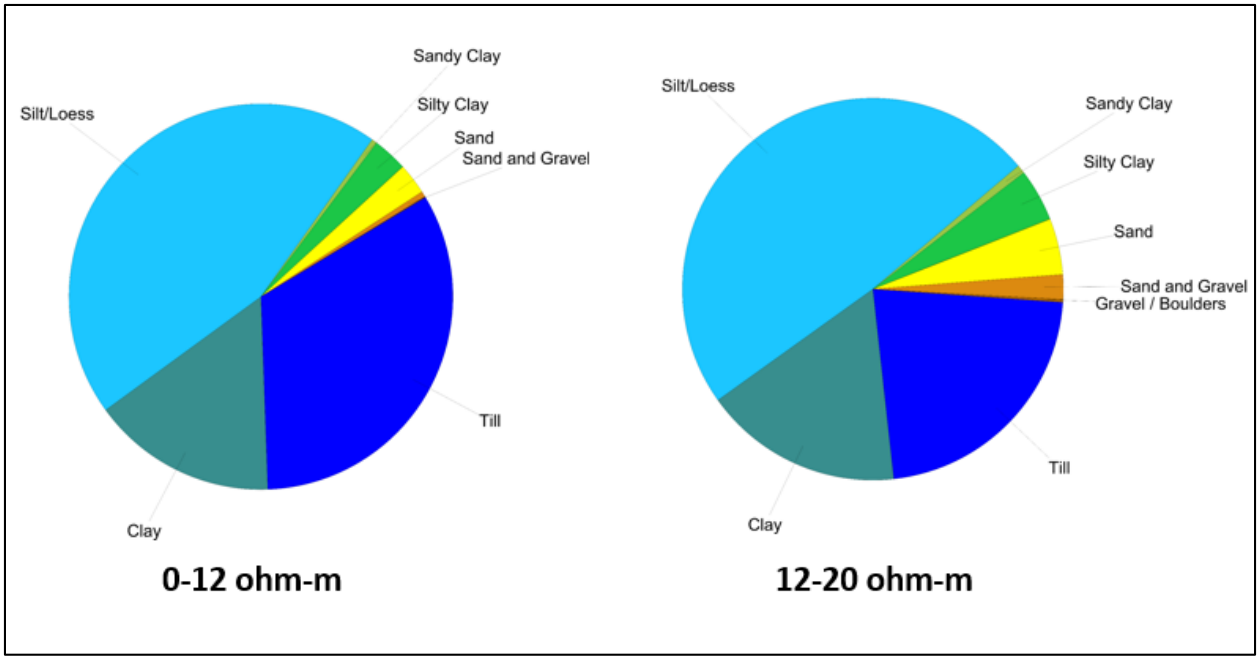



**Figure 5-5: Pie charts of the distribution of material within each resistivity range for the 4 aquifer materials used in the interpretation of the AEM data- 0-12 ohm-m (left) and 12-20 ohm-m (right).**

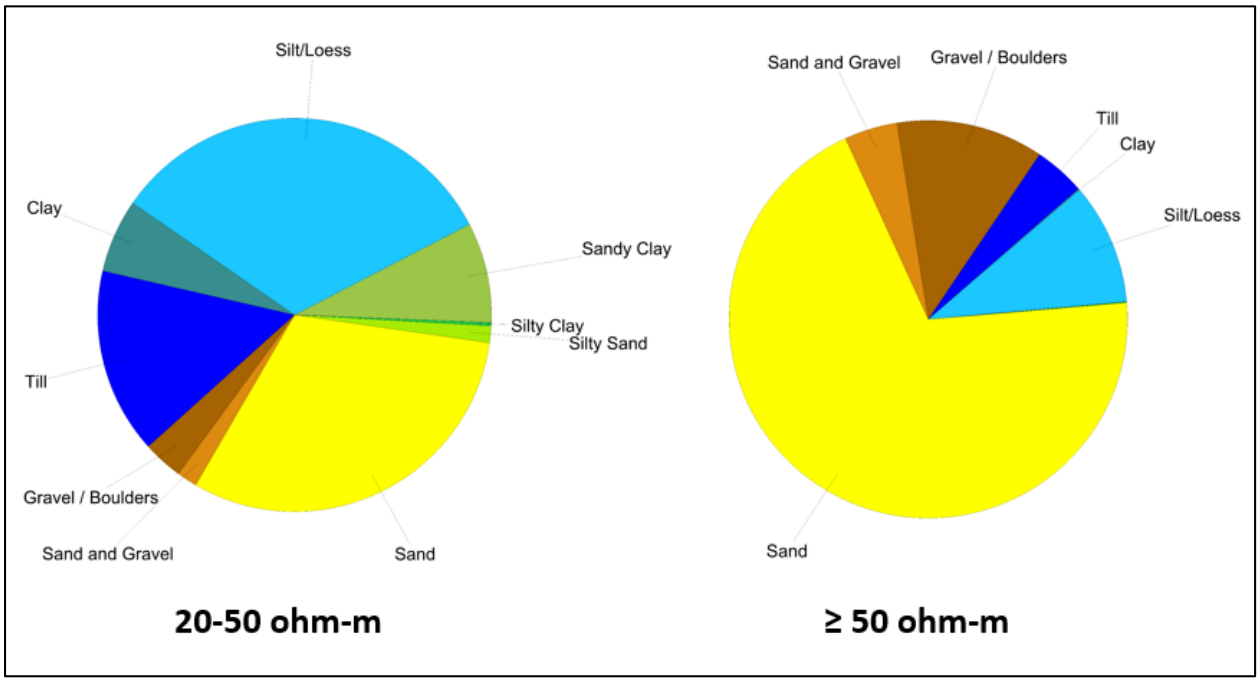



**Figure 5-6: Pie charts of the distribution of material within each resistivity range for the 4 aquifer materials used in the interpretation of the AEM data- 20-50 ohm-m (left), and 50 ohm-m (right) and above.**

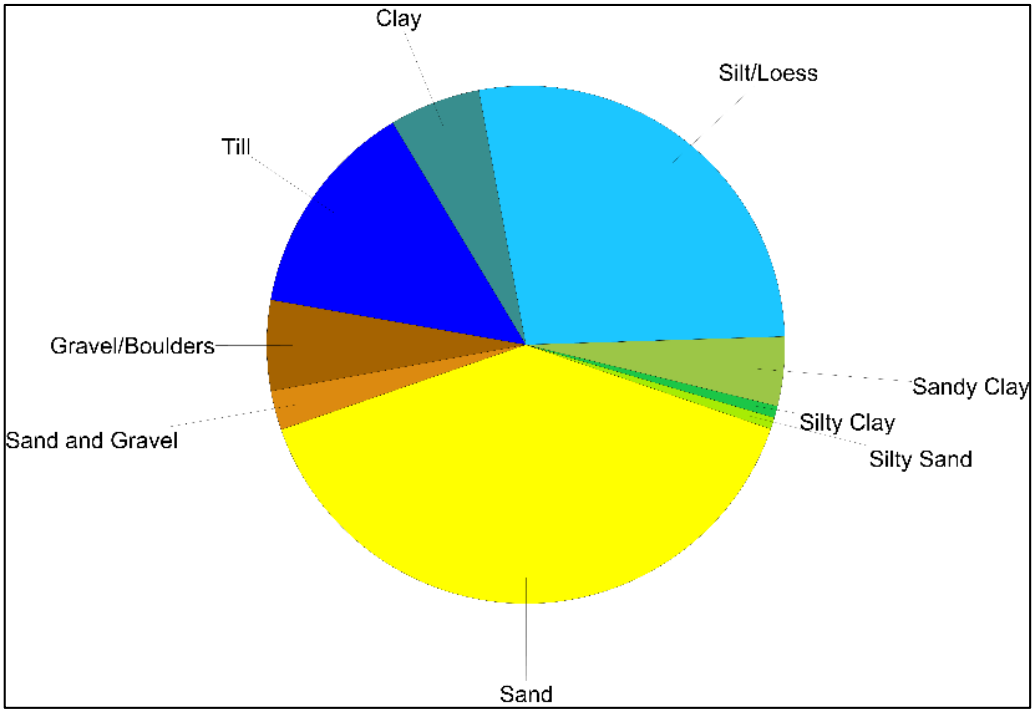



**Figure 5-7: Pie chart of the overall lithology indicated in the 58 e-logs used to characterize the relationship of lithology and resistivity in the project area.**

Figure 5-8 displays four pie charts showing overall percentage of lithologies in selected CSD test holes located within the southern half of the ENWRA project area. These charts are displayed with the CSD glacial till thickness map set in semi-transparent shading to demonstrate the relationship of the percentage of each major material with the extent and thickness of the till within the project area. CSD test hole 5-B-77, located in the southern LPNNRD, has the highest glacial till component in the holes displayed, with over a quarter of the Quaternary section of this hole consisting of glacial till. This area is mapped to be underlain by at least 150 ft of till according to the CSD glacial till thickness map. The abundance of coarse material in this chart also demonstrates that considerable thickness of aquifer materials can be present within, beneath, or above fine textured materials, such as encountered in paleovalleys of eastern Nebraska. At test hole 28-A-61, located in the eastern LPSNRD, silt/loess is the predominant material in the Quaternary section of this hole, comprising nearly two-thirds of the unconsolidated sediments analyzed in this hole. Of the remaining materials present, sand and gravel are the most abundant materials present. Test holes 3-B-73 and 8-A-67, located in the NNRD, each have close to 50 percent of the Quaternary section comprised of sand, with the remainder of the material consisting of fines. The abundance of coarse material at these locations should not be unexpected, as these holes are both located along major surface drainages in the NNRD.

These four pie charts demonstrate the variability in the materials encountered in the CSD test holes across the southern ENWRA area where e-logs were also available for assessing the relationship of resistivity with lithology. The general pattern of material distribution at three of these four locations is similar to the overall distribution of materials in holes from across the project area (Figure 5-8), which is composed of approximately 50% coarse deposits at all the CSD test hole locations used in this analysis.

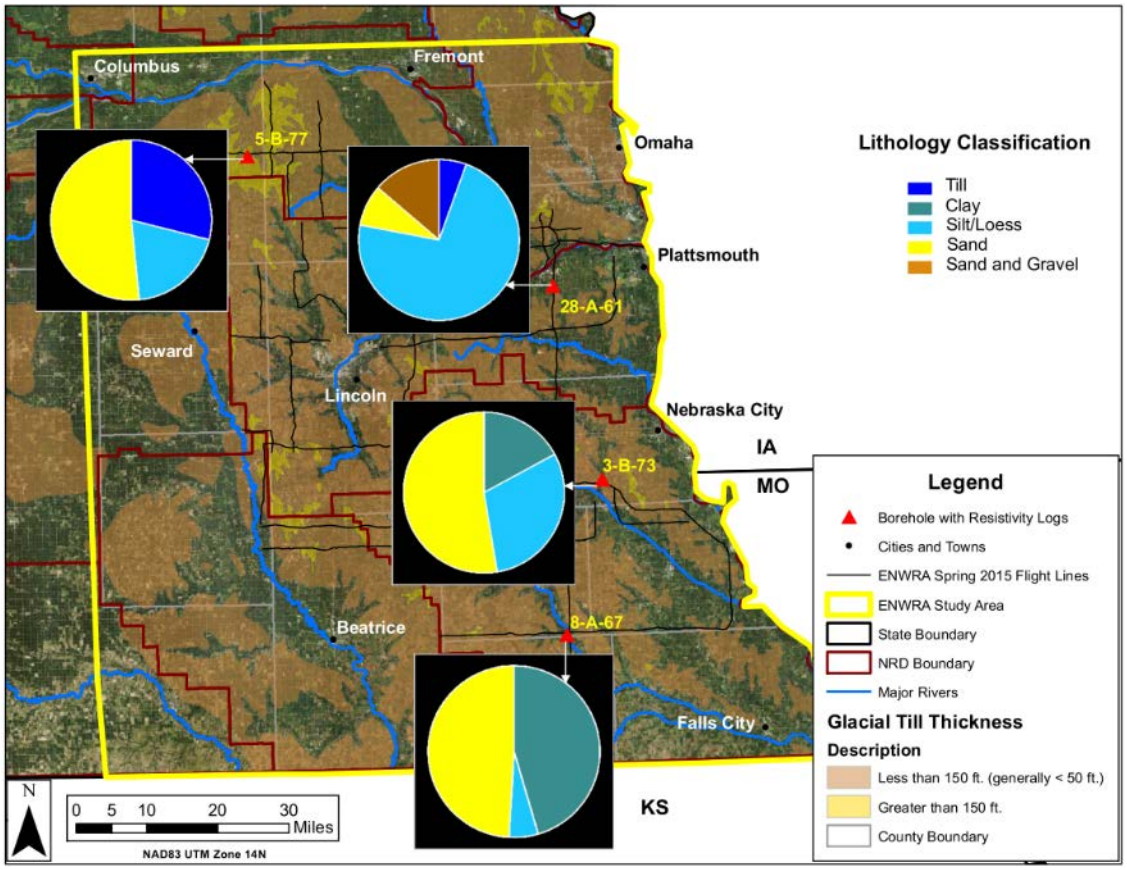



**Figure 5-8: Pie charts showing overall percentage of lithologies in selected CSD test holes in the southern ENWRA project area.**

For the fines in the Quaternary system at these locations, silt/loess is a ubiquitous material type across much of the southern ENWRA project area, but with varying percentages depending on location.

***Basis for Resistivity Thresholds in Quaternary System***

Based on the discussion above in Section 5.1.2, the Quaternary and Tertiary material were separated into four characteristic aquifer materials including non-aquifer (aquitard), marginal, principal, and coarse aquifer material. These breaks were determined based on the distribution of the resistivities (Figure 5-4) and the lithology (Figure 5-5 and Figure 5-6). However, the question can arise as to the sensitivity of the selection of the thresholds, specifically the lower threshold for the principal aquifer material (20 ohm-m). In order to assess this sensitivity, a test was conducted by analyzing the data set with thresholds of 20 and 21 ohm-m. The change in the percent thickness of the principle aquifer material was then calculated over the complete data set. It is important to note that the thickness was evaluated as being greater than or equal to both 20 and 21 ohm-m. For each of the thresholds (20 and 21 ohm-m), the materials were calculated based on the methodology outlined in Section 5.0. The thicknesses of the principal aquifer material were then compared using the following:

$$T_{Diff} = \frac{abs(T_{20} - T_{21})}{T_{20}}$$

where $T_{Diff}$ is the fractional difference in thickness, $T_{20}$ is thickness of the principle aquifer material with resistivities greater than or equal to 20 ohm-m, and $T_{21}$ is the thickness of the principal aquifer material with resistivities greater than or equal to 21 ohm-m.

For discussion purposes, this calculation was carried out for all data points within the Fall 2014 flight area, including the ENWRA and the LENRD flight areas (Figure 5-9). The statistics of this change in thickness analysis indicate that the median fractional difference is at 0.04, or 4%, and a first quartile of 0.01 (1 percent), and a third quartile of 0.10 (10%). This means that 75% of the data indicates a thickness change of the principal aquifer materials of less than 10% when comparing thicknesses derived from both 20 ohm-m and 21 ohm-m thresholds. Thus Figure 5-9 displays a histogram of the distribution of the variation in interpreted thickness of the principal aquifer material using 20 and 21 ohm-m thresholds.

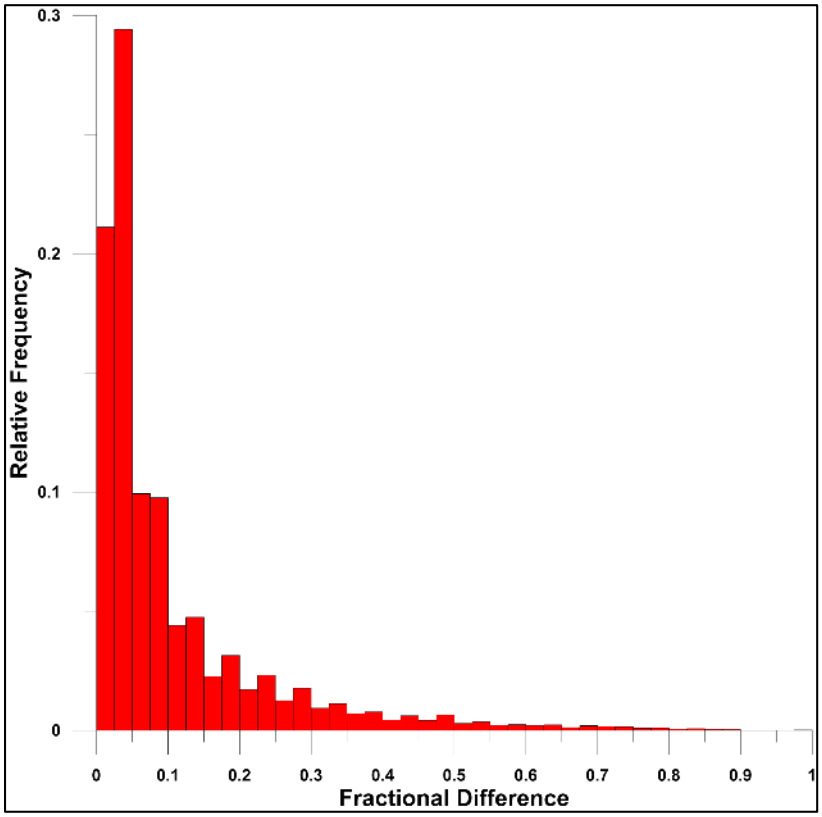



**Figure 5-9: Histogram of the distribution of the fractional difference in the thickness of the principal aquifer materials using 20 and 21 ohm-m resistivity thresholds.**

This analysis indicates that the sensitivity of picking 20 or 21 ohm-m is relatively insignificant for the overall interpretation of the thickness of the principal aquifer materials. Figure 5-10 demonstrates the impact on the interpreted cross sections with an example cross section showing both 20 and 21 ohm-m thresholds. This figure demonstrates that the area encompassed by the 20 ohm-m threshold (solid black line) is slightly greater than the 21 ohm-m aquifer extent (dotted black line), which results in a thicker estimation of the principal aquifer material. This result is not unexpected as the lower resistivity value should encompass a larger range of resistivities of greater than or equal to 20 ohm-m. However, it can

also be observed that the change in the interpretation is generally insignificant (see zoomed-in view in Figure 5-10), as the change in overall extent, when viewing the principal aquifer materials on a regional basis, is negligible when considering overall volume of the aquifer. It should be noted that in some areas where principal aquifer material is present at the land surface (indicated by blue arrow in Figure 5-10), but separate from the underlying main body of principal aquifer material, these intervals were included in the interpretation even if these features were separated by marginal aquifer material. This approach was warranted since this interpretation is a discussion on the major aquifer features in the subsurface of the LENRD. Surficial resistive materials are considered critical in assessing areas of aquifer recharge and, thus, are included in the principal aquifer zone even where separation from the main principal aquifer materials can occur.

In summary, the results of this sensitivity analysis indicate that for 75% of the data, a thickness change of less than 10% occurred between a threshold change of 20 to 21 ohm-m. Overall, the interpreted principal aquifer materials show a stable solution that is not sensitive to a 1 ohm-m change in the principal aquifer material threshold.

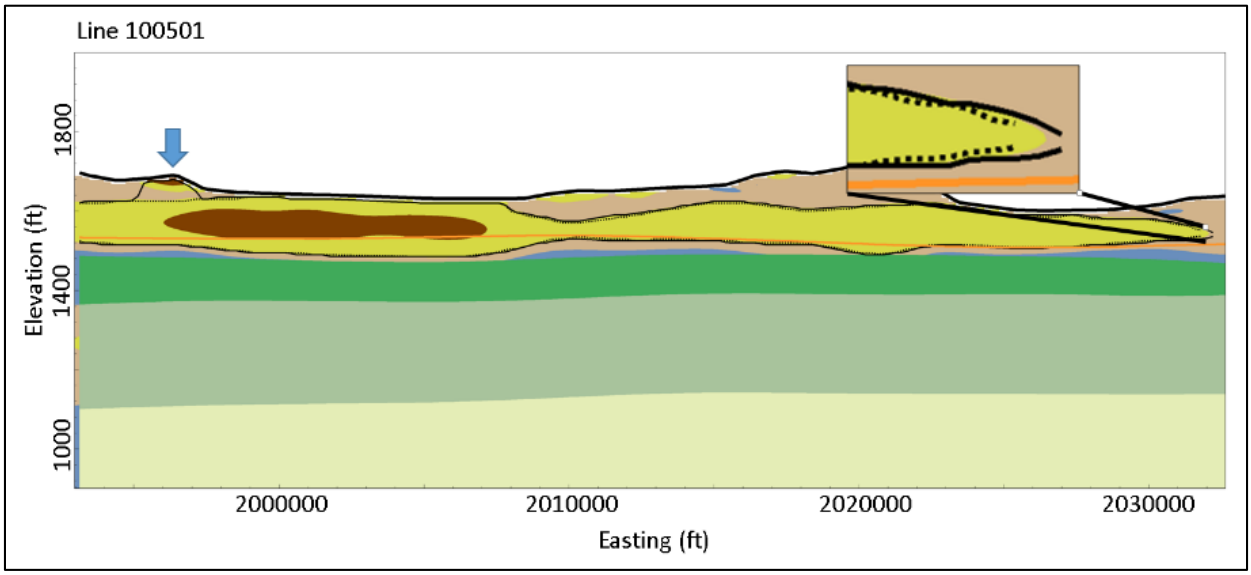



**Figure 5-10: Example cross section illustrating the small difference between selecting a 20 ohm-m threshold or a 21 ohm-m threshold to define the principal aquifer. The solid black line enclosing the yellow (principal aquifer material) represents the 20 ohm-m threshold and the dotted black line enclosing the principal aquifer material represents the 21 ohm-m threshold.**

#### *5.1.2.2 Bedrock Resistivity Thresholds*

Figure 5-11 displays a box and whiskers plot of the resistivity distribution for the bedrock strata described in the interpretation section, including the *To* (which is present only in the far northwest corner of the LPNNRD). Analysis of the bedrock data was conducted on e-logs from CSD test holes that penetrated into the bedrock. The analysis also included oil and gas wells with data on Paleozoic strata. Note that Figure 5-11 includes strata present in the northern ENWRA area only. These were included to demonstrate the overall distribution in resistivity of bedrock materials across the entire ENWRA area. The median resistivity values for each unit in Figure 5-11 are 40 ohm-m or less. *Kp* has the lowest median (9 ohm-m) and lowest overall value of resistivity, as would be expected for a lithologic unit

predominately composed of shale. *Kn* and *Kd* have similar distributions and maximum/minimum ranges, with one exception being the *Kd* having a lower median resistivity (approximately 20 ohm-m). The similarities in these two units on this plot exemplify how the *Kn*, which is predominately a shale and chalk, can contain resistive material, and the *Kd*, predominately a sandstone, can contain shale and other more conductive material. The *KcKgg*, and the undifferentiated Paleozoic strata also have similar resistivity characteristics, with median values around 16 ohm-m. The undifferentiated Paleozoic units show the widest range in detected resistivities, which should not be unexpected as this sequence contains resistive limestone and conductive shale units.

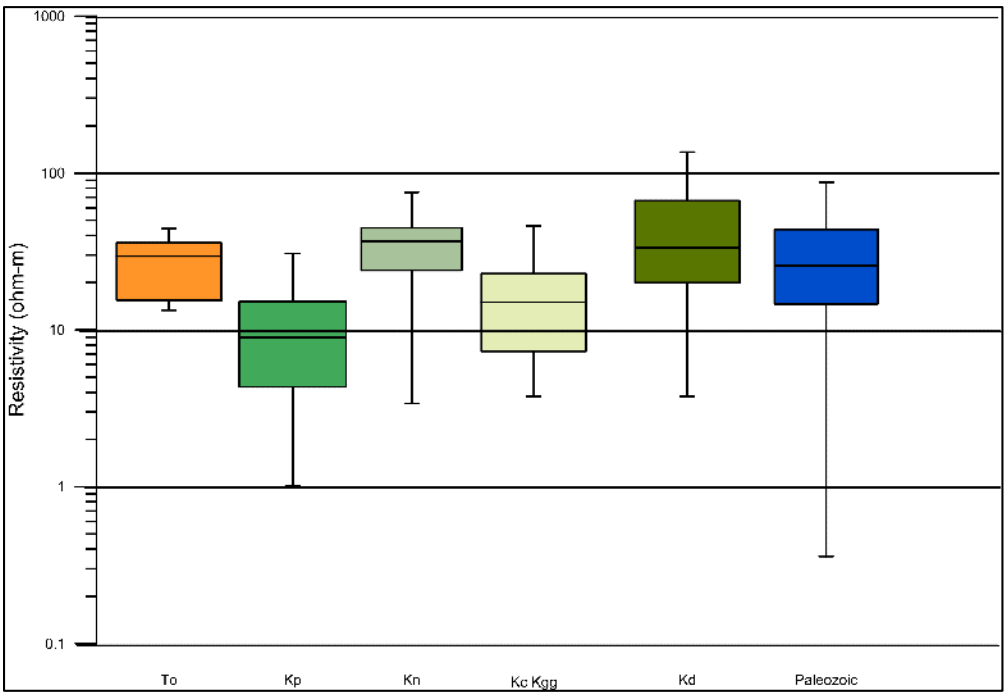



**Figure 5-11: Box and whiskers plot of the resistivity distribution of the Tertiary, Cretaceous and Paleozoic bedrock units discussed in the interpretation of the AEM data.**

The *To* has the narrowest distribution band of the formations displayed on Figure 5-11, with maximum and minimum resistivities of 45 and 12 ohm-m, respectively. The median value in the *To* is 30 ohm-m, a value that would be expected of interlayered sandstone, siltstone, sand, gravel, and silt. This narrow distribution for the *To* could be a result of the distal location of these sediments from their source area in the Rocky Mountains of Colorado and Wyoming. In regards to the NRDs discussed in this report, the *To* is present beneath only the far northwestern section of the LPNNRD.

Review of the NOGCC database provided three holes with electrical logs within three miles of a flight line across the entire ENWRA project area. Figure 5-12 displays the electrical resistivity logs compared with the closest AEM sounding for two NOGCC well locations in the northern ENWRA project area (wells 2616718000API and 2616721003API, 5,186 ft and 12,828 ft, respectfully, from the flight lines). This relatively close proximity allowed comparison of the AEM inversion model to the resistivity logs. It is important to note that the resistivity logs started within the Cretaceous strata. The comparisons show a general match to the AEM resistivities at depths in excess of 1,000 ft. It is also important to note that the averaging effect of the AEM models smooth out the thin resistive units around 600 ft in 261671900

and 500 ft in 2616721003. The logs compared to the AEM clearly indicate the inflection in the resistivity logs at 400 ft. This further provides assurance that the AEM is mapping the resistivity structure of the bedrock within the ENWRA survey area.

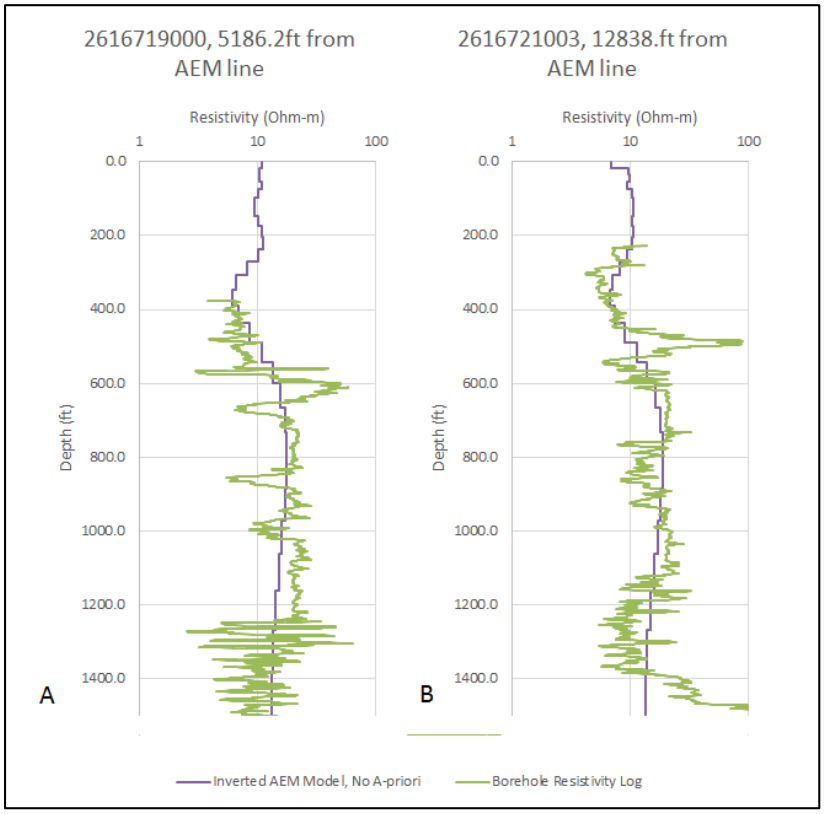



**Figure 5-12: Deep oil and gas borehole resistivity logs compared with inverted AEM models. A: Well 2616719000, 5,186 ft from the AEM line, B: Well 2616721003, 12,838ft from AEM line.**

***Kd Resistivity Threshold***

As a secondary aquifer resource in eastern Nebraska, the *Kd* holds potential as a new or additional groundwater source for users across parts of the ENWRA area. The AEM survey's DOI penetrated below the *Kd* in most locations, allowing for a full view of the formation electromagnetically, which can reveal changes in resistivity, and thus lithologic content and/or changes in water quality. To characterize the variability in the *Kd*'s resistivity, the relationship of lithology and resistivity was evaluated using the same method applied in associating unconsolidated lithologies to resistivity as described previously in this section. Resistivities were associated with each lithologic description in the CSD test holes that penetrated through the *Kd* in this process and are within the CSD's stratigraphic identification of the *Kd*. It should be noted that even what is presumably considered a consolidated formation, intervals of unconsolidated lithologies are noted in the CSD test hole descriptions.

Figure 5-13 shows a breakdown of textural size and nature of consolidation (unconsolidated (clay/silt) and consolidated fines (shale), unconsolidated (sand and gravel) and consolidated coarse (sandstone). The distribution for the coarse categories is similar, with the 25th quartile for each greater than 50 ohm-m, and median values over 70 ohm-m. Distributions for the fine textured materials are similar, with the

median values range from 25 to 30 ohm-m. In these plots, however, shale has a wider range of values detected in comparison to unconsolidated fines. Thus, in the analysis of the lithology-resistivity relationship for the *Kd*, unconsolidated and consolidated fines were grouped together, as well as coarse-textured unconsolidated and consolidated materials. The objective of this analysis was to determine if any natural breaks in the resistivity distribution were evident to base selection of categorical ranges for showing the variation in resistivity within the *Kd*.

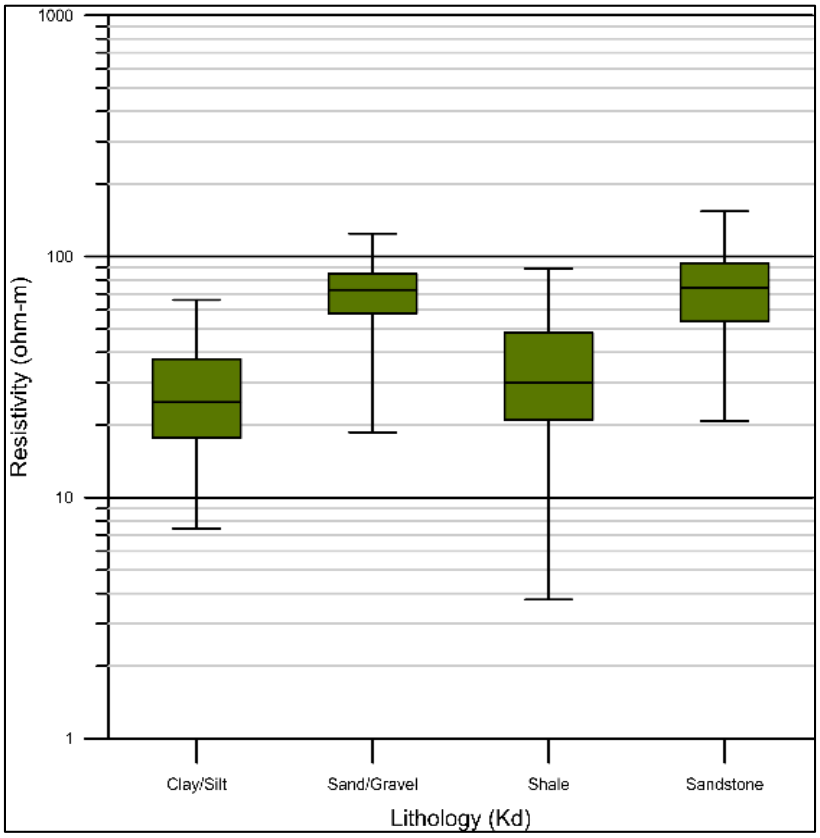



**Figure 5-13: Box and whisker plot for the major lithologic texture categories within the *Kd* from CSD e-logs located across the entire ENWRA project area.**

Figure 5-14 shows the count distribution of resistivity for coarse materials (top plot), fine materials (middle plot), and a composite of both major material distributions (bottom plot). From this distribution, it is evident that the bulk of fine textured materials are generally below 40 ohm-m, and that the bulk of the coarse textured distribution is above 30 ohm-m, with overlap of the two groups in the 20 to 40 ohm-m range. The plot for fine textured materials indicates bimodal distribution. The distribution below 10 ohm-m is likely due to brackish/saline water in the *Kd*, and the distribution greater than 10 ohm-m is most likely related to lithologic character. Thus, three general categories were selected from this distribution- 0-20 ohm-m, representing zones of the *Kd* predominately consisting of fines or high TDS pore water; 20-40 ohm-m, representing intervals of interbedded fine and coarse materials, and zones of 40 ohm-m or greater, which are intervals of the *Kd* where coarse textured deposits comprise the bulk of the material at that interval. These ranges are not categorized as “aquifer materials” as in the Quaternary system descriptions, since little is known about the aquifer potential in the *Kd* based on

resistivity alone. However, generalized inferences can be made in that the higher the resistivities encountered, the greater the probability the interval will produce beneficial flow to a well. To determine if any relationship exists between the resistivities revealed by the AEM data and production wells, XRI reviewed all DNR registered well records within 0.5 miles of the southern ENWRA area flight lines for production rates of wells screened in the *Kd*. Overall, no discernible pattern was evident, as nearly all wells along these lines near the CSD test holes penetrated only into the upper 10 to 20 ft of sandstone and were used for domestic purposes, with registered rates normally ranging from 10 to 20 gpm. It is unknown as to whether the *Kd* is capable of producing higher capacities to wells in these areas, since the wells currently existing at these locations typically do not require high pumping rates.

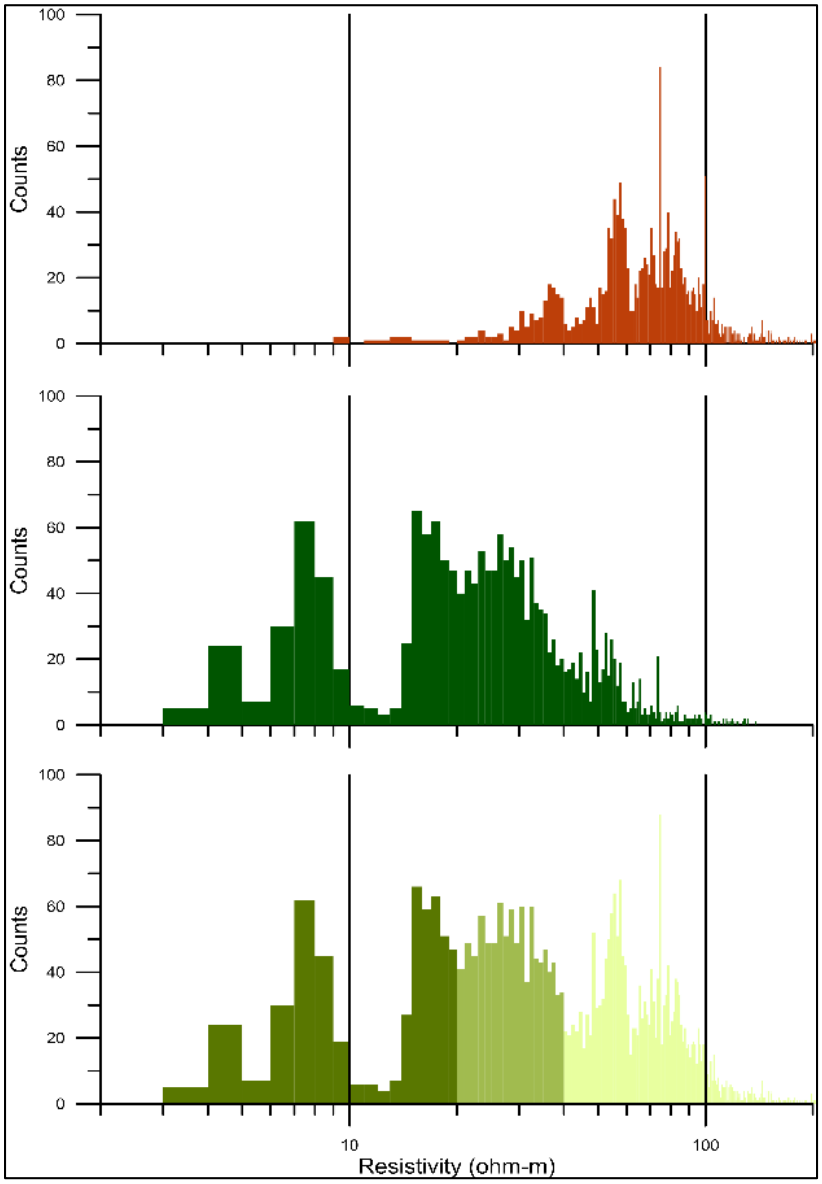



**Figure 5-14: Resistivity count distribution by major grain size category for CSD test holes screened in the *Kd*. Plot A (top) represents all coarse unconsolidated and consolidated deposits; plot B (middle) represents all unconsolidated and consolidated fines, and plot C (bottom) represents a composite of both coarse and fine materials, color coded by the ranges of 0-20, 20-40, and 40 ohm-m and above used in the interpretive figures of the *Kd* beneath the ENWRA project area.**

In conclusion, the evaluation of the relationship of lithology vs. resistivity in the *Kd* intervals resulted in 3 major intervals of resistivity, with the zones of 40 ohm-m or greater indicating the areas of higher likelihood of groundwater development from the *Kd* sequence beneath the project area.

## 5.2 Hydrogeologic Framework Interpretation

The AEM survey reveals considerable variability in the Quaternary system as well as the Cretaceous and Paleozoic strata deposits across the southern ENWRA project area. "Quaternary system" is a term used in the interpretative section of this report to describe all unconsolidated materials overlying the Cretaceous and Paleozoic bedrock, thus including aquifer and non-aquifer material alike. As mentioned in the prior section, *To* is present in the far northwestern section of the LPNNRD and will be discussed in further detail below in section 5.3.1. Figure 5-15 displays in 3D the overall distribution of materials (as described in the previous section) across the southern ENWRA area, along with major drainages and NRD boundaries. Overall, the most extensive principal aquifer deposits are found in the southern and eastern LPNNRD, the eastern and southern LPSNRD, and in the northwestern NNRD. Each of these areas of extensive principal aquifer material is associated with glacially derived paleovalleys or alluvial valley settings. Thicknesses of these features can range from 200-300 ft in places and extend for several miles with varying widths. Many of the intervals of principal aquifer in the subsurface contain many sand-rich zones (50 ohm-m or greater), including some areas such as the Todd Valley and Platte River valley where most of the resistivity signature of the Quaternary system is 50 ohm-m or greater.

Marginal aquifer is prevalent in the northern LPNNRD, throughout the LPSNRD as well as in many locations of the NNRD. Marginal aquifer materials range in thickness from over 250 ft (northern LPNNRD, western LPSNRD, and central NNRD) to less than 50 ft in the NNRD. In many locations, marginal aquifer materials are interlayered with, or overlain by, aquitard materials. Aquitard material thickness can range from less than 20 ft at locations scattered across the survey area to nearly 300 ft in the parts of the LPNNRD and LPSNRD. The AEM survey also revealed resistive variability in the *Kd*, with several areas of 40 ohm-m or greater ranging from 200-400 ft in thickness. The AEM resistivity profiles also revealed areas in the *Kd* where high TDS water is present, particularly north and west of Lincoln in the LPSNRD. The AEM also revealed considerable variability in the resistivity of the Paleozoic system and older deposits, including thick sequences of low-resistivity material, typically associated with shale/limestone sequences, and highly resistive zones, particularly in the far southern extent of the NNRD in the area of the Nemaha Uplift. Structural features are also evident in the AEM data. These features will be discussed further in Section 5.2.3.

To assist in the characterization of the aquifer underlying the project area, the 1995 Nebraska regional water table surface (CSD) was converted to a grid dataset and incorporated into the hydrostratigraphic interpretive profiles of the project area (blue dashed line in the profile figures). Overall, the regional water level surface conforms closely with the subsurface character revealed in the AEM profiles. In the drainage valleys, the surface matches closely with the land surface elevation, which would be expected where shallow groundwater conditions typically persist. Beneath the upland areas, the regional water level surface is typically found within the till deposits, indicating confined or semi-confined aquifer conditions, which are typical in the principal Quaternary aquifer in eastern Nebraska where thick till and loess sequences are present.

Note that all interpreted flight lines are included in Appendix 1. Select profiles showing major features are displayed in the following sub-sections, along with 3D images of the southern ENWRA area's hydrogeologic framework.

### *5.2.1 Quaternary Geologic and Depositional Features Revealed in the AEM Survey*

#### *5.2.1.1 Extent of Principal Aquifer Materials*

The aquifer materials in the ENWRA reconnaissance survey project area, including Quaternary and Tertiary deposits (where present), are identified with the colors tan (marginal aquifer- 12-20 ohm-m), yellow (principal aquifer- 20-50 ohm-m), and maroon (coarsest, sand-rich intervals of the principal aquifer- >50 ohm-m). These colors correspond to the resistivity ranges described at the beginning of Section 5.1. As displayed in Figure 5-15, Figure 5-16, and Figure 5-17, considerable variability exists in the aquifer resources that underlie the southern ENWRA project area, most notably in the overall thickness of the features, from less than 50 ft in parts of the LPSNRD and NNRD to over 400 ft in the western LPSNRD and LPNNRD.

Unlike the northern half of the ENWRA area where principal aquifer deposits are continuous and extensive throughout much of the western half of the surveyed area, the bodies of principal aquifer materials in the southern area are confined to more limited areas within paleovalleys and beneath modern-day valleys. Extensive intervals of marginal and aquitard material separate these features, many of which were deposited atop bedrock highs that further separate the paleovalleys. The resistive zones in the Quaternary system indicated by the AEM survey closely matched with known modern alluvial valley settings and paleovalleys displayed in Figure 2-11 and Figure 2-12. The data from the AEM survey demonstrates how airborne geophysical data can provide further refinement in the overall architecture of the buried aquifers, including improved detail in the basal elevation and contact with underlying bedrock, the nature of the valley edges and lateral extent of the aquifer deposits, and the thickness and character of overlying confining materials (Example- flight line 400803 in the NNRD). Even in areas of dense test hole/lithologic log control, the AEM data can reveal changes in the subsurface character that occur over short intervals.

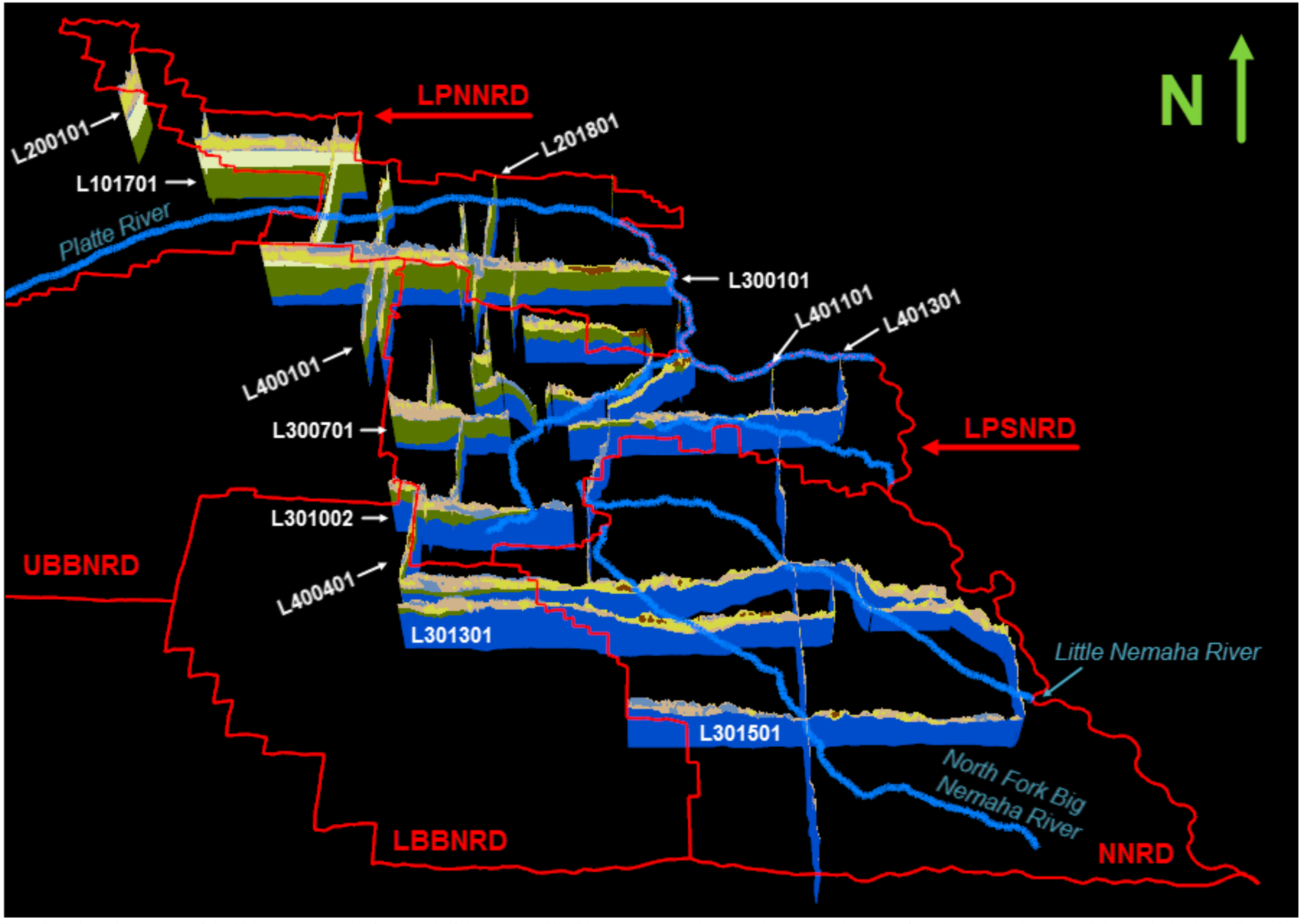



**Figure 5-15: A northward view of the 3D hydrostratigraphic framework of the southern ENWRA project area, including geologic materials ranging from Quaternary deposits to Paleozoic bedrock. See Figure 5-2 for the color codes of the materials and geologic strata displayed.**

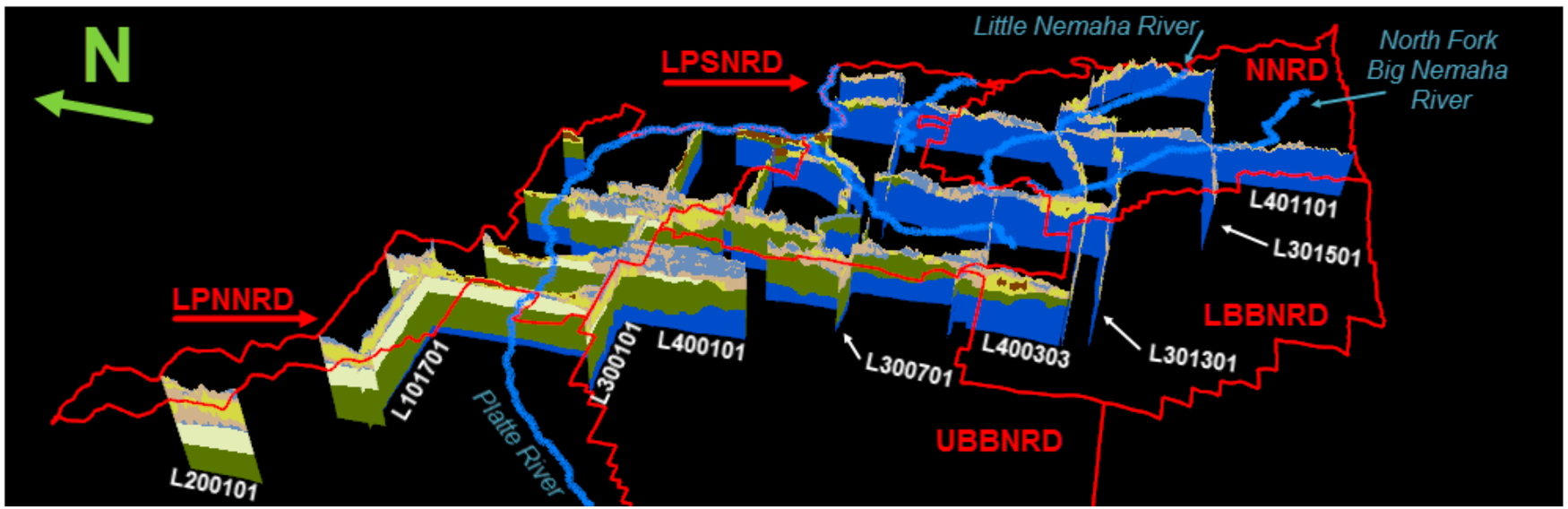



**Figure 5-16: An eastward view of the 3D hydrostratigraphic framework of the southern ENWRA project area. See Figure 5-2 for the color codes of the materials and geologic strata displayed.**

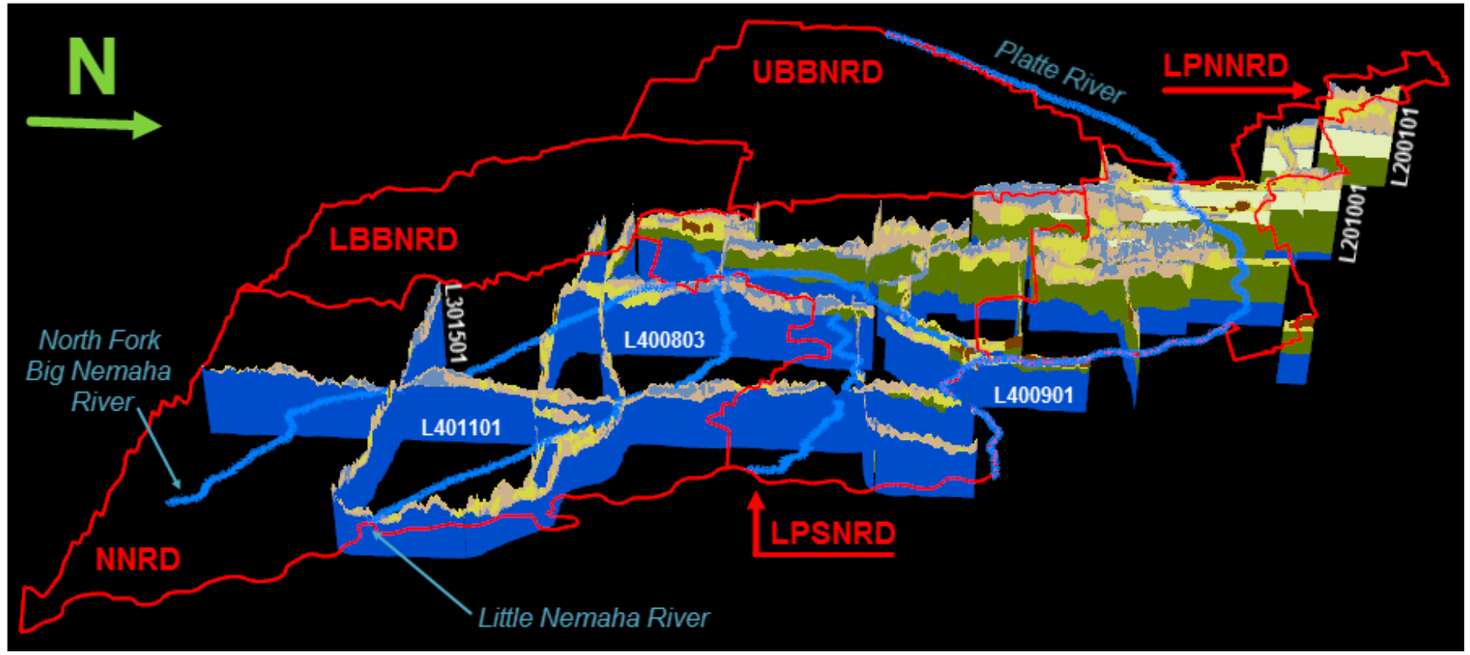



**Figure 5-17: A westward view of the 3D hydrostratigraphic framework of the southern ENWRA project area. See Figure 5-2 for the color codes of the materials and geologic strata displayed.**

As mentioned in the beginning of Section 5.2, each of the NRDs discussed in this report are underlain by principal aquifer deposits hosted in various depositional settings. Further detailed discussion on principal aquifer material features is provided in the individual NRD discussions in the following sub-sections of this report. The AEM survey also revealed several locations across the three NRDs in the survey area where principal aquifer materials are situated above the regional water table surface and are in close vertical distance to the land surface (e.g. flight line 301201 in the NNRD). These features are generally less thick (<100 ft) than the main bodies of underlying principal aquifer material, but nonetheless can play a critical role in the groundwater flow system, as such areas have the potential to experience higher rates of recharge, as well as increased vulnerability to water quality impacts. In other areas, the AEM reveals locations where principal aquifer materials are overlain by thick sequences of aquitard and interlayered aquitard/marginal aquifer material (e.g. flight lines 300101 in the LPNNRD (western half) and 400601 in the LPSNRD). At many of these locations, the principal Quaternary aquifer is confined by the till and loess that comprise the aquitard material. Defining these features from the AEM data can improve the conceptualization of the groundwater flow system, including storage dynamics, recharge rates, and water quality management practices.

Principal aquifer materials partially consist of the *To* in the northwestern corner of the LPNNRD (e.g. flight line 200101). In this area, the *To* ranges from 80 to over 200 ft thick and consists of principal and marginal aquifer material, and is overlain by upwards of 250 ft of Quaternary materials, mostly principal and marginal deposits with scattered aquitard intervals.

#### *5.2.1.2 Extent of Marginal Aquifer Materials*

Marginal aquifer materials are present throughout the southern ENWRA project area and are detected along every flight line in the AEM survey. Marginal aquifer material comprises a majority of the Quaternary system's aquifer resources beneath the survey area, acting as a matrix of unconsolidated material between the more isolated bodies of principal aquifer material. Thickness of the marginal aquifer material ranges from less than 100 ft in parts of the central and eastern LPSNRD and in east-central areas of the NNRD (e.g. flight lines 401301 and 300304 in the LPSNRD, 401201 in the NNRD), to over 400 ft in the western LPSNRD (e.g. flight line 300701). The degree of saturation of the marginal aquifer materials varies across the project area. The placement of the regional water table surface indicates relatively thick sections of saturated marginal aquifer material (>200 ft) in some areas (Example- flight line 300701), whereas in other locations, saturation is less than 50 ft to complete absence in some areas, particularly in the NNRD. Thick sequences of marginal aquifer material, oftentimes interlayered with aquitard deposits, are situated above the regional water table surface (e.g. flight lines 400701 and 201801 in the LPNNRD). In areas where unsaturated marginal aquifer material are present immediately below the land surface, recharge potential exists, but is likely more variable and at lower rates than where principal aquifer materials are present at the land surface, as marginal aquifer materials can contain a substantial percentage of fines (Figure 5-5). Thus, local studies would be required to estimate recharge rates above unsaturated marginal aquifer material in the project area.

#### *5.2.1.3 Non-Aquifer Materials*

Non-aquifer material ("aquitard") is present throughout the Quaternary system of the southern ENWRA flight area. This material is present in some places at the land surface and continues to considerable depths, as well as interlayered within marginal and principal aquifer materials. In some areas, aquitard

materials comprise basal Quaternary deposits that sit directly above Cretaceous and Paleozoic bedrock. From the central LPNNRD southward across the LPSNRD and in the far western NNRD, the glacial till is associated with the Cedar Bluffs moraine complex as mapped by Reed and Dreezen (1965). These deposits, consisting primarily of glacial till and loess, along with other low-permeability materials (mixtures of clay-rich sediments) are shown as light blue in the 3D hydrogeologic frameworks (Figure 5-15 and Figure 5-16), the AEM interpretive profiles and 3D framework images in this section and Appendix 1. In general, aquitard deposits are more extensive and thick beneath the LPSNRD and LPNNRD in comparison to the NNRD.

The AEM data reveals the combined thickness of these deposits in detail, with the intervals of greatest thickness (>200 ft) present in the central LPNNRD, southern LPSNRD, (e.g. flight lines 301002 and 400803 in the LPSNRD, 400301 in the LPNNRD). In some areas of these profiles, nearly the entire Quaternary system, from the land surface to the underlying bedrock, is comprised of aquitard materials. In other areas, aquitard deposits exceeding 150 ft in thickness overlie principal aquifer deposits within paleovalleys, creating confined aquifer conditions in places (e.g. flight line 400601 in the LPSNRD, and 101701 and 300101 in the LPNNRD). The AEM data provides greater detail in the presence, extent, and thickness of these low-permeability materials, information which can be critical in conceptualizing and modeling groundwater flow system dynamics, particularly in regards to storage and recharge. Additionally, water quality management planning can benefit by the identification of these materials that restrict downward vertical movement of unsaturated flow to the underlying principal aquifer materials.

#### *5.2.1.4 Cretaceous Stratigraphic Sequence*

***Niobrara Formation (Kn)***

The uppermost Cretaceous strata in the southern ENWRA project area are chalk, limestone, and shale deposits of the *Kn*, which extends under the northwestern half of the LPNNRD. The unit is present only in north-south flight lines 200101 and 200401 and a small interval of the west-east flight line 101701. The *Kn* is the uppermost bedrock unit immediately below the Quaternary system in this area. The thickness of the formation decreases from a maximum of 240 ft in flight line 200101 to approximately 80 ft in flight line 200401.

The resistivity profile reveals the lithologic variability in the formation, as resistivities range from around 12 ohm-m to nearly 40 ohm-m. The lower resistivities likely indicate shale and marl, the mid-range resistivities indicate chalk, and the highest resistivities are likely limestone. The *Kn* is not considered a widespread aquifer source in eastern Nebraska. However, beneath the major river valleys in the northern ENWRA project area, the uppermost interval of the *Kn* can contain fractures that transmit groundwater in hydraulic connection with overlying Quaternary aquifer materials. This condition is evident in resistivity profile along flight line 200801 (personal comm. with Sue Lackey, CSD, October 2013).

***Carlile Shale & Greenhorn Limestone/Graneros Shale (Kc, Kgg)***

In the interpretation of the northern ENWRA project area, the *Kc* was combined as one interpretive lithologic unit with the *Kgg*, as these two units showed similar resistivities in many locations, as well as the fact that both units act as aquitards in the Cretaceous sequence. Although the *Kc* was identifiable in

the resistivity data, the variability in resistivity within the *Kgg* made it difficult to discern clear contacts in the AEM data at all locations in the subsurface, thus, test hole data and 2D historic cross sections were relied on to guide the selection of the stratigraphic contacts of these units. Ultimately, these three units were grouped as one hydrostratigraphic unit in the interpretation of the AEM data. This combined hydrostratigraphic unit extends beneath only the LPNNRD in the southern ENWRA project area, where it terminates in the west-central part of the district.

The *KcKgg* is present across much of the western half of the LPNNRD. The unit is continuous with a relatively flat upper contact with overlying *Kn* and Quaternary deposits in this area, but becomes separated into individual bodies near its eastward terminus, as evident in flight lines 300101 and 201301. The *KcKgg* is over 300 ft thick along flight lines 200101 and 200401, but thins to approximately 200 ft thick along flight line 201301, where apparent erosion separated an isolated block of the unit beneath the Platte River valley. The apparent southern terminus of the unit is visible in flight line 201001, where it pinches out in a relatively short distance near the border of the LPNNRD and the LPSNRD. Beneath flight lines 201001 and 201301, the *KcKgg* serves as the basal bedrock unit beneath the Quaternary system, including below the extensive principal aquifer deposits that fill the Platte River valley.

***Dakota Formation (Kd)***

The *Kd,* which hosts the Maha aquifer in eastern Nebraska, is present beneath approximately the northwestern half of the project area. The overall thickness of the *Kd* within the project area ranges from approximately 600 ft in the northwest corner of the LPNNRD (flight lines 101701, 201001) to minimum thicknesses of less than 40 ft beneath the southern LPSNRD. The southeastern terminus of the *Kd* follows a southwest to northeast margin in the LPSNRD. In the eastern half of the LPSNRD, the *Kd* is present in isolated bodies separate from the continuous *Kd* sequence that extends westward to the Rocky Mountains. Many of these isolated bodies of *Kd* in the eastern LPSNRD are at shallow elevations and appear to have erosional drainage features present on the unit's upper surface. The unit has variable resistivity as indicated in the AEM profiles, ranging from less than 10 ohm-m to over 40 ohm-m. This variability arises due to be lithologic changes as well as changes in TDS content of the groundwater contained in the aquifer. The high TDS conditions are clearly evident along profiles north and west of the city of Lincoln in the northwestern LPSNRD.

Dip in the *Kd* strata is less pronounced compared locations in the northern ENWRA project area. Westward slope in the strata towards the Central Nebraska Basin is evident along flight line 300701 in the western LPSNRD. Overall, however, the *Kd* has generally little apparent slope in the LPSNRD and the LPNNRD.

The *Kd's* higher resistive zones (>20 ohm-m) are scattered beneath much of the LPNNRD and LPSNRD, including beneath the northwestern extent of the LPNNRD. Some of these resistive features approach 400 ft in thickness and extend laterally for several miles (Example- flight line 200801 in the LPNNRD). The *Kd* resistive intervals greater than 20 ohm-m are generally less thick beneath the LPSNRD, typically 200 ft or less, but still extend laterally for several miles beneath many locations of the district. The AEM survey detected several areas of the *Kd* where resistivities exceeded 40 ohm-m, including a large interval in the southeast LPNNRD (flight line 300201) that exceeds 200 ft in thickness and the central

LPSNRD (flight line 400801). Additionally, smaller, isolated intervals of 40 ohm-m or greater *Kd* are apparent throughout the AEM sequence in the southern ENWRA project area.

Sections of the *Kd* beneath the western LPSNRD, particularly to the west and north of Lincoln display low resistivities, typically in the range of less than 15 ohm-m throughout the entire interpreted *Kd* section (flight line 300701), as well as areas where an interface of resistive (fresh water) and more conductive intervals (high TDS water) exist (flight line 400302). Some of the interval of the *Kd* with resistivities below 15 ohm-m are present at relatively shallow depths, as indicated in flight line 300701. Unlike parts of the far northwestern sections of the northern ENWRA project area where the low-resistivity intervals extend over much wider zones of the westward dipping *Kd* strata, the low-resistivity *Kd* in the LPSNRD does not appear to extend westward beyond the southern ENWRA, as areas of resistive *Kd* are apparent in flight lines 400101 and 400201 in the northeastern corner of the UBBNRD and in the far western sections of the LPNNRD as indicated in flight lines 300101 and 200401. The presence of these low resistivity/potential high-TDS features could be the result of dissolution and transport of minerals from overlying or underlying units into the *Kd* (Helgesen et al., 1993). Further discussion on these conditions is included in Section 5.2.2.

The *Kd* bedrock surface topography that underlies the Quaternary materials varies across the southern ENWRA project area, from generally flat in some areas to more pronounced undulation in the eastern extent of the *Kd* near the margin of the unit, as well as in the western extent of the LPSNRD. In some locations, Quaternary principal aquifer materials fill the topographic depressions in the bedrock between the *Kd* bedrock highs (e.g. flight lines 400502, 400601, and 400602 in the LPSNRD, 400701 in the LPNNRD). The depth to the top of the *Kd* ranges from less than 50 ft beneath the major surface water drainages in the eastern sections of the LPSNRD and LPNNRD, to over 900 ft in far northwestern sections of the LPNNRD where the *Kd* is overlain by thick sequences of Quaternary deposits, *Kn*, and *KcKgg*.

#### *5.2.1.5 Paleozoic Stratigraphic Sequence*

The depth of investigation for the AEM survey allowed for detection of the Paleozoic strata that underlies southeastern Nebraska up to depths exceeding 1,000 ft bgl. As indicated in the geologic time scale and lithostratigraphic sequence (Figure 2-2), Paleozoic units from Permian through Cambrian age are present, primarily consisting of carbonates, evaporites, and clastic material indicative of cyclical transgressions and regressions of shallow seas inundating the region during the Paleozoic Era. Although test hole information was suitable for selection of individual Cretaceous units in the AEM data, sparse information at the depths of the Paleozoic units beneath the southern ENWRA project area prevented the selection and identification of individual Paleozoic formations. Thus, these units are identified only as “undifferentiated Paleozoic units” in the interpretive discussions in this report.

The depth to the top of the Paleozoic system is highly variable across the southern ENWRA project area. In the northwestern half of the surveyed area where Cretaceous strata are present, the top of the Paleozoic system was detected at depths of 1,200 to 1,500 ft bgl in the northwestern LPNNRD, to less than 200 ft in the central and eastern LPSNRD. In the southeastern half of the southern ENWRA project area, primarily within the NNRD, the Quaternary system directly overlies Paleozoic bedrock. In this area,

depth to the Paleozoic can range from essentially 0 to a few feet at outcrops and shallow subcrops to over 500 ft in the southwestern NNRD (flight line 300501).

Considerable variability in resistivity is detected in the Paleozoic strata, from as low as 10 ohm-m beneath parts of every profile in the NNRD to resistivities ranging upwards of 25 to 30 ohm-m beneath the southwestern NNRD. The highest resistivity detected, however, is associated with granite of the Nemaha Uplift and the Elk Creek Carbonatite in the southern NNRD along flight lines 301501 and 401101. These features, along with faults that are clearly evident in the Paleozoic resistivity section, will be discussed in greater detail in Section 5.2.3.

The surface of the top of the Paleozoic strata is irregular in many locations, particularly in the southern NNRD where numerous bedrock highs are revealed in the survey, and where surface drainages have cut into the upper strata of the Paleozoic sequence. This pronounced surface most likely was enhanced during the Pleistocene, when two major cycles of glaciation occurred in the region, each with multiple advancements and retreats of the continental ice sheet. These actions over tens of thousands of years provided the erosional and abrasive forces, along with further erosion by melt water from the glacial margin to further alter the terrain underlain by the Paleozoic system.

Although interpretation of the Paleozoic sequence is beyond the scope of this project, resistive features, some of which are several hundred feet in thickness, could indicate targets for future potential groundwater exploration projects. XRI evaluated NDNR well records along each of the flight lines of the southern ENWRA area to identify registered wells screened in bedrock to aide in the AEM interpretation. This evaluation revealed that some wells in the area surveyed are screened in limestone and shale south of the *Kd*'s eastern margin, indicating that some potential exists for groundwater production from the Paleozoic strata, most likely from fractures or cavities in numerous limestone intervals of the Paleozoic system.

### *5.2.2 Brackish/Saline Conditions in the Subsurface*

As discussed in the sections 5.2.1.4, 4.2.1, and 2.4.2, high TDS levels in the groundwater beneath parts of the southern ENWRA project area are present at shallow depths and are noted in surface water features in parts of the LPSNRD and the NNRD. The AEM survey was able to detect low resistivity (highly conductive) intervals within the shallow subsurface along several flight lines, most notably along immediately north and northwest of the city of Lincoln. Flight line 300701 provides a west-east cross section demonstrating eastwardly up-dipping *Kd* and the connection of this unit with conductive and shallow *Kd* with thin Quaternary deposits in the Salt Creek floodplain. Figure 5-18 displays a 3D image the AEM profiles in this area showing resistivities of 8 ohm-m or less in the subsurface, as well as resistivity values along the upper layer of the geophysical model, the latter of which indicates highly conductive (low resistivity) conditions at the land surface. Two profiles are of keen interest in this figure. Profile 300302 shows the up-dipping zone at 8 ohm-m or less within the *Kd*, and flight line 300303 that displays the 8 ohm-m or less material immediately below the land surface. Additionally, along flight line 300303, resistivities of 8 ohm-m or less are indicated at the land surface. 2D profiles and plan view of these surface conductivities of flight lines in 300302 and 300303 are shown in Figure 5-19 and Figure 5-20, respectively. For flight line 300302, the plan view map shows the conductivities at the top of the low resistivity interval within the *Kd*, and along flight line 300303, the conductivities displayed are at the

land surface. This map for flight line 300303 demonstrates areas where high-TDS groundwater is reaching the land surface or shallow soils from the *Kd*.

Regional water quality information from Helgesen et al. (1993) indicate TDS levels of 1,000 to 5,000 mg/l in Lancaster County within the *Kd*/Maha aquifer. Although the map from Helgesen et al. (1993) is regional in nature and lacks local detail for the southern ENWRA project area, it does indicate groundwater in the *Kd*/Maha aquifer to have elevated TDS content compared to the rest of the eastern margin of the *Kd* system beneath the High Plains region. Based on the resistivity levels detected in the AEM survey, it is likely that TDS levels are locally higher than indicated on this map, as flight line 300303 reveals where the full sequence of Quaternary deposits (less than 50 ft thick) exhibits a resistivity of 10 ohm-m or less that sits directly above *Kd* strata with similar resistivities. These low resistivity intervals are supported by local water quality information provided from an ecological study of wetlands conducted in the early 2000s. Harvey et al. (2007) reported TDS values from monitoring wells screened at depth in the *Kd* ranging from 12,000 to nearly 17,000 mg/l, whereas near the contact of the sandstone and the overlying shallow alluvium, the values are nearly 1,300 mg/l. The monitoring well from which these values were detected indicated an upward hydraulic gradient from the *Kd* to the shallow alluvial system, which is consistent with the evidence of conductive material connecting the near surface and the *Kd* along west-east AEM profile 300701. With verification of the upward gradient in this area, zones of high hydraulic connection between the *Kd* and the overlying alluvium, as indicated in Figure 5-19, can be characterized in greater detail at localized scales. The changes in high-TDS at the land surface indicate where permeability in the *Kd* is likely the greatest and where local confining intervals of fines (clay, shale) may restrict upward movement of high-TDS water in the *Kd*. The lithologic log of the *Kd* monitoring well in Harvey et al. (2007) indicated the upper 25 ft of *Kd* consisting of clay, which is likely limits rapid upward seepage of the saline water from the *Kd* to the overlying alluvium, as indicated by the order-of-magnitude decline in TDS levels.

The presence of high-TDS groundwater within the Kd and Quaternary deposits near Lincoln appears to be hydraulically connected with deeper strata. The extent of the high-TDS groundwater appears to be relatively limited on the north side of Lincoln to the *Kd*, but this area appears to be connected to a more widespread distribution of high TDS groundwater within the Paleozoic system beneath much of the southern ENWRA project area. Figure 5-21 displays this condition by showing areas of resistivity in the subsurface at 8 ohm-m or less, independent of geologic formation. However, the gridded surface of the top of the Paleozoic system is displayed and indicates that nearly all of the conductive features in the bedrock are hosted in the Paleozoic strata, with the exception of the area near Lincoln discussed previously in this section. Up-dipping conductive intervals along west-east flight lines in the southern area of the NNRD, similar to conditions in the *Kd* near Lincoln, are also present. The resistivity values of these zones are in the range of expected resistivity signature control resulting from fluid conditions and not likely lithology, although both factors could contribute to these conductive features mapped in the hydrogeologic framework of the region. The lack of interval-specific water quality data from the Paleozoic strata in this region limits further characterization of the groundwater present at these depths. It is recommended that further assessment of these high-TDS conditions is conducted with a test hole drilling program complimented with a water quality assessment and down-hole geophysical applications to characterize the nature of these high-TDS subsurface intervals.

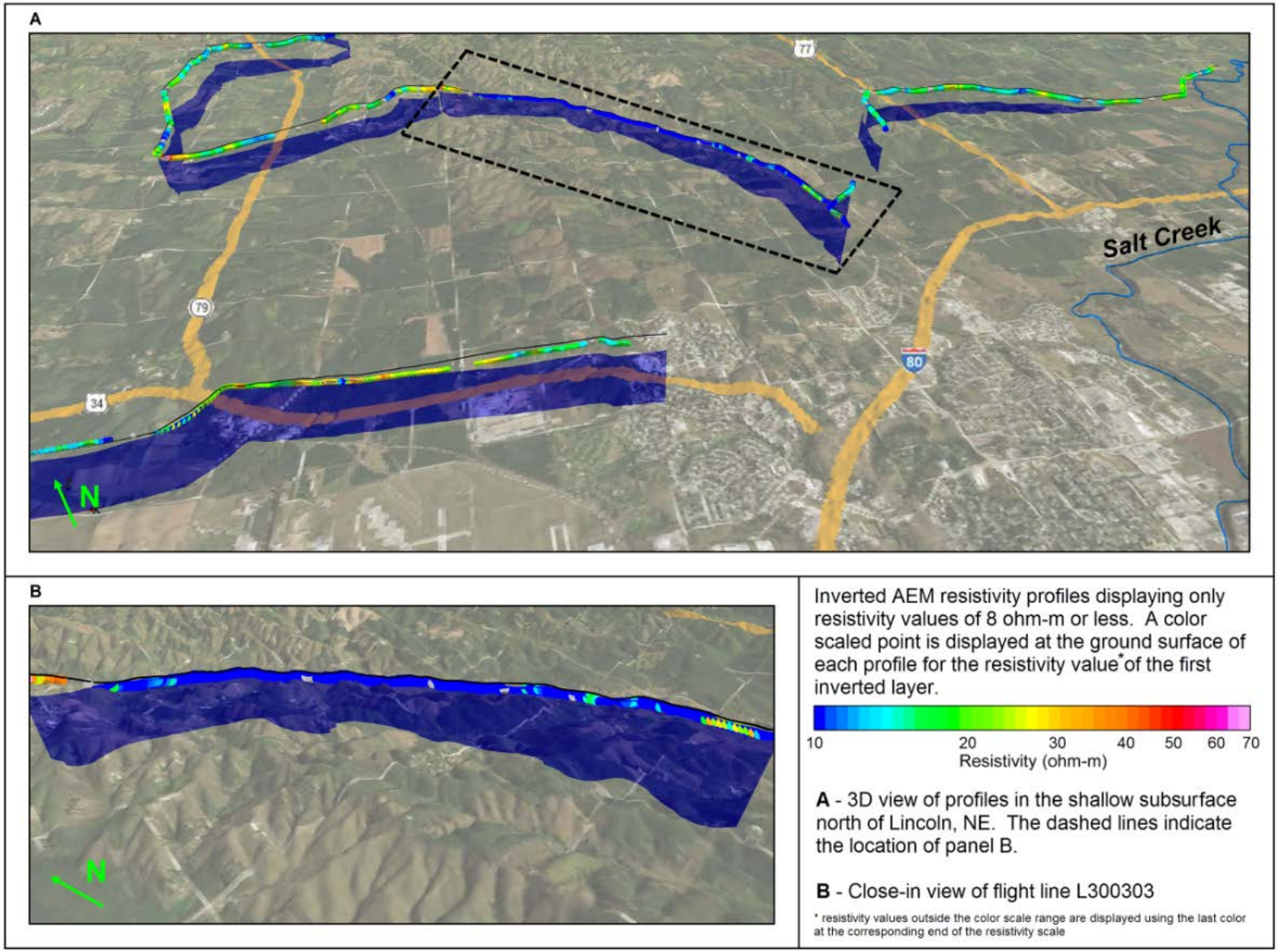



**Figure 5-18: 3D representation of shallow subsurface resistivity intervals of 8 ohm-m or less and at the land surface near the north side of the city of Lincoln in the LPSNRD.**

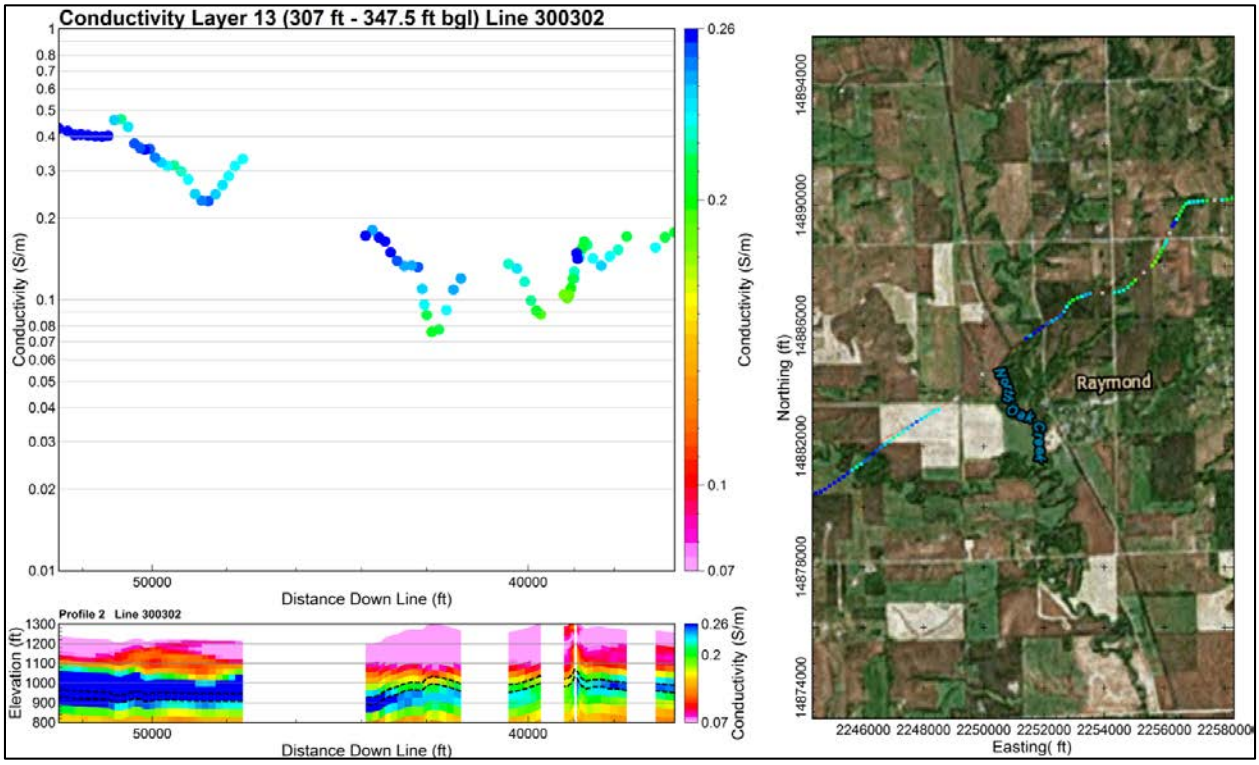



**Figure 5-19: Profile of conductivity (in Siemens/m) within the *Kd* along flight line 300302. The conductivity profile is from a depth at the top of the low resistivity interval within the *Kd*.**

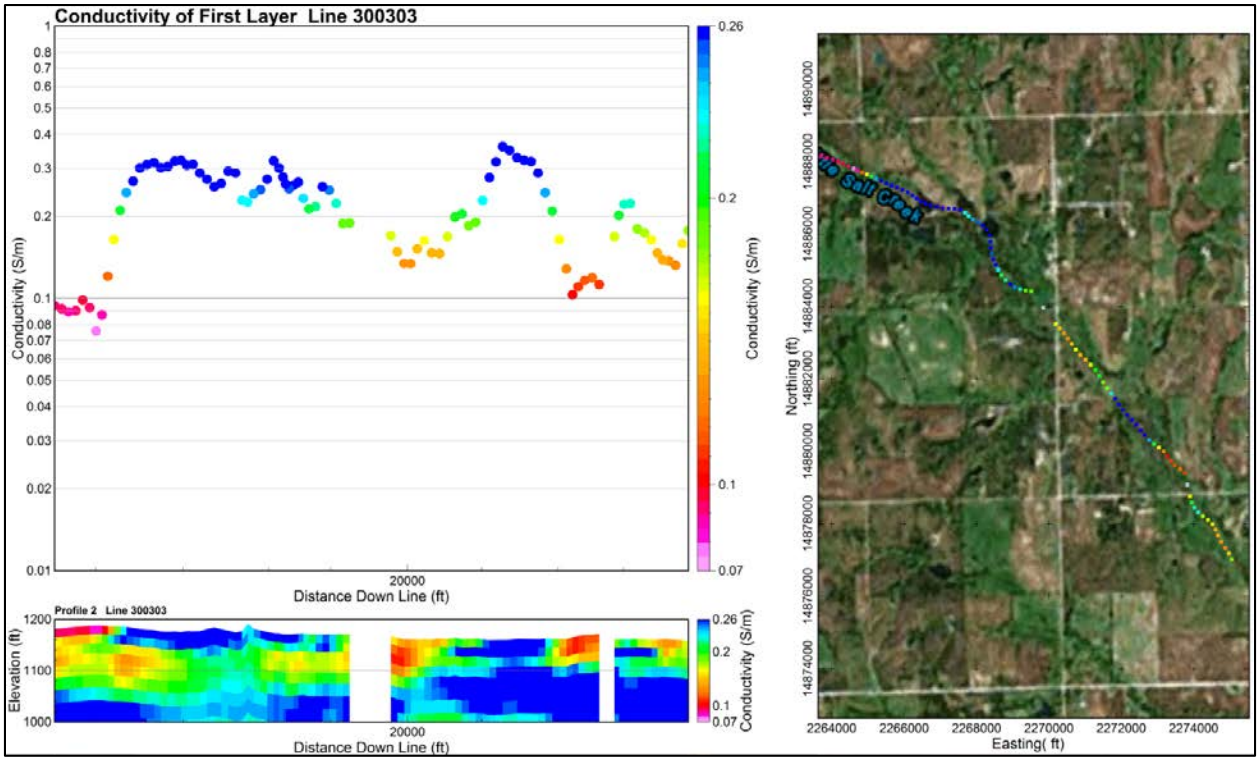



**Figure 5-20: Profile of conductivity (in Siemens/m) at the land surface along the Little Salt Creek drainage in the LPSNRD exhibiting areas of high TDS water in areas underlain by low-resistivity *Kd*.**

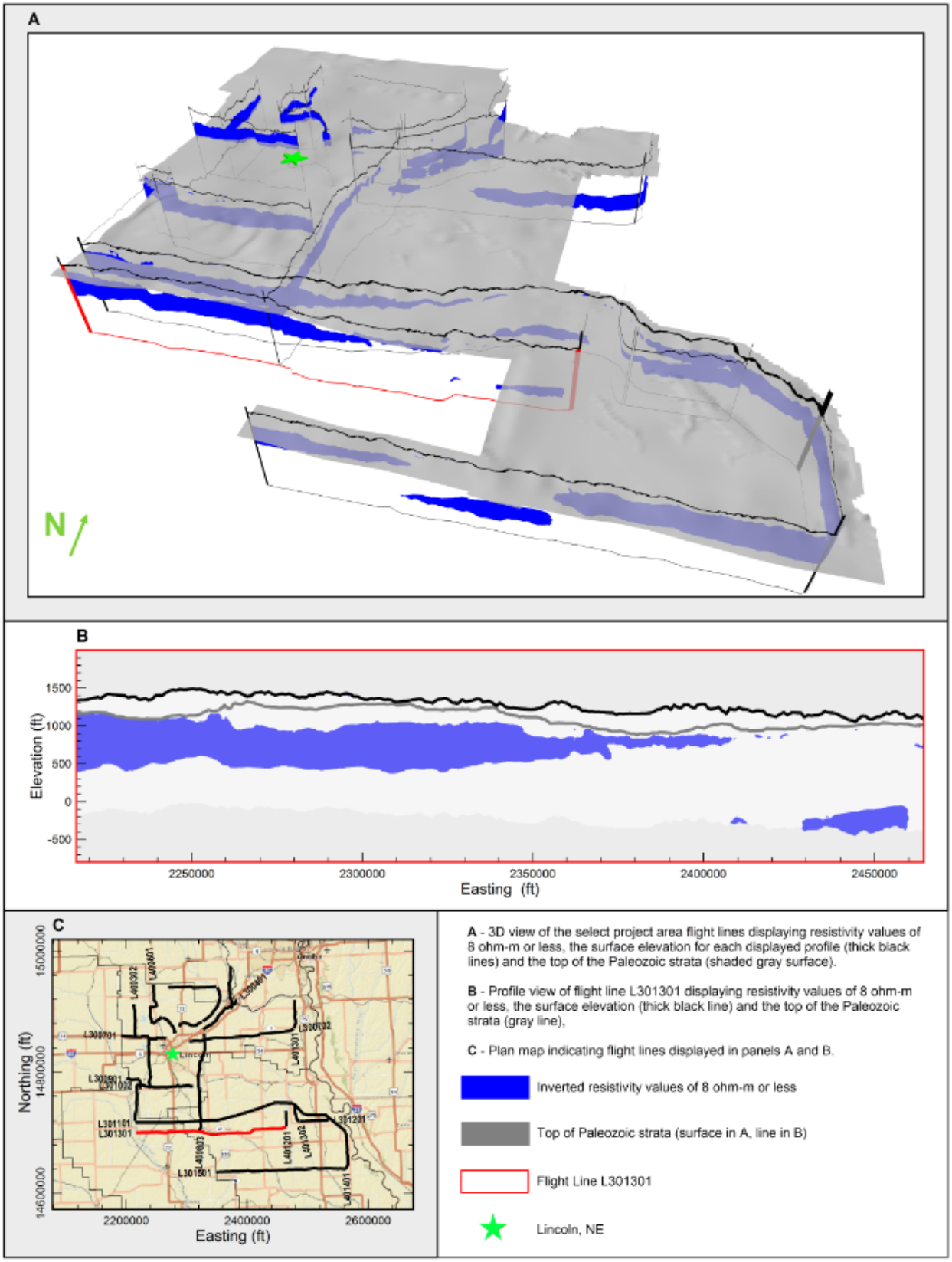



**Figure 5-21: 3D and 2D representations of regionally extensive, low-resistivity zones revealed in the southern ENWRA AEM survey. The gray surface demarcates the top of the Paleozoic system.**

### *5.2.3 Structural Features*

As indicated in Section 2.1.6, numerous structural features are present within the Paleozoic system that underlay the southern ENWRA project area. The AEM data revealed several locations where the Humboldt and Union faults were crossed by flight lines, as well as the Nemaha Uplift area and the Elk Creek Carbonatite. The Humboldt and Union Faults are clearly evident in the AEM profiles at multiple locations.

Flight line 401101 provides a north-south view of the subsurface between the Omaha metropolitan area on the north to the Nebraska-Kansas state line on the south (Figure 5-22). Along the profile, the Union Fault is apparent by the stark vertical contrast in the mapped resistivity near Northing value 14800000. Also displayed along this profile is the Nemaha Uplift area in the southern NNRD. The granite that comprises the Nemaha Uplift displays with a strong resistivity signature between Northing values 14600000 and 14650000. Tilt in the Paleozoic strata as a result of the uplift is indicated between Northing values 14650000 and 14700000. Viewing this area perpendicular to flight line 401101, the Nemaha Uplift, which hosts the Elk Creek Carbonatite is visible along flight line 301501 in the southern NNRD, along with the Humboldt Fault that is situated immediately adjacent to the east of the uplift area (Figure 5-23). The Paleozoic sequence shows a generally low resistivity east of the fault area within the western margin of the Forest City Basin. It is unclear as to whether this more conductive area is an artifact of lithology, water quality, or both within this stratigraphic sequence, however, since water quality samples were found from these depths during the project investigation. The Humboldt Fault is also detected further north along west-east flight line 301101 (Figure 5-24), where the fault in the Paleozoic strata is relatively shallow beneath a thin veneer of Quaternary deposits. The Humboldt Fault is also present along flight line 300402 as discussed in the PMRNRD section of Volume I of this report.

The Northern Bounding Fault is apparent along the northern side of flight line 400901 near the border of the LPNNRD and the PMRNRD (Figure 5-25). The fault is indicated in the CSD's Thurston to Pawnee County regional cross section beneath the Platte River valley (Korus et al., 2012), which provides insight into the offset Paleozoic strata beneath the Platte River valley. The Northern Bounding Fault as revealed in the AEM data matches closely with the fault indicated in the work by Korus et al. (2012).

The western extent of the mapped Union Fault trace is indicated in flight line 400803 near the NNRD-LPSNRD boundary in southeastern Lancaster County. The fault location on this profile is slightly southwest of the location of the fault indicated on the CSD's Thurston-Pawnee County cross section (Korus et al., 2012). The fault (Figure 5-26) shows an up-thrown block of Paleozoic strata on the south side of the fault. This faulted area also underlies a section of the large paleovalley that is present in the southern LPSNRD and the northern NNRD.

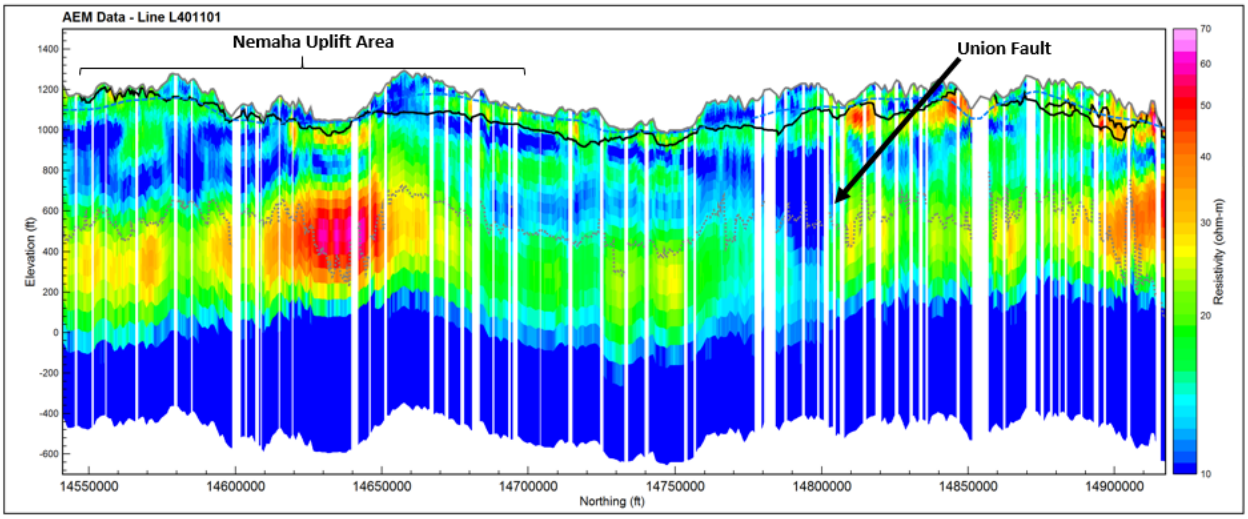



**Figure 5-22: AEM profile 401101 displaying the Nemaha Uplift area on the left and Union Fault within the Paleozoic system. Note the resistivity color scale ranges from 10 to 70 ohm-m.**

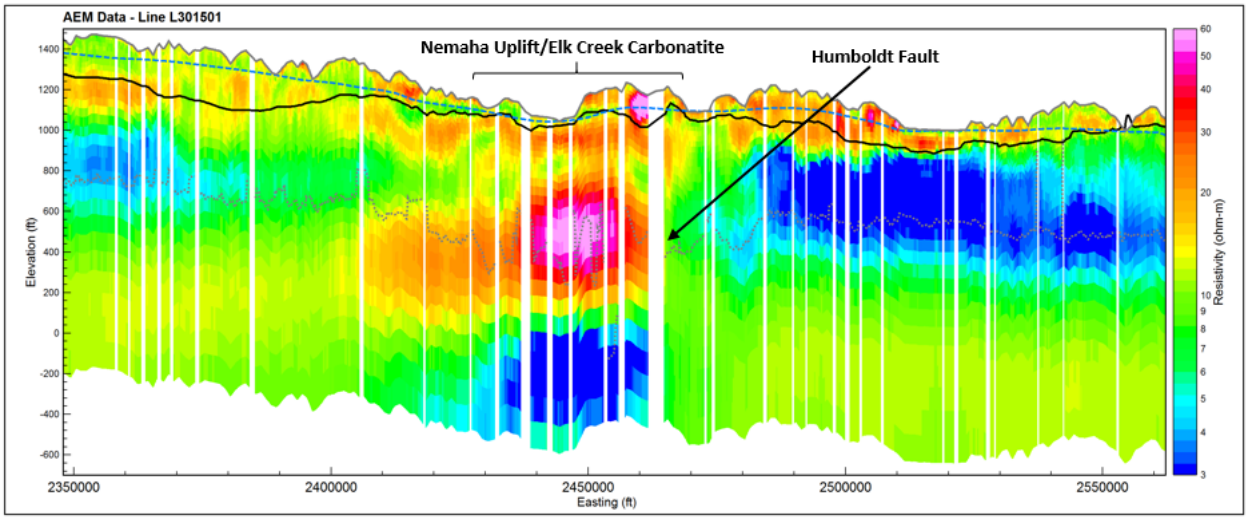



**Figure 5-23: AEM profile 301501 displaying the Nemaha Uplift/Elk Creek Carbonatite and the Humboldt Fault within the Paleozoic system. Note the resistivity color scale ranges from 3 to 60 ohm-m.**

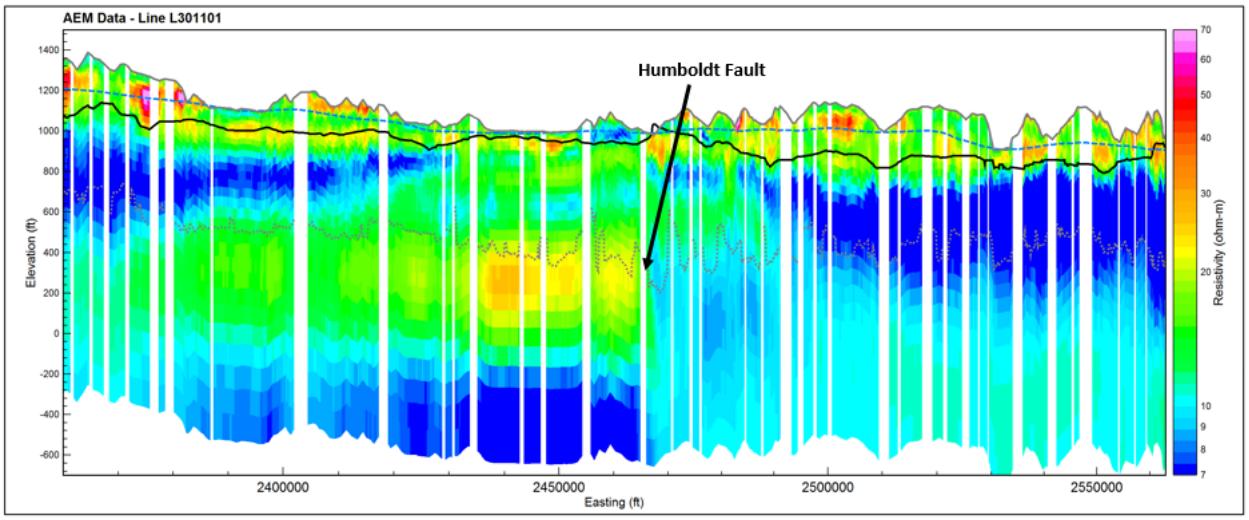



**Figure 5-24: AEM profile 301101 displaying the presence of the Humboldt Fault within the Paleozoic system. Note the resistivity color scale ranges from 7 to 70 ohm-m.**

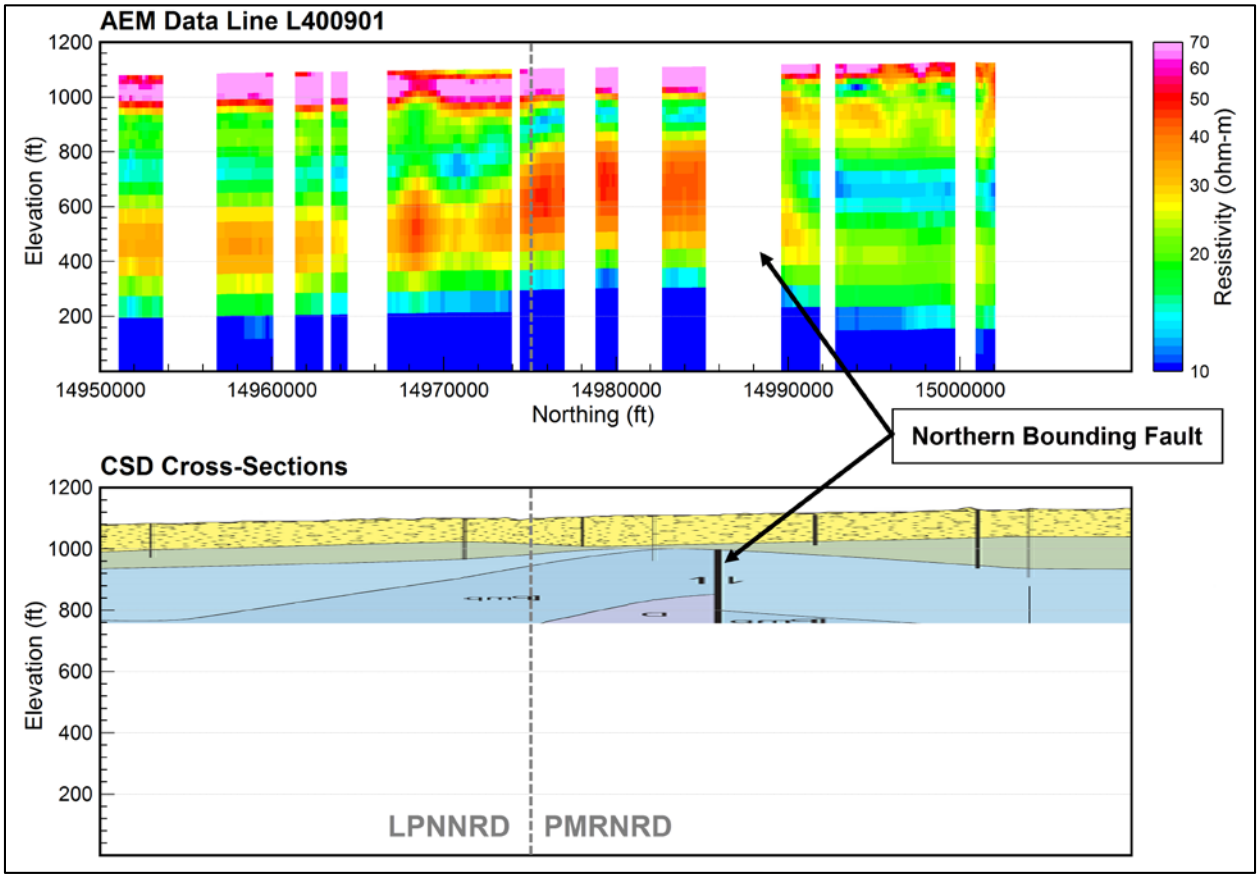



**Figure 5-25: AEM profile 400901 and CSD cross section on the LPNNRD-PMRNRD boundary displaying the Northern Bounding Fault beneath the Platte River valley. Note the resistivity color scale ranges from 10 to 70 ohm-m.**

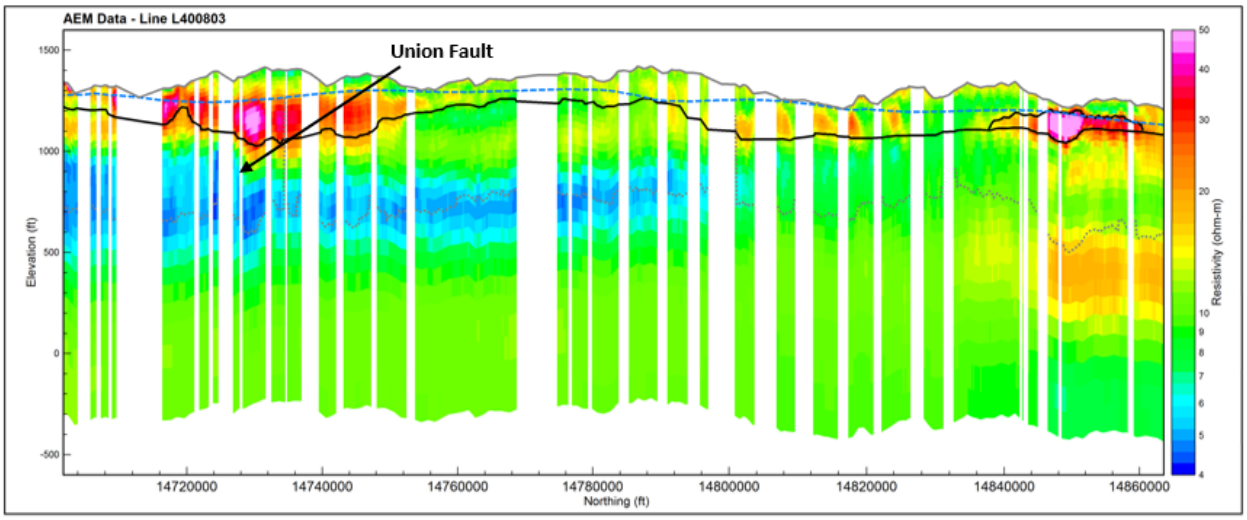



**Figure 5-26: AEM profile 400803 in the western NNRD showing the western extent of the Union Fault in the Paleozoic system. Note the resistivity color scale ranges from 4 to 50 ohm-m.**

### *5.2.4 Comparison with CSD Geologic Cross Sections and Test Holes*

Overall, the AEM profiles generally match the historic and contemporary (Divine et al., 2010; Korus et al., 2012) used in the AEM interpretive analysis. The multiple cross sections (Figure 5-27 and Figure 5-28) provided an additional background information dataset in the geologic interpretation process, which proved particularly useful in areas where Quaternary materials have similar resistivities as Cretaceous strata, or where Cretaceous and Paleozoic strata showed similar resistivities. The AEM profiles provide a resource for refinement of geologic cross sections previously created in eastern Nebraska, particularly in areas where formation contacts were estimated due to lack of test hole control.

AEM inherently has an averaging impact on the imaging of the subsurface, such that the inverted geophysical data cannot identify the fine lithologic details that can be gleaned from test hole logs such as thin laminae within thicker deposits or interbedded layers of a single formation. Section 4.6 (Spatially-Constrained Inversions) of this report indicates the thickness of the layers in the AEM inverted model. An example of this condition exists near CSD test hole 8-A-54 along a segment of flight line 201001 in the southeastern half of the LPNNRD. This section of flight line 201001 also corresponds with the historic geologic cross section 1601E1201E (Figure 5-29). In this area, the Quaternary material contains numerous thin layers of alternating fine and coarse materials. When the AEM is compared to the CSD test hole and cross section information, it is clear that not all of the interbedded detail of these materials can be identified in the AEM model due to the averaging effect that occurs during the inversion process. Figure 5-30 shows a zoomed-in view of CSD test hole 8-A-54. This plot exemplifies the nature of the aquifer that exists beneath much of the ENWRA project area where isolated bodies of aquifer material, either marginal or principal, are interlayered with aquitard material. The lithology profile in this figure displays the variability that can exist in the subsurface and demonstrates the importance of linking all historic and new lithologic data available with information from AEM surveys. This practice is particularly critical when planning local-scale exploratory test hole drilling programs.

Figure 5-31 and Figure 5-32 include comparisons of historic cross sections with AEM profiles and hydrogeologic interpretations at two additional profiles in the southern ENWRA area. Figure 5-31 shows profiles of AEM resistivity, hydrogeologic interpretation, and historic geologic cross section CCS18KDHD3 (Korus et al., 2012). In this figure, the AEM profile traces north to south along the Platte River valley and captures the 100-150 ft thick sequence of alluvium that occupies the valley. The AEM data reveals that most of this material is above 50 ohm-m, but has thinner intervals of less permeable (marginal aquifer) material at the top and the base of the Quaternary sequence above a thin band of *Kd*. The *Kd* mapped from the AEM data matches closely with the CSD cross section, but shows greater detail in the topographic relief of the contact between the Cretaceous and Paleozoic strata.

Figure 5-32 displays the same comparison of profiles along flight lines 300701 and 300702 that cross along nearly the entirety of the LPSNRD from west to east, with a small area removed near the city of Lincoln. While comparison of the data sources and interpretative profile shows general agreement in trends of strata, note how the AEM can also add detail where cross sections lack information between test holes. This is particularly evident along the top of the Paleozoic system (solid blue area along the interpretive profile) where the AEM survey reveals finer detail in the trace of this surface. Some disagreement exists between the data sources as well, particularly in the Quaternary sequence west of Lincoln, where the historic cross section indicates till in the upper interval at locations where the AEM profile indicates the existing of principal aquifer materials. A similar trend of disagreement exists to the east near Easting value 2400000 ft, where the AEM profile indicates resistive material 20 ohm-m or greater, and the historic cross section displays silt and till at this depth.

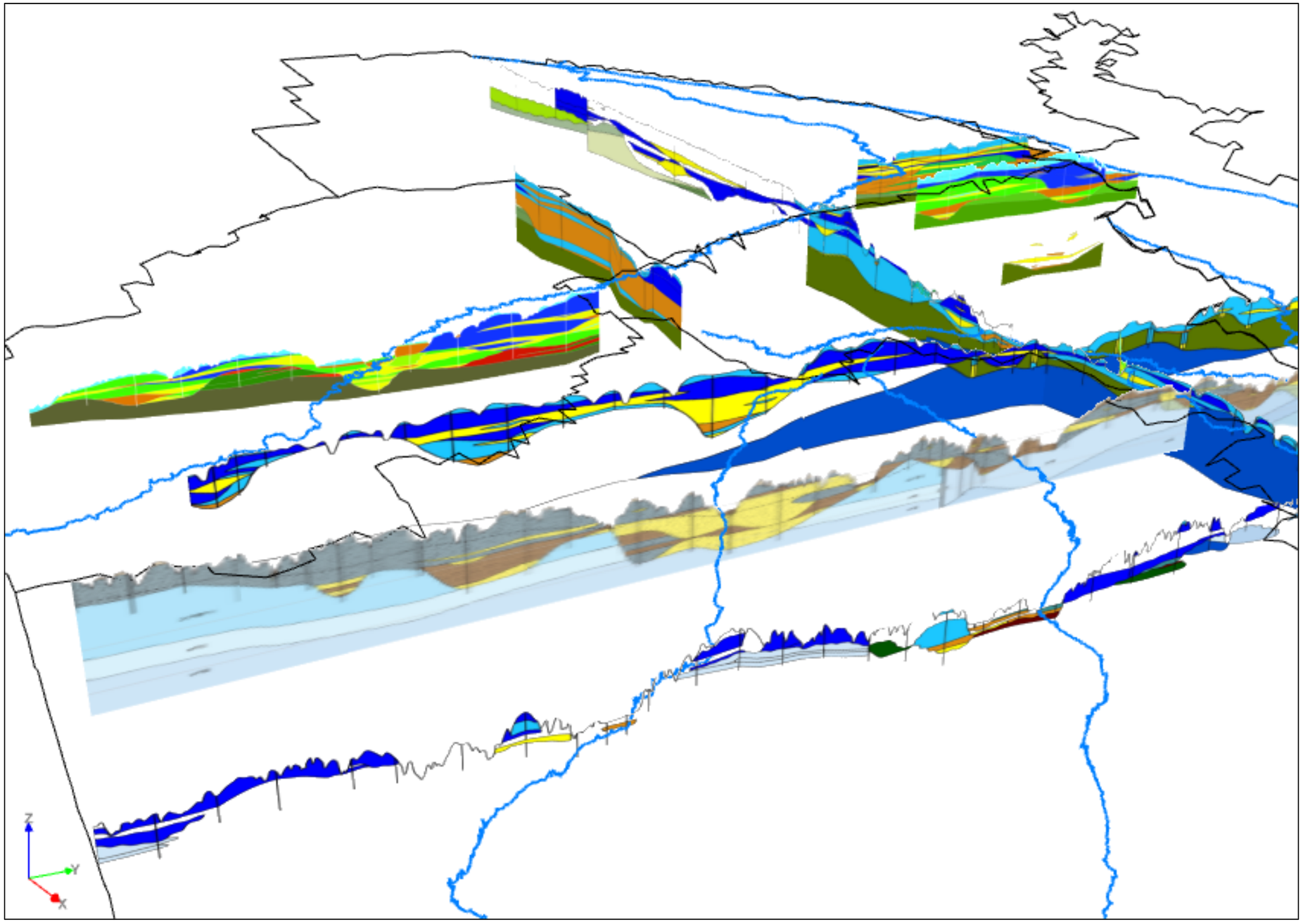



**Figure 5-27: Northwestward view of the southern ENWRA project area displaying the locations of historic and contemporary CSD geologic cross sections. The color scale is shown in Figure 5-2.**

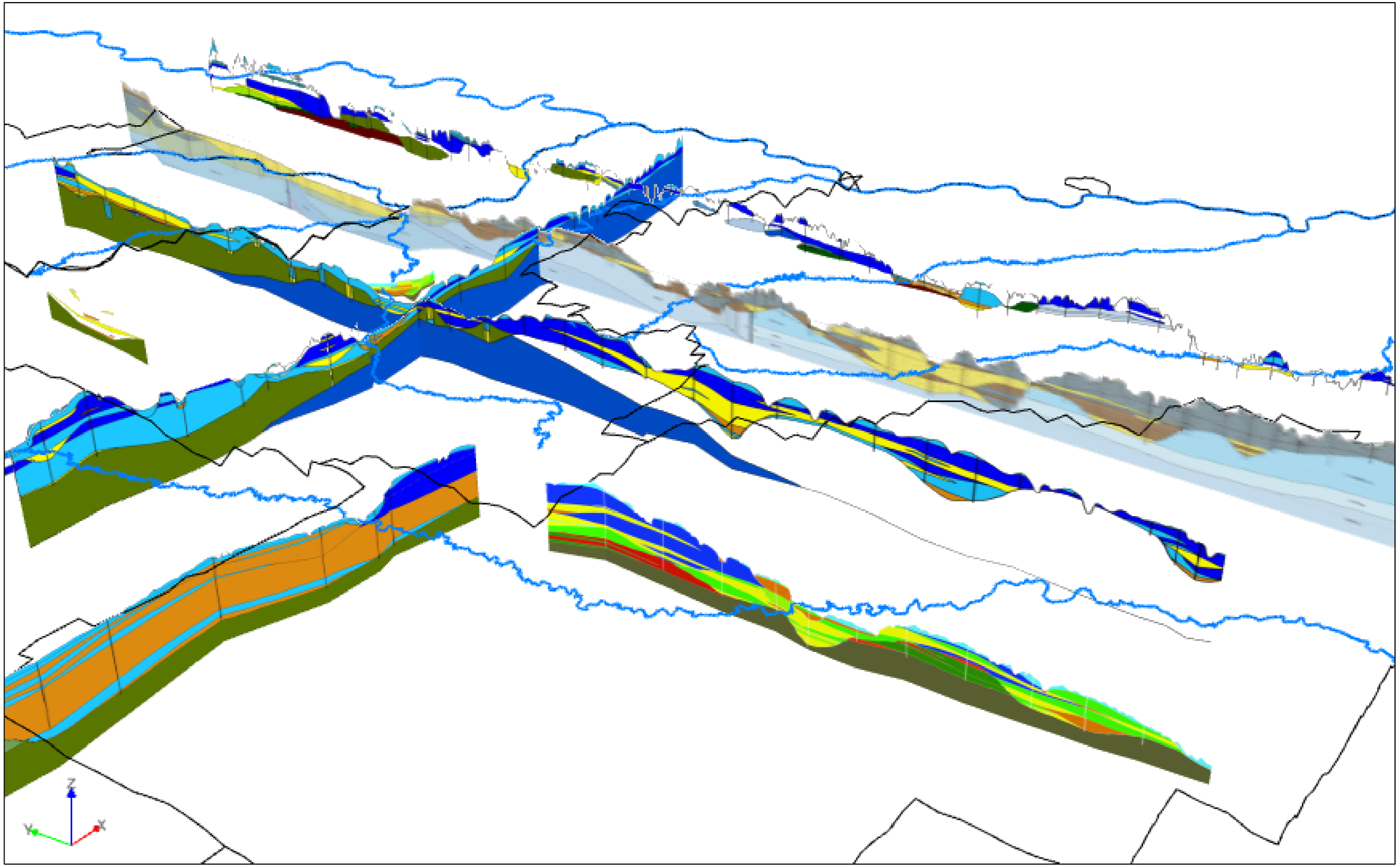



**Figure 5-28: Northeastward view of the southern ENWRA project area displaying the locations of historic and contemporary CSD geologic cross sections. The color scale is shown in Figure 5-2.**

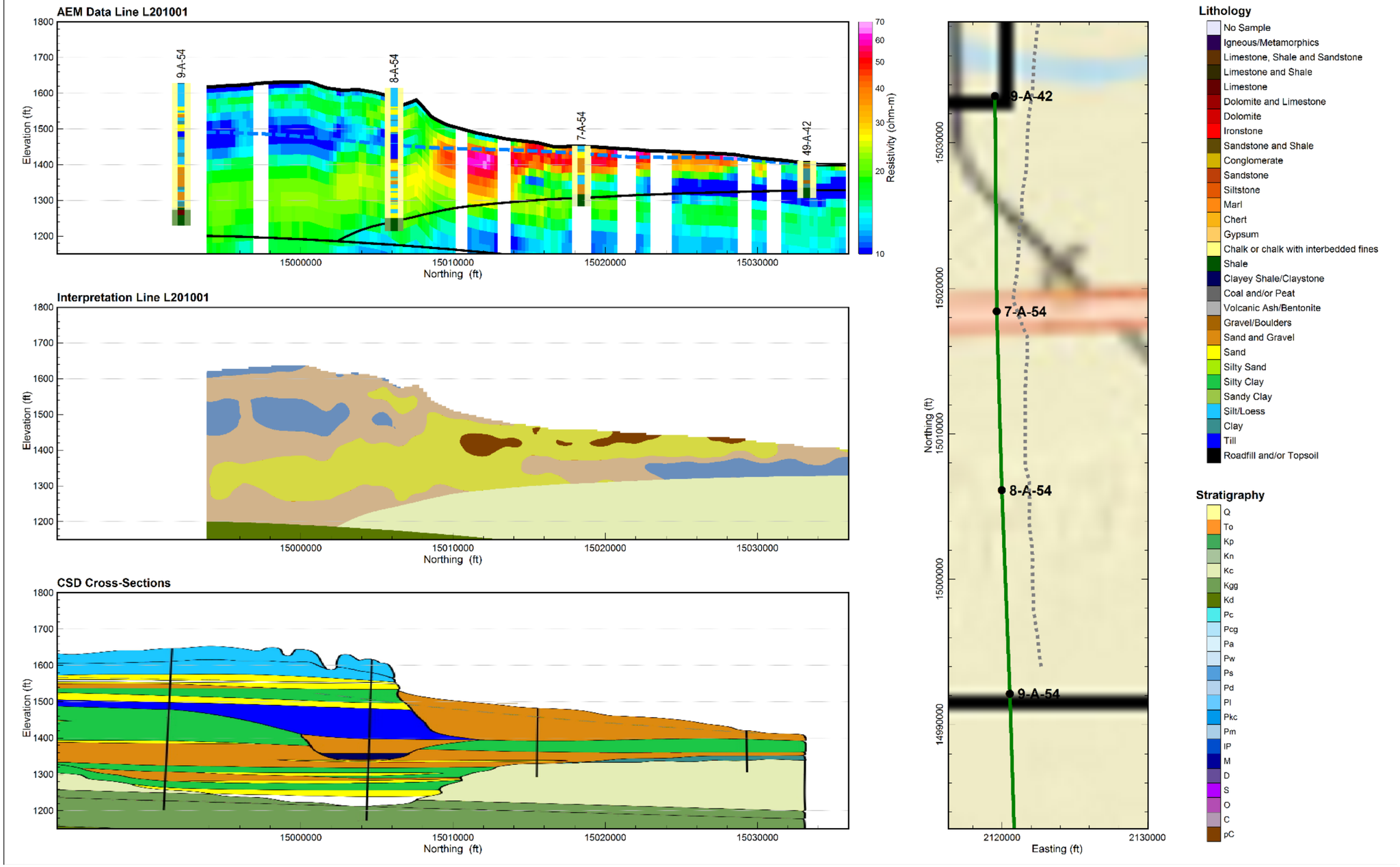



**Figure 5-29: Combined display of AEM data (top panel), hydrostratigraphic interpretation (middle panel), and CSD cross section (bottom panel) for a section of flight line 201001 in the southeastern half of the LPNNRD. The location of the AEM flight line and CSD cross section is displayed on the top pane to the right.**

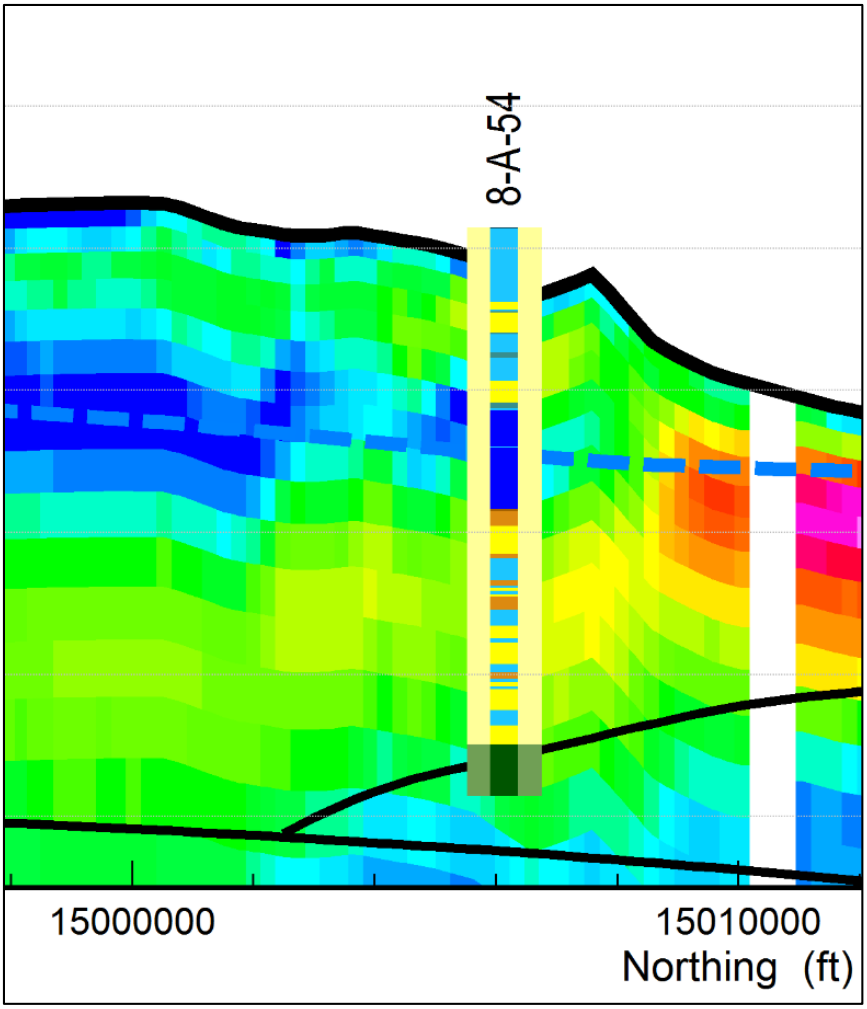



**Figure 5-30: Close-in view of CSD test hole 8-A-54 along a segment of the southern extent of AEM flight line 201001 in the LPNNRD, demonstrating the thin intervals of material indicated in the test hole logs that correspond to only the averaged resistivity data across intervals of greater thickness.**

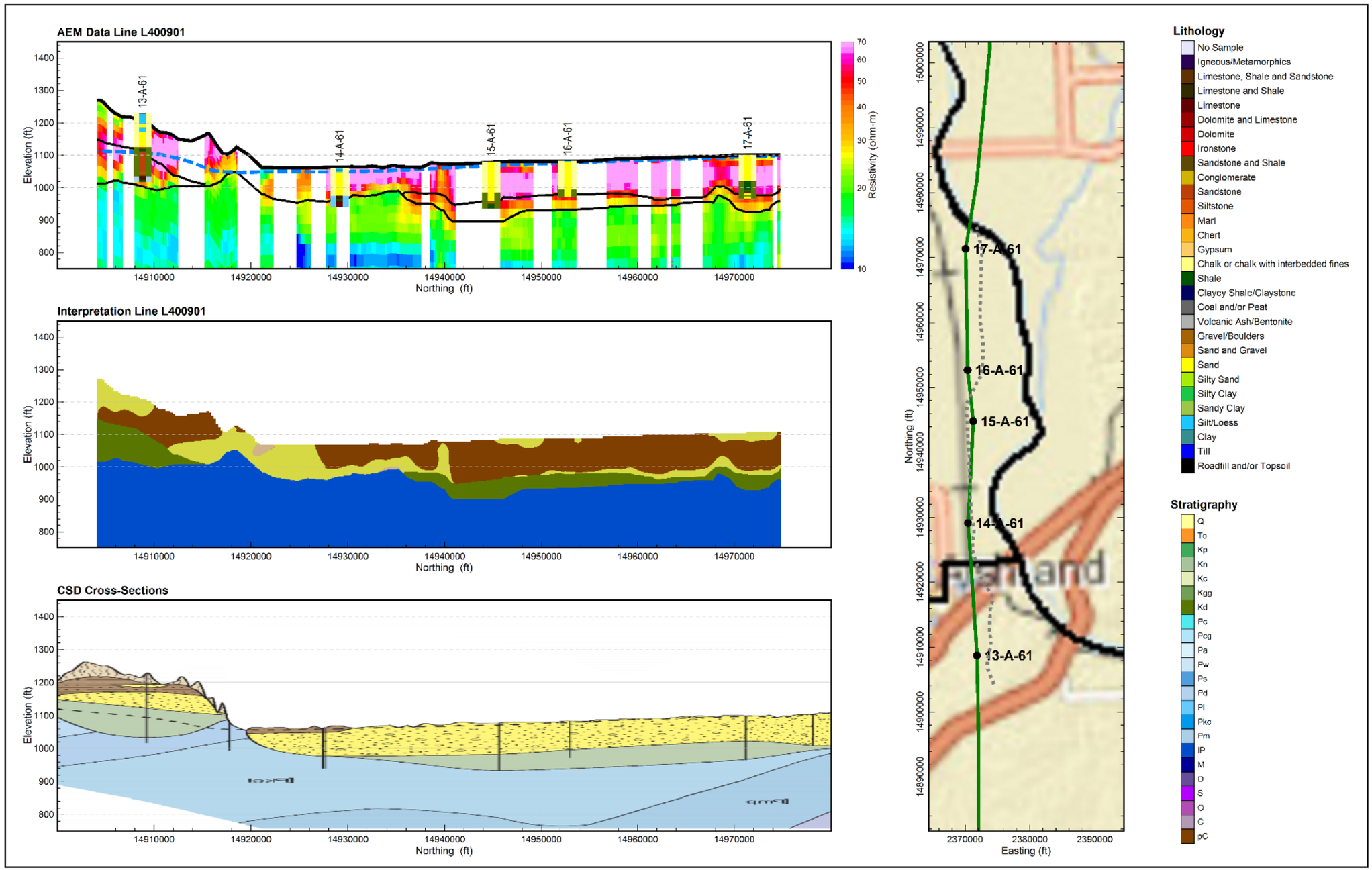



**Figure 5-31: Combined display of AEM data (top panel), hydrostratigraphic interpretation (middle panel), and CSD cross section (bottom panel) for flight line 400901 near Ashland, NE. The location of the AEM flight line and CSD cross section is displayed on the panel to the right.**

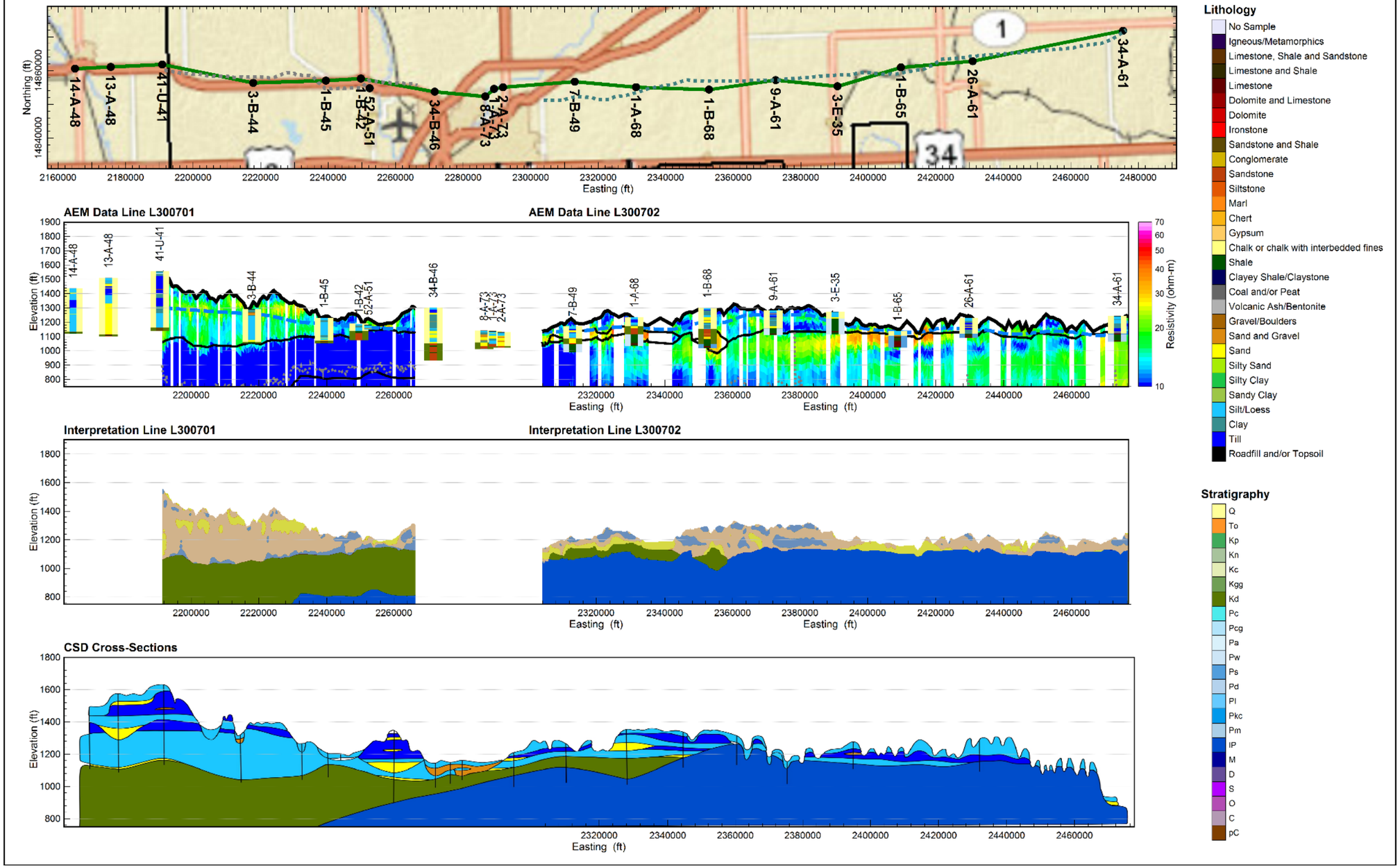



**Figure 5-32: Combined display of AEM data (second panel), hydrostratigraphic interpretation (third panel), and CSD cross section (bottom panel) for flight lines 300701 and 300702 which cross the LPSNRD from west to east. The location of the AEM flight line and CSD cross section is displayed in the top panel.**

Overall, the interpretations of the AEM data along the reconnaissance lines are in agreement with CSD test holes and historic CSD cross sections. Deviations mostly occur the most where test holes are at greater distances from the flight lines. The AEM data now allows users to visualize the character of the subsurface between test holes, thus greatly minimizing the amount of speculative estimation of how geologic materials change where no data exists. The AEM does not, however, map very thin layers on the order of a few feet in thickness due to averaging effects in the inversion modeling process. This condition is not considered to greatly affect how the AEM data would import to groundwater models, where such minor features cannot be accounted for and where averaging of hydraulic parameters occur over thick sequences of aquifer materials.

Volume I of this report includes a similar discussion on the comparisons from the eastern half of the LENRD where aquitard and marginal aquifer materials comprise the majority of the Quaternary sequence in the northern ENWRA project area. The reader is encouraged to review this section as well, which includes a comparison of the AEM resistivity model with lithology and stratigraphy at a CSD test hole that penetrates into the Cretaceous sequence. Note that all historic cross section-AEM comparison figures for the southern ENWRA project area are included in Appendix 2 of this report.

## 5.3 Hydrogeologic Interpretation for the Individual NRDs

### *5.3.1 Lower Platte North NRD*

AEM data for the LPNNRD were acquired during each of the ENWRA project's flight phases. Six north-south flight lines and one west-east flight line were acquired during the Fall 2014 survey. These flight lines covered areas in the northwest section of the LPNNRD, as well as along the Platte River valley between the cities of Columbus and Fremont. Flight lines from the Spring 2015 survey mainly the southern half of the NRD, and include an extension of flight line 201801 southward to the district boundary with the LPSNRD (Figure 5-33). The LPNNRD is roughly divided in half by the broad Platte River valley which is oriented west to east and separates rolling to hummocky uplands to the north and south that are composed of loess-mantled till. While select AEM profiles are displayed in this section, the remainder of the profiles are included in Appendix I of this report. Figure 5-34 displays the 3D hydrogeologic framework of the LPNNRD, which highlights the subsurface features described in this section. In map view, the shape of the district is described as the northwestern half, which includes the relatively narrow, northwest-southeast trending area in Platte, Boone, and Madison Counties. The southeastern half of the district describes the part of the district east of flight line 201001, and includes the Platte River valley.

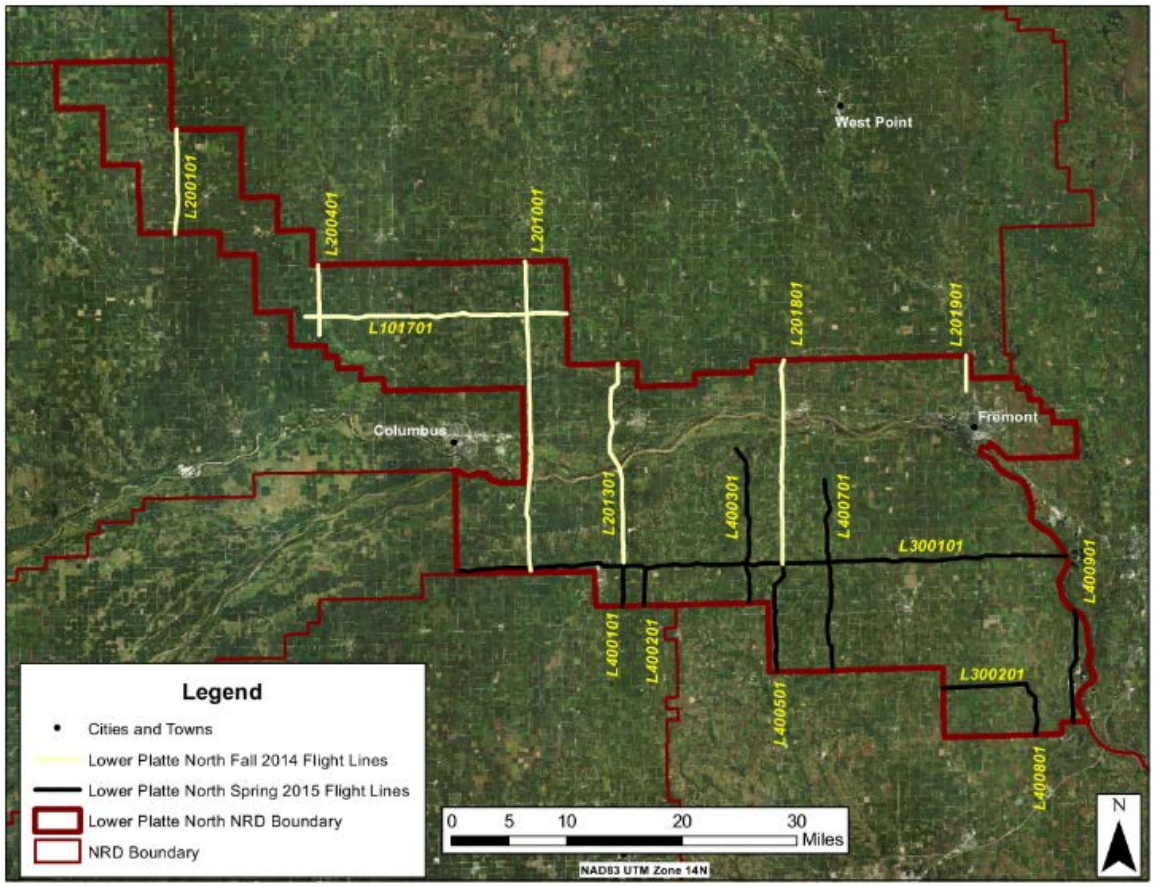



**Figure 5-33: Flight lines within the LPNNRD acquired in the both phases of the ENWRA AEM survey.**

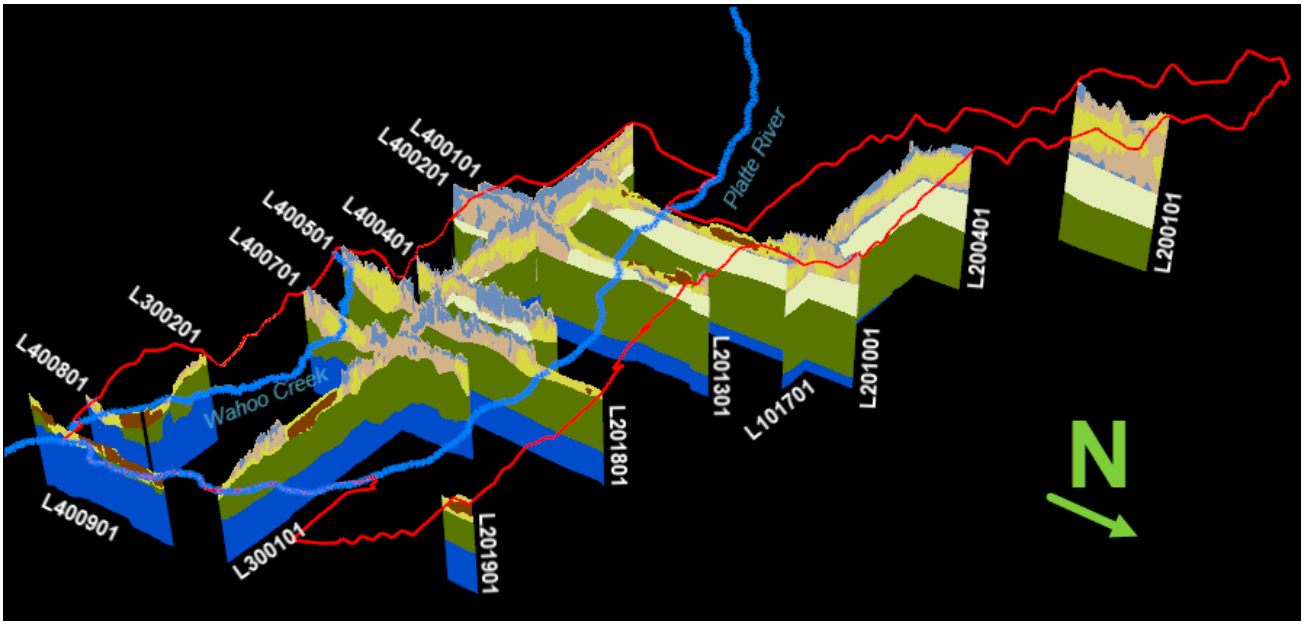



**Figure 5-34: 3D hydrogeologic framework from the reconnaissance AEM survey within the LPNNRD using flight lines from both the Fall 2014 and Spring 2015 AEM surveys. Vertical exaggeration is 60x.**

#### *5.3.1.1 Quaternary/Tertiary System beneath the LPNNRD*

The LPNNRD is underlain by a variety of Quaternary deposits across the district. Principal and sand-rich principal aquifer deposits are most prevalent in the following four areas: 1) the far northwest section of the district in Platte, Madison, and Boone Counties where principal aquifer materials are composed of both Quaternary and *To* deposits; 2) beneath the Platte River valley, 3) beneath the Todd Valley in eastern Saunders County; and 4) in a large buried paleovalley that extends beneath the south-central section of the district in southeastern Butler and western Saunders Counties.

***Northwest Area***

In the northwest corner of the district, combined Quaternary and *To* deposits form an aquifer ranging from less than 100 ft to over 300 ft thick, with much of the aquifer consisting of principal aquifer material (flight line 200101). In this area, the unsaturated zone above the 1995 CSD water level surface consists mostly of principal and marginal aquifer deposits, which creates conditions for higher recharge potential in this part of the district. Eastward from this area, the *To* terminates and Quaternary deposits form the sole principal aquifer material in the area, which has approximately 200 ft of saturated thickness near flight line 200401. In comparison to the area shown in flight line 200101, this area is overlain by thicker sequences of marginal and aquitard material.

***Platte River Alluvium***

The Platte River valley, which is filled with principal and sand-rich principal deposits interlayered with marginal and aquifer material, forms an extensive shallow aquifer resource across the northern extent of the southeastern half of the district. The valley angles southeastward in the eastern part of the district downstream of Fremont and forms a boundary with the PMRNRD. Five flight lines (201001, 201301, 201801, 201901, and 202001) from the reconnaissance survey extend to or cross the Platte River valley in the LPNNRD between the cities of Columbus and Fremont (Figure 5-35). These profiles reveal the thickness of the principal aquifer materials found in the valley (some of the extensive resistive features also extend northward into the LENRD), as well as the geomorphological structure of the valley bottomland and the surrounding uplands. Immediately east of Columbus, flight lines 201001 and 201301 reveal the extent of principal aquifer material beneath the valley, which approaches 15 miles in width at flight line 201001. Sand-rich, coarse principal aquifer material underlies much of the valley in this area, exceeding 100 ft in thickness beneath the northern half of the valley. The coarse deposits on the northern half of the valley appear to be possible terrace deposits, as they are within a flat, elevated feature that sits above the valley bottomland to the south. A 50-100 ft thick smaller body of sand-rich principal aquifer materials is also present on the south side of the valley that also extends beneath the uplands to the south of the valley. Between these two zones of highly resistive material is mostly marginal aquifer with a small body of non-aquifer material that could potentially be weathered bedrock. The presence of marginal aquifer material should be expected within the Platte River valley, as varying depositional patterns over recent geologic time have shifted, creating varying transport energies and load capacities, which resulted in fine materials interlayered with coarse deposits. This area underlies the modern day Platte River.

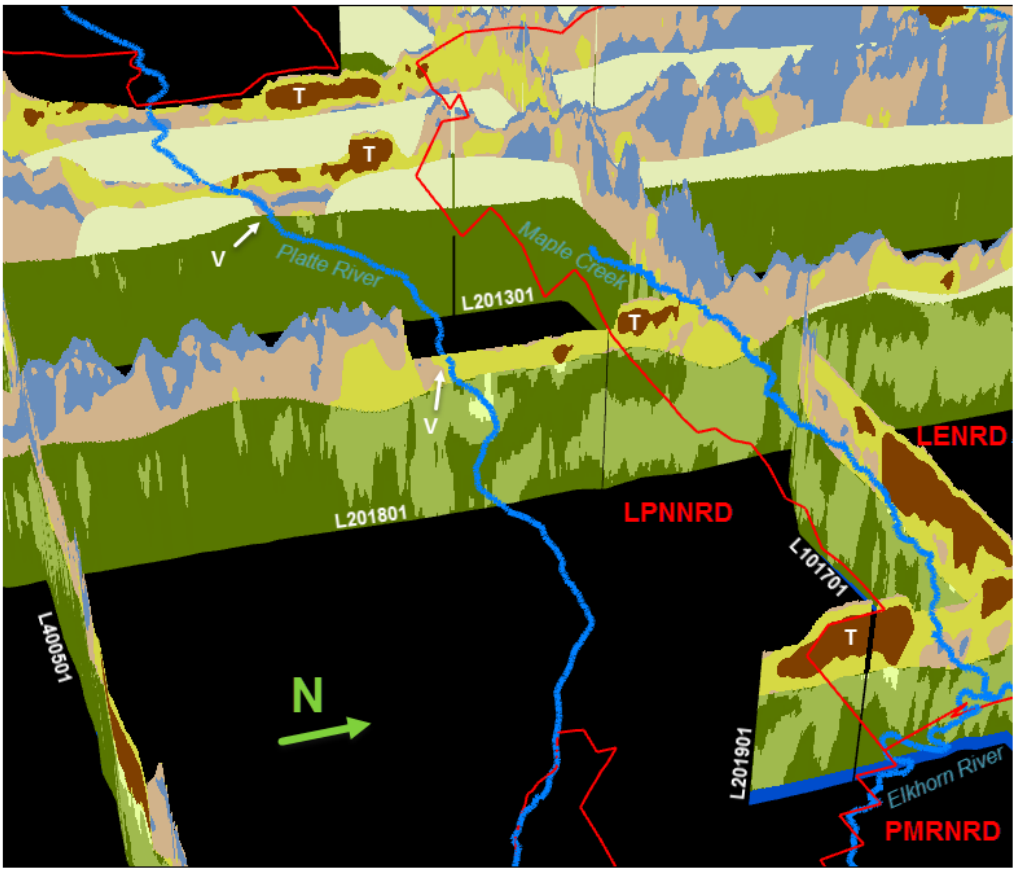



**Figure 5-35: A northwestward view of the 3D hydrostratigraphic framework interpretation in the LPNNRD displaying the hydrogeologic character of the Platte River valley. Terrace features are marked with a white "T", and the incised valley in flight line 201301 is marked with a white "V." Vertical exaggeration is 60x.**

Along flight line 201301, sand-rich principal aquifer material is present along the north side of the river from the uplands to near the present day river channel (Figure 5-35). Within the terrace deposits, these materials approach 140 ft in thickness, but thin to 40 to 80 ft beneath the valley bottomland. Beneath the northern half of the Platte River valley is an incised feature that cuts nearly 120 ft into the underlying *KcKgg* bedrock. This narrow feature is interlayered with marginal aquifer and aquitard material that underlies the shallower, more resistive principal aquifer material. South of the Platte River along this profile, principal aquifer between 20 and 50 ohm-m is the predominant material underlying the valley, typically less than 100 ft thick.

Along flight line 201801, the Platte River valley narrows to approximately 7 miles. The body of sand-rich, principal aquifer material along the north side of the valley detected upstream along flight lines 201001 and 201301 is also present in this area, and exceeds 100 ft in thickness beneath the terrace feature. Beneath the valley bottomland, the material is generally less than 100 ft in thickness and is composed primarily of principal aquifer material with minor intervals of sand-rich, coarse zones. The bedrock underlying this area is an irregular surface of *Kd*. Just north of the Platte River valley, a paleovalley appears to be carved from the *Kd* that is approximately 120 ft below the alluvium-bedrock contact immediately below the Platte River valley. This feature is filled with principal and marginal aquifer, and

appears to be in direct connection with the principal aquifer materials beneath the valley to the south. A similar but less pronounced feature is also present south of the Platte River valley.

Flight line 201901 terminates immediately south of the LPNNRD-LENRND boundary at the northern edge of the Platte River valley near Fremont. The valley along this profile is approximately 120 ft thick and is comprised primarily of sand-rich, principal aquifer material. This body of resistive material thickens to nearly 150 ft north of the Platte River valley on the tableland between the valley and the Maple Creek drainage in the southeast corner of the LENRD. The Quaternary system throughout this area sits atop *Kd*.

The southernmost extent of flight line 202001 extends into the Platte River valley southeast of Fremont. In this area, the flight line is semi-parallel to the Platte River, thus the view provided along this flight line is not a true cross-section across the valley, but does provide information on the character of the materials on the valley's east side. In this area, the valley is underlain by a mixture of materials-primarily marginal aquifer material interlayered with disconnected bodies of principal aquifer that includes sand-rich zones. The thickness of these materials ranges from approximately 50 to 100 ft. Marginal aquifer material extends a considerable distance northward beneath the uplands along this profile. Near the edge of the valley, the more resistive deposits are separated from this marginal aquifer material beneath the uplands by an interval of aquitard material. Flight line 400901, viewed in the 3D framework in Figure 5-34, reveals the character of the Platte River alluvium between Fremont and Ashland. In this area, the deposits range from less than 100 ft to over 150 ft in thickness and are comprised of sand-rich principal aquifer materials along much of the valley's extent. The valley is underlain by thin intervals of *Kd*, typically ranging from 50 to 100 ft in thickness with resistivities typically 20 ohm-m or greater.

***Todd Valley***

The Todd Valley is an abandoned alluvial valley of the ancestral Platte River (Mason and Joeckel, 2002). The topographically flat area extends approximately 25 miles from west of Fremont southeastward to the Mead/Ashland area in the southeast corner of the district (Figure 2-12). The valley is oriented approximately parallel to the modern-day Platte River valley, which is located 3-7 miles to the east. The two valleys are separated by an area of uplands comprised of marginal aquifer and aquitard materials.

The valley is evident in 3D framework of the LPNNRD (Figure 5-34) as well as in AEM profile 300101 (Figure 5-36). The AEM profile reveals that the thickness of the Todd Valley ranges from 150 to 200 ft in eastern Saunders County. The profile also reveals that the Todd Valley is situated 50 to 100 ft in elevation above the modern-day Platte River valley.

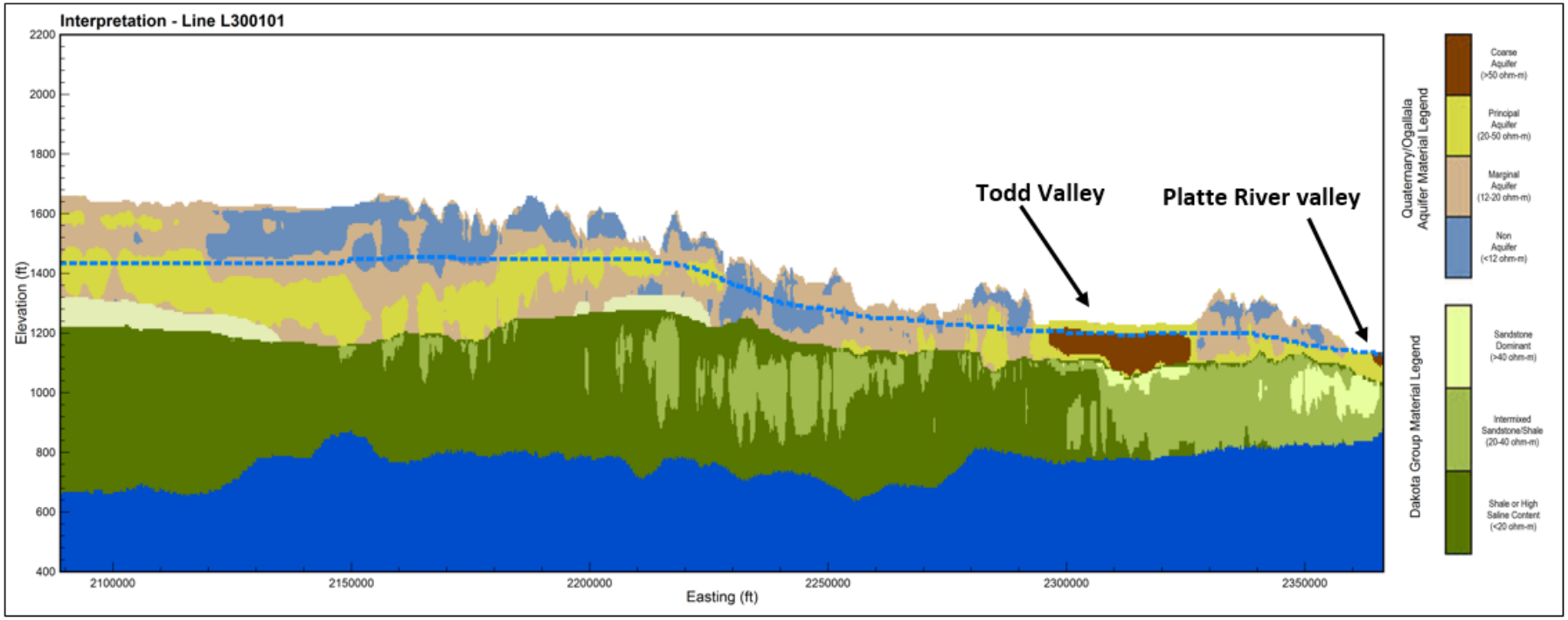



**Figure 5-36: AEM flight line 300101 across the center of the southeastern half of the LPNNRD. West is on the left, east to the right. The 1995 water level surface is displayed as a blue dashed line. The blue fill indicates undifferentiated Paleozoic strata.**

***Paleovalley beneath the southern LPNNRD***

The extensive paleovalley in the southeastern half of the LPNNRD (Figure 2-12) that merges with the Todd Valley in Saunders County is capture in detail by the AEM survey. Portions of this paleovalley are evident in flight line 300101 (Figure 5-36), where principal aquifer material, upwards of 200 ft thick in locations, are detected beneath 100 to 200 ft of marginal aquifer and aquitard material. Figure 5-36 also indicates sections of principal aquifer material above the paleovalley and the CSD 1995 water table surface on the west side of the AEM flight line. The placement of the 1995 water table surface in relation to the principal aquifer deposits of this paleovalley indicate that confined aquifer conditions likely persist throughout much of this paleovalley. Evident in flight lines 400301, 400501 (Figure 5-37), and 400701, the paleovalley exceeds 6 miles in north-south width in flight line 400501 and ranges from 100 to over 300 ft in thickness of principal aquifer materials, some of which extend close to the land surface in this area with minimal overlying marginal or aquitard materials. The southern half of flight line 400301 indicates the paleovalley deposits upwards of 300 ft in thickness near the LPNNRD-LPSNRD boundary, but thinning northward beneath thicker deposits of marginal and aquitard materials along this profile. These features appear to be the eastward extension of the Dwight-Valparaiso aquifer as defined by Druliner and Mason (2001).

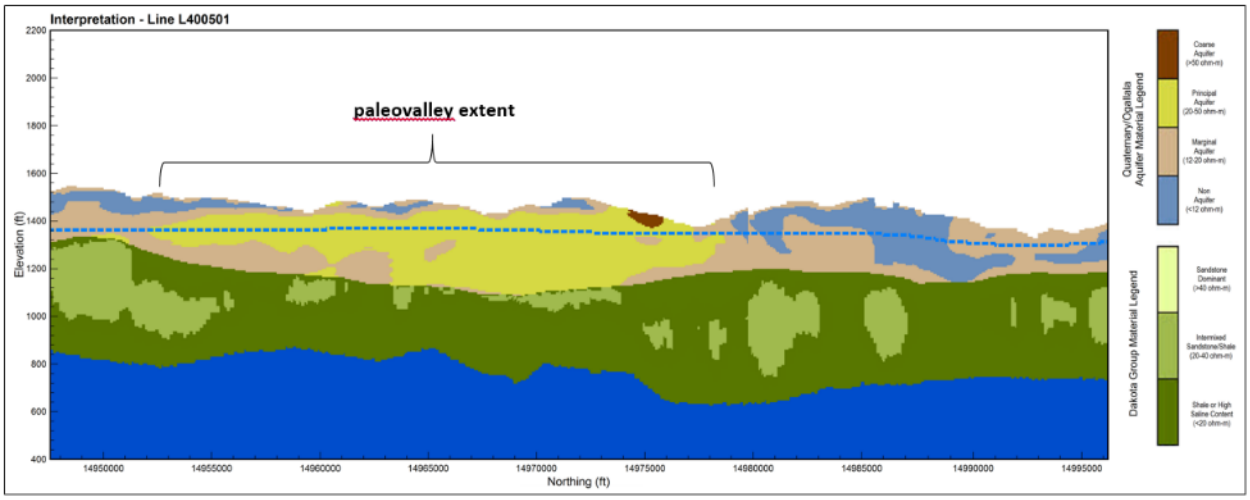



**Figure 5-37: AEM flight line 400501 across the south central section of the southeastern half of the LPNNRD. South is on the left, north to the right. The 1995 water level surface is displayed as a blue dashed line. The blue fill indicates undifferentiated Paleozoic strata.**

***Marginal and Aquitard Materials***

Separating the major aquifer features beneath the LPNNRD are sequences of marginal aquifer and aquitard material of varying thickness. In the northwestern half of the district, marginal aquifer materials range from 50 to over 150 ft in thickness, with only minimal isolated aquitard features that typically do not exceed 75 ft in thickness. In the southeastern half of the district, the upland area separating the Platte River valley and the southern paleovalley is underlain by predominately marginal and aquitard material. Flight lines 400301, 400501, and 400701 display thick sequences of marginal and aquitard material through the central portion of the southeastern half of the district. These deposits range from 200 ft to nearly 400 ft in thickness at some locations. Along flight line 400301, the Quaternary system consists almost entirely of aquitard material, with only minimal basal marginal

aquifer material present above the Cretaceous bedrock. Throughout much of the upland area, the marginal aquifer and aquitard materials are interlayered, with aquitard material present at the land surface at many locations. Flight line 300101 (Figure 5-36) shows examples of this distribution of the lower permeability materials above the principal aquifer between the western margin and Easting value 2250000 ft. This profile also displays the nearly 200 ft thick uplands between the Todd Valley and the Platte valley, which further exhibits the interbedded nature of the subsurface beyond the principal aquifer areas in the LPNNRD.

In the far southeast corner of the district, the Quaternary deposits are generally an interlayered combination of marginal and principal aquifer deposits that are relatively thin compared to the principal aquifer features in the district (Flight line 300201). Along this profile, the Quaternary sequence is generally less than 200 ft in thickness, with many areas being as thin as 100 ft with very little saturated thickness. This condition occurs along flight line 300201 just west of the Todd Valley where thin principal aquifer materials sit on top of a bedrock high of resistive *Kd.*

#### *5.3.1.2 Cretaceous and Paleozoic Sequence beneath the LPNNRD*

The Cretaceous sequence present beneath the LPNNRD includes the *Kn*, *KcKgg*, and the *Kd*. The *Kn* is the uppermost bedrock formation beneath the northwestern areas of the district, where the unit transitions from a thickness of approximately 225 ft along flight line 200101 to less than 100 ft along flight line 200401. The *Kn*'s eastward margin beneath the LPNNRD is located between flight line 200401 and 201001. The *KcKgg* is present beneath the western two-thirds of the district, where thickness ranges from approximately 300 ft along flight lines 200101 and 200401, and thins eastward to approximately 125 ft beneath the Platte River valley along flight line 201301. Beneath the center of the district along flight lines 201001 and 201301, the *KcKgg* is the uppermost bedrock unit in the Cretaceous sequence.

The *Kd* is present beneath nearly the entire LPNNRD, with the top of the formation ranging from 900 ft bgl along flight line 200101, to less than 100 ft bgl beneath the Platte River valley in the east-central area of the district. Maximum thickness of the unit approaches 600 ft beneath the northwestern half of the district. The *Kd* thins eastward to the 300-400 ft thickness near the center of the southeastern half of the district, and ultimately is less than 75 ft thick beneath the Platte River valley near the southeastern corner of the district (flight line 400901). The bedrock surface topography of the *Kd* varies from generally flat along flight lines in the northern half of the district's southeastern half, as well as beneath most of the northwestern half. South of the Platte River valley beneath the southeastern half of the district, the *Kd*'s topography is more pronounced, particularly from west to east along flight lines 300101 (Figure 5-36), 300201, 400501 (Figure 5-37), and 400701.

The *Kd*, considered a secondary aquifer source in the state of Nebraska, has extensive zones detected at 20 ohm-m or greater beneath much of the southeastern half of the district as well as in the area beneath flight line 200401 in the northwestern half of the district. Figure 5-36 demonstrates this eastward trend of increasing resistivity. From approximately the Todd Valley eastward, nearly the entire 350-400 ft thick *Kd* consists of material 20-40 ohm-m, with some intervals on the far eastern edge of this profile with resistivity greater than 40 ohm-m. Many of these high-resistivity areas are relatively shallow in the subsurface, within 200 ft of the land surface in some areas. In the area beneath flight line 201801,

several 20-40 ohm-m intervals are present beneath the Platte River valley and beneath the uplands to the south of the valley. Some of these features approach 400 ft in thickness. Additionally, beneath the northeast corner of the district (flight line 200901), several generally shallow intervals of 20-40 ohm-m with thicknesses approaching 300 ft are detected. Additionally, in the southeast corner of the district, a nearly 200 ft thick interval of *Kd* exceeding 40 ohm-m forms a bedrock high along flight line 300201 beneath the uplands adjacent to the Todd Valley. A slightly thinner interval of *Kd* exceeding 40 ohm-m is also present immediately east of this feature beneath the Todd Valley. Thus, with the presence of generally thick, resistive intervals in the sandstone in the *Kd*, potential exists in the LPNNRD for future groundwater exploration and development from the *Kd*. In the far northwest corner of the district, the *Kd* contains more conductive zones on the order of 10-12 ohm-m (Appendix 1). It is possible that the water quality (elevated TDS) is causing the decrease in resistivity in this area. It is recommended that to further character the water quality in the *Kd* in this area as well as in the more resistive zones, groundwater samples should be obtained from screened intervals set only in the *Kd* sandstone.

The undifferentiated Paleozoic units range in depth from over 1,300 ft bgl beneath the northwest corner of the district to less than 600 ft bgl in the east central portion of the district. Near the eastern edge of the district, the top of the Paleozoic system is less than 200 ft bgl and forms the bedrock immediately below the Quaternary system along parts of flight line 400901 in the Platte River valley. The contact between the *Kd* and the Paleozoic system varies, with the most pronounced topography beneath the central and eastern sections of the southeastern half of the district, as exemplified along flight lines 300101 (Figure 5-36), 400501 (Figure 5-37), and 400701. Resistivity within the undifferentiated Paleozoic units varies from as low as 10 ohm-m to nearly 25 ohm-m. The Paleozoic strata are primarily comprised of limestone and shale, which are not considered aquifer sources beneath eastern Nebraska. Further exploration for groundwater in the Paleozoic system beneath the LPNNRD is recommended where the highest resistivities are indicated in the AEM data.

### 5.3.2 Lower Platte South NRD

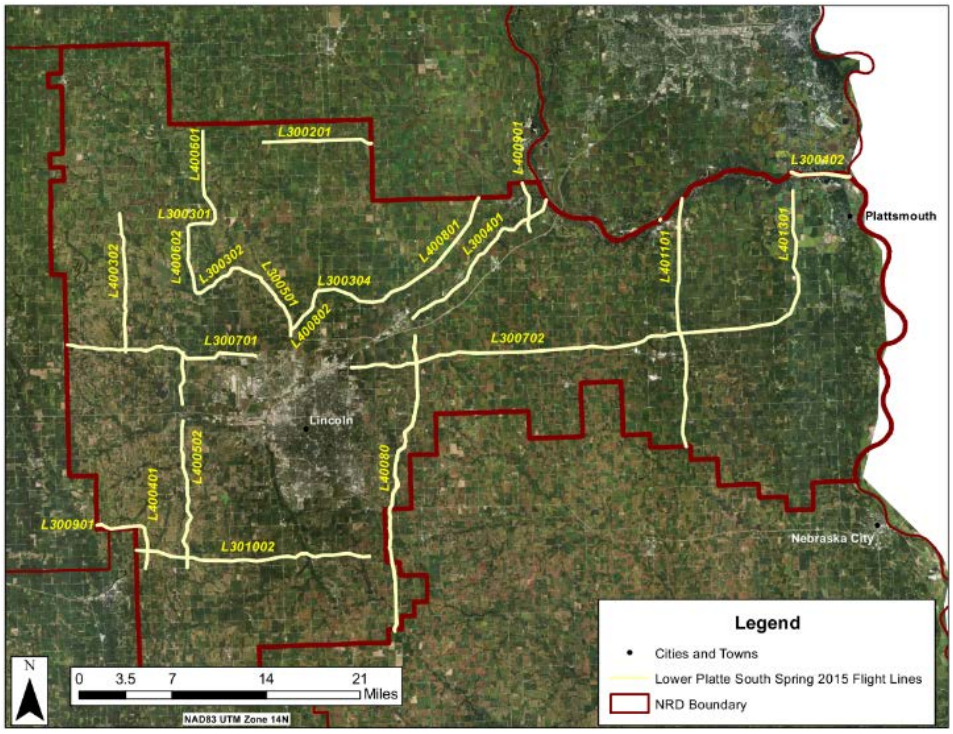



**Figure 5-38: Flight lines within the LPSNRD acquired in the second phase of the ENWRA AEM survey.**

The AEM survey in the LPSNRD revealed the geologic variability present beneath the district from the Quaternary system through the upper strata of the Paleozoic system, as well as local structural features that are associated with the TRSZ. Nine north-south and five west-east flight lines were surveyed in the LPSNRD, along with several diagonal lines to the north and northeast of Lincoln (Figure 5-38). The location of the city of Lincoln and surrounding communities in the west central area of the LPSNRD resulted in a large area devoid of AEM data. However, the flight lines were designed to capture as much AEM data as possible adjacent to Lincoln's developed areas. The electromagnetic data captured the numerous features in the district's subsurface, including the paleovalleys south of Lincoln and in the district's northwest corner, the extremely thin Quaternary deposits north of Lincoln with very low resistivities, the uplands of the eastern half of the district underlain by marginal and aquitard material, the isolated *Kd* features with elevated resistivities, and the variable topography and faults in the Paleozoic system. Many of these features and trends are apparent in the 3D hydrogeologic framework of the district (Figure 5-39).

#### 5.3.2.1 Quaternary System beneath the LPSNRD

As previously described and documented through numerous geologic studies, considerable variability in the character of the Quaternary system exists beneath the LPSNRD. For organization purposes, the interpretive discussion of both the Quaternary system and bedrock strata will be discussed by directional area in relation to Lincoln.

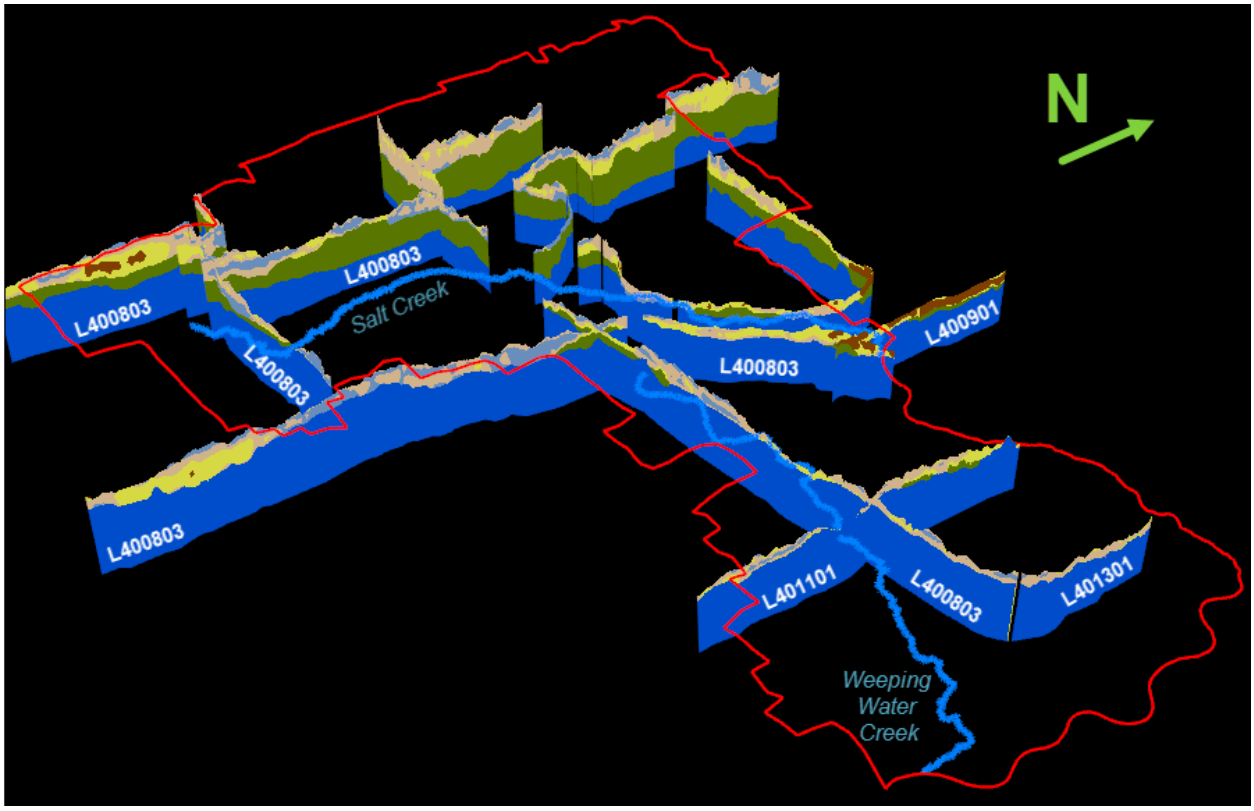



**Figure 5-39: 3D hydrogeologic framework from the reconnaissance AEM survey only within the LPSNRD. Vertical exaggeration is 30x.**

Aquifer resources west of the Lincoln area consist primarily of marginal aquifer material with isolated pockets of principal aquifer and aquitard materials, some of which sit above the 1995 regional water table surface as displayed along flight line 300701 (Figure 5-40). At the LPSNRD's western boundary, the Quaternary system exceeds 500 ft in thickness, although approximately half of the sequence is unsaturated. This pattern of deposits continues northward along flight line 400302, although thicker sequences of aquitard deposits above the regional water table surface are present on the north side of this flight line. Flight line 400502 reveals that the trend of minimal principal aquifer materials extends close to Lincoln, as the Quaternary system in this area is composed entirely of marginal aquifer and aquitard materials that ranges from 200-300 ft in thickness.

Northwest of Lincoln, principal aquifer material is detected beneath flight lines 300301 and 400601. Along this line, a 150 to 200 ft thick sequence of principal aquifer material sits atop Cretaceous bedrock and is overlain by nearly 200 ft of mostly aquitard material interlayered with marginal aquifer deposits. These materials are associated with the Dwight-Valparaiso aquifer as defined by Druliner and Mason (2001). This flight line coincides with the Dwight-Valparaiso area AEM survey conducted by XRI in 2013 (Carney et al., 2014), and provides a view of the subsurface beyond the local-scale, densely spaced grid lines used in the 2013 survey. Further comparison of these surveys is provided in Section 5.3.5.1.

Immediately north and northeast of Lincoln, along flight lines 300303, 300304, 300401, 400802, and 400801, the Quaternary system thins to less than 200 ft, and in some areas, the thickness ranges from 50 to 100 ft (flight lines 300303 and 400801). The deposits in this area are predominately marginal

aquifer material, with isolated intervals of principal aquifer deposits. However, in many areas, these materials sit above the regional water table surface. Along flight line 300303, the thin Quaternary deposits are mapped as aquitard material. This is the result of the resistivity threshold used to define aquifer materials in the Quaternary system. In this area, high TDS levels in the thin veneer of unconsolidated deposits that sit atop low resistivity *Kd* bedrock is likely the cause of low resistivity values in the Quaternary system. Along lines 400801 (Figure 5-41) and 300304, discontinuous principal aquifer deposits, some containing sand-rich principal aquifer material, are present within the mostly marginal aquifer material comprising the Quaternary system in this area. In some locations, the principal aquifer material, including sand-rich zones, are positioned above the regional water table surface and are likely areas of high potential recharge to the aquifer. Along flight line 300401, the Quaternary system ranges from 90 to 125 ft in thickness and contains a greater abundance of principal aquifer material relative to flight lines to the west, most of which is also saturated. In this area, the principal aquifer materials extend to near the land surface, thus increasing the potential for recharge to the shallow aquifer. This flight line roughly parallels the Salt Creek and the aquifer materials are considered part of the Lower Salt Creek aquifer as defined by the LPSNRD (Divine, 2014).

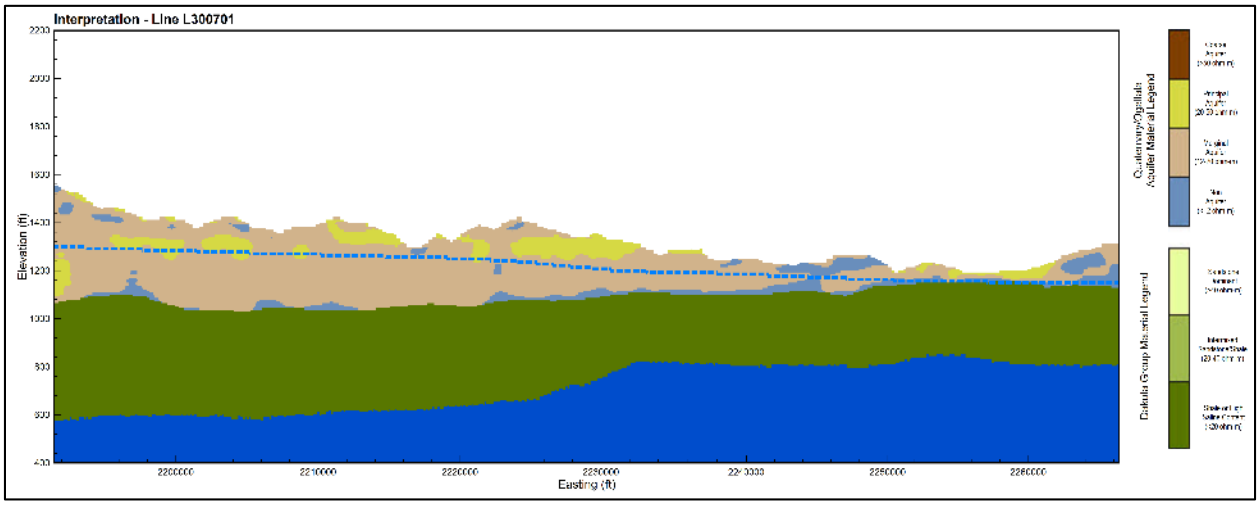



**Figure 5-40: Hydrogeologic interpretation of AEM profile 300701 west of Lincoln in the LPSNRD.**

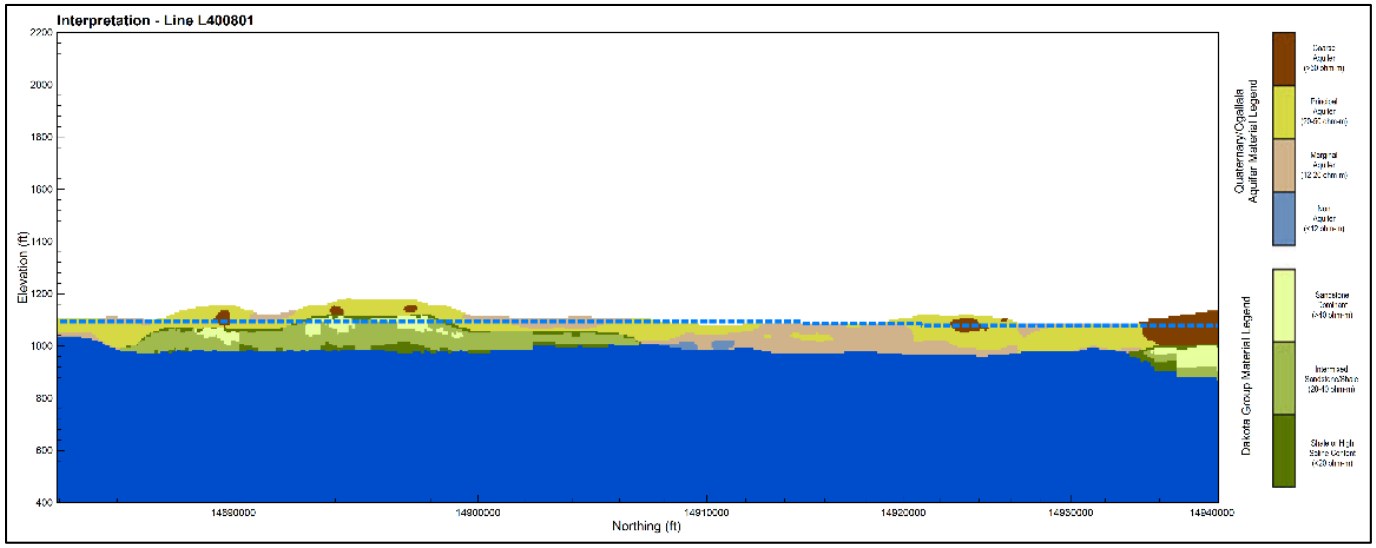



**Figure 5-41: Hydrogeologic interpretation of AEM profile 400801 northeast of Lincoln in the LPSNRD. The blue dashed line is the 1995 CSD regional water table surface and the solid blue color is undifferentiated Paleozoic strata.**

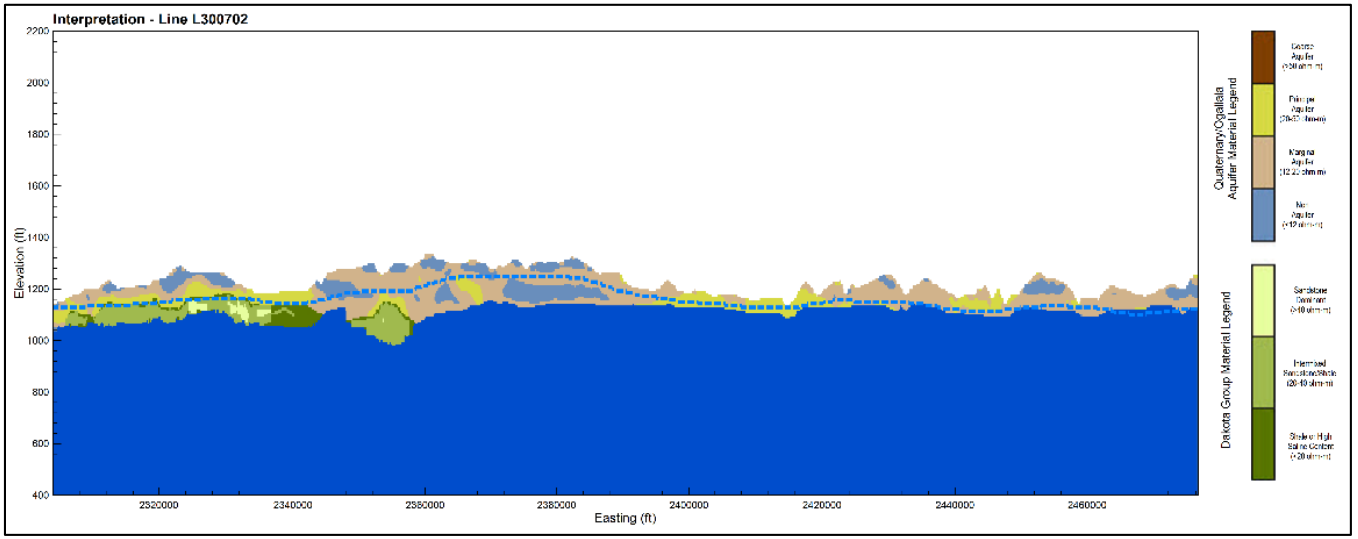



**Figure 5-42: Hydrogeologic interpretation of AEM profile 300702 east of Lincoln in the LPSNRD. The blue dashed line is the 1995 CSD regional water table surface and the solid blue color is undifferentiated Paleozoic strata.**

East of Lincoln, flight line 300702 reveals that the trend of mostly marginal aquifer and aquitard material continues to the eastern edge of the LPSNRD (Figure 5-42). Along this section, the maximum thickness of the Quaternary system approaches 250 ft, with minimal thickness of 80 to 100 ft beneath the Weeping Water Creek valley in central Cass County. Similar to areas west of Lincoln, only isolated intervals of principal aquifer material were detected along this profile, including some that are above the water table surface northeast of Lincoln. Along flight line 300702, the surface topography is hummocky, with numerous surface drainages crossing the landscape. Many of the hilltops in the AEM profile are underlain by aquitard material, which likely minimizes recharge to the groundwater flow system in this part of the LPSNRD. North and south of flight line 300702 in central Cass County, similar trends of predominately interlayered marginal aquifer/aquitard materials forming the entirety of the Quaternary system are indicated on flight line 401101. This profile indicates that at its crossing of Weeping Water Creek (near Northing value of 14850000 ft), Quaternary materials are essentially absent, as Paleozoic strata are present at the land surface. The lack of principal aquifer material in this area is further substantiated by the nearly complete absence of irrigation wells in the eastern LPSNRD (Figure 2-19, (2000s map)). On the far eastern side of the district, flight line 401301 indicates that the Quaternary system is almost entirely marginal aquifer ranging from 50-100 ft thick with varying degree of saturated thickness.

South of Lincoln, the Dorchester-Sterling paleovalley aquifer crosses beneath southern Lancaster County (Divine, 2014). However, the orientations and location of flight lines 400803 and 301002 in relation to the LPSNRD boundaries do not capture the expected resistive materials within this feature. However, the paleovalley is clearly detected in the AEM survey south of the LPSNRD boundary on flight line 400803 and is discussed in the interpretive section of the NNRD. Figure 5-43 displays the 3D hydrogeologic framework with an eastward view showing the paleovalley along 400801 and 400803. It should be noted that Druliner and Mason (2001) also call these deposits the Crete-Princeton-Adams aquifer.

Just beyond the northern boundary of this paleovalley and south of Lincoln, flight line 301002 reveals the Quaternary system to be similar to subsurface conditions west of Lincoln, with mostly marginal aquifer material interlayered with isolated bodies of aquitard material and scattered principal aquifer deposits. Along an approximately 8 mile extent between Easting values 2230000 and 2270000 is a 100 to 200 ft thick section of aquitard material that partially occupies a depression in the underlying *Kd* bedrock. The 1995 regional water table surface crosses the top of this aquitard feature. Hence, similar to areas in the eastern LPSNRD, this area has very few irrigation wells present (Figure 2-19 (2000s map)).

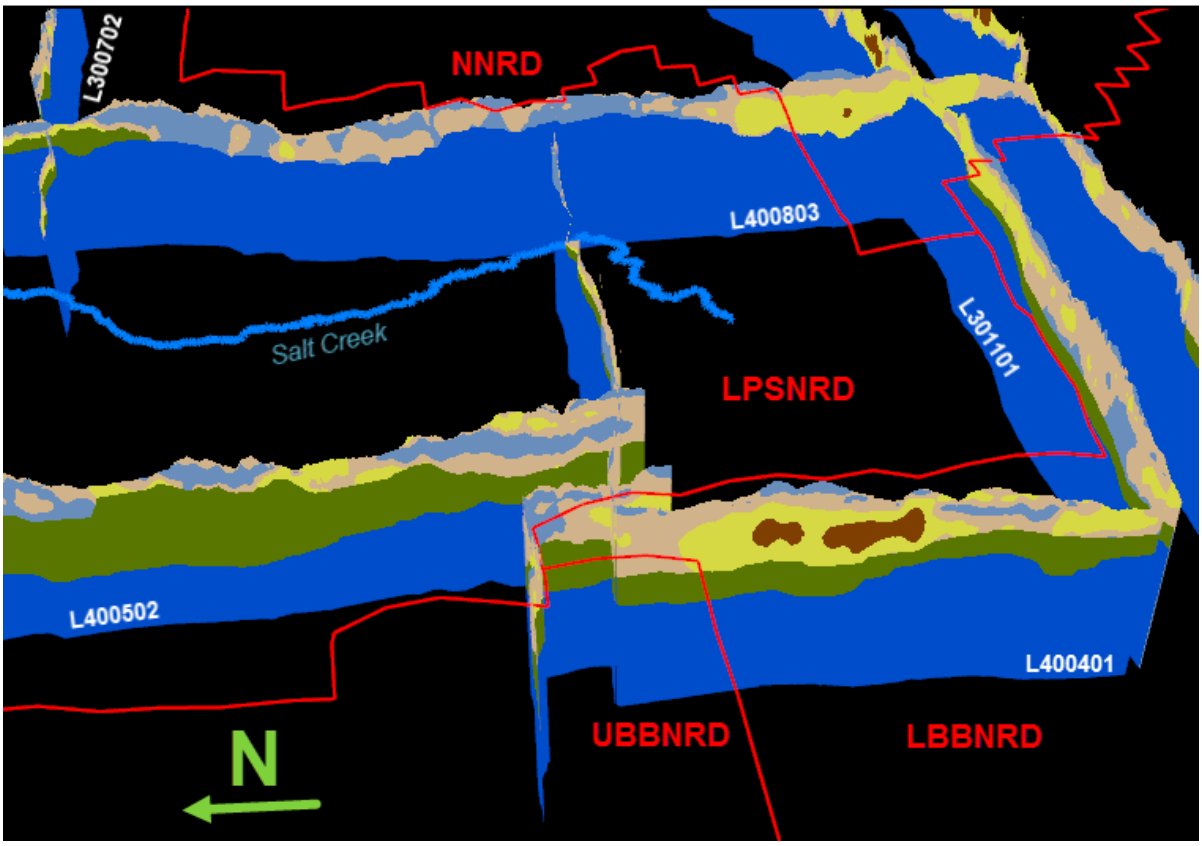



**Figure 5-43: Eastward view of the3D hydrogeologic framework of the southern LPSNRD showing principal aquifer materials of the Dorchester-Sterling paleovalley aquifer. Vertical exaggeration is 30x.**

#### *5.3.2.2 Cretaceous and Paleozoic Sequence beneath the LPSNRD*

The Cretaceous bedrock beneath the LPSNRD shows considerable variability in thickness, topographic expression, depth, and resistivity across the district. The southeastern terminus of the regionally extensive *Kd* occurs in the LPSNRD, which includes isolated blocks of the formation separate from the continuous unit. In the northwest corner of the district, the *KcKgg* is mapped in a peninsula-shaped subcrop (Figure 5-2) in the Dwight-Brainard area. However, no AEM flight line crossed this area, and the only Cretaceous unit mapped in the interpretation is the *Kd*.

West of Lincoln, the *Kd* approaches 500 ft in thickness, but thins eastward to around 300 ft near the city's northwest outskirts (Figure 5-40). At the western edge of the district, the westward dipping *Kd* is approximately 500 ft bgl, whereas on the northwest side of Lincoln, depth to the *Kd* is less than 50 ft in places. In the northwest corner of the district, the *Kd* ranges between 400 and 500 ft in thickness with undulating topographic relief in the bedrock surface. Along the western edge of Lincoln southward, the *Kd* thins from between 400 to 500 ft to approximately 150 ft (flight line 400502). Northwest and north of Lincoln, the *Kd* is detected with a resistivity of near 10 ohm-m. The eastwardly up-dipping strata of the *Kd* is less than 50 ft bgl north of the Lincoln Municipal Airport in the lowland valley of the Salt Creek watershed. As discussed in sections 5.2.2, between Easting values 2240000 and 2250000 ft, a zone of 10 ohm-m is detected between the shallow, thin Quaternary deposits and the top of the *Kd*. This apparent distribution of low resistivity from the AEM interpretation indicates likely connection of upwelling, high-TDS water from the *Kd* with the overlying Quaternary system, and the discharge of high-TDS

groundwater from the subcropping *Kd* creates the elevated salinity levels in the wetlands and marshes in the area northwest of Lincoln. The overall extent of this low resistivity trend in the *Kd* seems to be generally isolated, as within 3 mi to the south of flight line 300701, resistive intervals approaching 200 ft in thickness are detected in the 20-40 ohm-m range, and some greater than 40 ohm-m are present. Additionally, flight lines 400602 and 400601, immediately north of flight line 300701, also contain intervals of 20-40 ohm-m in the upper *Kd*.

North and northeast of Lincoln, the *Kd* thins considerably, with most of the AEM profiles detecting the southeast edge of the *Kd* subcrop and/or isolated bodies of the unit. Flight line 300304 captures the edge of the terminus of the *Kd*, where it thins from 120 ft to around 40 ft at the formation's edge. The formation in this area is primarily below 20 ohm-m, with small, isolated bodies of 20-40 ohm-m *Kd*. Eastward from the location, flight line 400801 (Figure 5-41) reveals an isolated section of *Kd* over 100 ft in thickness that is entirely composed of 20 ohm-m or greater sandstone. The topographic expression of the *Kd* in this area is generally flat to slightly uneven along flight line 400801.

East of Lincoln along flight line 300702 (Figure 5-42), the AEM survey captures an isolated interval of *Kd*, ranging from 50 to 100 ft in thickness with resistivities typically 20 ohm-m or greater with isolated zones exceeding 40 ohm-m. The top of the *Kd* in this area has a hummocky topographic expression that is overlain by 100-150 ft of Quaternary deposits. South of Lincoln, the *Kd* thins from nearly 250 ft thick, to less than 40 ft at its terminus near Easting value 2290000 ft. Within this area, zones of resistivity between 20-40 ohm-m are present within the *Kd*, and near the unit's eastern edge, the formation is entirely above 20 ohm-m.

The AEM survey detected resistivities several hundred feet into the Paleozoic system. As previously mentioned, the Paleozoic was undifferentiated in the interpretation plots of the AEM data. However, varying trends in Paleozoic resistivities are apparent throughout the survey area, including beneath the LPSNRD. The upper surface of the Paleozoic system is generally flat with slight undulations in the areas west and north of Lincoln, but becomes irregular with pronounced expression east of Lincoln as revealed in flight lines 400803 and 401101. Along most of these lines, the Paleozoic system forms the underlying bedrock beneath the Quaternary system.

The variable resistivity in the Paleozoic system also helps reveal structural trends and dipping strata within the AEM profiles. For example, flight line 401301 in the far eastern side of the district reveals Paleozoic strata dipping northward slightly, and flight line 300702 (Figure 5-42) reveals westward dipping strata. As discussed in prior sections, faults are present across southern ENWRA project area. However, intersections of flight lines with the mapped faults are present in the LPNNRD and NNRD and are discussed in those sections of this report.

### *5.3.3 Nemaha NRD*

The southernmost extent of the ENWRA AEM survey covered parts of the NNRD, including two west-east lines that nearly cover the entire district as well as a north-south line from the boundary of the LPSNRD to the Nebraska-Kansas state line (Figure 5-44). The highest density of flight lines cover the middle one-third of the district. The district is mostly rural with limited population centers or other

infrastructure that could cause interference to the data acquisition. Figure 5-45 displays the 3D hydrogeologic framework of the district.

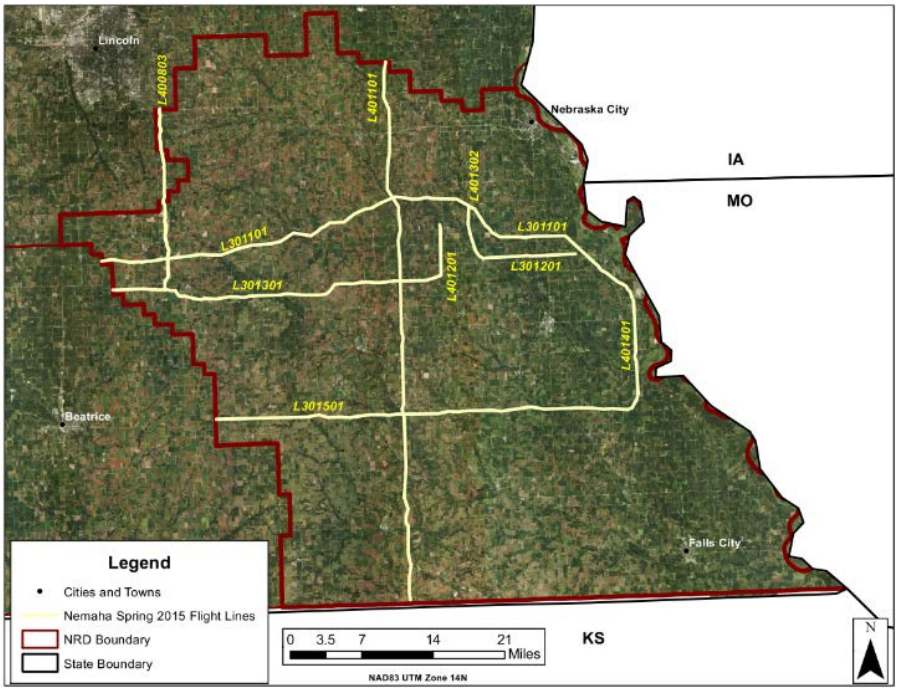



**Figure 5-44: Flight lines within the NNRD acquired in the ENWRA AEM survey.**

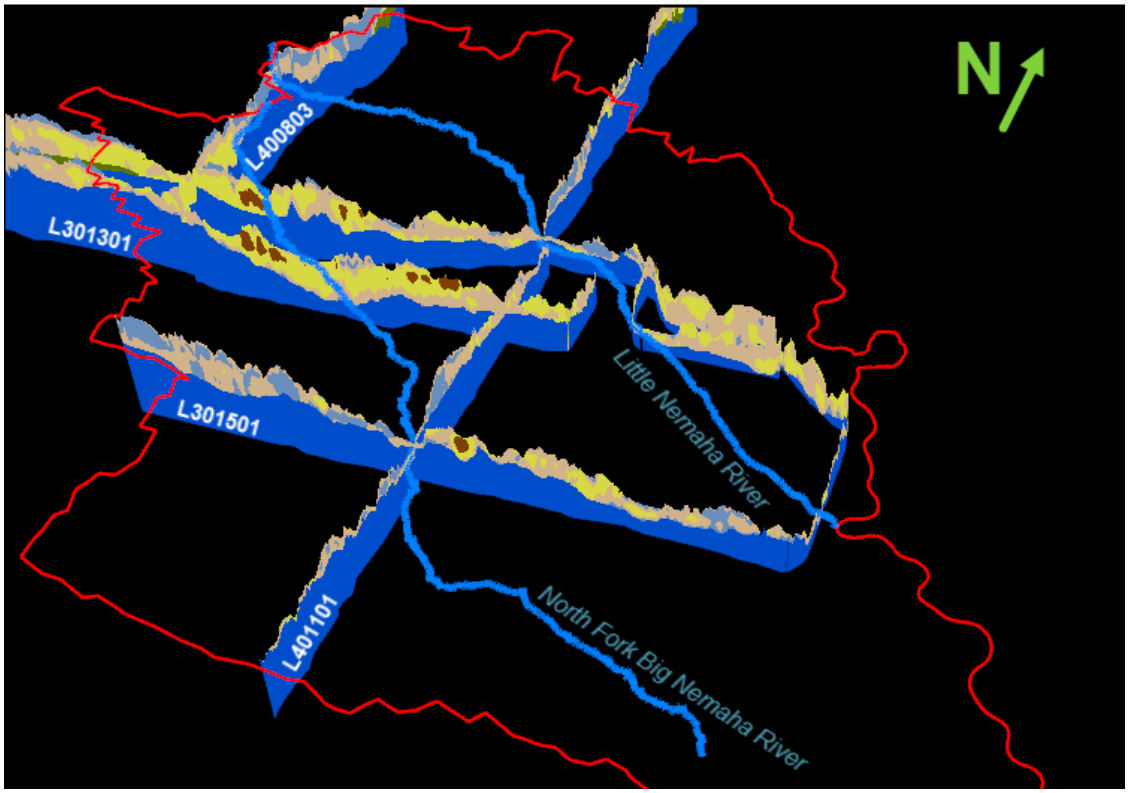



**Figure 5-45: 3D hydrogeologic framework from the reconnaissance AEM survey only within the NNRD.**

#### *5.3.3.1 Quaternary System beneath the NNRD*

The Quaternary system beneath the NNRD contains some of the greatest variability in thickness and resistivity in the entire ENWRA survey area. Thick, resistive Quaternary deposits occupy paleovalleys through much of the north-central section of the district, whereas in other locations, particularly in Pawnee County and along the easternmost flight lines, the Quaternary thickness is negligible, with only thin soils overlying Paleozoic bedrock. The most significant paleovalley aquifer is the eastward extension of the Dorchester-Sterling paleovalley aquifer that enters the district from the LPSNRD and LBBNRD to the west. The paleovalley is oriented west to east across the northern Gage, Johnson, and Nemaha Counties, as well as southern Otoe County (Figure 2-12). Figure 5-46 displays the 3D hydrogeologic framework of the NNRD with a close-in view of the paleovalleys in the northeast section of the district.

Along flight line 400803, which straddles the NNRD-LPSNRD boundary, the Dorchester-Sterling paleovalley aquifer is displayed in 2D on the southern one-third of the flight line (Figure 5-47). In this area, the principal aquifer deposits exceed 200 ft in thickness across an area over six miles wide along the profile. At this location, the paleovalley is overlain by marginal aquifer and aquitard material exceeding 100 ft in thickness. The regional water table surface is within the principal aquifer materials, indicating that aquifer conditions are likely unconfined in this area. Flight line 301301 captures the subsurface resistivity from west to east across most of the district, and includes the area of the paleovalley where it merges with a smaller, northeast-trending paleovalley in northeastern Johnson County (Figure 5-48, eastern half of profile). This confluence of paleovalleys ranges from 15-20 mi in width with principal aquifer deposits exceeding 200 ft in thickness in places with minimal overlying aquitard or marginal aquifer materials. At some locations, for example near Easting value 2350000 ft eastward, sand-rich zones of the principal aquifer materials are present at the land surface that extend downward to below the regional water table surface. These features are also apparent to the north along flight line 301301 (Appendix I). This extensive groundwater resource in the NNRD also stands out in the irrigation well map of the district (Figure 2-19), where the pattern of wells on the 2000s map closely resembles the extent of the paleovalleys in this area. In viewing the pattern of irrigation development in the district, the 1970's appear to be the time period when widespread development of this paleovalley aquifer resource occurred.

A second smaller paleovalley mapped by the CSD (Figure 2-12) is present in northwestern Richardson County. The northern edge of this valley is captured along flight line 501301 (Appendix 1) east of Easting value 2500000 ft. In this area, the paleovalley is less than 100 ft thick and consists of marginal and principal aquifer deposits. This area also corresponds with the present-day Muddy Creek watershed, thus it is unclear as to whether this resistive interval is actually composed of true paleovalley materials or Holocene alluvium. It is like the materials evident along flight line 501301 in the valley are a combination of these sources.

The remaining groundwater resources in the NNRD as revealed by the AEM data mostly consist of marginal aquifer materials with scattered distributions of principal aquifer material. In the southwest corner of the district, a nearly 200 ft thick sequence of marginal aquifer material is present along flight line 301501 west of Easting value 2400000 ft. In southern Pawnee County, along flight line 401401 (south of flight line 300501), the Quaternary system consists primarily of marginal and aquitard aquifer material that mantles the rolling Paleozoic bedrock topography. In this area, only local zones of

saturation or perched aquifers are likely present, as the regional water table surface is poorly constrained in this area. In the east-central section of the district east of flight line 401101, the Quaternary system is generally thin, and in many locations, unsaturated. Overall, the maximum thickness of Quaternary deposits exceeds 200 ft in locations along 301201 and 301101, but are typically 100 ft thick or less. An interval of principal aquifer material that is present in this area is revealed in flight line 401302 (Appendix I) that crosses the Otoe-Nemaha County line. The AEM data along this five mile profile indicates a thin interval (50 ft or less) of saturated principal aquifer material overlain by a thin veneer of mostly unsaturated marginal aquifer materials. These resistive features are associated with alluvium of the Little Nemaha River valley. This stream valley package of resistive alluvial deposits exemplifies how, in comparison with drainages to the north in the ENWRA area, stream valley aquifer resources in association with modern-day stream valleys are typically more limited in thickness and extent, and thus potential for groundwater development. Figure 5-49 displays the easternmost flight line of the southern ENWRA survey in the NNRD and exhibits the conditions in the Quaternary system in the eastern half of the district. Along this line, the Quaternary system is typically 75 ft thick or less and is comprised of marginal aquifer material with mostly thin saturated intervals.

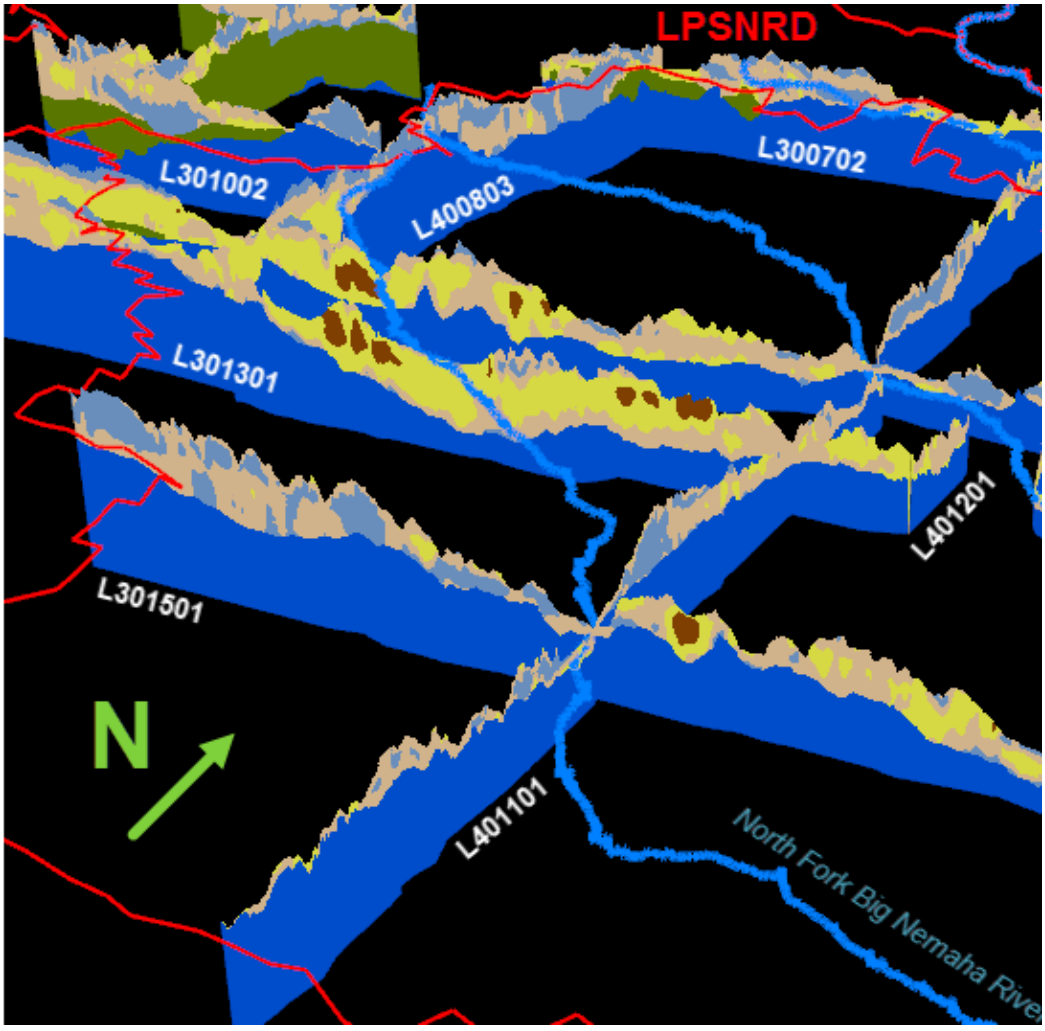



**Figure 5-46: Close-in view of the paleovalley system in the northwest NNRD. Vertical exaggeration is 50x.**

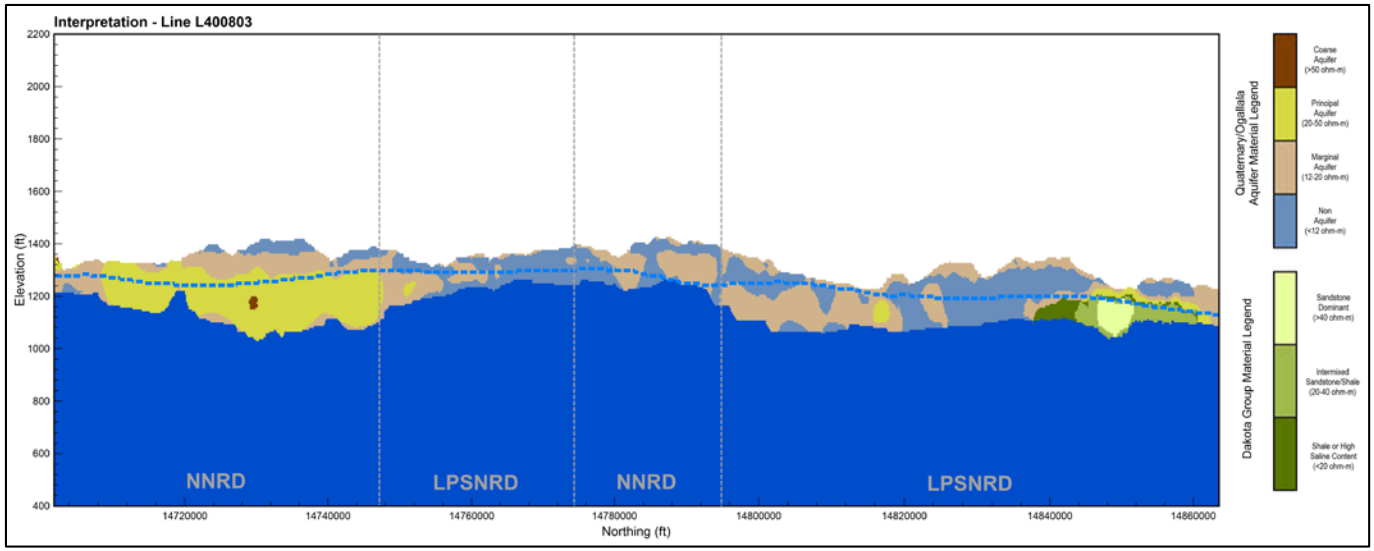



**Figure 5-47: View of flight line 400803 displaying the Dorchester-Sterling paleovalley on the south side (left) of the profile.**

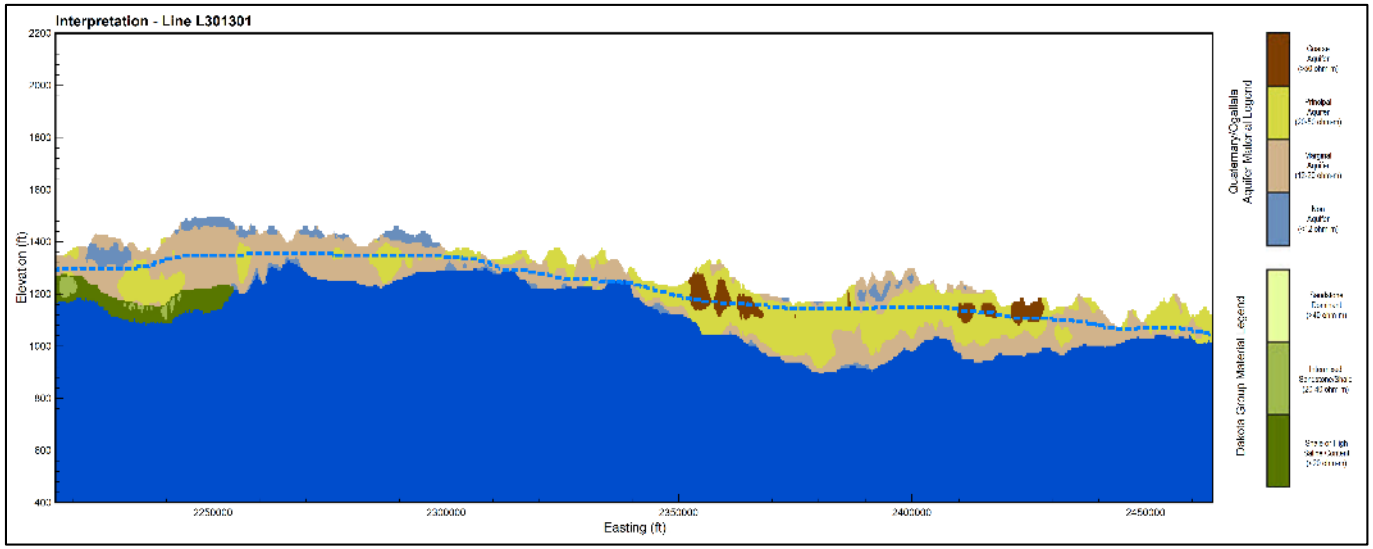



**Figure 5-48: AEM profile of flight line 301301 displaying the confluence of two paleovalleys in northeastern Johnson County.**

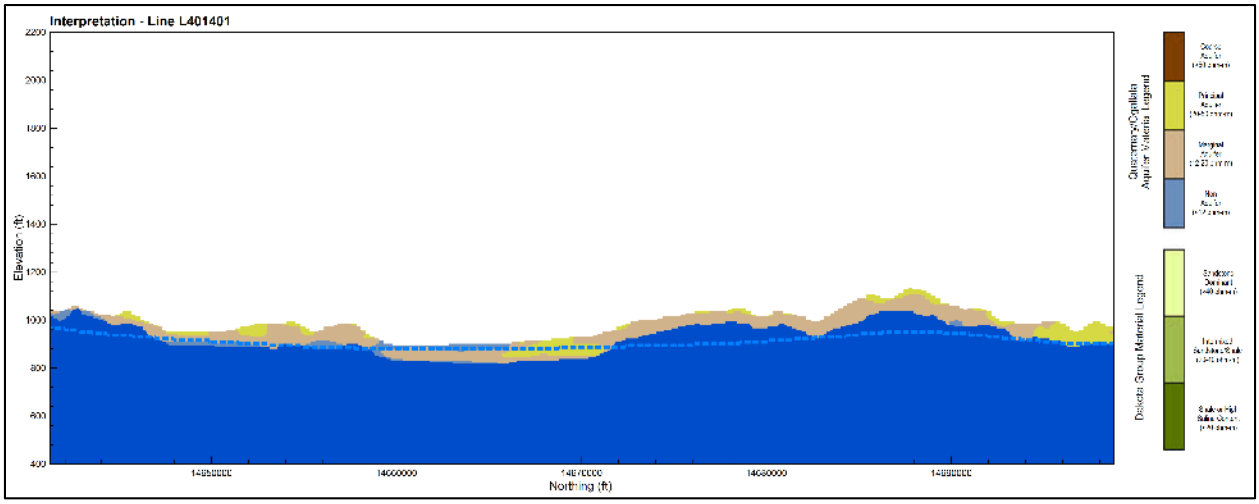



**Figure 5-49: Flight line from AEM profile 401401 in the eastern NNRD.**

### *5.3.3.2 Paleozoic Sequence beneath the NNRD*

The Paleozoic system beneath the NNRD has the most pronounced topographic expression of the entire ENWRA survey area. In some areas, local relief in the upper surface of the Paleozoic strata beneath the NNRD is nearly 300 ft in the north central section of the district (Figure 5-48) and 200-250 ft in southern Pawnee County. Overall, the resistivity of the undifferentiated Paleozoic strata is low, typically less than 15 ohm-m, and in along most profiles, is in the 10-12 ohm-m range. Exceptions to this pattern are evident, however, as along certain flight lines, particularly 401101, the eastern extent of flight line 301101, and near the center of flight line 301301 where resistivities approaching 20 ohm-m are apparent (resistivity profiles of these flight lines are available in Appendix I). Whether these elevated resistivities are related to lithologic character only, or whether groundwater is present, is unknown. Further research with exploratory test hole drilling would be required in these resistive units to determine whether groundwater resources are present in the Paleozoic strata beneath the NNRD.

In locations of the Paleozoic system with variability in resistivity, structural trends are clearly apparent. For example, along flight line 301301, westward dipping strata are present along the eastern half of the profile. As mentioned in Section 5.2.3, southeastern Nebraska, particularly beneath the NNRD, is underlain by several structural features that were detected by the AEM survey. Such features include the Union Fault, Humboldt Fault, and the Nemaha Uplift/Elk Creek Carbonatite complex. Each of these features is displayed in resistivity profiles included in Section 5.2.3. The hydrogeologic character and potential for groundwater development along these fault lines is unknown, however. In some regions, faults can act as conduits for groundwater movement, and in others, these features can act as a barrier to groundwater movement either within the fault or cross sectional flow between water-bearing porous or fractured strata. The AEM profiles of the southern ENWRA survey can be used to guide future potential exploratory drilling programs of these fault features to determine if groundwater development could occur along these faults.

Note that only a very small section of thin (less than 50 ft) *Kd* is present beneath the western edge of the NNRD along flight line 301101. This area of the *Kd* is discussed in the following section.

### *5.3.4 Flight Lines beyond the ENWRA Area*

Parts of five flight lines in the southern ENWRA survey extended beyond the boundaries of the NRD's participating in ENWRA. These include north-south flight lines 400101 and 400201 in the northeast corner of the UBBNRD (Figure 5-50) and flight lines 400303, 301101, and 301301 in the LBBNRD (Figure 5-51). These profiles are also revealed in the 3D representation of the southern ENWRA flight area in Figure 5-15 through Figure 5-17. In the UBBNRD, flight lines 400101 and 400201 reveal the character of the Quaternary system and the Cretaceous bedrock west of the LPSNRD, which includes the area flown in the 2013 AEM survey by XRI. Flight line 400101 (Figure 5-52) indicates that the Quaternary deposits are primarily interlayered marginal aquifer and aquitard material upwards of 300 ft in thickness, with only isolated intervals of principal aquifer ranging from 100 to 150 ft in thickness. Flight line 400201, located two miles east of flight line 400101, shows a similar pattern as flight line 400101, but with slightly wider and thicker intervals of principal aquifer materials. These bodies of more resistive material at the base of the Quaternary system could be connected to the larger intervals of principal aquifer materials comprising the large paleovalley in Figure 2-12 and described in sections 5.3.1 and 5.3.2.

In the Cretaceous bedrock displayed in these flight lines, a 50 to 100 ft thick interval of the *KcKgg* is present near the center of these profiles. The *Kd* in these profiles ranges from nearly 300 ft in the south to nearly 600 ft to the north, with isolated bodies of 20-40 ohm-m sandstone approaching 200 ft in thickness in both profiles. The presence of these resistive bodies indicates that the high-TDS zone along flight line 300701 to the southeast is not ubiquitous throughout the *Kd* immediately to the west of the ENWRA survey area, and that variability in the *Kd* potential for aquifer development exists in the northeastern area of the UBBNRD.

Flight lines 301101 and 301301 (Appendix I) extend into the LBBNRD from the NNRD to the east. These lines capture the widespread principal aquifer materials within the mapped paleovalley areas north of Beatrice, NE (Figure 2-12). In this area, a sequence of principal aquifer materials upwards of 200 ft in thickness that is interlayered within marginal aquifer material is present. These features are overlain by only thin intervals of aquitard material at the land surface. Based on the placement of the regional water table surface, the aquifer appears to be unconfined in this area, although localized testing would be required to determine this, as confining material can also be present at depth within marginal aquifer materials.

The terminus of the *Kd* is present in these profiles also, where the unit thins from approximately 120 ft on the western edge of the flight line to minimal thickness within 5-10 miles of the western edge of the survey area. Near the eastern edge of the *Kd*, resistive zones ranging from 20-40 ohm-m are present. The topographic expression of the top of the Paleozoic system has an uneven pattern beneath these flight lines, which is a pattern that continues eastward into the NNRD.

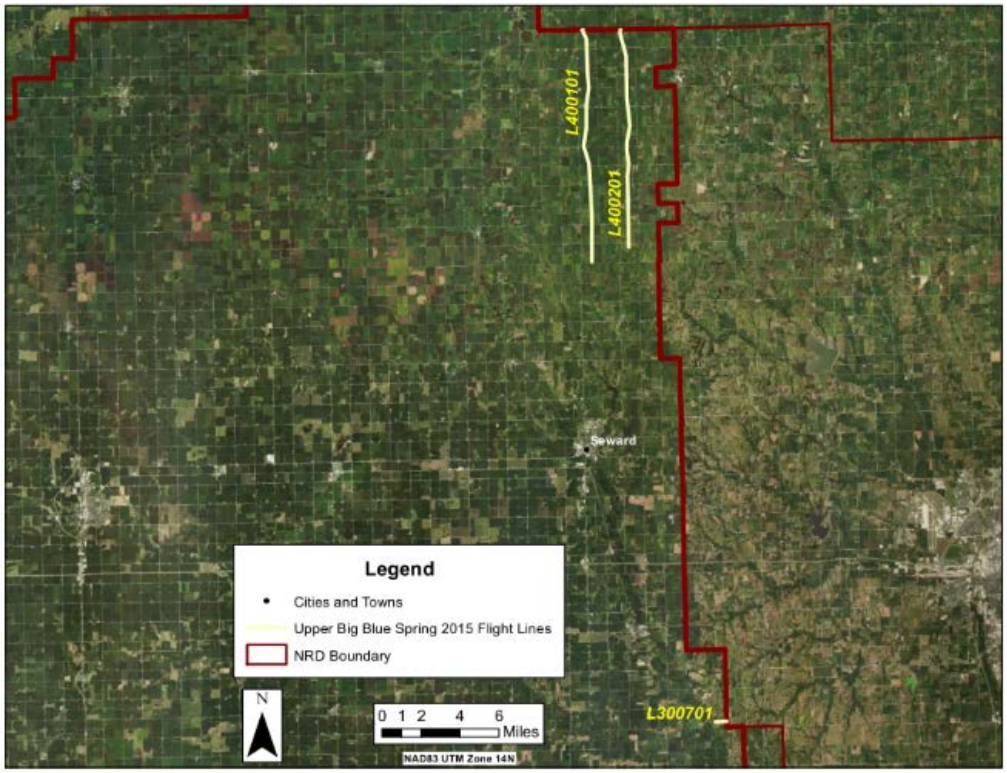



**Figure 5-50: Flight lines within the UBBNRD acquired in the second phase of the ENWRA AEM survey.**

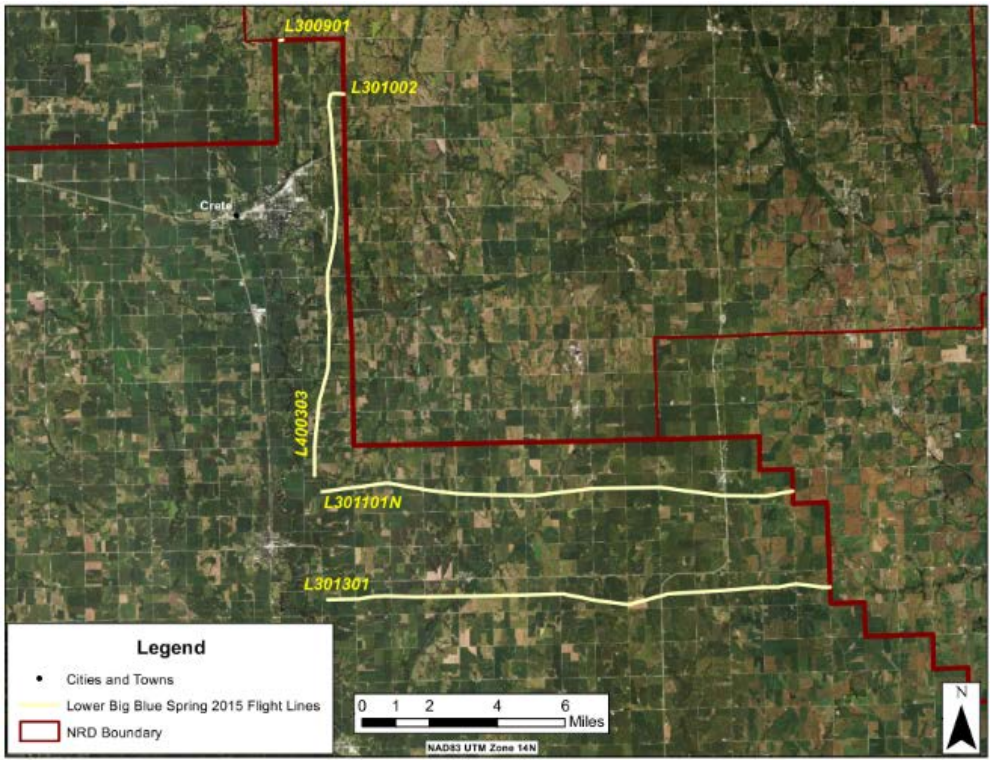



**Figure 5-51: Flight lines within the LBBNRD acquired in Phase 2 of the ENWRA AEM survey.**

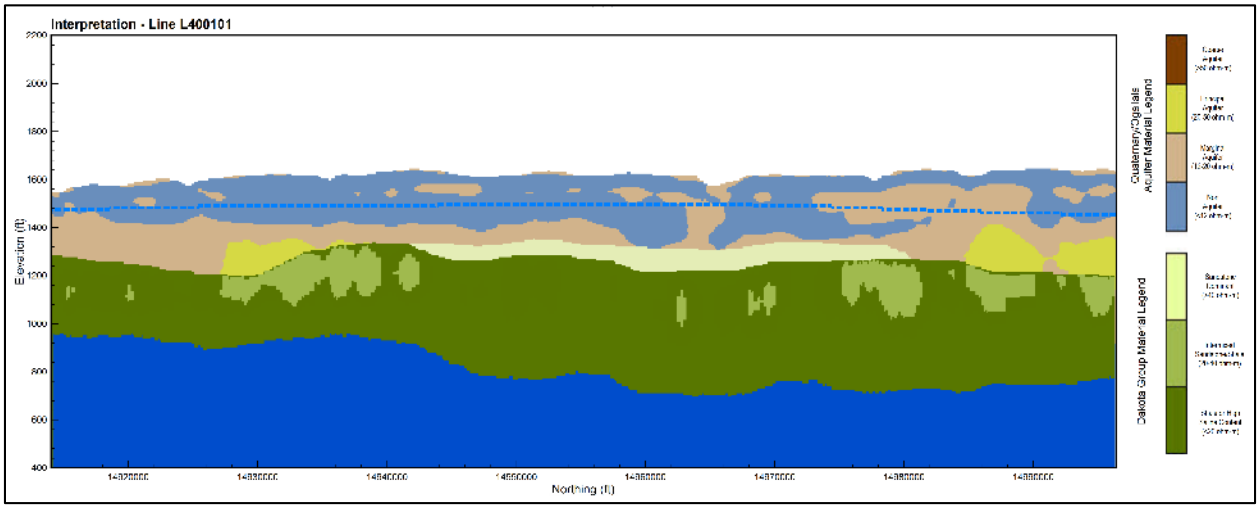



**Figure 5-52: AEM profile of flight line 400101 in the northeastern corner of the UBBNRD.**

Flight line 400303, which roughly parallels the LBBNRD-LPSNRD boundary in northeast Saline County, captures the western extent of the Dorchester-Sterling paleovalley aquifer system which extends from the northwestern NNRD through the LPSNRD (although the feature was not captured by flight lines within the LPSNRD). Along this profile, principal aquifer materials extend in a north-south width of over six miles, with a thickness approaching 250 ft. Within the principal aquifer materials are sand-rich zones with thicknesses approaching 100 ft in places. Overlying these coarse deposits are interlayered marginal aquifer and aquitard material ranging from 50 to over 100 ft in thickness. The placement of the regional water table surface indicates that aquifer conditions in this area are likely unconfined. But, similar to other areas with similar distribution of Quaternary materials, local field tests are required to characterize local aquifer conditions. Beneath the paleovalley, the *Kd* ranges from 100 to 200 ft in thickness, with intervals of 20-40 ohm-m material approaching 100 ft in thickness immediately below the overlying paleovalley.

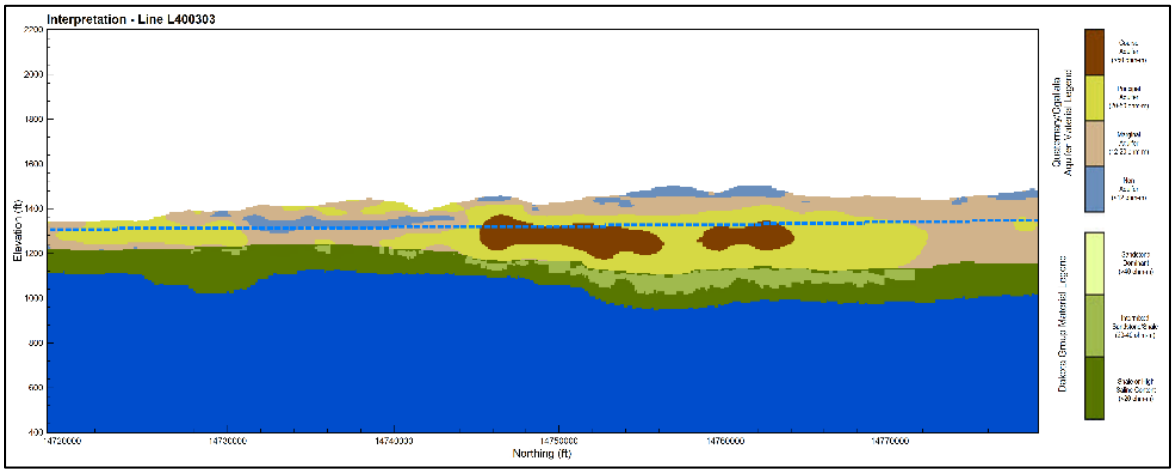



**Figure 5-53: AEM profile of flight line 400303 in the northern LBBNRD. See Figure 5-2 for the strata color coding.**

### *5.3.5 Comparison of AEM Results with Previous Studies*

Prior to and concurrent with the ENWRA project reconnaissance AEM surveys, XRI conducted an AEM survey in the northwestern area of the LPSNRD to provide a hydrogeologic framework of the aquifer in the area for groundwater management planning. Additionally, smaller, local scale airborne geophysical surveys were also conducted at several locations across the southern ENWRA project area by the CSD and USGS. The purpose of theses pilot studies was to assess the effectiveness of AEM at mapping the complex geology of Quaternary alluvial and glacial deposits. The pilot studies were conducted with a frequency-domain electromagnetic system (the SkyTEM is a time-domain type of electromagnetic system) at several sites that together encompass the wide range of hydrogeologic settings in eastern Nebraska. Figure 5-54 displays the locations of six survey areas (and two from the northern ENWRA survey area) conducted by the CSD and/or the USGS prior to the reconnaissance survey discussed in this report. These studies had various investigative objectives, with each providing insight into the subsurface conditions and the effectiveness of the AEM methodology implemented in the study. Discussion of the XRI and CSD/USGS pilot surveys are provided in the following subsections of this report.

The inversion results from ENWRA Fall 2014 were compared with ENWRA Spring 2015 at 2 locations where the flight lines approached each other. These locations are marked in Figure 5-55 while the models are shown in Figure 5-56. While the models compare well within the near surface, they diverge as the depth increases. The difference in panel A is approximately 5 ohm-m and 7 ohm-m in panel B. The calculated DOIs are also shown. This variance at depth could be due to the larger model layers (and the averaging that has to be done at those depths), or to a loss of resolution at greater depths, or due to the distance between the sounding locations on the flight lines from the two different survey events.

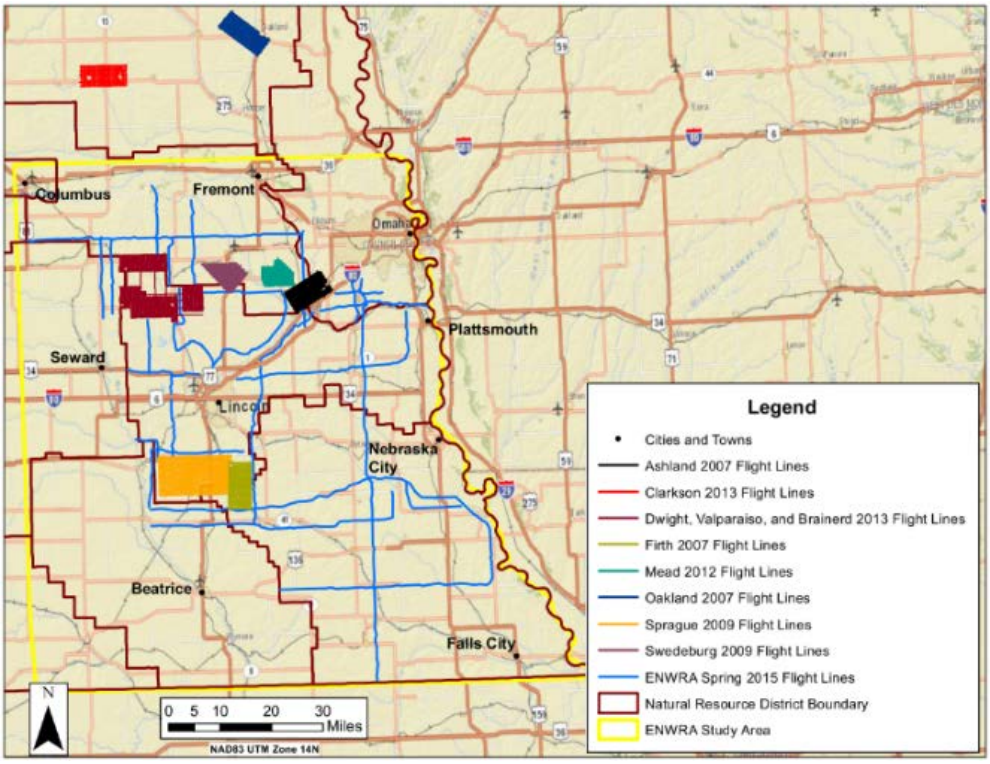



**Figure 5-54: Locations of prior study airborne geophysical survey studies in the southern ENWRA project area.**

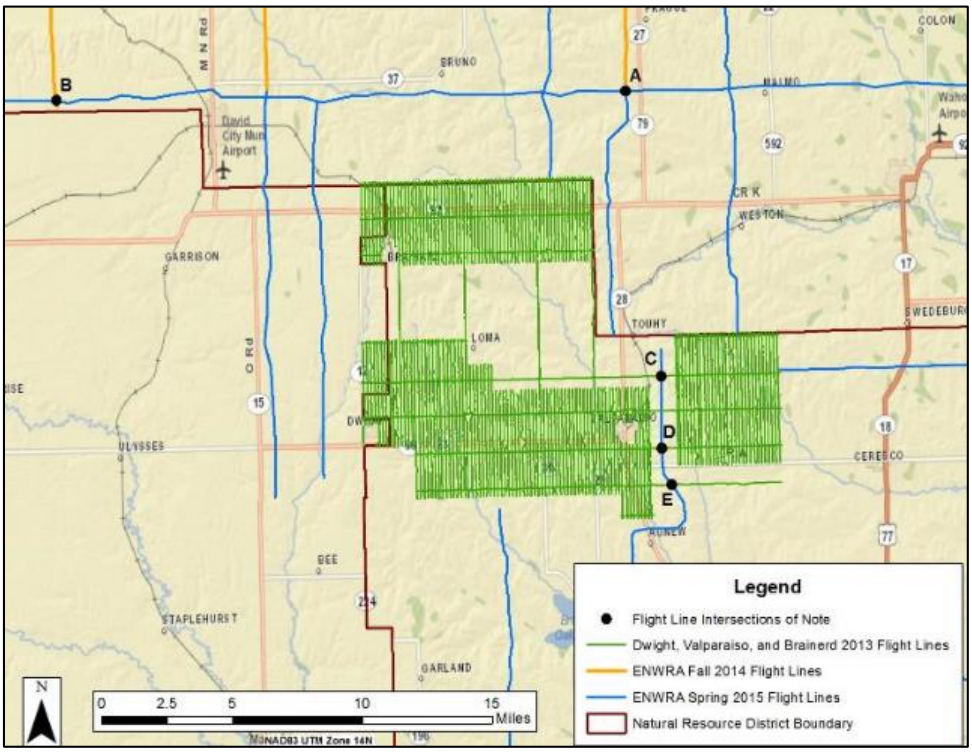



**Figure 5-55: Locations where inversion results between surveys were compared. ENWRA Fall 2014 and Spring 2015 were compared at points A and B. The compared models at point A were 252 ft apart and 601 ft at point B. ENWRA Spring 2015 were compared with the Dwight-Valparaiso-Brainard 2014 flights at points C, D, and E. The compared models were 77 ft, 48 ft, and 110 ft apart, respectively.**

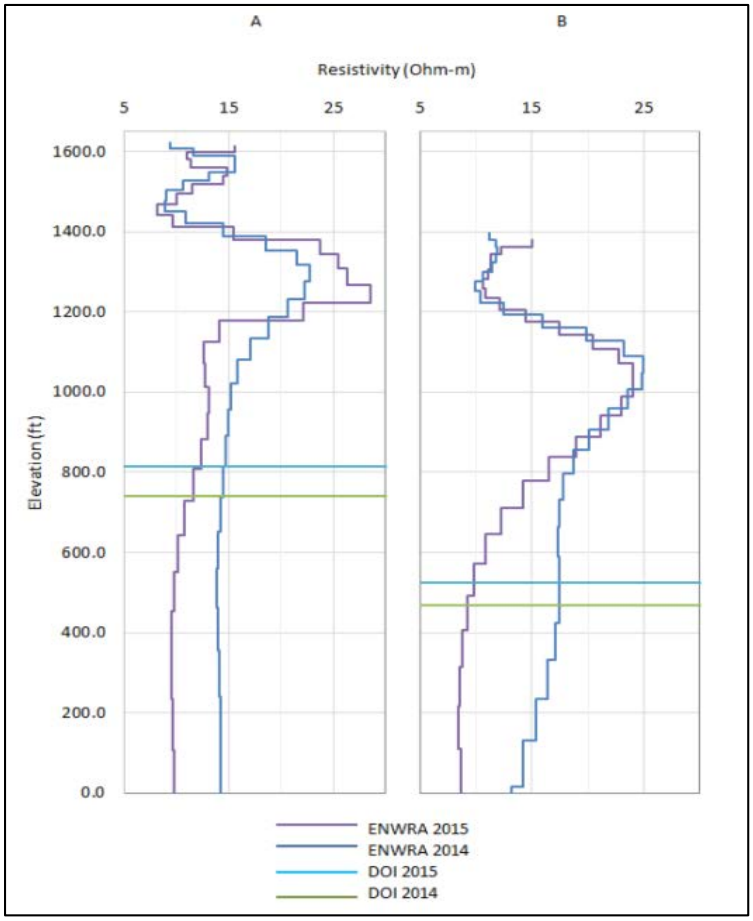



**Figure 5-56: Comparison of inverted model results between ENWRA 2015 and ENRWA 2014 at two locations. Depths of investigations for each survey are shown.**

### *5.3.5.1 Studies in the Lower Platte South and Nemaha NRDs*

***Dwight-Valparaiso-Brainard Area***

In August 2013, XRI conducted an AEM survey totaling 827 line-miles over three separate flight blocks in southern Butler and Saunders Counties, NE which resulted in a hydrogeological framework of the area between the towns of Dwight, Brainard, and Valparaiso. The survey implemented the SkyTEM 304 system, which was flown at a line spacing of approximately 700 ft, with some deviation in areas due to flight planning around infrastructure. Several tie-lines connected the 3 blocks to characterize the subsurface between the areas of interest. The purpose of the study was to assist the LPSNRD in groundwater management planning in the northwest part of the district. In addition to the airborne survey, ground-based time-domain electromagnetic data were acquired at four sounding locations for AEM data quality assurance. The flight blocks were planned in areas where known aquifer resources existed, but where extent and thickness of the aquifer materials was uncertain.

The survey revealed the extent and of two buried, east-trending paleovalley aquifers separated by a bedrock high of *Kc and Kgg* units in the north (Brainard) and south (Dwight) flight blocks, as well as an area of a more extensive shallow, resistive material across the east block (Valparaiso). The paleovalley

aquifer materials revealed in the north and south flight blocks in this survey were overlain by extensive intervals of more conductive material, comprised of till and loess. This contrasted considerably with the shallow, resistive deposits present near the land surface in the eastern block. In the north and south blocks, the aquifer is primarily confined, with the exception of near surface drainages, and is generally unconfined in the east block north and east of Valparaiso. The high density of flight lines allowed for development of a hydrogeologic framework from which voxel volumes could be constructed and used to estimate the volume of groundwater in storage beneath the survey area. Cumulatively, between the three areas, the survey estimated that nearly 884,000 ac-ft of water is present in the aquifer materials beneath the survey area with assumed specific yield of 0.15 based on work from Summeride et al. (2005). The study also revealed that resistive material is present near the upper contact of the *Kd*, which indicates areas where productive aquifer material is present. Some areas of the resistive material in the *Kd* underlie basal resistive deposits of the paleovalley aquifers, which are areas where hydrologic communication between the bedrock and overlying unconsolidated aquifers could exist. Results indicated the presence of aquifer materials in paleovalleys, aquitard thickness, potential groundwater recharge areas, connectivity of surface water and groundwater, and Cretaceous bedrock topography (Carney et al., 2014).

Three individual model locations were compared between the Spring 2015 survey and the Dwight-Valparasio-Brainard survey. The locations of these models are shown in Figure 5-55 while the models are compared in Figure 5-57. These models compare very well at all depths.

***Sprague***

The Sprague area (approximately 8 miles southwest of Lincoln, NE) overlies a paleovalley aquifer that is mantled by thick glacial deposits (gold area on Figure 5-54). Korus et al. (2012) demonstrated that major hydrostratigraphic boundaries in the upper 160 ft to 260 ft of the subsurface could be interpreted from HEM data in this geological setting. The results of the pilot study at Firth prompted resource managers to extend the study area to the west around the town of Sprague in southeastern Lancaster County. The primary goal of this study was to better understand the hydrostratigraphic framework and to address groundwater quality and quantity issues in the vicinity of Sprague, which overlies the western portion of the Crete-Princeton-Adams Groundwater Reservoir of the Lower Platte South Natural Resources District.

A frequency-domain HEM survey was conducted over the Sprague area in April and May of 2009. Detailed specifications of the survey are contained in Smith et al. (2011). The survey consisted of 44 east-west traverses with approximately 918 ft spacing, 5 north-south tie lines with variable spacing, and one southwest-northeast tie line for a total of 674 line miles. In addition, 4 east-west traverses were flown through parts of the 2007 Firth HEM flight area to tie the two surveys together.

The bedrock surface elevation and geometry of the lower aquifer material from the HEM results indicated that the paleovalley is not a continuous west-east feature through the study area as previously thought. Rather, the bedrock surface consists of a series of generally north-south trending highs and lows. The sedimentary fill of the paleovalley is complex. Sand and gravel bodies comprising the lower aquifer are discontinuous and their thicknesses are highly variable. In some areas the entire thickness of

the paleovalley fill appears to have been removed by erosion beneath overlying, channelized deposits. Materials comprising the upper aquifer are also highly complex. These shallow sands are much more wide-spread west of Highway 77 and are in hydraulic connection with the underlying lower aquifer throughout much of this area. This area therefore has a higher potential for groundwater recharge and greater vulnerability to contamination than areas east of Highway 77. Another important implication of this study is that Spring Creek is likely in hydraulic connection with the upper aquifer material for approximately half of its length.

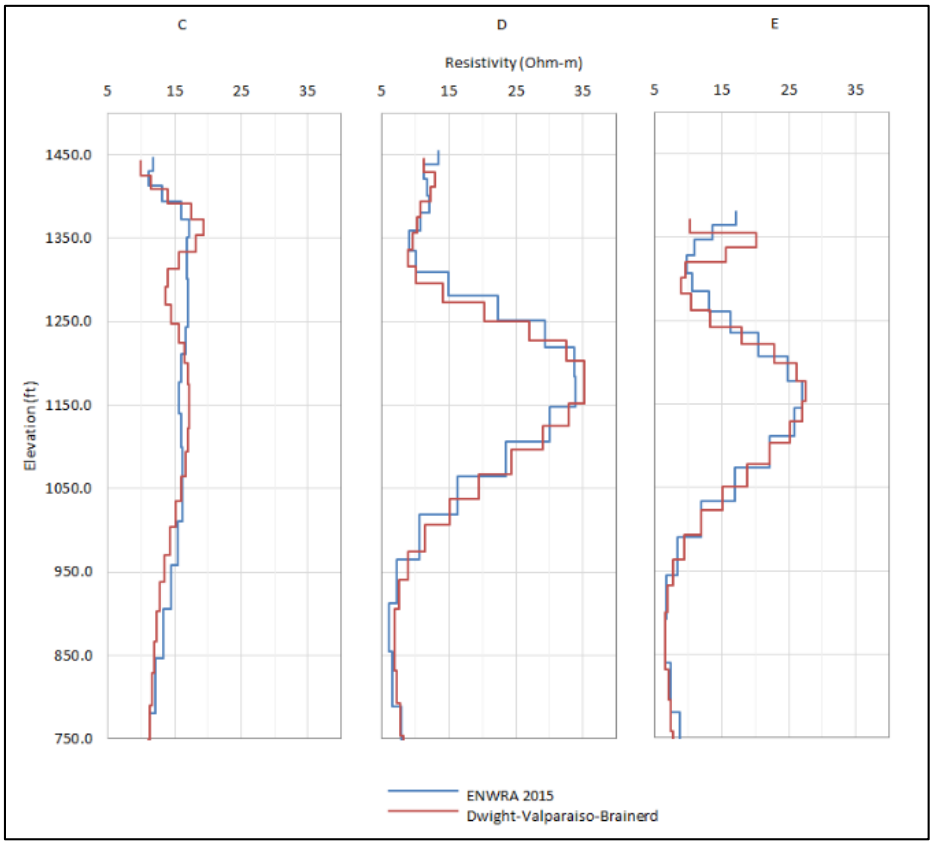



**Figure 5-57: Comparison of inverted models between the ENWRA 2015 survey and the Dwight-Valparaiso-Brainard surveys.**

***Firth***

The Firth site, which is located adjacent to the Sprague area, also overlies the buried paleovalley aquifer beneath southern Lancaster County that extends northwest to southeast across the southern LPSNRD and parts of the northern NNRD. The paleovalley aquifer is mantled by thick glacial deposits across much of the area. The Firth airborne survey area straddles the LPSNRD and NNRD boundary, which divides the study area approximately in half (olive green area on Figure 5-54). Korus et al. (2012) demonstrated that major hydrostratigraphic boundaries in the upper 160 to 260 ft of the subsurface could be interpreted from HEM data in this geological setting.

A helicopter electromagnetic (HEM) and magnetic field survey was conducted over the Firth study area in March, 2007 (Korus et al., 2013). Resistivity-depth sections with approximately 3 to 50 ft vertical

resolution and 10 ft horizontal resolution were produced. Detailed specifications of this survey are contained in Smith et al. (2008). The survey consisted of 52 east- west traverses with approximately 918 ft spacing and two north-south tie lines with approximately 3.7 mile spacing for a total of approximately 246 line miles flown. Apparent resistivity values were derived at six separate frequencies and were later transformed into resistivity-depth values using inversion algorithms as described in Smith et al. (2011).

The HEM resistivity patterns in the immediate vicinity of test holes and monitoring wells indicated that major aquifer/aquitard contacts can be correlated between borehole locations using a 20 ohm-m contour as a guide. Hydrostratigraphic unit contacts on resistivity-depth profiles were digitized, each contact elevation was interpreted, and the thicknesses of aquifers and aquitards were calculated. A multi-layer aquifer system with both small- and large- scale discontinuities was identified. The lower aquifer, which is largely confined, is connected to two areas of unconfined conditions that serve as sources of recharge. This framework revealed areas of potential aquifer vulnerability to overdevelopment and contamination. The HEM survey was able to characterize the hydrogeology in complex glaciated settings such as at Firth.

The high resistivity materials comprising the lower aquifer are continuous from north to south for nearly 6 miles and from east to west for over 4 miles. The lower aquifer is interpreted as a single hydrostratigraphic unit, but the geometries and lithologies of the materials from which it is composed suggest that it actually consists of distinct lower and upper sediment bodies. The lowermost body consists of sands and gravels of the Dorchester-Sterling paleovalley fill, the base of which lies between 1017 ft and 1181 ft asl in elevation. Gravels within this body include clasts of granite and potassium feldspar derived from the Rocky Mountains to the west (Stanley and Wayne, 1972). The upper sediment body, in contrast, consists of sands and gravels that do not appear to be genetically related to the paleovalley deposits. The base of the upper body lies between 1,279 ft and 1,312 ft asl in elevation. It is not constrained to the bedrock low in which the underlying paleovalley sediments were deposited. Rather, the upper sediment body overlies a bedrock high south of the paleovalley and its base lies at roughly the same elevation as the top of the paleovalley fill. The upper body contains granules and pebbles of red metaquartzite and dark-colored igneous and metasedimentary rocks, the origin of which is typically considered to be glacial (Stanley and Wayne, 1972). The juxtaposition of these two sediment bodies in the valley of the Middle Branch of the Big Nemaha River, however, provides a hydrologic connection and makes them indistinguishable in HEM profiles.

The Firth study highlighted several limitations of frequency-domain HEM (FDHEM): (1) the depth of investigation of FDHEM is relatively shallow and may not be sufficient to fully penetrate the primary aquifers of southeastern Nebraska; (2) thick, fine- grained glacial deposits may further reduce the depth of investigation, and (3) interpretation of the data is non-unique, so it must be accompanied by detailed lithologic, stratigraphic, hydrochemical, and hydraulic head data from multiple test holes and monitoring wells.

### *5.3.5.2 Studies in the Lower Platte North NRD*

***Ashland***

As part of the ENWRA, a FDHEM geophysical investigation was conducted in conjunction with subsurface data to map the hydrostratigraphy of the Platte River valley and adjacent uplands near Ashland, NE (black area on Figure 5-54). The HEM survey was performed over 36 square-mile study area, with the approximately western half of the survey within the LPNNRD, and a small segment along the southern edge of the flight area in the LPSNRD (approximately 0.6 $mi^2$). The eastern half of this HEM study was within the PMRNRD and is discussed in Volume I of this report. Specific data sets generated during the HEM survey at the Ashland site can be found in Smith et al. (2008). The survey was conducted in March 2007 on a flight line spacing of approximately 890 feet and the helicopter flew at a height of approximately 115 ft above the ground surface. Flight elevations were determined by onboard GPS and final ground elevations were corrected using differential GPS. Ground surface elevation errors are expected to be on the order of ± 6.5 ft. The survey used six frequencies, ranging from 400 Hz to 114,000 Hz and individual soundings were acquired at 11 ft intervals. The higher electromagnetic frequencies have shallow penetration depths whereas the lower frequencies can penetrate deeper into geological materials.

Following completion of the inversion, CSD compared the results of particle size analysis, borehole geophysics, and hydrochemistry from test holes and monitoring wells installed during the study to the inverted HEM profiles. In addition, CSD used registered groundwater wells, oil and gas borehole logs, and other pre-existing data that were not used in the inversion process. Hydrostratigraphic unit contacts were identified using subsurface data. Where these contacts correlated to contrasts in resistivity, the contacts were traced along HEM profiles. In some cases, there was no resistivity contrast at the unit contact (i.e. between sand/sandstone or sandstone/limestone). Therefore, only borehole data were used for correlation.

Hydrostratigraphic units were interpreted using earth resistivity models from the FDHEM survey and subsurface data, including CSD test holes, NGOCC deep oil and gas well logs, and registered well logs. Deposits of highly conductive materials (clay and silt) 80 to 100 ft thick limited the effectiveness of the HEM results for hydrostratigraphic mapping in the uplands. However, hydrostratigraphic units in recent and abandoned alluvial deposits of the Platte River, even where covered by 10-15 ft of fine sediments, could be mapped in detail using the FDHEM survey results. The investigation showed that the Platte River and Quaternary aquifer materials are apparently connected hydrologically throughout the study area and that the Quaternary and *Kd* aquifers can be hydrologically connected except where the discontinuous aquitard strata in the *Kd* separates them.

Interpretive cross-sections drawn with the use of the available subsurface data and the HEM survey results show the relationships between subsurface hydrostratigraphic units. A cross-section drawn in the northern section of the Ashland HEM area shows up to approximately 175 feet (53 m) of Quaternary sediment and Cretaceous rock overlying Pennsylvanian bedrock. The area immediately adjacent to the modern day Elkhorn and Platte River channels is surrounded by Quaternary aquifer material. Quaternary fine material (aquitard) is found at the land surface along the edges of the Platte River valley and

covering the Todd Valley. Within the Platte River valley, Quaternary aquitard material is comprised of overbank alluvium fines, but the Q fines mantling the Todd Valley is primarily loess. The alluvium within the Platte River valley in most locations coarsens with depth. Throughout most of the Ashland HEM area, the Platte River valley alluvium directly overlies *Kd* except for a small area east of the active Platte River channel where aquitard of the *Kd* is present. Through most of this portion of the Platte River valley the Quaternary aquifer materials and the *Kd* units are hydrologically connected. Underlying the *Kd* units are low resistivity Paleozoic shale.

A cross-section along a southeastern flight line shows that a small remnant of *Kd* underlies the Todd Valley and the far western edge of the Platte River valley. To the west of the Todd Valley, Wahoo Creek valley is underlain by Quaternary aquitard material. There is only a remnant of Quaternary aquifer material below the Todd Valley on the western side of the survey line. Pennsylvanian strata is found directly under the Quaternary aquifer deposits beneath much of the valley.

***Swedeburg***

A FDHEM survey was conducted over a 28 square mile study area around Swedeburg in Saunders County in April and May of 2009 (purple area on Figure 5-54). Detailed specifications of this survey are contained in Smith et al. (2011). The survey consisted of 30 southeast-northwest traverses with approximately 918 ft line spacing, and four southwest-northeast tie lines with variable spacing for a total of 190 miles.

The objective of this study was to better understand the hydrostratigraphic framework in the vicinity of Swedeburg, NE. The HEM profiles of the Swedeburg area show, approximately, the top approximately 200 ft of the subsurface. Except in the southwestern-most part of the study area, this 200 ft is sufficient to image the entire thickness of Quaternary deposits and the top of bedrock.

An upper resistive unit was defined based on comparison between CSD test holes and FDHEM data. The upper resistive unit consists of both unconsolidated Quaternary deposits and consolidated *Kd* bedrock. The upper resistive unit appears to consist of aquifer materials in most locations, but at other localities, the *Kd* consist of materials that have poor aquifer properties such as shale and clay. The saturated thickness of the upper resistive unit is generally greatest on the north and west sides of the study area. Isolated areas of relatively thick saturation occur in T14N, R7E, section 26 and 34. The saturated thickness shown for section 34 occurs in unconsolidated Quaternary deposits. Much of the saturated thickness in section 26, however, occurs in fine materials with low transmissivity.

The use of resistivity values to map hydrostratigraphic units, however, appears to be limited to, approximately, the upper 82 ft of the subsurface. Below this depth, lithology and resistivity do not appear to have a consistent relationship. The inability to use FDHEM to map units at this depth may be attributed to the effects of groundwater salinity on FDHEM, the limited resolution of the HEM data at depth, and the highly variable nature of lithology in the Quaternary deposits and in bedrock.

The resolution of FDHEM at depth was insufficient to map the aquifers occurring near the town of Swedeburg and in T14N, R7E, sections 20 and 21. Elevated TDS concentrations in shallow portions of the *Kd* were apparent on the HEM profiles though high TDS groundwater that occurs deeper than 200 ft

were not imaged. Scattered areas of potentially high groundwater recharge rates and vulnerability to contamination exist around the survey area, with the most continuous area occurring in the eastern Wahoo Creek valley. Hydrostratigraphic profiles under the creeks indicate that portions of the Wahoo Creek valley in the east part of the survey area are likely in hydrologic connection with the upper resistive unit. None of the other creeks in the survey area appear to have significant hydrologic connection with groundwater.

***Mead***

In October 2012, an airborne FDHEM and magnetic field survey occurred at the former Nebraska Ordnance Plant (NOP) in Mead, NE (Fugro, 2013a). The flight area is shown in green on Figure 5-54. The HEM geophysical survey was conducted to support the Groundwater Monitoring Program Optimization efforts in accordance with the *Helicopter Electromagnetic and Magnetic Geophysical Survey Work Plan, Former Nebraska Ordnance Plant, Mead, Nebraska* (ECC/GEO, 2012). The purpose of this project was to perform a FDHEM survey to map the electrical conductivity and subsurface properties at the former NOP. A helicopter-borne multi-coil, multi-frequency, electromagnetic system supplemented by a high-sensitivity cesium magnetometer was used to complete the survey. The survey mapped the subsurface properties in an area that covers existing former NOP groundwater plumes. In particular, the purpose of the survey was to map the geology, structure, and depth to bedrock of the area. Data were acquired using a Fugro RESOLVE electromagnetic system, supplemented by two high-sensitivity cesium magnetometers. Six frequencies were measured, nominally ranging from 400 Hz to 140, 000 Hz. The information from these sensors was processed to produce maps and images that display the magnetic and conductive properties of the survey area.

The inversion model results from the FDHEM survey provided a general understanding of the Todd Valley aquifer and the definition and location of the Platte Valley and Wahoo Valley boundaries (Fugro, 2013b). The FDHEM survey indicated highly conductive areas (Platte River valley and silty clay zone) and the occurrence of shale is visible at greater depths. Overall, a strong correlation was indicated between boring logs and the FDHEM survey with respect to the depth of the loess/overburden material. However, a poor correlation existed between individual log information for certain bedrock formations and the HEM inversion model cross sections pertaining to this bedrock unit. The potential explanations for this include error in the Z (vertical) field and lack of resistive contrast between sand and sandstone.

In general, the FDHEM survey data accomplished the following goals: 1) identifying the Wahoo Valley and Platte Valley boundaries; 2) identifying the silt and clay zones; and 3) estimating the loess and overburden thicknesses. The FDHEM survey did not provide additional resolution for the: 1) top of the upper bedrock intervals; 2) depth to the Paleozoic strata; 3) geochemical distribution and plume correlation; and 4) hydraulic conductivity or variations in the unconsolidated sands.

Future FDHEM surveys should include the removal of power lines and other cultural features from the data set to the extent possible and collection of additional geologic and hydrogeologic information for comparison to survey results.

## 5.4 Summary and Recommendations

### *5.4.1 Key AEM Survey Findings*

The AEM reconnaissance survey of the southern half of the ENWRA project area has provided information that have been used to develop a detailed interpretation of the subsurface hydrogeologic conditions at the variable flight line spacing and design utilized in this investigation. The AEM survey detected subsurface conditions well beyond 1,000 ft bgl and provided a characterization of the Quaternary system, the *Kd* (where present), and the Paleozoic system beneath southeastern Nebraska. The following list of items summarizes the findings resulting from this survey:

- General - Aquifer resources beneath the southern ENWRA project area vary considerably within the Quaternary system, and with the exception of the Platte River valley, aquifer materials, whether principal or marginal, are considerably more limited in areal extent as compared to the northern half of the ENWRA project area (Volume I). The distribution of aquifer material is also revealed in the pattern of irrigation wells in the project area, with the greatest density of wells being located in the LPNNRD and parts of the LPSNRD.

- LPNNRD - In the LPNNRD, the AEM survey provides a characterization of where the Platte River valley hosts a high density of irrigation wells, the Quaternary system is composed of widespread deposits of principal aquifer material, and in many locations, sand-rich principal aquifer materials. In the uplands south of the Platte River valley across the southern LPNNRD and northern LPSNRD, the Quaternary system primarily consists of marginal and aquitard materials, and in some areas, nearly the entire Quaternary sequence consists of aquitard materials. In the south central area of the southeastern half of the LPNNRD, a paleovalley is present that consists of upwards of 200 ft of principal aquifer deposits underlain by 100-200 ft of marginal and aquitard deposits. The hydrogeologic framework resulting from the AEM survey provides further insight into the width, thickness, and extent of this body of coarse deposits that are the eastward extension of the Dwight-Valparaiso aquifer present beneath the northwest corner of the LPSNRD (Druliner and Mason, 2001). In the far western area of the northwestern half of the LPNNRD, the principal aquifer consists of Quaternary deposits and *To* materials. On the eastern side of the district, the Todd Valley hosts sand-rich principal aquifer material through nearly the entire thickness of the valley, which exceeds 200 ft along flight line 300101. In the far southeast corner of the district, the Quaternary system is relatively thin compared to other sections of the LPNNRD and consists of interlayered marginal and principal aquifer material with variable degrees of saturation.

- LPSNRD - In the LPSNRD, the Quaternary system is variable in material thickness and texture, with a majority of the materials west of Lincoln consisting of marginal and aquitard deposits with isolated intervals of principal aquifer. The most extensive bodies of principal aquifer deposits are found in the northwest corner of the district where paleovalleys are underlain by aquitard and marginal aquifer deposits, and to the south of Lincoln where a paleovalley crosses

beneath the district with variable width, depth, and thickness. In the northwest, the principal aquifer material thickness ranges from 150 to 200 ft and underlies 100 to 200 ft of aquitard and marginal aquifer materials. South of Lincoln, the principal aquifer exceeds 250 ft in thickness near the LPSNRD-NNRD boundary. The unit thins westward, but is 150-200 ft thick near the LPSNRD-UBBNRD boundary. Immediately north of Lincoln, the Quaternary system is relatively thin, typically not exceeding 200 ft in thickness, and in many locations, less than 200 ft thick with variation in resistivity. This trend continues along the Salt Creek valley northeast of Lincoln, where less than 100 ft of interlayered marginal and principal aquifer materials comprise the local groundwater source. On the northern outskirts of Lincoln, low resistivity (conductive) intervals were detected in the shallow subsurface, which corresponds to high-TDS conditions in the shallow aquifer and surface water features. The source of these conditions has been attributed to seepage from a conductive area of the up-dipping *Kd* that is present less than 100 ft bgl in this area. East of Lincoln, the Quaternary system consists primarily of marginal aquifer and aquitard material ranging from 100 to 200 ft in thickness, with only isolated principal aquifer features, mostly overlying the underlying *Kd* and Paleozoic bedrock. The Quaternary system generally thins eastward, and along the easternmost flight line (400301), the AEM revealed that the Quaternary system is mostly marginal aquifer material ranging from 100 to 150 ft in thickness. Saturated thickness in this area is variable, ranging from areas where saturation approaches 100 ft, and in other locations, no saturated intervals are present.

- NNRD - Beneath the NNRD, the Quaternary system ranges from areas of thick paleovalleys in the northwest and north-central areas of the district to areas of only thin, unsaturated marginal aquifer and aquitard materials overlying Paleozoic bedrock. The AEM survey revealed insight into the structure of known palevalleys that exist beneath parts of Johnson, Nemaha, Gage, Otoe, and Lancaster Counties. The width of the valley can range from 1-2 miles in some areas to upwards of seven miles at other locations, with thicknesses exceeding 250 ft. In some areas of Johnson County, principal aquifer materials are present near the land surface and extend to near the base of the Quaternary system, a condition that provides greater potential for aquifer recharge. The trace of the paleovalley is also expressed in the distribution of irrigation wells in the area, as many areas of the NNRD lacking adequate principal or even marginal aquifer materials are completely devoid of irrigation wells. In the east-central area of the NNRD, the AEM survey revealed a thin distribution of marginal aquifer material with isolated areas of principal aquifer materials. Overall, the Quaternary system is less than 100 ft thick with variable saturated thickness in this area of the district.

- Cretaceous Strata *KcKgg* - The AEM survey detected the combined *KcKgg* beneath the western half of the LPNNRD and in the two flight lines in the northeast UBBNRD. The eastern margin of the *KcKgg* is detected along flight line 400301, where the unit's thickness ranges from approximately 50 to 125 ft. The *KcKgg* terminates between flight line 400301 and 400501. It is apparent that the flight lines will aid in refining the extent of the *KcKgg* as mapped by Burchett (1986). For example, along flight line 201301 (from the Fall 2014 flights), the AEM indicated isolated features of *KcKgg* in comparison to a continuous extent of the unit as indicated in the

1986 map, particularly in the area beneath the Platte River valley. Additionally, flight line 400301, where *KcKgg* has been mapped by the AEM, is beyond Burchett's easternmost extent of the *Kc* in this area. Thus slight modifications to the regional geologic map can be made in this area as well.

- Cretaceous Strata *Kd* - The full extent and thickness of the *Kd*, a secondary aquifer resource in eastern Nebraska, is revealed in the AEM survey of the southern ENWRA area. The southeastern terminus of this regionally extensive formation is evident in the AEM data, which also includes isolated remnants of the formation beyond the primary eastern *Kd* margin in the LPSNRD. The *Kd* ranges in thickness from nearly 600 ft beneath parts of the western LPNNRD to less than 40 ft along the margin of the formation. Very slight apparent dip to the west in the *Kd* is indicated along west-east flight lines in the LPNNRD, especially in comparison to the more pronounced slope indicated in the *Kd* as revealed in flight lines in the northern half of the ENWRA project area. The topographic expression of the *Kd* is generally flat beneath much of the southern ENWRA project area's western half, with more local relief ranging from 50 to over 100 ft in some areas in the eastern LPNNRD and LPSNRD. The depth to the top of the *Kd* ranged from over 900 ft in the northwestern half of the LPNNRD to less than 50 ft in some locations along drainages in the eastern LPNNRD and LPSNRD. The eastern fringe of the *Kd* is present along the NNRD-LBBNRD boundary and extends only a few miles beneath the NNRD along flight line 301101.

  The AEM data captured the variability in resistivity of the *Kd*, which provides an inventory of potential drill targets in this formation for bedrock aquifer development. Interpretation of the *Kd* was divided into three zones, with the areas of 20-40 and greater than 40 ohm-m revealing the most resistive sections of the unit, with the higher resistivities indicating sandstone with very minimal clay and silt content. Intervals of 20-40 ohm-m ranging from less than 100 ft to nearly 400 ft are present throughout much of the LPNNRD and the eastern half of the LPSNRD, some containing thinner intervals of 40 ohm-m or greater material. An area of expected high TDS water within the *Kd* is evident in the central LPSNRD (immediately north of Lincoln) where the *Kd* is relatively shallow and where high TDS surface water is detected in numerous wetlands and surface drainages. This area of the *Kd* extends westward along flight line 300701, but does not appear to extend north or south, as resistive intervals are found in the *Kd* within flight lines in both directions from this conductive area. The *Kd*, which hosts the Maha aquifer in eastern Nebraska, is a viable groundwater resource where the sandstone has suitable permeability and porosity. The likelihood of encountering intervals of potable water within the *Kd* with sufficient permeability and porosity is higher in intervals of highest resistivity. Thus, it is recommended that future drilling investigations targeting the *Kd* occur over locations above the intervals with highest resistivity in the *Kd*. In some locations where principal aquifer material of the Quaternary system sits atop of *Kd*, particularly in the *Kd*'s most resistive zones, hydraulic communication between the two aquifer sources could occur. Further analysis of local vertical head gradients as well as water quality samples would provide greater understanding of the relationship between the two aquifers in these areas.

- Paleozoic Strata - The AEM survey of the southern ENWRA project area revealed over 1,000 ft of Paleozoic strata beneath much of the surveyed locations, particularly in the eastern LPSNRD and most of the NNRD. Although undifferentiated in the interpretation in this report, the AEM data revealed considerable variability in the resistive nature of the Paleozoic deposits, from bodies with resistivities exceeding 30 ohm-m, to other strata with resistivity less than 10 ohm-m. Resistivities greater than 60 ohm-m are encountered along flight lines 401101 and 301501 in the southern NNRD that are associated with granite of the Nemaha Uplift. Depth to the Paleozoic sequences range from over 1,500 ft bgl beneath the northwestern half of the LPNNRD to only a few feet beneath overburden along gullies and valleys of the southern NNRD. Numerous Paleozoic outcrops are present across the NNRD and the parts of the LPSNRD. Although the Paleozoic units are not relied upon as a groundwater source over widespread areas of southeastern Nebraska, isolated wells are known to exist that tap Paleozoic strata for low yield wells. The AEM data can provide potential target areas for future exploration of groundwater resources in the region, particularly in resistive bodies. It is recommended that where known currently existing wells tap Paleozoic units, the resistivity of the subsurface from this study is evaluated with the well characteristics (depth, screened interval) to determine if any relationship exists between resistivity and the a well's production potential and water quality.

  The AEM survey revealed several structural features in the Paleozoic system beneath the southern ENWRA survey area, including faults and dipping strata associated with the TRSZ and resistive zones the Nemaha Uplift and Elk Creek Carbonatite complex. These features are identified in the AEM profiles by vertical or near-vertical offsets in the Paleozoic strata as indicated by abrupt changes in resistivity. The Union and Humboldt Faults are evident on several AEM profiles, and tilted strata are clearly evident along flight line 401101. The basement rock of the Nemaha Uplift, consisting of Precambrian granite, is also evident along flight line 401101 and 301501. This uplift, which also hosts the Elk Creek Carbonatite, is indicated as a large resistor immediately west of the Humboldt Fault. Although interpretation of Paleozoic features was beyond the purview of this project, the depth and detail revealed within the Paleozoic sequence can allow for refined interpretation of regional structure, as well as identifying possible sources for groundwater exploration in southeast Nebraska, particularly along faults.

- Flight Line Grid Spacing - The variable grid spacing across the southern ENWRA project area provided insight and information on a regional scale, allowing for greater understanding of where future investigations could potentially provide more detailed characterization of the subsurface. Due to the larger population centers and infrastructure, along with areas of particular interest from ENWRA, the design of the survey lines was more variable as compared to the more gridded design of the northern ENWRA survey area conducted in the Fall of 2014 (Volume I). Denser grid spacing is required for smaller, specific water supply projects such as the survey conducted for the Dwight-Valparaiso-Brainard area within the LPSNRD (Carney et. al, 2014). This survey, located in the northwestern LPSNRD, provides an example of the benefits of tightly spaced flight lines in defining paleovalleys, bedrock highs, and the connection of principal aquifer materials with local surface water features. Volume I of this final survey report provides

an additional example of the importance of flight line spacing with characterizing buried paleovalleys in the Clarkson/Howells area of the southern LENRD.

Only local scale flight line density provides the detail in the subsurface information suitable to create 3D voxel models of aquifer features. The previous example from the Clarkson, NE area demonstrates how densely collected data provides the ability to estimate the aquifer material volume and estimates of groundwater in storage. Without closely spaced flight lines providing fine detail of the subsurface, it is not recommended that these volume and storage calculation be made.

### *5.4.2 Applicability and Recommendations Regarding Future Groundwater Investigations*

The hydrostratigraphic framework resulting from the AEM reconnaissance survey provides a database of information on the geologic characteristics of materials hosting groundwater resources available beneath the southern half the ENWRA project area. The survey of the southern half of the ENWRA area reveals the contrast in the subsurface character beneath southeastern Nebraska in comparison to the northern half of the ENWRA project area. The irregularly shaped flight line layout was necessitated by the presence of population centers and infrastructure as well as the presence of known subsurface targets such as previously mapped paleovalleys and structures in the Paleozoic system. The resulting datasets from this survey provide readily useable information for managers from multiple NRDs in southeast Nebraska. Although the flight line pattern undoubtedly misses some local subsurface features, the framework provided from the AEM survey helps further characterize major subsurface trends, information from which can help identify areas where future surveys with more densely spaced flight lines can be conducted to assess localized hydrogeologic conditions. Such information can include the type of aquifer material present (if any), the depths to the aquifer top and base, as well as the thickness of the intervals of interest. For example, a tighter spaced grid could along the Dorchester-Sterling paleovalley in the northern NNRD could provide detailed control of the paleovalley's structure and volume of groundwater in storage, as well as identify locations where the aquifer could be vulnerable to contamination where overlying marginal or aquitard material is thin to absent. In regards to non-aquifer materials, the extent and thickness of these deposits is also provided in detail in the AEM data, which can assist in planning locations for managed groundwater recharge projects or developing groundwater quality protection plans (i.e. wellhead protection plans, best management practices for application of agri-chemicals). Additionally, for non-water development needs, the AEM survey data can be utilized to assess current or locate future sand and gravel mining operations in southeast Nebraska.

In regards to principal aquifer materials, particularly in the extensive paleovalleys where sediments are relatively thick and provide ample yields to irrigation wells, the lithologic character distributions based on resistivity as indicated in Figure 5-8 can also provide preliminary estimated ranges of hydraulic conductivity (*k*) for each of the aquifer materials. For the non-aquifer/aquitard category, which is predominately till, silt/loess, and clay, *k* values could range from $2.8 \times 10^{-6}$ feet per day (ft/d) to $2.8 \times 10^{-1}$ ft/d. For the marginal aquifer materials, much of the material distribution is similar to the aquitard material, with the exception of a larger interval of coarse material (nearly 15 percent). Thus, *k* values could be expected to increase in these areas toward the range of 1-3 ft/d where coarse materials are

present. For the principal aquifer, more expanded areas of *k* values ranging from 30 to nearly 300 ft/d could be present. For areas of the principal aquifer with resistivity over 50 ohm-m, especially where well-sorted gravel is present, *k* values could exceed 1,000 ft/d. For this condition to occur, however, the gravel would need to be angular and well-sorted with a minimal component of sand or silt in the matrix (Fetter, 1994). Specific yield values in the sand-rich portion of the principal aquifer could range from 0.21 to 0.27, with values of the parameter ranging from 0.02 to 0.18 in clay, silt, and sandy clay deposits that are predominant in the marginal aquifer and aquitard materials (Johnson 1967). For the *To* portion of the principal aquifer, *k* values can range from 1 to 50 ft/d, with specific yield values ranging from less than 0.01 to 0.3 (Gutentag, et al. 1984).

Helgesen and others (1993) report transmissivity within the *Kd*/Maha aquifer beneath the project area ranging from approximately 7,500 to 75,000 gpd/ft (converted from reported values of 1,000 to 10,000 $ft^2/d$). With an assumed thickness of 500 ft, these transmissivity values would equate to a *k* range of 2 to 20 ft/d, with the higher values of this range likely occurring in the more resistive intervals of the *Kd* identified in the interpretive profiles of Appendix 1. These reported values are only estimates of the *k* that could be encountered in the *Kd*, and it is highly recommended that aquifer tests and other geophysical methods be implemented to specifically characterize local conditions in this bedrock aquifer source.

To more accurately characterize the physical parameters of the Quaternary aquifers and Cretaceous resistive intervals, as well as for further verification of the lithologic-resistivity relationship described in section 5.2.4, it is recommended that sonic cores are acquired to obtain specific lithologic samples that are minimally altered by drill bits or drilling mud. This would provide undisturbed core of the subsurface with only minimal disturbance of fine material that is normally lost during mud-rotary drilling. Following retrieval of the core, implementation of a calibrated, full-suite geophysical log is recommended. The resulting data would provide specific resistivity and gamma log data that could be more reliably correlated with the lithology present at that interval. Additionally, nuclear magnetic resonance (NMR) technology could be utilized to characterize porosity and permeability of the materials encountered at the location of interest. It is possible that a sonic core could provide tighter constraints on the resistivity ranges, particularly with the maximum and minimum ranges for glacial till and sand. If the fines are lost in the mud rotary-based drill hole, it would be nearly impossible to assess the quantity of fines in these intervals identified as till or sand, which would thus result in erroneous lithologic characterization, even if those intervals resulted in lower than expected resistivities from the geophysical log for that lithology type.

It is also recommended that sonic coring efforts focus on a location where bedrock resistors are present, particularly in the *Kd*, ideally with one in the northwest portion of the project area where less resistive intervals were detected in the AEM as well as higher resistive areas in the eastern half of the project area. A core would provide beneficial insight into the understanding of the cause of the higher conductive areas in the *Kd*, which could be related to lithologic or pore water characteristics. Sonic core data can also provide insight into the nature of the resistive intervals revealed in the Paleozoic strata.

Based on the experience and knowledge gained from this effort, the following preliminary recommendations are presented to guide future investigations in support of groundwater characterization and management in eastern Nebraska. They are as follows:

- Additional AEM surveys can now be conducted in areas where the reconnaissance survey located potentially extensive zones of sand-rich, principal aquifer materials. Examples of these locations include, but are not limited to:
    - The Dorchester-Sterling paleovalley aquifer in the southern LPSNRD and northern NNRD;
    - The west-east paleovalley in the southern LPNNRD;
    - The character of the Platte River valley aquifer materials. A survey of this valley at a tightly-spaced flight line pattern could help identify and assess the structure of the valley, recharge areas, and estimates of groundwater volumes in storage; and
    - The paleovalley indicated along flight line 300501 in northeast Richardson County in the NNRD.

- AEM surveys can assist in characterization of features in the *Kd* bedrock, including, but not limited to:
    - The area of the *Kd* in the northwest LPSNRD showing low resistivity that appears to contribute high-TDS water to the overlying thin Quaternary deposits north of Lincoln; and
    - Further delineation of the high resistivity intervals (20 ohm-m or greater) in the eastern LPSNRD and LPNNRD, particularly in areas where resistive *Kd* underlies Quaternary principal aquifer materials, which are locations where interaction of groundwater in the two subsurface groundwater resources can occur.

- The connectivity between groundwater and surface water features along the streams and rivers within the project area is not well understood at all locations, particularly in areas where high densities of irrigation wells exist. The addition of a near-surface, high resolution AEM streambed mapping program of the riparian areas is recommended. This data would provide finer detail of the lithology of these critical areas, and more precisely characterize the extent and shape of the aquifers and aquitards that affect hydrologic connection to streams. This is of particular importance in the narrow stream valleys in the NNRD where alluvium volume is limited.

- A tightly-spaced AEM flight line grid in the area northeast of Lincoln of the shallow subsurface, to complement an investigation of the *Kd* beneath this area, could further characterize the extent of the areas affected by the high-TDS groundwater in the shallow subsurface, which can assist in planning and development of new groundwater resources in the rapidly growing areas of suburban Lincoln.

- For locations where the target of the investigation involves localized aquifer features, a tighter grid spacing is recommended, on the order of 600 to 1,500 ft flight line separation. Surveys of

this scale will allow for creation of 3D voxel models of aquifer materials, from which calculations of aquifer volume and groundwater in storage can be made, which can provide NRD managers greater insight into the quantity of groundwater available in the area of interest.

- A CSD test hole program that includes penetration through the *Kd*, ideally in the areas where the most extensive *Kd* resistors were detected in the AEM survey. Following drilling and lithologic analysis, interval-specific water quality testing and assessment of potential well yield via aquifer tests is recommended. It is suggested that future test hole locations be selected with knowledge gained from the AEM survey.

- A similar test hole program to explore the conductive zones within the Paleozoic system present beneath the LPSNRD and the NNRD that were detected in the AEM survey. Such a program could further the understanding of the presence of fluids in the Paleozoic system and potential for groundwater development. Such a program should include drilling and lithologic analysis, interval-specific water quality testing (including age dating), and assessment of potential well yield via aquifer tests is recommended. It is suggested that future test hole locations be selected with knowledge gained from the AEM survey.

- The AEM survey identified areas along the flight lines where a greater probability of groundwater recharge is likely to occur. A high resolution AEM survey of these areas would quantify the geographic extent of these areas and the hydrologic connection to the subsurface. This information could then be used to specifically site recharge studies in known locations that provide the greatest benefit to understanding the meteoric contribution to the water balance of locations of interest within the ENWRA area.

- Utilize aquifer characterization techniques in conjunction with the AEM survey flight lines to improve the understanding of important changes in hydraulic conductivity, storage, and yield. This information can then be used directly with future groundwater modeling endeavors to improve model calibration and predictive capability.

# 6 Description of Data Delivered

The geophysical and borehole electronic data are included as Appendix 4. Electronic interpretation results are also included.

Table 6-1 describes the data columns in the .xyz file EM_20150428_Nebraska_Final01.xyz. This file contains the raw geophysical data, including magnetic, as supplied directly from SkyTEM. The result of the SCI is included in xyz files and ENWRA2015_SCI_Results.xyz and the data columns of these databases are described in Table 6-2. The borehole data used to constrain the SCI inversion and to assist in the interpretation of the inversion results are included in the files listed in Table 6-3. Each type of borehole information has both a collar file containing the location of each of the wells, and a second file containing the borehole data for the individual wells. The data column descriptions for the collar files are listed in

Table 6-4. Table 6-5 describes the channels in all of the borehole data files as well as indicates which type of data contains each channel. The various interpretation results are included in data files ENWRA_south_AEMData_Interpretation.xyz. Table 6-6 describes the data columns of those files.

In addition to the data delivered in .xyz format, Google Earth .kmz files were created to view the geophysical AEM flight line locations, and interpreted geologic data. Unique .kmz files were created for each individual flight line, as well as a .kmz file for all flight lines. Within the .kmz file, the AEM flight line is shown, as well as place marks at each location where there are interpreted geologic results. The attribute data for each unique place mark contains information, including the top elevations of various geologic units, the presence of aquifer material, and the top elevation of the water table. These .kmz files are located within the "ENWRA_2015" folder. The file "read_me.txt" provides instructions in regards to the "Settings" changes that may need to be made in Google Earth, and how to use the .kmz files in Google Earth. A Microsoft Word document is also included, which serves as a legend for the attributes in the .kmz files.

**Table 6-1: Channel name, description, and units for EM_20150428_Nebraska_Final01.xyz with EM, mag, DGPS, Inclinometer, altitude, and associated data.**

| Parameter | Description | Unit |
|---|---|---|
| FID | Unique Fiducial Number | Seconds |
| LINE | Line Number | LLLLLL |
| FLIGHT | Name of Flight | yyyymmdd.ff |
| DATETIME | DateTime Format | Decimal days |
| DATE | DateTime Format | yyyymmdd |
| TIME | Time | hhmmss.sss |
| ANGLEX | Angle (in flight direction) | Degrees |
| ANGLEY | Angle (perpendicular to flight direction) | Degrees |
| HEIGHT | Filtered Height Measurement | Meters [m] |
| LON | Longitude, WGS84 | Decimal Degrees |
| LAT | Latitude, WGS84 | Decimal Degrees |
| E | Easting, NAD83 UTM Zone 13N | Meters [m] |
| N | Northing, NAD83 UTM Zone 13N | Meters [m] |
| DEM | Digital Elevation | Meters [m] |
| ALT | DGPS Altitude | Meters above sea level |
| GDSPEED | Ground Speed | Kilometers/hour [km/h] |
| CURR_2 | Current, Low Moment | Amps |
| CURR_1 | Current, High Moment | Amps |
| LMZ_G01 | Normalized (PFC-Corrected) Low Moment Z-RxCoil value | pV/($m^4$*A) |
| HMZ_G01 | Normalized (PFC-Corrected) High Moment Z-RxCoil value | pV/($m^4$*A) |
| LMX_G01 | Normalized (PFC-Corrected) Low Moment X-RxCoil value | pV/($m^4$*A) |
| HMX_G01 | Normalized (PFC-Corrected) High Moment X-RxCoil value | pV/($m^4$*A) |
| BMAG_RAW | Raw Base Station Mag Data | nanoTesla [nT] |
| DIURNAL | Diurnal Mag Data | nanoTesla [nT] |
| MAG_RAW | Raw Mag Data | nanoTesla [nT] |
| MAG_COR | Mag Data Corrected for Diurnal Drift | nanoTesla [nT] |
| PLNI | Power Line Noise Intensity monitor | C*V/sqrt(Hz) |
| X_ft | Easting, NAD83 UTM Zone 13N | Feet [ft] |
| Y_ft | Northing, NAD83 UTM Zone 13N | Feet [ft] |

**Table 6-2: Channel name, description, and units for ENWRA2015_SCI_Results.xyz with EM inversion results.**

| Parameter | Description | Unit |
|---|---|---|
| X_ft | Easting NAD83, UTM Zone 14 | Feet [ft] |
| Y_ft | Northing NAD83, UTM Zone 14 | Feet [ft] |
| X_m | Easting NAD83, UTM Zone 14 | Meters [m] |
| Y_m | Northing NAD83, UTM Zone 14 | Meters [m] |
| TOPO | Topography | Feet [ft] |
| FID | Unique Fiducial Number | |
| LINE | Line Number | |
| ALT | Altitude | Feet [ft] |
| INVALT | Inverted Altitude | Feet [ft] |
| INVALTSTD | Inverted Altitude Standard Deviation | |
| DELTAALT | Change in Altitude | Feet [ft] |
| NUMDATA | Number of data points | |
| RESDATA | Residual of individual sounding | |
| RESTOTAL | Total residual for inverted section | |
| DOI_LOWER | Less conservative estimate of DOI | Feet [ft] |
| DOI_UPPER | More conservative estimate of DOI | Feet [ft] |
| RHO_I_1 THROUGH RHO_I_30 | Inverted resistivity of each later | Ohm-m |
| RHO_I_STD1 THROUGH RHO_I_STD2 | Standard deviation of inverted resistivity | |
| SIGMA_I_1 THROUGH SIGMA_I_30 | Conductivity | mS/m |
| DEP_BOT_1 THROUGH DEP_BOT_29 | Depth to the bottom of individual layers | Feet [ft] |
| DEP_TOP_1 THROUGH DEP_TOP_30 | Depth to the top of individual layers | Feet [ft] |
| THK_1 THROUGH THK_30 | Thickness of individual layers | Feet [ft] |

**Table 6-3: Files containing borehole information.**

| Database | Description |
|---|---|
| CSD2015ELogs_Collar.xyz<br>CSD2015ELogs _Data.xyz | Electrical logs from CSD wells |
| DNR2015Lith_Collar.xyz<br>DNR2015Lith_Data.xyz | Lithology logs from DNR wells |
| CSD2015Lith_Collar.xyz<br>CSD2015Lith_Data.xyz<br>CSDAddendumLith_Collar.xzy<br>CSDAddendumLith_Data.xyz | Lithology logs from CSD wells |
| CSD2015Strat_Collar.xyz<br>CSD2015Strat_Data.xyz | Stratigraphy logs from CSD wells |
| GP-logs-inv-constrain_Collar.gdb<br>GP-logs-inv-constrain_data.gdb | Geophysical logs used to constrain the SCIs |
| NOGCC2015GP_Collar.xyz<br>NOGCC2015GP _Data. xyz | Geophysical logs from the oil and gas wells |
| NOGCC2015GPLith_Collar.xyz<br>NOGCC2015GPLith_Data.xyz | Lithology logs from the oil and gas wells |
| NOGCC2015GPStrat_Collar.xyz<br>NOGCC2015GPStrat_Collar.xyz | Stratigraphy logs from the oil and gas wells |

**Table 6-4: Channel name, description, and units for collar files.**

| Parameter | Description | Unit |
|---|---|---|
| DH_Hole | Name of individual boreholes | |
| DH_East | Easting of boreholes, NAD83, UTM Zone 14 | Feet [ft] |
| DH_North | Northing of boreholes, NAD83, UTM Zone 14 | Feet [ft] |
| DH_RL | Elevation of top of borehole | Feet [ft] |
| DH_Dip | Dip of borehole | Degrees |
| DH_Azimuth | Azimuth of borehole | Degrees |
| DH_Top | Depth to top of borehole | Feet [ft] |
| DH_Bottom | Depth to bottom of borehole | Feet [ft] |
| DH_ZMin | Minimum elevation in borehole | Feet [ft] |
| DH_ZMax | Maximum elevation in borehole | Feet [ft] |

**Table 6-5: Channel name description and units for borehole data.**

| Parameter | Description | Unit | Type of Log |
|---|---|---|---|
| DH_East | Easting of boreholes, NAD83, UTM Zone 14 | Feet [ft] | All |
| DH_North | Northing of boreholes, NAD83, UTM Zone 14 | Feet [ft] | All |
| DH_RL | Elevation of top of borehole | Feet [ft] | All |
| DH_From | End of interval | Feet[ft] | Strat, Lith |
| DH_To | Start of interval | Feet [ft] | Strat, Lith |
| DH_Strat_Code | Code used to indicate type of stratigraphy | | Strat |
| DH_Soil_Code | Code used to indicate type of lithology | | Lith |
| DH_Description | Description of stratigraphy or lithology | | Strat, Lith |
| DH_Depth | Depth | Feet [ft] | GP |
| DH_SP | Self Potential | milliVolt [mV] | GP, E, Geo |
| DH_SN | Short Normal Resistivity | Ohm-m | GP |
| DH_SFL | Spherically Focus Log | Ohm-m] | GP |
| DH_ILD | Induction Log Deep | Siemens/m [S/m] | GP |
| DH_ILM | Induction Log Medium | Siemens/m [S/m] | GP |
| DH_LAT | Laterolog | Ohm-m | GP |
| DH_Res | Resistivity | Ohm-m | Constrain, E |
| DH_Nat_Gam | Natural Gamma | Counts | Geo |
| DH_Res_SnglPt | Resistivity Single Point | Ohm-m | Geo |
| DH_Res_16 | Resistivity 16in | Ohm-m | Geo |
| DH_Res_64 | Resistivity 65in | Ohm-m | Geo |
| DH_Res_Lat | Res Laterolog | Ohm-m | Geo |
| DH_SP_Cond | Self Potential Induction | milliVolt [mV] | Geo |
| DH_Res_FL | Resistivity of the fluid | Ohm-m | Geo |
| DH_Tmp_FL | Temperature of the fluid | Degrees F | Geo |
| DH_Del_Tmp | Change in temperature of the fluid | Degrees F | Geo |

**Table 6-6: Channel name description and units for the interpretation results file.**

| Parameter | Description | Unit |
|---|---|---|
| X_ft | Easting NAD83, UTM Zone 14 | Feet [ft] |
| Y_ft | Northing NAD83, UTM Zone 14 | Feet [ft] |
| Z_ft | Topography at 1000ft sampling (NAVD 1988) | Feet [ft] |
| Distance | Down line distance from start of flight line | Feet [ft] |
| RHO_I[0] through RHO_I[28] | Inverted resistivity of each later | Ohm-m |
| DEP_BOT[0] through DEP_BOT[28] | Depth to the bottom of individual layers | Feet [ft] |
| DEP_TOP[0] through DEP_TOP[28] | Depth to the top of individual layers | Feet [ft] |
| RESDATA | Residual of individual sounding | NA |
| RESTOTAL | Total residual for inverted section | NA |
| DOI_LOWER | Less conservative estimate of DOI | Feet [ft] |
| DOI_UPPER | More conservative estimate of DOI | Feet [ft] |
| WT_1995 | Elevation of the top of the water table from the Nebraska School of Natural Resources Configuration Report, 1995. | Feet [ft] |
| Bedrock | Elevation of interpreted bedrock surface | Feet [ft] |
| PrincipalAquifer_Top | Elevation of top of principal aquifer material (>21 ohm-m) | Feet [ft] |
| CoarseAquifer_Top | Elevation of top of coarse aquifer material (>50 ohm-m) | Feet [ft] |
| CoarseAquifer_Bot | Elevation of bottom of coarse aquifer material (>50 ohm-m) | Feet [ft] |
| PrincipalAquifer_Bot | Elevation of bottom of principal aquifer material (>21 ohm-m) | Feet [ft] |
| *To* | Elevation of the top of the Tertiary Ogalla Group. | Feet [ft] |
| *Kp* | Elevation of the top of the Cretaceous Pierre shale. | Feet [ft] |
| *Kn* | Elevation of the top of the Cretaceous Niobrara Formation. | Feet [ft] |
| *Kc_Kgg* | Elevation of the top of the Cretaceous Carlile Shale. | Feet [ft] |
| *Kd* | Elevation of the top of the Cretaceous Dakota Formation. | Feet [ft] |
| *P* | Elevation of the top of the Paleozoic Strata. | Feet [ft] |
| * | No data or unit not detected | |

# 7 References

Abraham, J. D., Carney, C.P., and J. C. Cannia. 2013. Data Report on Mapping the Hydrogeology of the Clarkson Area within the Lower Elkhorn Natural Resources District Using an Airborne Electromagnetic Survey. Project findings report prepared for the Lower Elkhorn Natural Resources District.

Abraham, J. D., Bedrosian, P.A., Asch, T.H., Ball, L.B., Cannia, J. C., Phillips, J.D., and S. Olafsen-Lackey. 2011. Evaluation of Geophysical Techniques for the Detection of Paleochannels in the Oakland Area of Eastern Nebraska as Part of the Eastern Nebraska Water Resource Assessment. U.S. Geological Survey Scientific Investigations Report 2011-5228.

Anderson, R.R. 1988. Phanerozoic Structural Features in the Northern Midcontinent, U.S.A. U.S. Geological Survey Miscellaneous Field Studies Map MF-1835-E in cooperation with the Iowa Department of Natural Resources Geological Survey Bureau.

Arnold, T.L., K.L. Warner, G.E. Groschen, J.P. Caldwell, and S.J. Kalkhoff. 2008. Hydrochemical regions of the glacial aquifer system, northern United States, and their environmental and water-quality characteristics. U.S. Geological Survey Scientific Investigations Report 2008-5015, 84 p.

Bankey, V., Cuevas, A., David, D., Finn, C.A., Hernandez, I., Hill, P., Kucks, R., Miles, W., Pilkington, M., Roberts, C., Roest, W., Rystrom, V., Shearer, S., Snyder, S., Sweeney, R., Velez, J., Philips, J.D., and D. Ravat. 2002. Digital data grids for the magnetic anomaly map of North America. U.S. Geological Survey Open-File Report 02-414, Denver, CO: U.S. Geological Survey.

Bentall, R. 1971. Water supplies and the land, the ELkhorn River Basin of Nebraska; Lincoln. University of Nebraska-Lincoln Conservation and Survey Division Resource Atlas No. 1.

Blessington, M.J. 2014. A Niobium Deposit Hosted by a Magnetiite-Dolomite Carbonatite, Elk Creek Carbonatite Complex, Nebraska, USA. Master's Thesis, University of Nebraska-Lincoln, Lincoln, Nebraska. Available online at: http://digitalcommons.unl.edu/geoscidiss/62/.

Burberry, C.M., Joeckel, R.M., and J.T. Korus. Submitted in 2014. In review. Pulsed Reactivation on the Nemaha Tectonic Zone and Midcontinent Rift System, Southeast Nebraska and Northern Kansas. The Mountain Geologist- Journal of the Rocky Mountain Association of Geologists.

Burchett, R.R., V.H. Dreezen, E.C. Reed, and G.E. Prichard. 1972. Bedrock geologic map showing thickness of overlying Quaternary deposits, Lincoln quadrangle and part of Nebraska City quadrangle, Nebraska and Kansas. U.S. Geological Survey, Miscellaneous Geologic Investigations Map I-729, scale 1:250,000; Available at: http://ngmdb.usgs.gov/Prodesc/proddesc_9487.htm [Accessed April 1, 2015].

Burchett, R.R., E.C. Reed, V.H. Dreeszen, and G.E. Prichard. 1975. Bedrock geologic map showing thickness of overlying Quaternary deposits, Fremont quadrangle and part of Omaha quadrangle, Nebraska. U.S. Geological Survey, Miscellaneous Investigations Series Map I-905, scale 1:250,000; Available at: http://ngmdb.usgs.gov/Prodesc/proddesc_9797.htm [Accessed April 1, 2015].

Burchett, R. R. 1982. Thickness and structure maps of the Pennsylvanian and Permian rocks across southern Nebraska. Nebraska Geological Survey Report of Investigations No. 7. Conservation and Survey Division, School of Natural Resources, Institute of Agriculture and Natural Resources, University of Nebraska-Lincoln. 15 p.

Burchett, R. R. 1983. Surface and subsurface correlation of Pennsylvanian and Lower Permian rocks across southern Nebraska. Nebraska Geological Survey Report of Investigations No. 8. Conservation and Survey Division, School of Natural Resources, Institute of Agriculture and Natural Resources, University of Nebraska-Lincoln. 24 p.

Burchett, R.R., Luza, K.V., Van Eck, O.J., and F.W. Wilson. 1985. Seismicity and Tectonic Relationships of the Nemaha Uplift and Midcontinent Geophysical Anomaly (Final Project Summary). U.S. Nuclear Regulatory Commission NUREG/CR-3117.

Burchett, R. R. 1986. Bedrock geology of Nebraska. University of Nebraska-Lincoln, School of Natural Resources. http://snr.unl.edu/data/geographygis/NebrGISgeology.asp#bedrock

CALMIT. 2007. Delineation of 2005 land use patterns for the State of Nebraska Department of Natural Resources. Center for Advanced Land Management Information Technologies, School of Natural Resources, University of Nebraska-Lincoln, 1:840,000, Available at: http://snr.unl.edu/data/geographygis/NebrGISland.asp#landuse05 [Accessed January 12, 2015]

Carlson, M.P. 1971. Eastern Nebraska and North-Central Kansas, in Adler, F.J., et al., Future Petroleum Provinces of the Mid-Continent, Region 7, in Cram, I.H., Future Petrolume Provinces of the United States, Their Geology and Potential, : American Association of Petroleum Geologists Memoir 15, p. 1103-1108.

Carlson, M., and S. Treves. 2005. The Elk Creek Carbonatite, southeast Nebraska- an Overview. Natural Resources Research, v. 14, p. 39-45.

Carlson, M.P. 2011. The Forest City Basin- Back to the Future. Nebraska Oil and Gas Conservation Comission. Available online at: www.nogcc.ne.gov

Carney, C. P., Pierce, K.S., Abraham, J. D., Steele, G.V., Genco, A.G., and J. C. Cannia. 2014. Hydrogeologic Assessment and Framework Development of the Aquifers beneath the Brainard-Valparaiso Area of the Lower Platte South Natural Resources District in Eastern Nebraska.

Christensen, N. B., J. E. Reid, and M. Halkjaer. 2009. Fast, laterally smooth inversion of airborne time-domain elecromagnetic data. Near Surface Geophysics, 599-612.

Christiansen, A. V., and E. Auken. 2012. A global measure for depth of investigation. Geophysics,Vol. 77, No. 4, WB171-177.

Condra, G. E., and C. E. Reed. 1959. The geolgogical section of Nebraska with current revisions by C.E. Reed. Nebraska Geological Survey Bulletin, Lincoln, Nebraska: University of Nebraska-Lincoln, Consevation and Survey Division.

Conservation and Survey Division. 1951. Topographic regions of Nebraska. Conservation and Survey Division, University of Nebraska-Lincoln, 1:1,000,000, Available at: *http://snr.unl.edu/data/geographygis/NebrGISgeology.asp#topography*

Diffendal, R. F. 1995. Geology of the Ogallala/High Plains regional aquifer system in Nebraska, field trip No.6 in Geological Society of America. Annual Meetings of the North-Central and South Central Sections.

Divine, D.P., R.M. Joeckel, J.T. Korus, P.R. Hanson, and S.O. Lackey. 2009. Eastern Nebraska Water Resources Assessment (ENWRA), Introduction to a hydrogeological study. Conservation and Survey Division, School of Natural Resources, Institute of Agriculture and Natural Resources, University of Nebraska-Lincoln, Bull. 1 (New Ser.), 31 p.

Divine, D. P. 2012. Geologic cross section across eastern Nebraska from Pierce County to Dakota County. Correlations and Cross Sections, Conservation and Survey Division, School of Natural Resources, Institute of Agriculture and Natrual Resources, University of Nebraska-Lincoln.

Divine, D. P., and J. T. Korus. 2012. Eastern Water Resources Assessment. Three-dimensional Hydrostratigraphy of the Sprague Nebraska Area: Results from Helicopter Electromagnetic (HEM) Mapping in the Eastern Nebraska Water Resources Assessment (ENWRA), http://www.enwra.org/media/2012ENWRA_Sprague_final.pdf (accessed Jan 8, 2015).

Divine, D.P. and Korus, J.T. 2013. Three-dimensional Hydrostratigraphy of the Swedeburg, Nebraska Area: Results from Helicopter Electromagnetic (HEM) Mapping for the Eastern Nebraska Water Resources Assessment (ENWRA). Conservation and Survey Division, School of Natural Resources, Institute of Agriculture and Natural Resources, University of Nebraska-Lincoln. Conservation Bulletin 5 (New Series), 31 p.

Divine, D. P., R. M. Joeckel, J. T. Korus, P. R. Hanson, and S. Olafsen-Lackey. 2009. Eastern Nebraska Water Resources Assessment, Introduction to Hydrogeological Study. Conservation and Survey Division, School of Natural Resources, Institute of Agriculture and Natural Resources, University of Nebraska-Lincoln.

Divine, D. P., S. Ross, and J. Korus. 2010. Compilation of Geologic Cross Sections of Eastern Nebraska. Open-File Report 109, Lincoln, Nebraska: Conservation and Survey Division, School of Natural Resources, Institute of Agriculture and Natural Resources, University of Nebraska-Lincoln.

Divine, D.P. 2014. The Groundwater Atlas of Lancaster County, Nebraska. Resource Atlas No. 7. Conservation and Survey Division, School of Natural Resources, Institute of Agriculture and Natural Resources, University of Nebraska-Lincoln.

Dolton, G.L. and T.M. Finn. 1989. Petroleum Geology of the Nemaha Uplift, Central Mid-Continent. U.S. Geological Survey Open File Report 88-450D.

Drenth, B.J. 2014. Geophysical Expression of a Buried Niobium and Rare Earth Element Deposit: The Elk Creek Carbonatite, Nebraska, USA. Interpretation, 2(4), SJ23-SJ33. DOI: 10.1190/INT-2014-0002.1

Druliner, A.D., and J.P. Mason. 2001. Hydrogeology and Water Quality in Five Principal Aquifers in the Lower Platte South Natural Resources District, Eastern Nebraska, 1994. U.S. Geological Survey Water-Resources Investigations Report 00-4155. http://pubs.usgs.gov/wri/wri004155/pdf/WRIR00-4155.pdf

ECC/GEO, 2012. Final Helicopter Electromagnetic and Magnetic Geophysical Survey Work Plan, Former Nebraska Ordnance Plant, Mead, Nebraska.

Elder, J. A., V. H. Dreesen, and E. C. Weakly. 1951. Topographic Regions of Nebraska. University of Nebraska-Lincoln, School of Natural Resources. http://snr.unl.edu/data/geographygis/NebrGISgeology.asp#topography

Ellis, M. J. 1984. Overview of the Dakota aquifer system in Nebraska, in Jorgensen, D.G. and Signor, D.C., eds., Geohydrology of the Dakota aquifer. National Water Well Association Proceedings, p. 48-55.

Exploration Resources International Geophysics, LLC. 2015. Airborne Electromagnetic Geophysical Surveys and Hydrogeologic Framework Development for Selected Sites in the Lower Elkhorn Natural Resources District, Project findings report prepared for the Lower Elkhorn Natural Resources District.

Flowerday, C. A., R. D. Kuzelka, and D. T. Pederson. 1998. The Groundwater Atlas of Nebraska. Resorce Atlas No. 4A, Lincoln, Nebraska: Conservation and Survey Division, School of Natural Resoirces, Institute of Agriculture and Natural Resoruces, University of Nebraska-Lincoln.

Foged, Nikolaj, Esben Auken, Anders Vest Christiansen, and Kurt Ingvard Sorensen. 2013. Test-site calibration and validation of airborne and ground based TEM systems. Geophysics 78, No.2, E95-E106.

Fredrick, B. S., J. I. Linard, and J. L. Carpenter. 2006. Environmental setting of Maple Creek watershed Nebraska. Scientific Investigations Report 2006-5037, U.S. Geological Survey.

Fugro, 2013a, Final - Helicopter Electromagnetic and Magnetic Geophysical Survey Report, Former Nebraska Ordnance Plant, Mead, Nebraska: prepared for the U.S. Army Corps of Engineers, Kansas City District, May 2013, 126 p.

Fugro, 2013b, FINAL - Helicopter Electromagnetic and Magnetic Geophysical Survey Interpretation Study, Former Nebraska Ordnance Plant, Mead, Nebraska: prepared for the U.S. Army Corps of Engineers, Kansas City District, May 2013, 87 p.

Gates, J. B., G. V. Steele, P. Nasta, and J. Szilagyi. 2014. Lithologic influenes on groundwater recharge through incised glacial till from profile to regional scales: Evidence from glaciated Eastern Nebraska. Water Resources 50, 466-481.

Gosselin, D. C., F. E. Harvey, and C. D. Frost. 2001. Geochemical evolution of groundwater in the Great Plains (Dakota) aquifer of Nebraska: implications for the management of a regional aquifer system. Ground Water 31, 98-108.

Gosselin, D.C., J. Headrick, X-H Chen, and S. Summerside. 1996. Regional Analysis of Rural Domestic Well-water Quality – Southeastern Glacial Drift Area. Conservation and Survey Division, School of Natural Resources, Institute of Agriculture and Natural Resources, University of Nebraska−Lincoln, GIM–112. 11 p.

Gosselin, D. C., J. Headrick, X. Chen, S. Summerside, and R. Tremblay. 1996. Northeast glacial drift area hydrogeologic summary from domestic well-water quality in rural Nebraska. Lincoln, Nebraska: University of Nebraska-Lincoln, Conservation and Survey Division GIM.

Gutentag, E. D., Heimes, F.J., Krothe, N.C., Luckey, R.R., and J. B. Weeks. 1984. Geohydrology of the High Plains aquifer in parts of Colorado, Kansas, Nebraska, New Mexico, Oklahoma, South Dakota, Texas, and Wyoming. Professional Paper 1400-B, U.S. Geological Survey.

Hanson, P. R., Korus, J.T., and D. P. Divine. 2012. Three-dimensional hydrostratigraphy of the Platte River Valley near Ashland, Nebraska: Results from Helicopter Electromagnetic mapping in the Eastern Nebraska Water Resources Assessment. Bulletin 2, Conservation and Survey Division, School of Natural Resources, Institute of Agricultutre and National Resources, University of Nebraska-Lincoln.

Hanson, P.R., A.R. Young and L.M. Howard. 2012. Surficial Geology of the Emerald 7.5 Minute Quadrangle, Nebraska. Conservation and Survey Division, School of Natural Resources, University of Nebraska-Lincoln. http://snr.unl.edu/data/geologysoils/STATEMAP/quads.aspx?lincoln_nebrcity

Harvey, F.E., J.F. Ayers, and D.C. Gosselin. 2007. Ground water dependence of endangered ecosystems: Nebraska's eastern saline wetlands. Ground Water, v. 45, no. 6, 17 p. Available at: http://onlinelibrary.wiley.com/doi/10.1111/j.1745-6584.2007.00371.x/abstract

Helgesen, J. O., R. B. Leonard, and R. J. Wolf. 1993. Hydrology of the Great Plains aquifer system in Nebraska, Colorado, Kansas, and adjacent areas. Regional Aquifer-System Analysis—Central Midwest, Professional Paper 1414-E, U.S. Geological Survey.

HydroGeophysics Group Aarhus University. 2011. Guide for processing and inversion of SkyTEM data in Aarhus Workbench, Version 2.0.

HydroGeophysics Group Aarhus University. 2010. Validation of the SkyTEM system at the extended TEM test site.

Joeckel, R.M. and J.S. Dillon. 2005. Surficial Geology of the Bennet Quadrangle, Nebraska. Conservation and Survye Division, School of Natural Resources, University of Nebraska-Lincoln, Department of Geography, University of Nebraska-Kearney. http://snr.unl.edu/data/geologysoils/STATEMAP/quads.aspx?lincoln_nebrcity

Joeckel, R.M. and J.S. Dillon. 2005. Surficial Geology of the Roca Quadrangle, Nebraska. Conservation and Survye Division, School of Natural Resources, University of Nebraska-Lincoln, Department of Geography, University of Nebraska-Kearney. http://snr.unl.edu/data/geologysoils/STATEMAP/quads.aspx?lincoln_nebrcity

Johnson, A. I. 1967. Specific yield- Compliation of specific yeilds for various materials. Water- Supply Paper 1662-D, U.S. Geological Survey.

Jorgensen, D. G., Helgesen, J.O, Signor, D.C., Leonard, R.B., Limes, J., and S. C. Christenson. 1993. Analysis of regional aquifers in the central Midwest of the United States in Kansas, Nebraska, and parts of Arkansas, Colorado, Missouri, New Mexico, Oklahoma, South Dakota, Texas, and Wyoming Geohydrologic framework. Professional Paper 1414-B, U.S. Geologic Survey.

Korus, J. T. 2012. Geologic cross section across eastern Nebraska from Thurston County to Pawnee County. Conservation and Survey Division, School of Natural Resources Institute of Agriculture and Natural Resources, University of Nebraska-Lincoln.

Korus, J. T., and R. M. Joeckel. 2011. Generalized geologic and hydrostratigraphic framework of Nebraska 2011, version 2. Conservation and Survey Division, School of Natural Resources, Institute of Agriculture and Natural Resources, University of Nebraska-Lincoln.

Korus, J. T., Divine, D.P., Hanson, P.R., and J. S. Dilion. 2012. Three geologic cross sections across portions of eastern Nebraska showing Quaternary lithologic units and stratigraphy of uppermost bedrock. Correlations and Cross Sections, Conservation and Survey Division, School of Natural Resources, Institute of Agriculture and Natural Resources, University of Nebraska-Lincoln.

Korus, J.T., Joeckel, R.M. and Divine, D.P. 2013a. Three-dimensional hydrostratigraphy of the Firth, Nebraska Area: Results from Helicopter Electromagnetic (HEM) mapping in the Eastern Nebraska Water Resources Assessment (ENWRA). Conservation and Survey Division, School of Natural

Resources, Institute of Agriculture and Natural Resources, University of Nebraska-Lincoln. Conservation Bulletin 3 (New Series), 100 p.

Korus, J.T., Howard, L.M., Young, A.R., Divine, D.P., Burbach, M.E., Jess, J.M., and D.R. Hallum (with contributions from Diffendal, R.F., and R.M. Joeckel). 2013b. The Groundwater Atlas of Nebraska. Conservation and Survey Division, School of Natural Resources, Institute of Agriculture and Natural Resources, University of Nebraska-Lincoln. 64 p.

Korus, J.T., Howard, L.M., Kuzila, M.S., and R.M. Joeckel. 2014. Surficial Geology of the Table Rock 7.5 Minute Quadrangle, Nebraska. Conservation and Survey Division, School of Natural Resources, Institute of Agriculture and Natural Resources, University of Nebraska-Lincoln. http://snr.unl.edu/data/geologysoils/STATEMAP/quads.aspx?lincoln_nebrcity

Lohman, S.W. 1972. Ground-water hydraulics. U.S. Geological Survey Professional Paper 708, 70 p., 9 pls.

Maher, H.D. 2014. Distributed Normal Faults in the Niobrara Chalk and Pierre Shale of the central Great Plains of the United States. Lithosphere, 6(5) p. 319-334. DOI 10.1130/L367.1.

Mason, J.A., and R.M. Joeckel. 2000. Surficial Geology of the Wann Quadrangle, Nebraska. Conservation and Survey Division, University of Nebraska-Lincoln. http://snr.unl.edu/data/geologysoils/STATEMAP/quads.aspx?fremont_omaha

Mason, J. A., Joeckel, R.M, 2002, Surficial geology of the Platte River Valley, Fremont to Ashland (Fremont East, Arlington, Valley, Wann, and Ashland East 7.5-Minute Quadrangles), Conservation and Survey Division Open-File Report 68, University of Nebraska, Lincoln, 39 p.

Miller, J. A., and C. L. Appel. 1997. Ground water atlas of the United States; Segment 3 Kansas, Missouri, and Nebraska. Hydraulic Atlas 730D, U.S. Geological Survey.

Miller, R. D., Van Horn, R., Dobrovolny, E., and L. P. Buck, 1964. Geology of Franklin, Webster, and Nuckolls Counties, Nebraska Bulletin 1165, http://pubs.er.usgs.gov/publication/b1165 (accessed Mar 20, 2015).

Nebraska Department of Economic Development. 2015. Geography – Nebraska Incorporated Communities by Legal Classification. Available at: http://www.neded.org/business/data-a-research/geography [Accessed March 31, 2015]

Nebraska Game and Parks Commission. 2015. Branched Oak State Recreation Area. Available at: http://outdoornebraska.ne.gov/parks/guides/parksearch/showpark.asp?Area_No=34

Nebraska Oil and Gas Conservation Commision. 2008. Nebraska Oil and Gas Conservation Commission Data and Publications, http://www.nogcc.ne.gov/NOGCCPublications.aspx (accessed Jan 5, 2015).

Nolan, B. T., Healy, R.W., Taber, P.E., Perkins, K., Hitt, K.J., and D. M. Wolock. 2007. Factors influencing ground-water recharge in the eastern United States. Journal of Hydrology 332, 187-205.

Ojakangas, R.W., Morey, G.B., and Green, J.C. 2001. The Mesoproterozoic Midcontinent Rift System, Lake Superior region, USA: Sedimentary Geology, v. 141-142, p. 319-341.

Olafsen-Lackey, S. 2005a. Specific yield of principal aquifer Sioux City Quadrangle, Nebraska. Conservation and Survey Division, School of Natural Resources, Institute of Agriculture and Natural Resources, University of Nebraska-Lincoln.

Olafsen-Lackey, S. 2005b. Transmissivity of principal aquifer Sioux City Quadrangle, Nebraska. Conservation and Survey Division, School of Natural Resources, Institute of Agriculture and Natural Resources, University of Nebraska-Lincoln.

Olafsen-Lackey, S., and S. Summerside. 2005. Specific yeild of principal aquifer Fremont and Omaha Quadrangles, Nebraska. Conservation and Survey Division, School of Natural Resources, Institute of Agriculture and Natural Resources, University of Nebraska-Lincoln.

Panday, S., Langevin, C.D., Niswonger, R.G., Ibaraki, M. and J. D. Hughes. 2013. MODFLOW–USG version 1: An unstructured grid version of MODFLOW for simulating groundwater flow and tightly coupled processes using a control volume finite-difference formulation. U.S. Geological Survey Techniques and Methods, book 6, chap. A45, 66 p.

pbEncom, 2015, pbEncom Discover Profile Analyst, available on the world wide web at: http://www.pitneybowes.com/pbencom/products/Geophysics/encom-pa.html

Peterson, J. A. 1984. Stratigraphy and Sedimentary Facies of the Madison Limestone and Associated Rocks in Parts of Montana, Nebraska, North Dakota, South Dakota and Wyoming. Professional Paper 1273-A, U.S. Geological Survey.

Platt. 2014. Platts McGraw Hill Financial, http://www.platts.com (accessed Oct 2014).

Schamper, C., E. Auken, and K. Sorensen. 2014. Coil response inversion for very early time modelling of helicopter-borne time-domain electromagnetic data and mapping of near-surface Geologic Layers. European Association of Geoscientistis & Engineers, Geophysical Prospecting.

School of Natural Resources University of Nebraska-Lincoln. 2005. Delineation of 2005 land use patterns for the Sate of Nebraska Department of Natural Recorces. http://snr.unl.edu/data/geographygis/NebrGISland.asp#landuse05 (accessed Jan 12, 2015).

Signor, D. C., Helgesen, J.O., Jorgensen, D.G., and R. B. Leonard. 1996. Geohydrology and simulation of steady-state flow conditions in regional aquifer systems in Cretaceous and older rocks underlying Kansas, Nebraska, and parts of Arkansas, Colorado, Missouri, New Mexico, Oklahoma, South Dakota, Texas, and Wyoming. Professional Paper 1414-C, U.S. Geological Survey, http://pubs.usgs.gov/pp/1414c/report.pdf

SkyTEM Airborne Surveys Worldwide. 2012. SkyTEM survey: Mary Creek Canada data report.

SkyTem Airborne Surveys Worldwide. 2015. Appendix A, Specifications of the SkyTEM508 System 60 Hz, http://skytem.com/wp-content/uploads/2015/01/SkyTEM508-60-Hz.pdf (accessed March 18, 2015).

Smith, B.D., Abraham, J.A., Cannia, J.C., Steele, G.V., and Hill, P.L. 2008. Helicopter electromagnetic and magnetic geophysical survey data, Oakland, Ashland, and Firth study areas, Eastern Nebraska, March 2007: U.S. Geological Survey Open-File Report 2008-1018, 16 p.

Smith, B. D., Abraham, J.D., Cannia, J.C., Minsley, B. J., Ball, L. B., Steele, G. V., and M. Deszcz-Pan. 2009. Helicopter Electromagnetic Geophysical Survey Data, Swedeburg and Sprague Areas, Eastern Nebraska. U.S. Geological Survey Open-File Report 2010-1288.

Souders, V. L. 2000. Geologic maps and cross sections showing configurations of bedrock surfaces, Broken Bow 1° x 2° quadrangle, east-central Nebraska. Geologic Investigations Series I–2725, U.S. Geological Survey.

Stander, T.W. 1989. Structural Nature of the Humboldt Fault Zone in Northeastern Nemaha County, Kansas. Kansas Geological Survey Bulletin 226- Geophysics in Kansas.

Stanton, J. S., Steele, G. V., and J. R. Vogel. 2007. Occurrence of agricultural chemicals in shallow ground water and the unstaturated zone, northeast Nebraska glacial till, Scientific Investigations Report 2002-04, U.S. Geological Survey.

Stanton, J. S., Peterson, S. M., and M. N. Fienen. 2010. Simulation of groundwater flow and effects of groundwater irrigation on stream base flow in the Elkhorn and Loup River Basins, Nebraska Phase Two. Scientific Investigations Report, U.S. Geological Survey, 78.

Summerside, S., Ponte, M., Dreezen, V. H., Harung, S. L., Khisty, M. J., and J. Szilagyi. 2001. Update and revision of regional 1x2 degree water-table configuration maps for the State of Nebraska. Lincoln, Nebraska: Conservation and Survey Division, Institute of Agriculture and Natural Resoruces University of Nebraska-Lincoln.

Summerside, S., and W. Myers. 2005a. Specific yield of the principal aquifer, Lincoln and Nebraska City Quadrangles, Nebraska. Conservation and Survey Division, School of Natural Resources, Institute of Agriculture and Natural Resources, University of Nebraska−Lincoln, 1 plate 1:250,000.

Summerside, S., and W. Myers. 2005b. Transmissivity of the principal aquifer, Lincoln and Nebraska City Quadrangles, Nebraska. Conservation and Survey Division, School of Natural Resources, Institute of Agriculture and Natural Resources, University of Nebraska−Lincoln, 1 plate 1:250,000.

Szilagyi, J., and J. Jozsa. 2013. MODIS-Aided statewide net groundwater-recharge estimation in Nebraska. Ground Water 51, 735-744.

Szilagyi, J., Harvey, F. E., and I. F. Ayers. 2005. Regional estimation of total recharge to ground water in Nebraska. Ground Water 43, 63-69.

Tanner, D.Q., and G.V. Steele. 1991. Ground-water quality in the Nemaha Natural Resources District, southeast Nebraska, 1989. U.S. Geological Survey Water-Resources Investigations Report 90-4184. 52 p. Available at: http://pubs.er.usgs.gov/publication/wri904184 [Accessed April 2, 2015]

Tikoff, B., and J. Maxson. 2001. Lithospheric Buckling of the Laramide Foreland during Late Cretaceous and Paleogene, Western United States. Rocky Mountain Geology 36(1) p. 13-35.

Tukey, J. W. 1977. Exploratory data analysis, Reading, PA, Addison-Weasley.

U.S. Census Bureau, 2015. Demographic profile, total population: U.S. CensusBureau, American FactFinder. Available at: http://factfinder.census.gov/faces/nav/jsf/pages/index.xhtml [Accessed March 31, 2015].

U.S. Geological Survey, 1966a, Burr, NE: USGS Topographic map, 24:000 scale.

U.S. Geological Survey, 1966b, Cook, NE: USGS Topographic map, 24:000 scale.

U.S. Geological Survey. 2015. USGS surface-water data for Nebraska. http://waterdata.usgs.gov/ne/nwis/sw/ (accessed Jan 8, 2015).

U.S. Department of Agriculture. 2014. USDA Natural Resources Conservation Service. http://www.nrcs.usda.gov/wps/portal/nrcs/detail/oh/technical/dma/gis/?cid=nrcs144p2_029531 (accessed Oct 2014).

University of Nebraska-Lincoln School of Natural Resources. 2014. Nebraska statewide test-hole database. http://snr.unl.edu/data/geologysoils/NebraskaTestHole/NebraskaTestHoleIntro.asp (accessed October 15, 2014).

Viezzoli, A., Christiansen, A. V., Auken, E., and K. Sorensen. 2008. Quasi-3D modeling of airborne TEM data by spatially constrainted inversion. Geophysics Vol. 73 No. 3, F105-F113.

Witzke, B.J. and G.A. Ludvigson. 1994. The Dakota Formation in Iowa and the type area, Geological Society of America Special Paper 287.

Witzke, B.J., Anderson, R.R., Bunker, B.J., and G.A. Ludvigson. 2003. Bedrock Geologic Map of Southwest Iowa. Iowa Department of Natural Resources and the Iowa Geological Survey. Available online at: http://s-iihr34.iihr.uiowa.edu/publications/uploads/ofm-2003-1_txt.pdf.

Young, H.L. 1992. Summary of Ground-Water Hydrology of the Cambrian-Ordovician Aquifer System in the Northern Midwest, United States. U.S. Geological Survey Professional Paper 1405-A- Regional Aquifer-System Analysis- Northern Midwest.